GEOCHEMISTRY OF THE CAMBRIAN MANGANESE DEPOSITS OF EASTERN NEWFOUNDLAND

JOHN LESLIE DOUGLAS

CANADIAN THESES ON MICROFICHE

I.S.B.N.

THESES CANADIENNES SUR MICROFICHE

National Library of Canada
Collections Development Branch

Canadian Theses on
Microfiche Service

Ottawa, Canada
K1A 0N4

Bibliothèque nationale du Canada
Direction du développement des collections

Service des thèses canadiennes
sur microfiche

NOTICE

The quality of this microfiche is heavily dependent upon the quality of the original thesis submitted for microfilming. Every effort has been made to ensure the highest quality of reproduction possible.

If pages are missing, contact the university which granted the degree.

Some pages may have indistinct print especially if the original pages were typed with a poor typewriter ribbon or if the university sent us a poor photocopy.

Previously copyrighted materials (journal articles, published tests, etc.) are not filmed.

Reproduction in full or in part of this film is governed by the Canadian Copyright Act, R.S.C. 1970, c. C-30. Please read the authorization forms which accompany this thesis.

THIS DISSERTATION
HAS BEEN MICROFILMED
EXACTLY AS RECEIVED

AVIS

La qualité de cette microfiche dépend grandement de la qualité de la thèse soumise au microfilmage. Nous avons tout fait pour assurer une qualité supérieure de reproduction.

S'il manque des pages, veuillez communiquer avec l'université qui a conféré le grade.

La qualité d'impression de certaines pages peut laisser à désirer, surtout si les pages originales ont été dactylographiées à l'aide d'un ruban usé ou si l'université nous a fait parvenir une photocopie de mauvaise qualité.

Les documents qui font déjà l'objet d'un droit d'auteur (articles de revue, examens publiés, etc.) ne sont pas microfilmés.

La reproduction, même partielle, de ce microfilm est soumise à la Loi canadienne sur le droit d'auteur, SRC 1970, c. C-30. Veuillez prendre connaissance des formules d'autorisation qui accompagnent cette thèse.

LA THÈSE A ÉTÉ
MICROFILMÉE TELLE QUE
NOUS L'AVONS REÇUE

NL-339 (r. 82/08)

Canada

GEOCHEMISTRY OF THE CAMBRIAN MANGANESE DEPOSITS OF EASTERN NEWFOUNDLAND

John Leslie Douglas, B.Sc.

A Thesis submitted in partial fulfillment of the
requirements for the degree of
Doctor of Philosophy

Department of Geology
Memorial University of Newfoundland
August 1983

St. John's Newfoundland

ABSTRACT

Manganese-rich sedimentary rocks are exposed intermittently throughout an area of 40,000 km^2 in the Avalon Zone in southeastern Newfoundland. Paleontological data indicate that the manganese-rich rocks form a stratiform deposit of basal Middle Cambrian age and that the manganese horizon is related to a disconformity whose duration increases from south to north. Stratigraphic measurements and chemical analyses show that the manganese horizon becomes thinner (from 25 to 1 m) and progressively enriched in Mn relative to Fe (Mn/Fe from <1 to ≃3.0) towards the north as the magnitude of the disconformity increases. The manganese horizon is enriched in Mn, Fe, Mg, Ba, and P relative to enclosing red and green mudrocks.

Petrographic study of manganese horizon samples shows that the horizon is fossiliferous, containing a fauna which includes trilobites and algal structures. Most of the manganese is present in carbonate minerals (rhodochrosite and manganiferous calcite), although secondary manganese oxide minerals also occur. In part, the manganese horizon contains anomalous concentrations of Fe-rich chlorite (chamosite). Phosphatic nodules and euhedral crystals of barite and pyrite are also present in some manganese horizon samples. Carbonate nodules are abundant and these are believed to have been formed during diagenesis.

The available evidence suggests that the manganese accumulated slowly in shallow marine waters in a partially restricted basin during a break in normal sedimentation characterized by reduced rates of

clastic sedimentation. The manganese was originally precipitated in oxide form, with subsequent alteration during early diagenesis producing the manganese carbonate which now characterizes the horizon. The Mn was derived from the weathering of Late Precambrian rock assemblages exposed around the Middle Cambrian basin. Mn was separated from Fe during transportation of the Mn towards the north within the partially restricted basin. In this regard, the restricted rate of clastic sedimentation is critical, as it permitted the gradual transportation and concentration of manganese at a given site over long periods of time with no dilution by clastic minerals.

The shallow marine origin, the stable tectonic environment, the manganese carbonate mineralogy, and the pronounced influence of diagenesis upon the rocks suggest similarities between the Newfoundland manganese horizon and modern oceanic ferromanganese deposits of the diagenetic type (Rona et al., 1978; Bonatti et al., 1972) and with the Nicopol' Formation type of ancient deposit (Varentzov, 1964). Manganese-rich rocks of basal Middle Cambrian age present in the Harlech Dome region in North Wales are stratigraphically, tectonically, and chemically similar to the Newfoundland manganese horizon (Mohr, 1966) and may be correlative with the latter.

ACKNOWLEDGEMENTS

The author would like to express his thanks to Memorial University of Newfoundland for the financial support given him to conduct this study. The assistance and constructive criticism of Dr. V.S. Papezik and Dr. R.N. Hiscott, and especially the unflagging support provided by Dr. D.F. Strong were of great help to the author. My thanks also to J. Vahtra and G. Andrews for their assistance in conducting chemical analyses.

My sincerest thanks are due to S. Merrick and M. Poppenroth for their excellent typing of the final draft under less than ideal conditions. Finally, I would like to express my appreciation to C. Danby for her continued encouragement and to Dr. A.B. Baldwin for the incentive provided me in this work.

TABLE OF CONTENTS

CHAPTER Page

LIST OF TABLES

TABLE Page

TABLE Page

Appendices:

LIST OF FIGURES

FIGURE Page

Appendices (Continued)

CHAPTER I

INTRODUCTION

1.1 Nature and Purpose of the Study

A stratiform deposit of manganese-rich sedimentary rocks of basal Middle Cambrian age is exposed intermittently over an area of at least 40,000 km^2 in the Avalon Zone of southeastern Newfoundland. The manganese horizon was formed in a shallow-water marine environment. Most of the manganese present in the horizon occurs in carbonate minerals (Dale, 1915). At this time, a great deal of research is being carried out on ferromanganese deposits. Most is concerned with recent, deep-sea manganese deposits (Rona, 1978) and to date deposits such as that on the Avalon Peninsula have been largely ignored.

The current study was undertaken with the objectives of determining the origin of the Newfoundland manganese horizon and of assessing its economic potential. An additional objective was to compare data obtained from the Newfoundland deposit with that available for recent and other ancient manganese deposits, to determine if it is analogous with any of these.

1.2 Current Status of Research on Sedimentary Manganese Deposits

Recent Deposits:

Ferromanganese deposits are widely distributed on the ocean floors (Horn et al., 1972), occurring in the form of manganese nodule concentrations or as more or less continuous ferromanganese crusts. The deposits form in several ways and each type possesses characteristic concentrations of manganese and iron (Bonatti, et al., 1972; and see discussion below). However, as a group the deposits are distinguished by high manganese concentrations and by Mn/Fe ratios which commonly reach or exceed unity. Some deposits contain appreciable contents of trace metals such as Cu, Ni, and Co, while others contain or are associated with high Ba and/or P concentrations. Mineralogically, the oceanic ferromanganese deposits are dominated by iron and manganese oxide and hydroxide minerals, though manganese carbonate minerals produced during diagenesis also occur in some deposits (Bonatti et al., 1972; Callender, 1973). The deposits occur under a wide range of environmental conditions, with the depth of water varying from abyssal to shallow marine in deposits present in epicontinental basins (Manheim, 1965). Ferromanganese deposits also occur in fresh water lacustrine environments (e.g., Cronan & Tooms, 1970; Callender, 1973).

The origin of oceanic ferromanganese deposits has been a subject of investigation for more than 100 years, since their discovery during the expedition of the H.M.S. Challenger (Murray & Irvine, 1895). The recognition, in recent years, that some pelagic deposits contain economic concentrations of Cu, Ni, and Co (e.g. an average of 2.5% Cu + Ni for nodules in the Northeastern Equatorial Pacific; McKelvey et al., 1979), has greatly expanded the volume of research on their distribution, character, and origin. Oceanic ferromanganese deposits exhibit regional variations in composition (Cronan, 1972) and form in a variety of environments. Deposits formed by various methods differ chiefly in the source of the manganese contained, though this difference is in turn reflected by differences in chemical and mineralogical composition.

Different processes which appear to be responsible for the formation of oceanic ferromanganese deposits are briefly discussed below. The names given the various types are those proposed in the genetic classification of Bonatti et al. (1972). The compositional and environmental differences between them are more fully discussed in Chapter 7.

<u>Hydrogenous Deposits</u>: these form by the direct, albeit slow, precipitation of manganese, iron and other chemical constituents from 'normal' sea water. Physicochemical conditions within the oceans are believed to favor the precipitation of iron and manganese oxides as stable species (Burns & Brown, 1972; Crerar & Barnes, 1974). The deposits form over a range of water depths, with deeper water favoring the production of nodules and shallower water, ferromanganese crusts (Bonatti <u>et al</u>., 1972). The deposits form very slowly (with estimated rates of growth of 1 cm/10^6 years; Kuenvolden <u>et al</u>., 1979), and the anomalous trace metal contents present in pelagic deposits of this nature are believed to be due to a combination of the low growth rates and the scavenging of trace metals from sea water by the accumulating iron and manganese oxides and hydroxides (Goldberg, 1954).

Hydrothermal Deposits: are formed by the precipitation of iron and manganese minerals from hydrothermal solutions. The latter are produced in regions of the oceans in which active volcanism is occurring, such as in the vicinity of oceanic ridges and in rifting environments (Bonatti et al., 1972). Examples of this type of deposit are the deposits in the neighborhood of the East Pacific Rise (Bostrom & Peterson, 1969), the iron and manganese oxide-rich sediments observed immediately above basaltic basement on some of the cores of the Deep Sea Drilling Project (Rex, 1969; Dymond et al., 1972), and the TAG area on the mid-Atlantic Ridge (Rona, 1978). While the manganese in these deposits is presumed to be largely of hydrothermal origin, analytical data suggest that some constituents are probably extracted from sea water (Dymond et al., 1973).

Diagenetic Deposits: are formed by the diagenetic remobilization of manganese in buried sediments, in a reducing environment generated by the decay of organic matter. The manganese mobilized in this way is precipitated at or near the sediment/water interface, upon entry into an oxidizing environment, though locally conditions in the sediment favor the diagenetic production of manganese carbonate minerals (Bonatti et al., 1972). Diagenetic ferromanganese deposits are associated with shallow marine environments and with sediments containing relatively high concentrations of organic matters.

Halmyrolytic Deposits: are formed by the interaction of fine-grained basaltic glass with sea water on the ocean floor, with the Mn freed during alteration of the volcanic material being precipitated as manganese oxides.

Possible Organic Control on Deposits:

Bacteria are known to be capable of reducing and oxidizing iron and manganese in sediments (Berner, 1981; Erlich, 1972). Erlich (op. cit.) has further shown that such bacteria are present in oceanic ferromanganese deposits, and concludes that the bacteria play a role in their production. He believes that the concentration of organic carbon in the sediments determines whether oxidation or reduction of manganese and/or iron will prevail, with high concentrations favoring bacterial reduction and low concentrations bacterial oxidation. The bacteria may not be essential to the production of ferromanganese deposits, but rather serve as catalytic agents speeding up the deposition of geochemically stable manganese and iron oxide minerals. The quantitative importance of such bacterial activity in the production of oceanic ferromanganese deposits remains undetermined.

Ancient Sedimentary Deposits:

More than 90% of the world's conventional (i.e., land-based) manganese ores are of sedimentary origin, with other types of manganese deposits, such as those formed in direct association with the intrusion of igneous bodies, accounting for only a small proportion of the total reserves (Wissink, 1972). The characteristics of ancient sedimentary manganese deposits are more fully discussed in Chapter 7.

Wissink (1972) and Varentsov (1964) have formulated classifications of sedimentary manganese deposits, subdividing them upon the basis of differences in composition, in the nature of the associated sedimentary rocks, and in the tectonic setting in which they occur. Quantitatively, the most important type of sedimentary manganese deposit forms in association with predominantly detrital sequences, though deposits present in carbonate sequences and in direct association with volcanic rocks also occur. Most of the sedimentary manganese deposits originate in shallow marine waters in tectonically stable regions. Mineralogically, manganese oxide and carbonate minerals are most abundant, though manganese silicate minerals occur in metamorphosed deposits such as those in North Wales (Woodland, 1939). Chemically, the deposits are dominated by Mn, which is much more enriched than any other element, though lesser enrichments in other elements such as P and Ba occur in some deposits.

The source of the manganese in the sedimentary deposits is interpreted to have been either from the weathering of rocks of 'normal' composition around the margins of the depositional basins or from hydrothermal solutions produced during the extrusion of time-equivalent volcanic rocks. A direct volcanic source of manganese cannot be factually sustained in the case of most of the shallow marine deposits, such as those in the Nicopol' Formation in the U.S.S.R., as no volcanic rocks occur in close association with the manganese-rich rocks.

1.3 Approach to Current Study

Samples collected from exposures of the Newfoundland manganese horizon were chemically analyzed, and subjected to x-ray diffraction for the purpose of obtaining mineralogical information. The chemical and mineralogical data obtained in this manner were used in conjunction with stratigraphic and paleontological data to formulate a model for the origin of the manganese horizon and to compare the horizon with other manganese deposits.

Descriptions of the stratigraphic sections which were examined in detail for this study and of the method used to sample these sections are provided in Chapter 3.

1.4 Location and Access

The Cambrian sequence in which the manganese horizon occurs is exposed on the Avalon Peninsula and vicinity in southeastern Newfoundland in a number of discrete erosional remnants preserved by downfolding or downfaulting of the stratigraphic succession (McCartney, 1967). The locations of the stratigraphic sections sampled for this thesis are shown on Figure 1.1.

The whole of the Avalon Peninsula was affected by Wisconsin glaciation which directly or indirectly shaped much of the present topography (Henderson, 1960, 1972). Inland exposures of bedrock are restricted by the presence of a stony till cover, glacially-formed lakes, and post-glacial peat bogs. This is particularly true of Cambrian exposures, as the Cambrian succession consists principally of soft and easily-eroded mudrock. In consequence, the best Cambrian bedrock exposures are found in cliff sections along the coast of the Avalon Peninsula. Conception Bay exposures (Figure 1.1) are accessible by road and foot, as are the sections

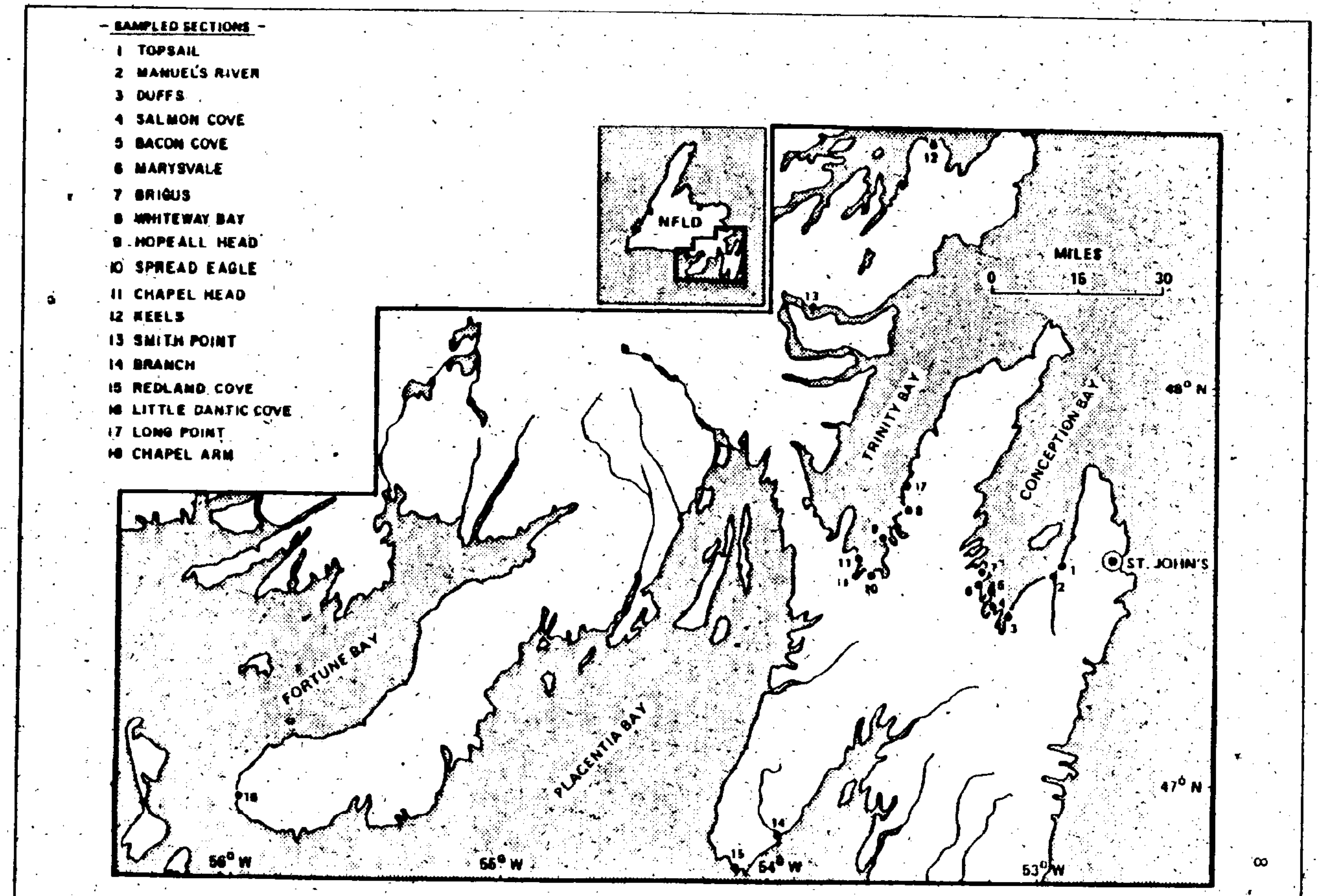

FIG. 1.1 LOCATION OF SAMPLED CAMBRIAN EXPOSURES IN SOUTHEASTERN NEWFOUNDLAND

exposed at Little Dantzic Cove on the Burin Peninsula and along the north shore of Smith Sound on Trinity Bay (Figure 1.1). A boat is necessary to gain access to the other sample localities shown on Figure 1.1.

CHAPTER 2

GENERAL GEOLOGY

2.1 Introduction

The island of Newfoundland is part of the Appalachian Structural Province (Williams et al., 1972) located along the southeastern margin of the North American continent, running in a northeasterly direction along the Atlantic seaboard of the United States, through the Canadian Maritime provinces, and thence into Newfoundland. The island constitutes the northeastern termination of the exposted Appalachian System in North America, though it is probable that the orogen is extended offshore northeast of the island on the Grand Banks (Sheridan & Drake, 1969). Reconstruction of the Appalachian System before the Mesozoic opening of the Atlantic Ocean (e.g., Bullard et al., 1965) indicates that the orogenic belt continues into the Caledonides through Britain, Norway and Sweden.

The reconstruction of Cowie (1971) given in Figure 2.1, shows the relative positions of southeastern Newfoundland and paleontologically correlative areas in North America, Britain and Scandinavia which lie along the southeastern or European flank of the Appalachian-Caledonian orogen. The Lower Paleozoic trilobite fauna of Acado-Baltic affinity (Hutchinson, 1962; Fletcher, 1972) present in these regions contrasts with the Lower Paleozoic trilobite fauna of the Pacific Faunal Realm which is present in western Newfoundland and other areas located on the northwestern flank of the orogen (Fig. 2.1).

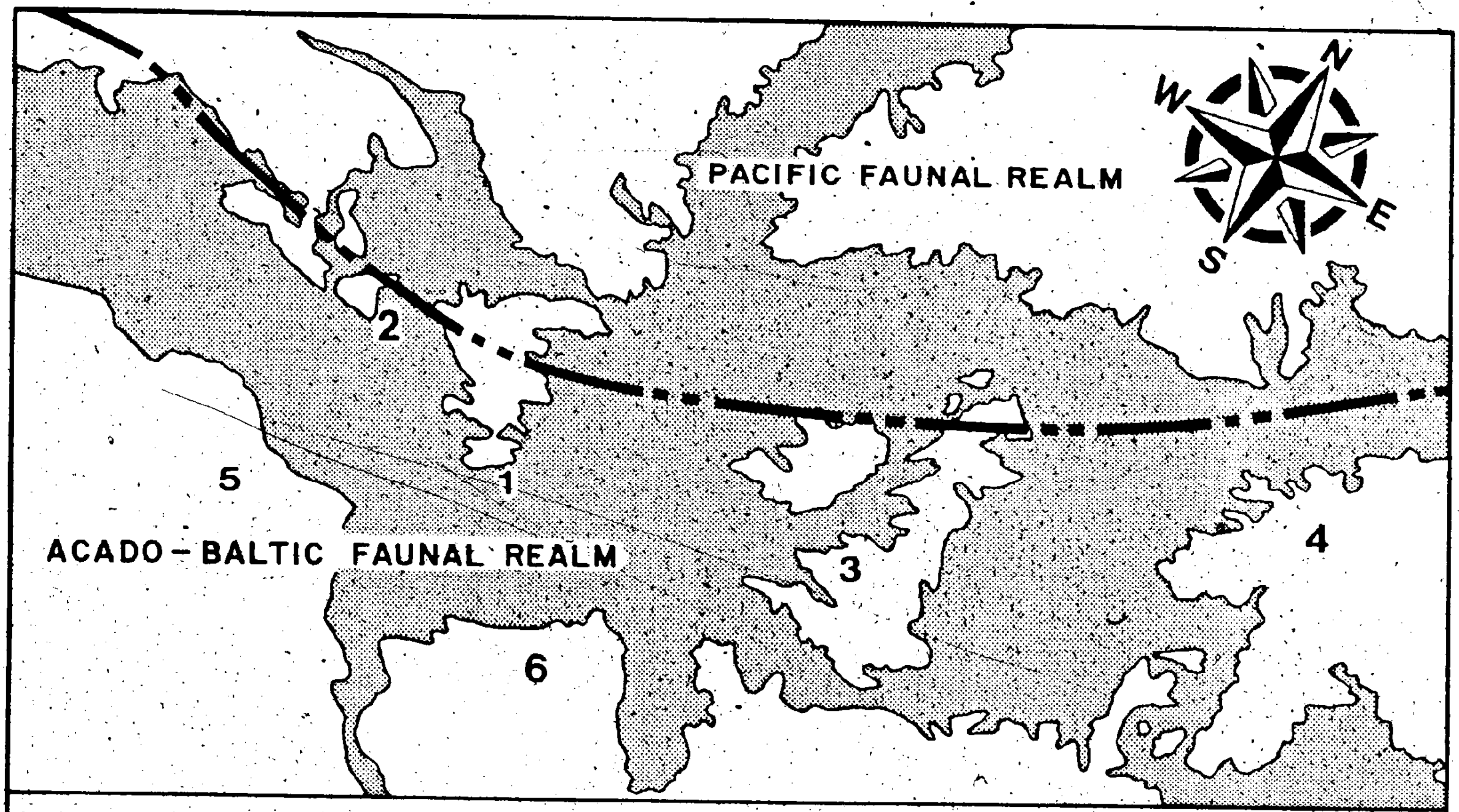

1. SOUTHEASTERN NEWFOUNDLAND
2. CAPE BRETON ISLAND
3. WALES AND THE BRITISH MIDLANDS
4. SCANDINAVIA
5. MOROCCO
6. SPAIN

▬ ▪ ▪ ▬ AXIS OF APPALACHIAN - CALEDONIAN OROGEN

FIGURE 2.1 PRE-MESOZOIC PALEOGEOGRAPHICAL RECONSTRUCTION OF APPALACHIAN-CALEDONIAN OROGEN REGION (AFTER COWIE, 1971)

These paleontological relationships led Wilson (1966) to propose that during the Lower Paleozoic, areas containing the two faunal elements were situated on opposite sides of a proto-Atlantic Ocean, and that subsequent closure of that ocean, followed by renewed crustal rifting to produce the present Atlantic Ocean, was responsible for the present spatial distribution of the two faunal realms. Wilson's concept of a proto-Atlantic Ocean has been incorporated into a number of plate tectonic models for the evolution of the Appalachian-Caledonian orogen (e.g., Bird & Dewey, 1970; Church & Stevens, 1971; Dewey & Bird, 1971; Schenk, 1971; Strong et al., 1974). These models suggest that in the Lower Paleozoic the stratigraphic sequences belonging to the two faunal realms were separated by an ocean (Iapetus) wide enough to prevent faunal mixing and homogenization. Estimates for the width of Iapetus during the early Paleozoic are in the order of 2000 km or more (Williams, 1980; McKerrow et al., 1976). Subsequently, the destruction by subduction of Iapetus during later Paleozoic time resulted in collision of the two bordering continental masses, producing the structures and deformation associated with the Appalachian-Caledonian orogen.

In Newfoundland, the Appalachian System can be divided into three fundamental units (Williams, 1964), viz. a central Paleozoic mobile belt falnked east and west by platformal sequences composed primarily of Late Precambrian and Lower Paleozoic sedimentary rocks. More recently, the central mobile zone has been subdivided (Williams, 1979) into the Dunnage and Gander zones (Figure 2.2).

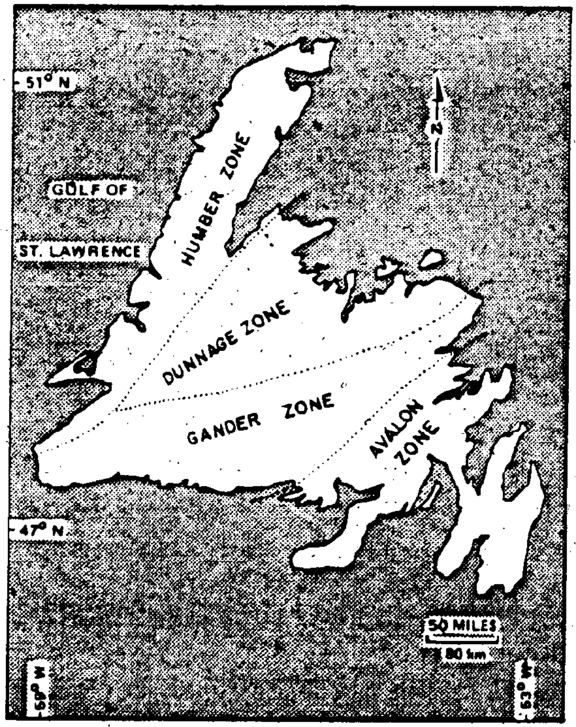

.... BOUNDARIES OF TECTONOSTRATIGRAPHIC ZONES

FIG. 2.2 TECTONOSTRATIGRAPHIC ZONES OF NEWFOUNDLAND
(AFTER WILLIAMS ET AL, 1980)

The Humber Zone in Figure 2.2 comprises a platformal sequence which is believed to represent the eastern continental margin of ancient North America, located to the west of Iapetus during the Lower Paleozoic. The Dunnage Zone contains island arc sequences built upon oceanic crust and is believed to contain the remnants of Iapetus per se, while the Gander Zone records the development and destruction of a continental margin on the east side of Iapetus (Williams, 1979).

The Late Precambrian history of the Avalon Zone is uncertain and may relate either to rifting associated with the initiation of Iapetus (Strong, 1979; Strong _et al._, 1978b) or to the development of an island arc sequence (Hughes and Brueckner, 1971) associated with a pre-Iapetus, Late Precambrian Subduction Zone (Rast _et al._, 1976). The Avalon Zone remained a stable platform during the Cambrian and Ordovician when construction and destruction of Iapetus in the Dunnage Zone was most intensive, and this suggests that the Avalon Zone was not in direct contact with the main body of Iapetus during this time (Williams, 1979).

The manganese horizon with which this work is concerned is developed in Cambrian sedimentary rocks of the Avalon Zone and the geology of this zone is discussed in greater detail in the remainder of this chapter.

2.2 Previous Work

Introduction

The Avalon Zone is predominantly underlain by a thick series of Late Precambrian volcanic and sedimentary rocks. These rocks are locally cut by granitic intrusives of several ages. Cambrian and Ordovician sedimentary rocks locally overlie the Late Precambrian rocks, forming a sequence up to 2,500 meters thick (King et al., 1974). The distribution of the Late Precambrian and Early Paleozoic rocks which comprise the Avalon Zone in southeastern Newfoundland is shown in Figure 2.3.

Previous Work

The earliest work on the geology of the Avalon Peninsula was carried out by J. B. Jukes in 1839 and 1840. Other early studies in this area include those by A. Murray and J.P. Howley (reports between 1869 and 1883), who jointly published a geological map of the Avalon Peninsula in 1881. The trilobite fauna present in the Cambrian sequence of sedimentary rocks was investigated by G. F. Matthew and C.D. Walcott in the 1880's and 1890's. These early workers recognized one group of Precambrian and another of Paleozoic sedimentary rocks, and separately mapped the igneous and volcanic rocks present in the region.

Van Ingen (1914) and Howell (1925) studied the paleontology and stratigraphy of the Lower Paleozoic sequence, while Dale (1915) was the first to examine in detail the manganese-rich sedimentary rocks of Lower Middle Cambrian age exposed in a number of localities around Trinity and Conception Bays. Hayes (1915, 1929) studied the oolitic iron ores present in Ordovician rocks exposed on Bell Island in Conception Bay, while Buddington (1916, 1919) investigated the petrology of Precambrian volcanic and plutonic rocks exposed in the northern half of the Peninsula. White (1939) and Widmer (1950) studied the geology of the Avalon Zone terrace in areas north of Fortune Bay southwest of the Avalon Peninsula.

The Geological Survey of Canada conducted a mapping program during the 1940's and 1950's which covered about half of the Avalon Peninsula. Rose (1952) mapped the Torbay area on the northeastern part of the Peninsula, modifying and extending knowledge of the Precambrian volcanic rocks of the Harbour Main Group. Hutchinson (1953) mapped Precambrian and Paleozoic rocks exposed in the Harbour Grace area in the north-central part of the Peninsula, and subsequently (in 1962) published a report on the Cambrian stratigraphy and trilobite faunas of southeastern Newfoundland. In the 1950's, McCartney (1959, 1967) mapped a large part of the central and western portions of the Avalon Peninsula, proposing lithostratigraphic correlations between the Precambrian volcanic, plutonic, and sedimentary rocks which underlie the bulk of the Peninsula. Henderson (1960, 1972) studied the glacial deposits and structures present on the Avalon Peninsula. Jenness (1963) mapped rocks of the Avalon Zone in the Bonavista and Terra Nova map areas northwest of the Avalon Peninsula proper, while Williams (1971) studied rocks in the Fortune Bay district southwest of the Peninsula.

In recent years, much of the work on the Avalon Peninsula has been undertaken by the faculty and students of Memorial University of Newfoundland. Various aspects of Avalon Peninsula geology have been the subjects of reports by Papezik (1970, 1972, 1973, 1980), Hughes (1970, 1973), Hughes and Brueckner (1971), Brueckner (1969), Anderson (1972), Brueckner and Anderson (1971), Anderson and Misra (1968), and King (1971, 1980). Student theses and dissertations have mainly been concerned with the Precambrian geology of the region (e.g., Keats, 1970; Hsu, 1972; Misra, 1969; Maher, 1972; and Malpas, 1971), but several have been directed towards the Lower Paleozoic rocks of the Peninsula (Nautiyal, 1966; Greene, 1962).

Several reports concerned with the economic geology of the Avalon Peninsula have been released by the Newfoundland Department of Mines and Energy (Butler & Bartlett, 1967; DeGrace, 1974). In recent years, an increasing amount of work has been done on the geology of the southern part of the Avalon Peninsula and on the adjacent Burin Peninsula (Fletcher, 1972; Greene & Williams, 1974; Williams & King, 1976; O'Brien _et al._, 1977; Strong _et al._, 1978).

2.3 General Geology of the Avalon Peninsula

King _et al._ (1974) separate the rocks of the Avalon Zone into three assemblages (Figure 2.3). Their "Lower Assemblage" and "Middle Assemblages comprise Late Precambrian volcanic and sedimentary rocks which underlie most of the Avalon Peninsula. Their "Upper Assemblage" includes quartzites of Lower Cambrian age (e.g., Random Formation; Anderson, 1981) and a series of mudrock, limestone, and sandstone of Cambrian and Ordovician age.

Strong _et al._ (1978b) provide a recent review of the stratigraphy, structure, and possible origin of the Late Precambrian rocks present in the Avalon Zone. These rocks are not further discussed here as they are not directly relevant to the present study.

Rocks of the "Upper Assemblage" are preserved in down-

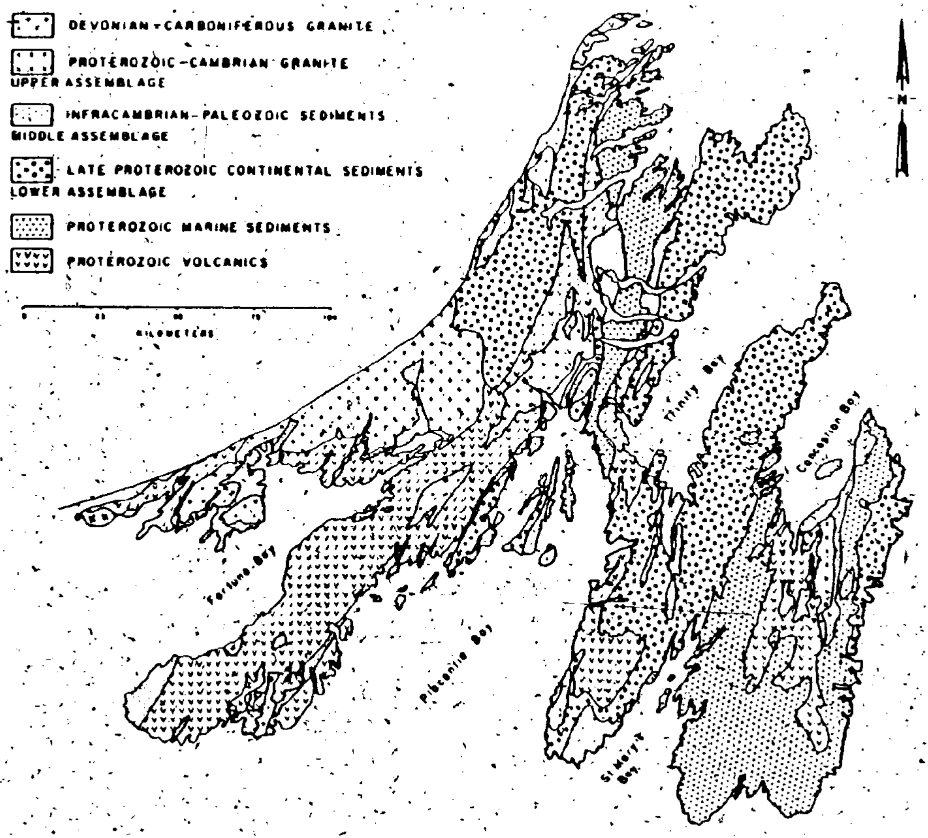

FIG. 2.3 GEOLOGY OF AVALON ZONE, SOUTHEASTERN NEWFOUNDLAND (FROM STRONG et al, 1978b)

faulted or downfolded erosional remnants in the Avalon Zone (Figure 2.3). The assemblage is subdivided into a number of units which persist over large areas. The stratigraphic sequence in various portions of the Avalon Zone is given in Table 2.1. The stratigraphic succession developed in the northern and eastern portions of the Avalon Zone is used in the remainder of this section as most of the study area is situated within this region. For discussions of correlations between this area and the Burin Peninsula and Fortune Bay areas, the reader is referred to recent reports by Strong <u>et al</u>.(1978a)and O'Brien <u>et al</u>. (1977).

Contact relationships between formation members in the Lower Paleozoic succession are in general conformable. Hutchinson (1962) and Fletcher (1972) consider the contact between the Lower (Brigus Fm.) and Middle (Chamberlain's Brook Fm.) Cambrian disconformable, primarily on paleontological grounds. The manganese-rich sedimentary rocks with which this study is concerned are related to this discomformity.

In eastern Avalon Peninsula exposures, fossiliferous Cambrian rocks overlie Precambrian volcanic and sedimentary rocks with angular unconformity. Elsewhere in Avalon Peninsula exposures, fossiliferous Cambrian rocks disconformably overlie quartzites of the Random Formation (Table 2.1). West of the Avalon Peninsula, sedimentation across the Precambrian-Cambrian boundary appears to have continued without interruption (Anderson, 1981, Bengston and Fletcher, Ms). The base of the Cambrian in this region is placed within the green and red siltstones, argillites, sandstones and minor limestones which comprise the Chapel Island Formation (Table 2.1).

TABLE 2.1 TABLE OF FORMATIONS, LOWER PALEOZOIC ROCK UNITS, AVALON ZONE, NEWFOUNDLAND (AFTER ANDERSON, 1981; HUTCHINSON, 1962)

AGE	FORTUNE BAY	SOUTHWESTERN BURIN. PENINSULA	SOUTHEASTERN BURIN PENINSULA	NORTHERN & EASTERN AVALON ZONE		
LOWER ORDOVICIAN				WABANA GROUP		
				BELL ISLAND GROUP		
				CLARENVILLE GROUP		
UPPER CAMBRIAN	SALMONIER COVE FORMATION			ELLIOT COVE FORMATION	HARCOURT GP.	DARK GREY TO BLACK SHALE & MUDROCK, MINOR CARBONATE, SORT
MIDDLE CAMBRIAN	YOUNGS COVE FORMATION	MANUEL'S RIVER FORM.	MANUEL'S RIVER FORM.	MANUEL'S RIVER FORM.	ADEYTON GROUP	RED AND GREEN MUDROCKS SUBORDINATE LIMESTONE
		CHAMBERLAIN'S BROOK FORM.	CHAMBERLAIN'S BROOK FORM.	CHAMBERLAIN'S BROOK FORM.		
LOWER CAMBRIAN	NON-SEQUENCE	BRIGUS FORMATION	BRIGUS FORMATION	BRIGUS FORMATION		
		NON-SEQUENCE	SMITH POINT LST.	SMITH POINT LST.		
			BONAVISTA FORM.	BONAVISTA FORM.		
	RANDOM FM.	RANDOM FM.	RANDOM FORM.	RANDOM FORM.		
PRE-CAMBRIAN	CHAPEL ISLAND FM.	CHAPEL ISLAND FORM.	CHAPEL ISLAND FM.			
	RENCONTRE FM.	DOTEN COVE FORM.	DOTEN COVE FORM.			
LATE PRECAMBRIAN VOLCANIC ROCKS						

The upper portion of the Chapel Island Formation contains the oldest fossiliferous Cambrian rocks of the Avalon Zone and it follows that the initial Cambrian transgression occurred in the Fortune Bay region to the west of the Avalon Peninsula (Anderson, 1981).

2.3.1 The Random Formation

The Random Formation comprises a sequence of white quartzites and intercalated grey siltstones which ranges in thickness from 0 to 150 meters. It is present over most of the Avalon Peninsula, but is absent in Conception Bay exposures. Lithologically similar quartzites in the Burin Peninsula and the area north of Fortune Bay (e.g. the Blue Pinion Formation of Widmer, 1950) have been correlated with the Random Formation (Hutchinson, 1962; Greene and Williams, 1974; Anderson, 1981). The Random Formation contains no shelly fossils but does locally contain trace fossils. It has been interpreted as a shallow water deposit, possibly intertidal in part (Fletcher, 1972).

Contact Relationships and Age

The Age of the Random Formation has been problematical since the formation was first described (Walcott, 1900). Various authors have considered the Random Formation to be of late Precambrian age (Walcott, 1900, Hutchinson, 1962), of Cambrian age (Rose, 1948; Van Alstine, 1948), of either late Precambrian or Cambrian age (McCartney, 1967), or as being markedly diachranous and ranging in age from Late Precambrian to Early Middle Cambrian (Greene and Williams, 1974). Recent studies by Anderson (1981) and by Bengston and Fletcher (MS) suggest that the Random Formation, though diachronous, is of early

Cambrian age; this age has been adopted for the purposes of this work.

Contact relationships suggested by the recent studies referred to above indicate that in Eastern and Northern Avalon Zone exposures, the Random Formation disconformably overlies sedimentary rocks of Late Precambrian age and is in turn disconformably overlain by fossiliferous Lower Cambrian rocks (Bonavista Formation in Table 2.1). In the Burin Peninsula - Fortune Bay region, which marks the western limit of the exposed Avalon Zone, the Random Formation conformably overlies fossiliferous Early Cambrian rocks (Chapel Island Formation in Table 2.1) and is disconformably overlain by sedimentary rocks of Lower to Middle Cambrian age.

2.3.2 Paleozoic Rocks

The Cambrian and Ordovician rocks exposed in the Avalon Zone comprise a sequence of red, green, and black mudrock, with minor limestone also present. The Cambrian sequence of sedimentary rocks is subdivided into the Adeyton and Harcourt Groups (Jenness, 1963). The Adeyton Group consists of a sequence of red and green mudrocks and minor intercalated limestone ranging in age from Lower Cambrian through Lower Middle Cambrian. The manganese horizon with which this work deals is developed within the mudrocks of the Adeyton Group. The Harcourt Group conformably overlies the Adeyton Group, and comprises black to grey mudrocks with minor intercalated grey limestone and fine-grained sandstone. It ranges in age from middle Middle Cambrian through Upper Cambrian.

The Harcourt Group in turn is overlain, probably conformably (Rose, 1952), by sandstone and shale of Lower Ordovician age. The

Adeyton and Harcourt Groups vary in exposed thickness from 300 to 1200 m (King et al., 1974). The sedimentary rocks unconformably overlie Late Precambrian volcanic, sedimentary, and plutonic (viz. the Holyrood Granite) rocks in the Conception Bay region of the Avalon Peninsula; elsewhere, the Adeyton Group unconformably (Fletcher, 1972) overlies quartzites of the Random Formation.

Locally, volcanic flows of Middle Cambrian Age are present in the Cambrian Sequence on the Avalon Peninsula. The volcanic rocks are present in the uppermost portion of the Chamberlain's Brook Formation (Hay Cove volcanics of Fletcher, 1972) and in the overlying Manuel's River Formation (McCartney, 1967). The volcanic rocks are restricted to a narrow, north-south trending zone which extends from Hopeall Head, Trinity Bay south to the Cape Dog, St. Mary's Bay area. The volcanic rocks include submarine pillow lavas and associated marine pyroclastics; these rocks are chemically altered but petrographically resemble tholeites or alkali basalts (Papezik, 1980). Small intrusive bodies of diabasic gabbro cut Middle Cambrian sedimentary rocks within the linear belt in which volcanic rocks were deposited and probably were feeders for the Middle Cambrian lavas (McCartney, 1967). Individual flows appear to be of limited lateral extent (Fletcher, 1972).

Diabasic dykes and sills are present throughout the Adeyton Group. Some are undeformed and therefore postdate Acadian (Devonian) deformation.

The stratigraphic units into which the Harcourt and Adeyton Groups are divided on the Avalon Peninsula are shown in Table 2.1.

These units are discussed individually below.

2.3.2.1 Adeyton Group

Bonavista Formation: The red and green mudstones which comprise the Bonavista Formation are up to 150 meters thick. Limestone is present in the formation in subordinate amounts, occurring in thin intercalated limestone beds and in limestone nodules. The latter are commonly concentrated along specific horizons and define the bedding in the sequence. The Bonavista Formation is thickest along an axis running south through Trinity Bay, across the isthmus of Avalon, and continuing south through Placentia Bay. It thins east and west of this axis, and is absent in eastern Conception Bay exposures (Hutchinson, 1962). The Bonavista Formation is also missing in Western Burin Peninsula and in Fortune Bay exposures (Anderson, 1981). The Bonavista Formation disconformably overlies Random Formation quartzites on the Avalon Peninsula (Fletcher, 1972).

Smith Point Limestone Formation: The Smith Point Limestone conformably overlies the Bonavista Formation, and consists of pink, grey, and red massive limestone up to 15 meters thick. Red argillaceous interbeds occur in the limestone, which also contains stromatolitic algal colonies (Hutchinson, 1962; McCartney, 1967). The uppermost half-meter of the formation contains the oldest trilobite fauna recorded in southeastern Newfoundland (Fletcher, 1972). The Smith Point Limestone, like the older Bonavista Formation, is absent from eastern Conception Bay exposures and in western Burin Peninsula exposures (Hutchinson, 1962).

Brigus Formation; The Brigus Formation overlies the Smith Point Limestone Formation, and constitutes the youngest Lower Cambrian formation on the Avalon Peninsula. It is composed principally of massive red and green mudrock and slate, though lesser amounts of limestone, generally present in thin nodular limestone beds, also occur. The formation ranges between 10 and 210 meters in thickness on the Avalon Peninsula, thinning east and west of an axis running south through Trinity and Placentia Bays, as do the preceding Lower Cambrian formations (Hutchinson, 1962). It contains a trilobite fauna ranging in age from middle to late Lower Cambrian (Fletcher, 1972).

In Conception Bay exposures, the Brigus Formation unconformably overlies Late Precambrian volcanic, sedimentary, and plutonic rocks. Older members of the Adeyton Group are absent in this area. In these exposures, the base of the Brigus Formation is marked by a thin conglomerate bed. This conglomerate characteristically has a calcareous cement and is rarely more than one meter thick. In some of the Conception Bay exposures (i.e., at Brigus and Bacon Cove), the calcareous conglomerate fills fractures in underlying Precambrian rocks to a depth of one meter or more. Locally, stromatolites are present in the basal conglomerate at the base of the Brigus Formation in this area.

Chamberlain's Brook Formation: The Chamberlain's Brook Formation contains the oldest Middle Cambrian rocks present in southeastern Newfoundland. The formation disconformably overlies the preceding Brigus Formation, with the disconformable contact marked by deposition of a horizon of manganese-rich sedimentary rocks. The character and regional variations in development of this horizon are considered in greater detail in the next chapter. The base of the Chamberlain's Brook Formation marks the base of the Middle Cambrian portion of the stratigraphic sequence throughout the Avalon Peninsula region (Fletcher, 1972; Hutchinson, 1962), while the upper contact of the unit constitutes the boundary between the Adeyton and overlying Harcourt Groups (see Table 2.1). The Chamberlain's Brook Formation, up to 150 meters thick, consists mainly of green to grey mudrocks, although red mudrocks occur locally. Thin limestone interbeds also occur in the formation, and in the Hopeall Head, Trinity Bay exposure, an intercalated volcanic breccia unit about 5 meters thick occurs some 60 meters above the base (McCartney, 1967). Volcanic rocks of equivalent age also occur in the formation in the Cape St. Mary's region in the southern Avalon Peninsula (Fletcher, 1972).

2.3.2.2 Harcourt Group

Manuel's River Formation: The Manuel's River Formation gradationally overlies the Chamberlain's Brook Formation, and consists of medium grey to black shale and slate with lenses of grey limestone. The formation, up to 30 meters thick, contains a trilobite fauna ranging in age from middle to late Middle Cambrian. The color change between the dark shales of the Manuel's River Formation and the green shales and mudrocks of the underlying Chamberlain's Brook Formation is gradational. Fletcher (1972) uses a widespread bentonite bed to separate the two, defining the bentonite bed as the base of the Manuel's River Formation. On the western half of the Avalon Peninsula, around the head of Trinity Bay and on the Cape St. Mary's Peninsula, andesitic pillow lavas and breccias (the Chapel Arm member of McCartney, 1967) are interbedded in the Manuel's River Formation. Two flows, separated by about 5 meters of slate, make up the Chapel Arm member in most Trinity Bay locations (McCartney, 1967). The andesitic flows are pale to dark grey in color and generally contain calcite amygdules. Individual flows are up to 60 meters thick (Fletcher, 1972) but thin rapidly and are of limited lateral extent.

Elliot Cove Formation: The Elliot Cove Formation consists of dark grey to black, locally pyritiferous shales, with grey limestone concretions and grey, micaceous sandstone beds in the upper part. No complete sections are known, but the formation attains a maximum exposed thickness of about 200 meters (Hutchinson, 1962). The Elliot Cove Formation contains a trilobite fauna of Upper Cambrian age and its base defines the Middle-Upper Cambrian boundary in the Avalon Zone (Hutchinson, 1962). The contact between the formation and the underlying Manuel's River Formation is believed to be disconformable and is locally marked by the presence of a thin conglomerate bed (Poulson and Anderson, 1975). The Elliot Cove Formation is overlain by sedimentary rocks of Lower Ordovician age but the contact between the two is not exposed (Hutchinson, 1962).

2.3.3 Fossils Present in Lower Adeyton Group

The Cambrian sequence contains a trilobite fauna belonging to the Acado-Baltic realm (Fletcher, 1972; Hutchinson, 1962). The oldest Adeyton Group rocks on the Avalon Peninsula predate the appearance of trilobites in the uppermost 0.5 meter of the Smith Point Limestone (Fletcher, 1972). However, other fossil forms are present in these older sedimentary rocks, including *Hyolithes*, *Coleoloides*, and the gastropod *Straparollina remota* Billing (Fletcher, 1972). Locally, these shelly fossils are present at the base of the Bonavista Formation where this overlies the Random Formation (e.g., section exposed at Cuslett Point on the St. Mary's Peninsula; Fletcher and Brueckner in King *et al*., 1974, p. 38).

The Adeyton Group also contains algal stromatolites at intervals throughout, as well as algal textures attributable to the algae *Ephiphyton* and *Girvanella* (M. M. Anderson, pers. comm., 1975). Sponge spicules also occur in these sedimentary rocks (Dale, 1915).

The significance of the fauna present in the Adeyton and Harcourt Groups as to the conditions present during sedimentation is considered below.

2.3 Depositional History of Adeyton and Harcourt Groups

The Avalon Zone remained a stable, gently subsiding tectonic element throughout the Lower Paleozoic (Williams *et al*., 1974; Williams, 1979).

The Cambrian sedimentary rocks are almost exclusively fine-grained, except for a thin basal conglomerate and minor grey sandstone towards the top of the Harcourt Group. The fine-grained nature of the sequence suggests that deposition took place in a low-energy environment. Coarser material is absent because the basin was in some way restricted or because there was little erosion of the source areas. The presence of a trilobite fauna and especially of algal remains at intervals throughout the Adeyton Group suggest that deposition took place in shallow water, in neritic to intertidal environments.

The oldest fossiliferous Cambrian sedimentary rocks in the Avalon Zone (Chapel Island Formation) were deposited in the Burin Peninsula - Fortune Bay area and it would therefore appear that the initial Cambrian transgression occurred in this region. The initial transgression was extended eastwards and northwards over the Avalon Peninsula and was accompanied by deposition of the quartzites and sandstones of the Random Formation (Anderson, 1981).

The sea then withdrew from the area, resulting in the partial erosion of the Random Formation (Anderson, 1981). A renewed marine transgression from the northeastern part of the Avalon Zone (i.e. the Avalon Peninsula area) was accompanied by the deposition of the oldest member of the Adeyton Group, the Bonavista Formation.

Isopach maps for members of the Adeyton Group (Hutchinson, 1962) suggest that throughout the remainder of the Lower and Middle Cambrian, the Cambrian sedimentary basin formed a trough elongated in a north-south direction and bounded by positive areas east and west of an axis running south through Trinity and Placentia Bays. The basin was initially relatively narrow and the Bonavista Formation was not deposited in the eastern (i.e. Conception Bay) part of the Avalon Peninsula or in the Fortune Bay region to the west (Hutchinson, 1962). The basin continued to widen throughout the Lower Cambrian and by the early Middle Cambrian covered the present-day limits of the Avalon Zone in southeastern Newfoundland. Sedimention continued in the basin throughout the remainder of the Cambrian, though not without interruption (see below).

During the Middle Cambrian, increased tectonic instability, centred along the north-south depositional axis of the basin, led to the deposition of volcanic flows and the emplacement of related gabbroic intrusives (Papezik, 1980; McCartney, 1967). The volcanic activity did not intensify, however, and had ceased by the close of the Middle Cambrian.

The Lower-Middle (Hutchinson, 1962; Fletcher, 1972) and Middle-Upper (Poulson and Anderson, 1975) Cambrian boundaries in the Avalon Zone are disconformable and mark significant regressive events within the Cambrian basin. Additional minor breaks in sedimentation probably also occur (Fletcher, 1972).

The manganese horizon with which this study is concerned is associated with and was deposited during the Lower-Middle Cambrian regression. The horizon is characterized by manganese carbonate minerals (Chapters 4 and 5) and is best developed in northern Avalon Peninsula exposures. Paleontological studies by Fletcher (1972) show that the hiatus in sedimentation lasted longest in the northern Avalon Peninsula area where the manganese horizon is best developed. The 'non-sequence' becomes progressively less significant towards the south and sedimentation at the Lower-Middle Cambrian boundary was essentially uninterrupted in southernmost Avalon Peninsula exposures. Fletcher (1972) concludes that the break in sedimentation was caused by differential uplift of the northern Avalon Peninsula.

area at the close of Lower Cambrian time. This was followed by erosion of Brigus Formation sedimentary rocks in the north and the deposition of the manganese horizon. The manganese horizon is discussed in more detail in Chapter 3.

2.5 Structure

Most of the structures present within the study area can be related to the compressive Acadian Orogeny of Devonian Age (Williams et al., 1974). This event has produced open folds and axial planar cleavage in the Cambrian sedimentary rocks, though some areas (e.g. Manuel's, Conception Bay) are less affected than others. The Acadian Orogeny is also believed responsible for the faulting which now controls the distribution of the Lower Paleozoic rocks.

Locally, Late Precambrian rocks were tilted and folded prior to Cambrian sedimentation (e.g., Bacon Cove, Conception Bay; King et al., 1974) and this provides evidence for an older period of deformation. This, however, is poorly understood at this time and it is not known whether there was a single Precambrian 'orogeny' or several unrelated periods of deformation in the Avalon Zone (Strong et al., 1976).

2.6 Comparison of Avalon Zone to Paleontologically Correlative Areas

Lower Paleozoic sedimentary rocks in southeastern Newfoundland were deposited in a shallow-water, marine environment in a stable, gently subsiding continental/epicontinental environment (Williams, 1979). Tectonically, the same holds true for paleontologically correlative rocks deposited in maritime North America, England, Wales, Scandinavia, France (Brittany), Spain, and Morocco in Africa (e.g., Rast et al., 1976; Strong, 1979; Schenck, 1971; Martinsson, 1974).

The latest Precambrian-Lower Paleozoic sedimentary rocks deposited in these areas share the following lithological and depositional properties:

(1) the Cambrian/Precambrian boundary is not clearly defined, i.e., is marked by continuous sedimentation (the pre-trilobite zone of Fletcher, 1972; the Eocambrian sequence of Scandinavia described by various authors);

(2) the presence of glacial sediments in latest Precambrian sedimentary rocks (Anderson, 1972; Bjørlykke, 1978);

(3) orthoquartzites present at or near the Precambrian/Cambrian boundary (Bjørlykke, 1978; Strong, 1979);

(4) transgressive Lower Cambrian sediments which are arenaceous or dominated by mudrocks, as in southeastern Newfoundland, Cape Breton Island (Hutchinson, 1962), and Britain (Cowie & Rushton, 1974). Arenaceous sequences such as those typical of the Baltic Shield in Scandinavia are characterized by numerous 'breaks' in sedimentation which are marked by conglomeratic horizons commonly enriched in glauconite, phosphorous, or pyrite (Martinsson, 1974);

(5) a disconformable Lower-Middle Cambrian boundary (see below); and

(6) a Middle and Upper Cambrian sequence dominated by black and grey mudrocks and shale (e.g., the Alum Shale present in

Scandinavia-Gee, 1972; Bjorlykke, 1974).

Volcanic rocks are in general rare in these sequences. Where present, they are usually of Middle Cambrian age and restricted in areal extent (e.g., in Cape Breton Island-Hutchinson, 1952; and Newfoundland-McCartney, 1967; Fletcher, 1972), though in Morocco volcanic rocks of Lower Cambrian age occur.

Paleogeographically, Lower Paleozoic sedimentary rocks in the Acado-Baltic realm were deposited in epicontinental stable basins (Gee, 1972) or in discrete, linear troughs not in direct contact with the main Lower Paleozoic (Cambrian) ocean basin (e.g., Wales-Crimes, 1970; parts of Scandinavia-Bjorlykke, 1978; and Newfoundland-Hutchinson, 1962).

The Lower-Middle Cambrian disconformity in southeastern Newfoundland with which manganese-rich sedimentary rocks are associated is present in many correlative areas in the Acado-Baltic Faunal Realm, as can be seen in Table 2.2. Indeed, Newfoundland (and North Wales) can be seen to be atypical in that sedimentation across the Lower-Middle Cambrian boundary is much less effected by the regressive event than other regions, such as Scandinavia, Shropshire, etc.

Palmer and James (1980) have recently documented a Lower-Middle Cambrian break in sedimentation in western Newfoundland and correlative areas, i.e., in the Pacific Faunal Realm or on the American side of Iapetus (Figure 2.1).

Thus, it is possible that the Lower-Middle Cambrian regression in southeastern Newfoundland is part of a 'global' event effecting sedimentation on both sides of Iapetus, perhaps a eustatic lowering of sea-level (Palmer and James, 1980).

Acado-Baltic strata in North Wales are of particular interest

TABLE 8.1 CORRELATION CHART (after Fletcher, 1972)

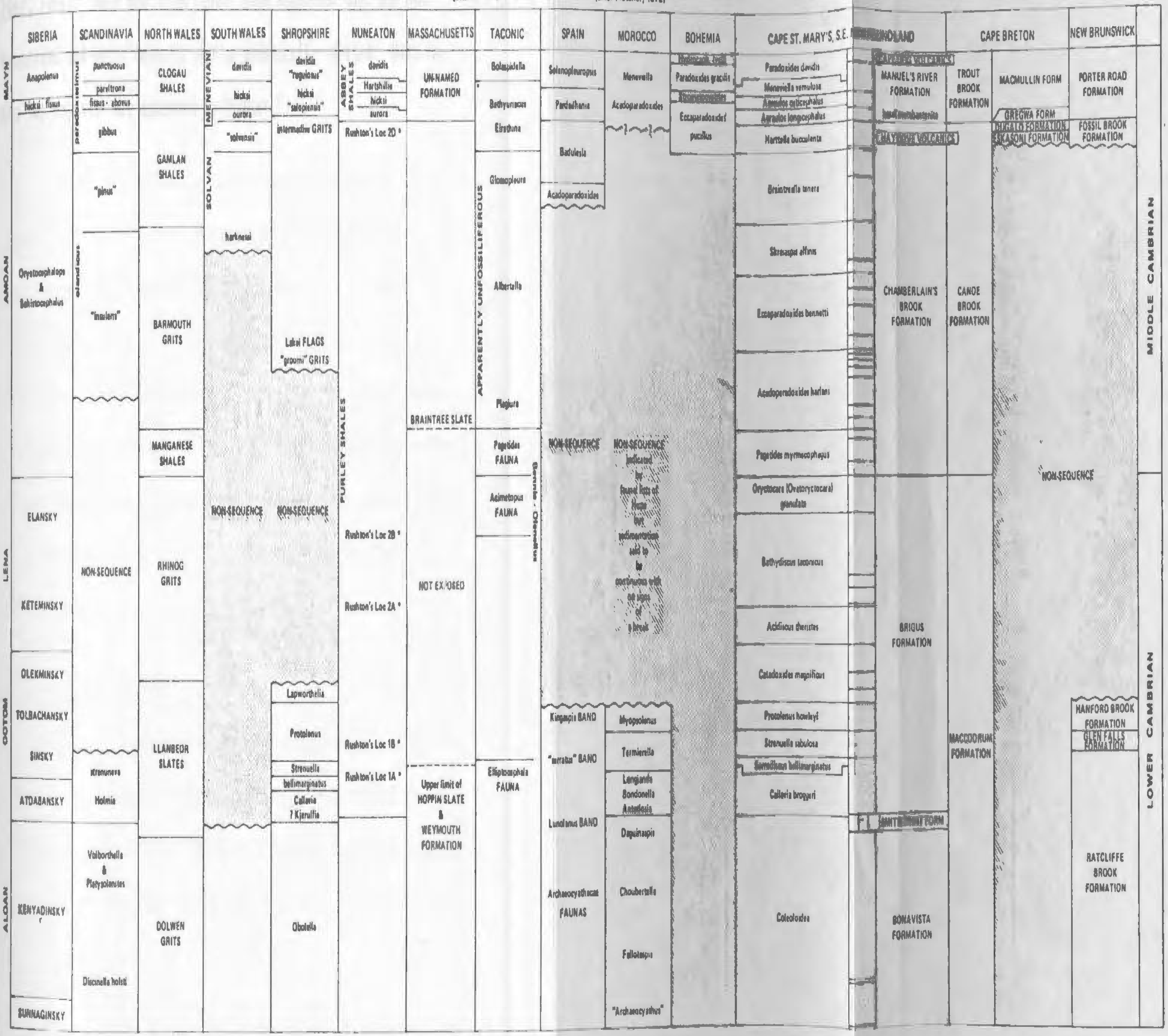

to this study because of the presence there of a sedimentary manganese horizon of basal Middle Cambrian age (Woodland, 1939; Mohr, 1964, 1966). Mohr and Allen (1965) have suggested that the Newfoundland and Welsh deposits may be genetically related. Data on the two deposits are compared in Chapter 7.

CHAPTER 3

GEOLOGY OF SAMPLED CAMBRIAN STRATIGRAPHIC SECTIONS

3.1 Introduction

In the previous chapter, the geological setting of the Avalon Zone and the general character of the Lower Paleozoic sequence present in southeastern Newfoundland were discussed. In this chapter, additional information is given on the geology of individual stratigraphic exposures sampled for the present study. The lithological character of the Lower Middle Cambrian manganese-rich rocks included in these exposures is described, and the nature of regional changes in the horizon containing the manganese-rich rocks examined.

3.2 Location of Rock Samples

Cambrian stratigraphic exposures located on the Avalon and Burin Peninsulas in southeastern Newfoundland were sampled in the summers of 1971 and 1972. The areas from which these rock samples were collected are identified on Figure 1.1.

Method of Sampling

Rock samples were collected from the Bonavista, Smith Point Limestone, Brigus, and Chamberlain's Brook Formations, which collectively form the Lower and Lower Middle Cambrian Adeyton Group (Jenness, 1963). In general, the calcareous conglomerate developed at the base of the Cambrian succession marks the lower stratigraphic limit of sampling, and the upper contact of the Chamberlain's Brook Formation with dark shales of the Harcourt Group the upper sampling limit. A few samples were collected for comparative purposes from the Precambrian rocks underlying the Cambrian succession and from the black and dark grey shales of the Manuel's River Formation and Elliot Cove Formation.

Sampling was concentrated in 'key' sections exposed in the Trinity-Conception Bay area. This area was selected for detailed examination because the manganese horizon ~~at the~~ base of the Chamberlain's Brook Formation is best developed there (in terms of manganese concentration). Other sections in the Trinity-Conception Bay region and sections exposed in the St. Mary's Bay area on the southern part of the Avalon Peninsula were sampled in reconnaissance fashion only, primarily to obtain comparative material from the manganese horizon and the mudrocks immediately above and below it. The section exposed at Little Dantzic Cove on the Burin Peninsula was examined briefly to obtain comparative manganese horizon samples. Other sections present in the Burin Peninsula-Fortune Bay area were not examined due to the limited amount of time available. The section located at Keel's, Bonavista Bay (Figure 1.1) was not examined in any detail as no manganese horizon was found there.

Within the 'key' Trinity-Conception Bay sections referred to above, samples were located in the stratigraphic succession according to stratigraphic sections measured by Hutchinson (1962) and Fletcher (1972), except for the stratigraphic sections exposed at Brigus, Conception Bay and Smith Point on Smith Sound, Trinity Bay, where portions of the Lower and Lower Middle Cambrian succession were remeasured. In these 'key' sections, material was collected from all major lithological subdivisions of exposed Adeyton Group formations. Particular attention was paid to the manganese horizon in these sections, where grab samples were collected on a bed-to-bed basis.

The stratigraphic position of rock samples from the 'key' sections which are used in Chapter 5 to identify chemical trends in the Cambrian sequence in general and the manganese horizon in particular is shown in Figures 5.5.1 - 5.5.5 (Adeyton Group samples) and Figures 5.5.1'a' - 5.5.5'a' (manganese horizon samples) in that chapter.

3.3 Geology of Sampled Cambrian Stratigraphic Sections

General Remarks

All of the 'key' sections discussed below were deformed to a greater or lesser extent by the Devonian (Acadian) orogeny which influenced all tectonic-stratigraphic provinces in Newfoundland. In the Avalon Zone, the deformation has produced simple open folds and both transverse and thrust faults with a single slaty cleavage in the mudrocks. The sections exposed in southeastern Conception Bay (e.g., Manuel's River section) and along the northern shore of Smith Sound on Trinity Bay have not been deformed and are exceptions to the above generalizations. In the discussions of individual stratigraphic sections which follow, the Bonavista and Brigus Formations are discussed collectively becuase of their lithological similarity.

Manuel's River, Conception Bay (No. 2 on Figure 1.1)

The Manuel's River section is located on the southeastern margin of Conception Bay on the Avalon Peninsula, near the northeastern limit of Cambrian rock exposure. The local geology and a stratigraphic column for the Cambrian succession are shown on Figure 3.1.

The Cambrian rocks unconformably overlie volcanic rocks of the Harbour Main Group and granites of the Holyrood Plutonic Series. The basal Cambrian conglomerate is more than 5 meters thick; much thicker than in other Cambrian exposures on the Avalon Peninsula. The well-rounded volcanic and granitic clasts in the conglomerate suggest local derivation. It has been interpreted as a beach deposit of local extent (King et al., 1974). The Lower Cambrian sequence is approximately 20 meters thick at Manuel's River, much thinner than in other exposures of Lower Cambrian rocks towards the west. The two oldest formations of the Adeyton Group, the Bonavista and Smith Point Limestone Formations, are unrepresented at Manuel's River, and paleontological data indicate that Cambrian sedimentation in this region began later than in sections located further west towards the axis of the Cambrian basin. The Lower Cambrian sequence is dominated by green mudrocks in which several thin limestone interbeds occur.

The Chamberlain's Brook Formation at Manuel's River, the type section for this unit (Hutchinson, 1962), is 75 meters thick, and consists principally of green mudrocks, with occasional thin limestone interbeds. The manganese horizon located at the base of this formation is here about 5.5 meters thick.

Dark grey to black mudrocks of the Harcourt Group overlie the Chamberlain's Brook Formation and have an exposed thickness of

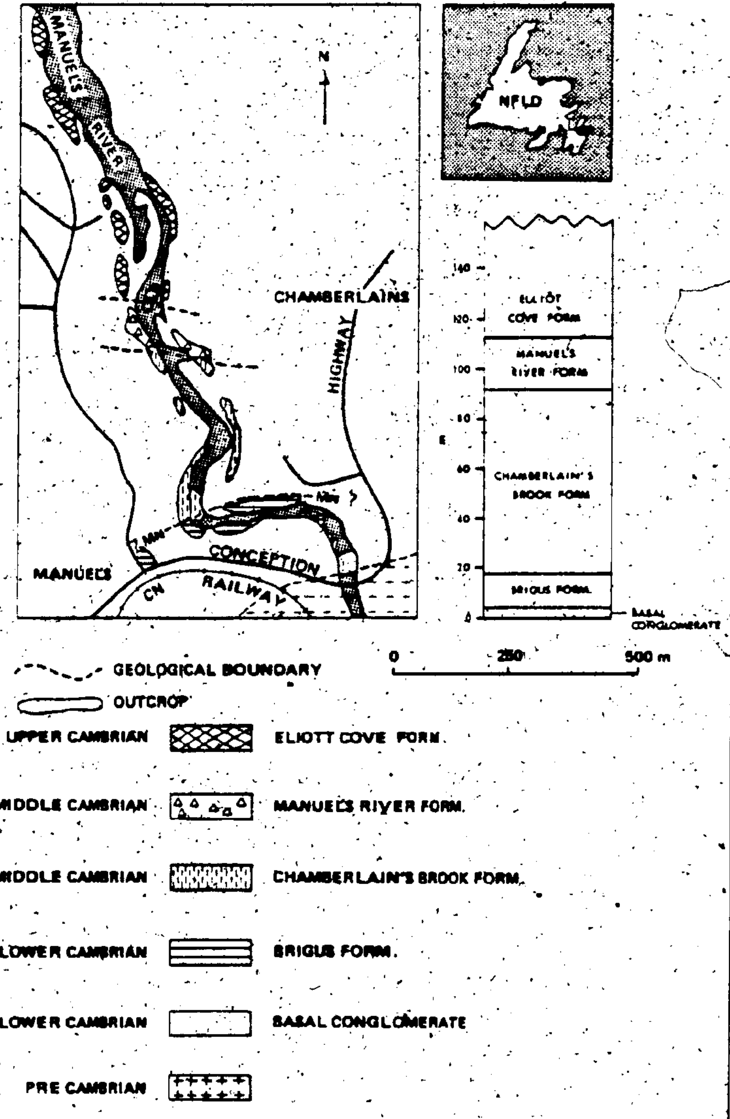

FIG. 3.1 GEOLOGY IN VICINITY OF MANUELS RIVER SECTION (AFTER KING et al, 1974)

200 meters. Minor amounts of grey limestone, commonly nodular, are present in the Harcourt Group, and locally the rocks are pyritiferous. Thin interbeds of micaceous, fine-grained sandstone, commonly cross-bedded, are present in the upper exposed portion of the Harcourt Group. The Manuel's River section is the type section for the lowest stratigraphic division of the Harcourt Group, the Manuel's River Formation, here some 20 meters thick (Hutchinson, 1962).

Ordovician sandstones and shales of the Bell Island and Wabana Groups are believed to conformably overlie the Harcourt Group rocks, though the contact is not exposed (Rose, 1952).

Brigus, Conception Bay (No. 7 of Figure 1.1)

The Cambrian stratigraphic section exposed near the town of Brigus is located on the southwestern shore of Conception Bay. Details of the local geology are shown in Figure 3.2.

The exposed thickness of Cambrian rocks in the Brigus section (in part estimated) is 150 meters. The Cambrian succession unconformably overlies red sandstones and siltstones of the Harbour Main Group. The latter were tilted before the initiation of Cambrian sedimentation so that the basal Cambrian beds form a right angle with bedding in the Precambrian rocks. The Harbour Main sedimentary rocks are in fault contact with Harbour Main volcanic rocks 60 meters south of the basal Cambrian conglomerate exposed on the eastern shore of Brigus Bay. Further south, the Harbour Main Group is in fault contact with silicious green siltstones of the Conception Group.

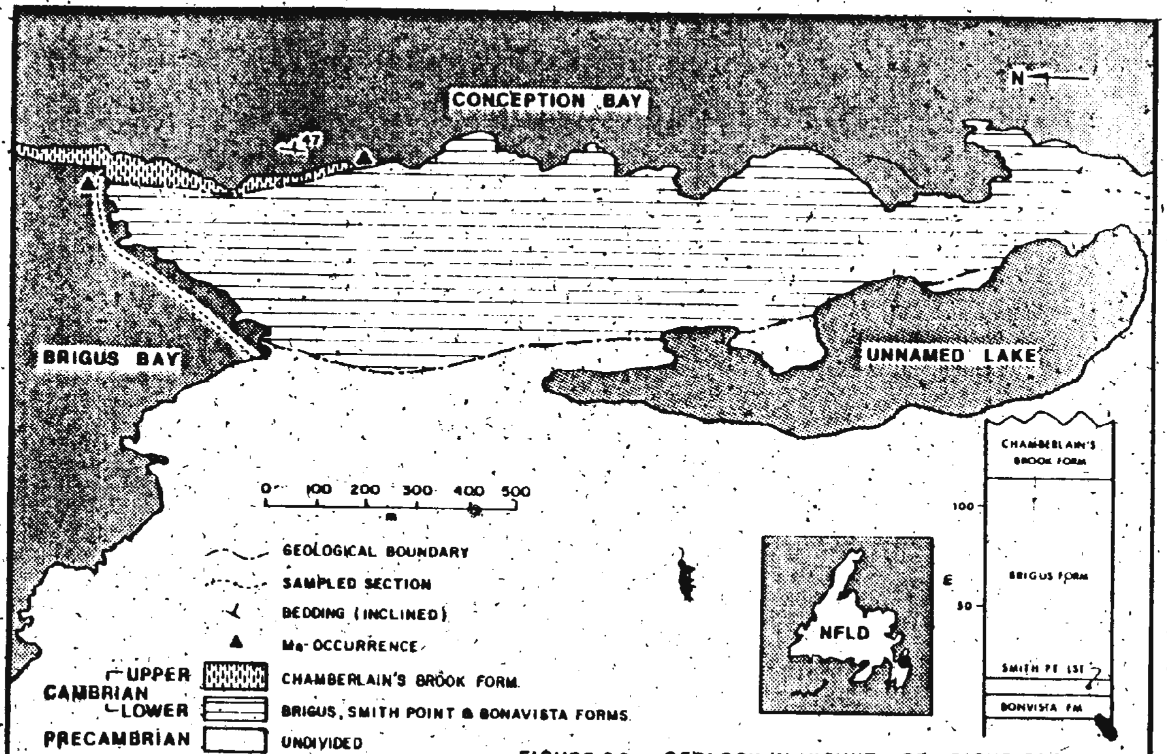

FIGURE 3.2 GEOLOGY IN VICINITY OF BRIGUS SECTION

The basal Cambrian congolmerate varies in thickness up to a maximum of about 1 meter. In addition, the conglomerate fills fractures in the underlying Precambrian rocks to a depth of 1 meter or more. The conglomerate consists of quartz pebbles set in a limy matrix. Most of the quartz clasts are less than 1 cm in diameter. Red mudrock clasts also occur in the conglomerate.

The Bonavista and Brigus Formations consist of red and green mudrock and slate, with thin, commonly nodular, limestone interbeds present at intervals in the sequence. Two exceptionally thick limestone beds, each between 3 - 4 meters thick, occur towards the base of the Brigus Formation. The Brigus section is the type locality for the Brigus Formation (Hutchinson, 1962), though recent paleontological and stratigraphic investigations suggest the formation is more fully developed in the St. Mary's Bay region on the southern part of the Avalon Peninsula (Fletcher, 1972).

The Smith Point Limestone Formation, 10 meters thick in the Brigus section, consists of pink to red limestone which at intervals contains thin red argillaceous interbeds. Locally, algal colonies are numerous in the limestone.

The Chamberlain's Brook Formation at Brigus is approximately 30 meters thick, though it is not completely exposed, as the upper portion has been removed by erosion. It consists of green mudrocks in which occasional thin limestone beds are intercalated. Some of the mudrocks in the Chamberlain's Brook Formation are laminated, consisting of alternating bands and lenses of black-colored, chlorite-rich material and normal green mudrock. The manganese horizon at the base of this formation is about 5 meters thick at Brigus.

The red and green mudrocks comprising the Lower Cambrian Bonavista and Brigus Formations are more irregularly distributed with respect to bedding in the Brigus section than in other Lower Cambrian exposures in the Trinity Bay and St. Mary's Bay regions of the Avalon Peninsula. Though the color changes at Brigus, as elsewhere, commonly conform with bedding, in places large, irregularly shaped masses of green mudrock occur enclosed in red mudrock. Comparison of portions of the stratigraphic succession exposed at more than one locality along the coastline demonstrates that the color of the mudrocks in the sequence changes along strike. Thus, for example, numerous green mudrock beds are included in the succession exposed along the Conception Bay coastline, while the section exposed along the eastern shore of Brigus Bay consists almost entirely of red mudrocks. Again, in places the uppermost 2 meters of the Brigus Formation, immediately below the manganese horizon, are green, while elsewhere the equivalent strata are red. The presence of green mudrock along fractures in red mudrock and the local development in red mudrock of green reduction spheres indicate that part of the green mudrocks have been formed by secondary alteration of red mudrocks in the succession.

The mudrocks in the Brigus section contain a single, well-developed cleavage.

Hopeall Head, Trinity Bay (No. 9 on Figure 1.1)

This section is exposed along the southwestern flank of Hopeall Head on the eastern shore of Trinity Bay. Details of the geology and stratigraphy for this section are given in Figure 3.3.

The Cambrian sequence at Hopeall Head rests disconformably upon massive white quartzite of the Random Formation. The conglomerate at the base of the Cambrian succession is up to 1 meter thick and consists of quartz pebbles to 1 cm in diameter set in an arenaceous and/or limy matrix.

The Bonavista and Brigus Formations, 30 and 140 meters thick respectively, consist of green and red mudrocks, which occur in discrete, massive beds. At intervals, the mudrocks contain many limestone nodules, commonly concentrated along bedding planes; occasionally, thicker limestone beds up to 0.5 meters thick are present. Locally, the green mudrocks are laminated, containing thin lenses (some less than 0.5 cm thick) of dark rock alternating with typical apple-green mudrock. Rarely, pyrite cubes and concretions are present in the green mudstone beds.

The Smith Point Limestone Formation is 12 meters thick in the Hopeall Head section, and, as in other sections, consists of massive pink to red, locally algal limestone.

The Chamberlain's Brook Formation at Hopeall Head is approximately 125 meters thick, and consists primarily of green to grey mudrock, with the latter increasingly common towards the top of the formation. Several limestone beds up to 1 meter thick are intercalated with the mudrocks. A volcanic breccia bed, approximately 5 meters thick, occurs in the Chamberlain's Brook Formation about 15 meters below its top. The breccia consists of angular volcanic fragments set in a white, calcareous matrix. The manganese horizon at the base of the Chamberlain's Brook Formation

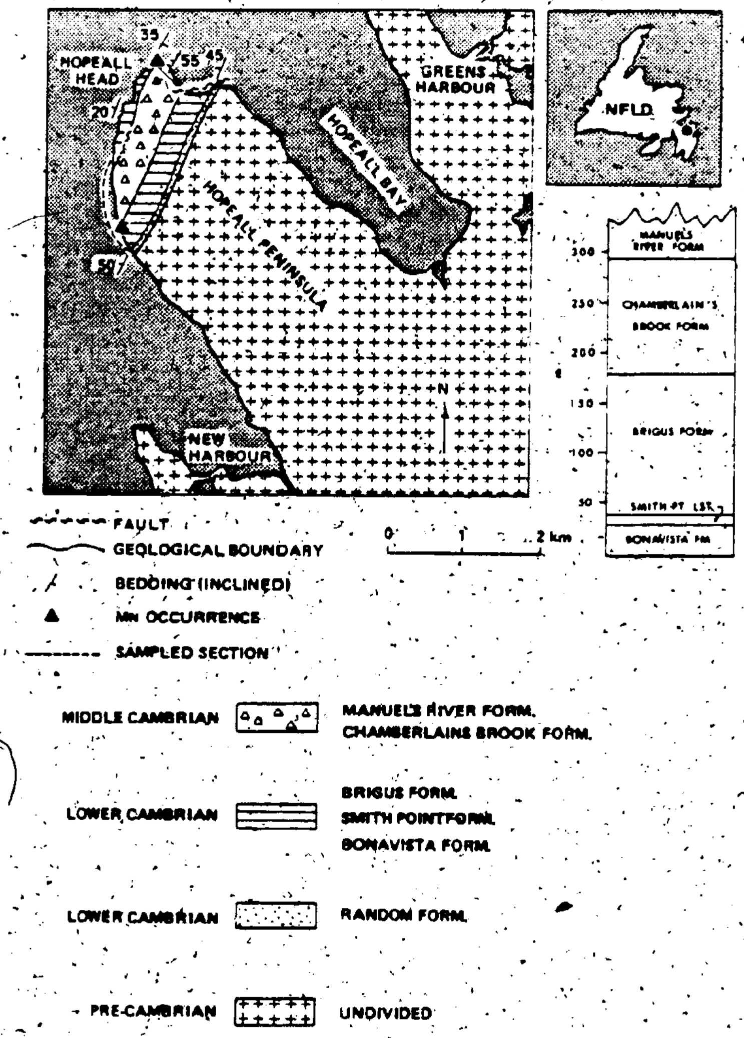

FIG. 3.3 GEOLOGY IN VICINITY OF HOPEALL HEAD SECTION (AFTER McCARTNEY, 1956)

at Hopeall Head is between 1 - 2 meters thick.

Chapel Head, Trinity Bay (No. 11 on Figure 1.1)

The Chapel Head section is a composite one, with the two lowest Lower Cambrian rock units (Bonavista and Smith Point Limestone Formations) sampled where exposed along the shore of Long Cove on Trinity Bay, and the remainder of the section sampled along the western shore of Chapel Head, located several hundred meters east of Long Cove. Geological and stratigraphic aspects of this composite section are shown in Figure 3.4.

The Cambrian rocks in this section disconformably overlie red and green quartzites of the Random Formation. The basal Cambrian conglomerate atop these quartzites is less than 0.5 meters thick, and consists of quartz pebbles set in a limy matrix.

The Brigus and Bonavista Formations in the Chapel Head section are dominated by massive bedded red and green mudrocks, which in places contain thin nodular limestone interbeds up to 0.5 meters thick. The Bonavista and Brigus Formations attain thicknesses of 22 and 225 meters respectively. In places, the green mudrocks contain thin black laminae as in other sections, and occasionally they contain pyrite concretions.

The Smith Point Limestone Formation is 6.5 meters thick in the Chapel Head section, and consists of red limestone, which contains thin red argillaceous interbeds and locally abundant algal colonies.

The Chamberlain's Brook Formation is approximately 50 meters thick, but is incomplete with the upper portion removed by erosion.

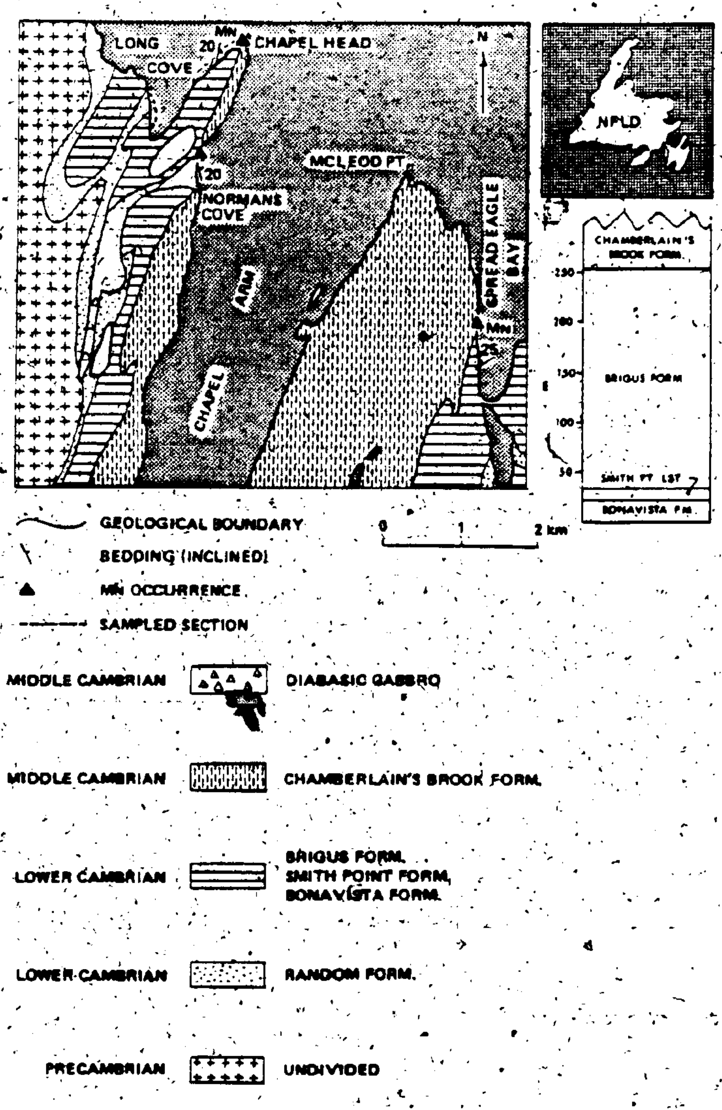

FIG. 3.4 GEOLOGY IN VICINITY OF CHAPEL HEAD SECTION, TRINITY BAY (AFTER McCARTNEY, 1967)

It is composed of red and green mudrocks. The manganese horizon at the base of the formation is about 2 meters thick.

Smith Point, Trinity Bay (No. 13 on Figure 1.1)

The Smith Point section is located on the north shore of Smith Sound on the western side of Trinity Bay, immediately northwest of the Avalon Peninsula proper. The section lies near the northwestern limit of Cambrian exposures in the Avalon Zone. Figure 3.5 shows details of the local geology and stratigraphy.

The disconformable contact of the Cambrian rocks with quartzites of the Random Formation is exposed to the east of Smith Point proper on the north shore of Smith Sound. The limy quartz pebble conglomerate overlying the Random quartzites is less than a meter thick and resembles the basal Cambrian conglomerate present in other 'key' sections.

The exposed thickness of the Bonavista Formation is approximately 135 meters, though the basal part of the unit is hidden. Hutchinson (1962) has estimated that an additional 60 meters of Bonavists Formation are unexposed. He proposed that the Smith Point section be the type section for the Bonavista Formation, which (assuming the hidden 60 meters to be present) is thicker here than anywhere else on the Avalon or Burin Peninsulas. The Brigus Formation at Smith Point is approximately 100 meters thick. The Bonavista and Brigus Formations consist of massive bedded red and green mudrock, in which thin limestone interbeds (commonly nodular) occur.

The Smith Point section is the type locality for the Smith

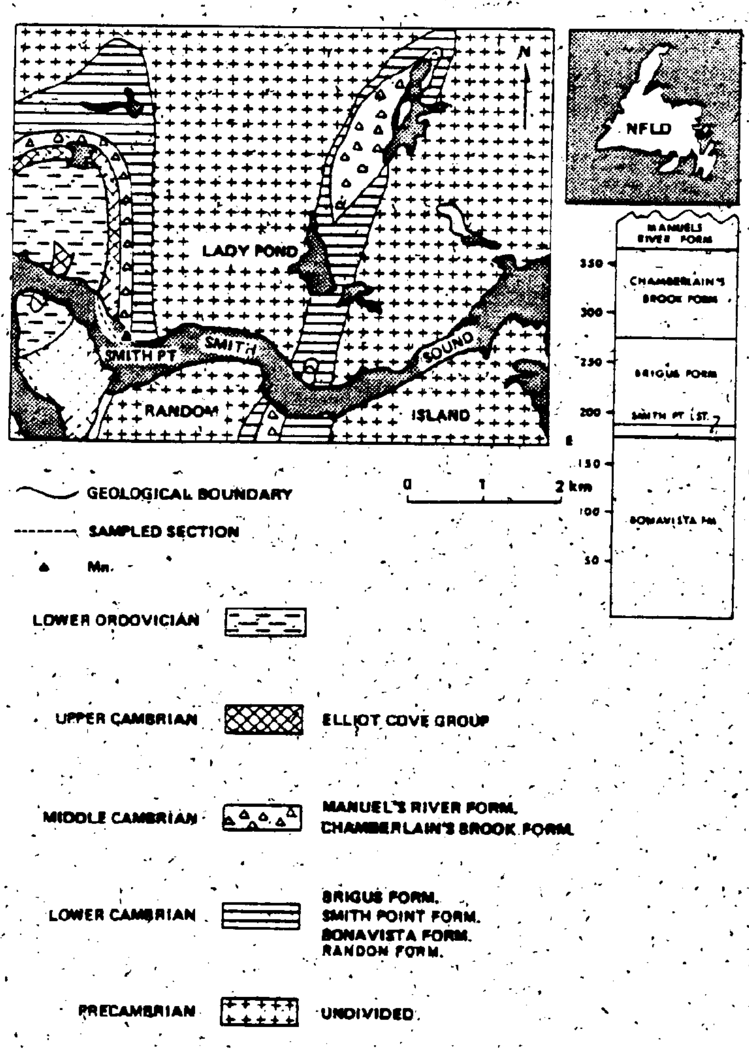

FIG. 3.5 GEOLOGY IN VICINITY OF SMITH POINT SECTION, SMITH SOUND, TRINITY BAY

Point Limestone Formation (Walcott, 1900), which is 7 meters thick and lithologically similar to previously described exposures of the formation.

The Chamberlain's Brook Formation has an estimated minimum thickness of 100 meters (Hutchinson, 1962), though Jenness (1963) concludes on the basis of lithological correlation with nearby exposures that some of the uppermost part of the unit included in the 100 meters may belong to the overlying Harcourt Group. The formation consists of massive bedded red and green mudrock, with red mudrock restricted to the lower part of the formation. Nodular limestone beds are intercalated with the red and green mudrocks.

The manganese horizon at the base of the Chamberlain's Brook Formation is one meter thick.

Dark grey to black shales of the Harcourt Group, of undetermined thickness, overlie the mudrocks comprising the Chamberlain's Brook Formation.

3.4 The Manganese Horizon

General Remarks

The manganese horizon comprises manganese-rich sedimentary rocks present in the basal part of the Lower Middle Cambrian Chamberlain's Brook Formation. The horizon occurs in all stratigraphic sections on the Avalon Peninsula in which the basal part of the Chamberlain's Brook Formation is exposed, and also occurs in equivalent strata in Cambrian exposures on the Burin Peninsula. It consists of a mixture of manganese-bearing and calcium-bearing carbonate minerals (hereafter referred to as the carbonate fraction of the manganese horizon) and a suite of silicate minerals. The mineralogical composition of the manganese horizon is further considered in Chapter 4. Thickness variations and lithological changes occur in the manganese horizon from one section to the next, and are discussed in the remainder of this section.

The manganese-rich rocks were deposited during a break in normal conditions of sedimentation within the Cambrian basin with paleontological and stratigraphic thickness relationships over the Avalon Peninsula area indicating that the manganese horizon was formed during a period characterized by very slow rates of clastic sedimentation. The horizon may represent a disconformity (e.g., Hutchinson, 1962) or a non-sequence (e.g., Fletcher, 1972). As there is no physical evidence of erosion or disruption present at the base of the manganese horizon, the latter term (= paraconformity) is considered more applicable.

3.4.1 Contact Relationships

The lower stratigraphic limit of the manganese horizon coincides with the contact between the Chamberlain's Brook and Brigus Formations. In the 'key' Trinity-Conception Bay exposures on the Avalon Peninsula, this contact is abrupt, and the lower boundary of the manganese horizon can be accurately positioned. The lowest bed in the manganese horizon in these exposures consists of Mn-bearing, dark bluish-black weathered carbonate. Though the contact of this lowest manganese-rich carbonate bed with underlying Brigus mudrocks is sharp, in no case was any physical evidence of disruption, such as the occurrence of conglomerate, observed.

The upper boundary of the manganese horizon with overlying manganese-poor green mudrock of the Chamberlain's Brook Formation is gradational, with the proportion of Mn-bearing carbonate becoming progressively less until the sequence consists entirely of mudrock. For sampling purposes, the upper contact of the manganese horizon was arbitrarily defined as the uppermost recognizable Mn-bearing carbonate bed or layer.

The thicknesses obtained for the manganese horizon in Trinity-Conception Bay sections using the above criteria correspond well with other estimates for the same exposures (*e.g.*, by Hutchinson, 1962; Dale, 1915).

In Southern Avalon Peninsula stratigraphic exposures, the manganese horizon thicknesses determined by Fletcher (1972) have been used in the discussion of regional variations in its character.

3.4.2 Age of Manganese Horizon

Paleontological studies of the trilobite fauna present in the Cambrian stratigraphic succession indicate that the manganese horizon is everywhere of basal Middle Cambrian age, and that the lower boundary of the horizon defines the Lower-Middle Cambrian boundary (Fletcher, 1972; Hutchinson, 1962). The horizon thus occupies a definite and restricted stratigraphic position throughout the Avalon and Burin Peninsula area.

3.4.3 Regional Variations in Manganese Horizon

Lithological and paleontological investigations have identified a number of regional changes in the character of the manganese horizon. All changes in the Avalon Peninsula region occur in a north-south direction, with no apparent changes of any magnitude taking place in an east-west direction. Regional trends in the development of the manganese horizon are individually discussed below, and are schematically summarized in Figures 3.6 and 3.7 (N-S and E-W cross sections of the horizon in the Avalon Peninsula region, respectively).

3.4.3.1 Thickness

The manganese horizon becomes progressively thicker in a north to south direction. The thinnest exposures occur along the northern shore of Smith Sound on Trinity Bay, where the manganese horizon is only 1 meter thick. Southwards, it becomes progressively thicker, measuring 25 meters in thickness in the southernmost Avalon Peninsula exposures in the St. Mary's Bay area.

3.4.3.2 Lithological Character

A lithofacies change from carbonates in the north to a mudrock facies in the southernmost sections occurs in a north to south direction. In the northernmost Trinity Bay exposures (e.g., Smith Point section, No. 13 on Figure 1.1), the manganese horizon consists of a single massive, albeit impure, Mn-Ca carbonate bed. In the southernmost Avalon Peninsula exposures in the St. Mary's Bay area, the manganese horizon consists primarily of red and green mudrock. Manganese carbonate in these exposures is restricted to a few scattered nodular beds in the mudrocks, and the horizon is not the lithologically distinct entity it is in the north. In

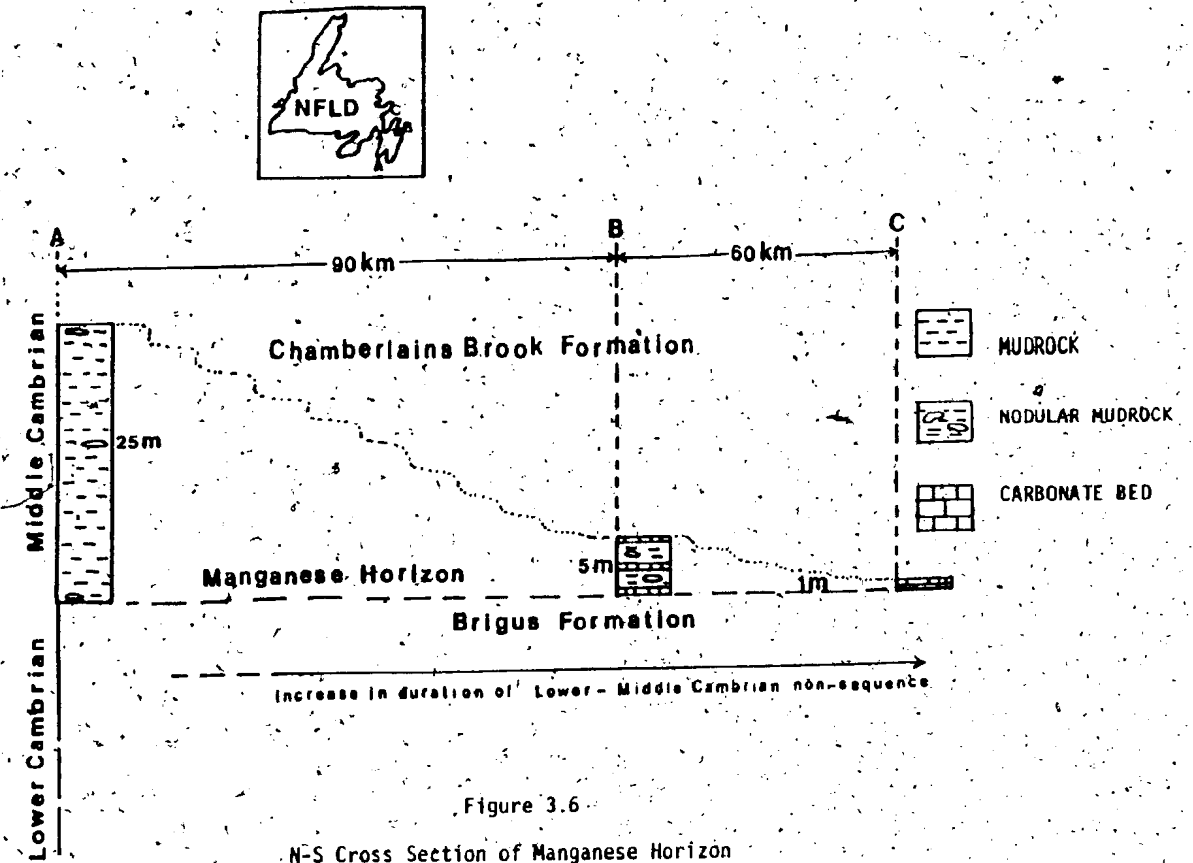

Figure 3.6

N-S Cross Section of Manganese Horizon

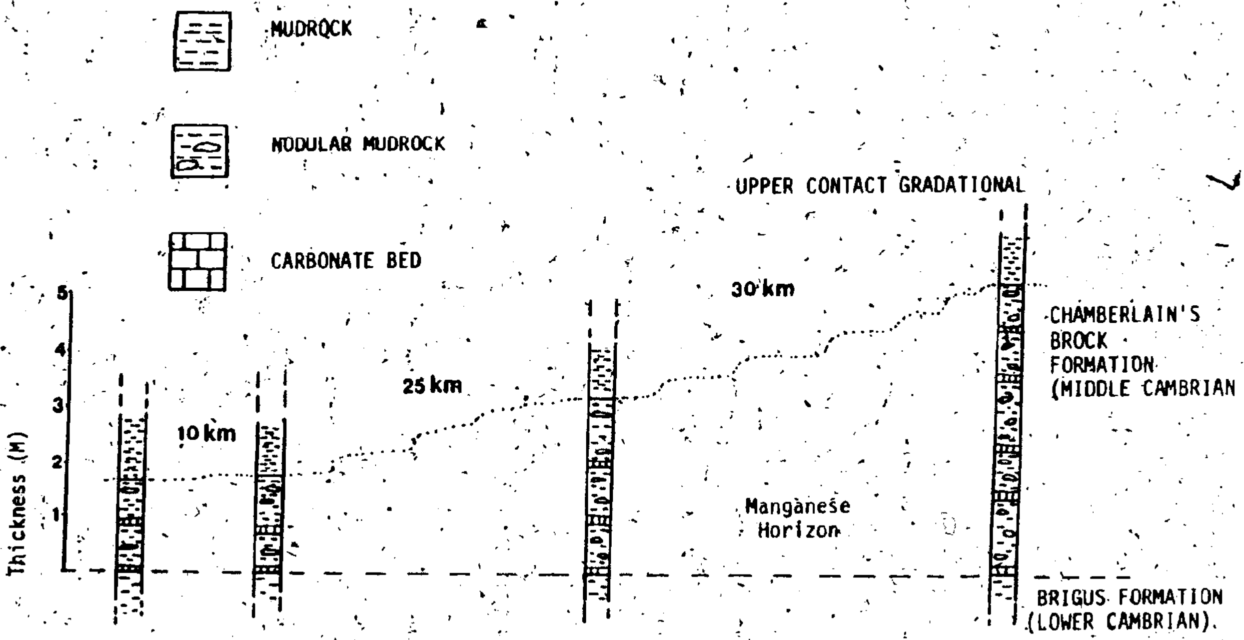

Figure 3.7

E-W Cross Section of Manganese Horizon

stratigraphic sections located in intermediate positions around the heads of Trinity and Conception Bays, the manganese horizon consists of interbedded carbonate and argillaceous beds. The carbonate beds vary in thickness (up to 0.3 meters) and in length with some thin lenses only centimeters in length and others exceeding the limits of outcrop exposure. Carbonate concretions, locally concentrated along bedding planes, are common in these sections.

The variation in lithological character of the manganese horizon from north to south on the Avalon Peninsula suggests that the carbonate facies in the north grades laterally by interfingering with the thicker mudrock facies in the south.

3.4.3.3 Chemical Variation

The horizon is progressively enriched in Mn (relative to Fe) in a northerly direction (Sec. 5.3.2), in part because the proportion of carbonate minerals with which the Mn is associated (Chapter 4) increases as the horizon becomes thinner in this direction.

3.4.3.4 Fossils in Manganese Horizon

The manganese horizon is fossiliferous in all stratigraphic exposures, containing a fauna including trilobites, Hyolithes, sponge spicules, and several kinds of algal textures (Fletcher, 1972; M. M. Anderson, pers. comm., 1975).

CHAPTER 4

PETROLOGY

4.1 Introduction

The following petrological work was carried out on samples of the Cambrian sedimentary rocks comprising the Adeyton Group:

(1) a total of 137 thin sections, more than half from the manganese horizon, were examined under the microscope with the aims of identifying the mineral species and fossil forms present and the amount of diagenetic alteration in the manganese horizon and other rock groups;

(2) 180 samples were examined with X-ray diffraction. The principle mineral species present in major rock groups were identified and the diffractogram mineral peak areas used to calculate relative mineral proportions for the samples; and

(3) chemical analytical data obtained from the Cambrian sedimentary rocks was used to obtain normative estimates of the mineralogical composition for them.

Details on sample preparation methods and the analytical techniques employed are given in Appendix I.

4.2 Results of Petrographic Examination

Thin sections prepared from rocks representing all lithologies and from all formations in the Adeyton Group were examined with a polarizing microscope, with the majority from samples of the various sampled stratigraphic exposures of the manganese horizon. As seen in the thin sections the sedimentary rocks are uniformly fine-grained, and contain the same identifiable mineral species throughout. The rocks can be separated into two groups: argillaceous rocks (typified by the red and green mudrocks) and carbonate-rich rocks (e.g., limestones, samples from the manganese horizon). The two groups are gradational.

The Cambrian rocks are in general very fine-grained, except for the basal Cambrian conglomerate, where clasts ranging in size up to 0.5 meters occur. Several of the minerals in the mudrocks - feldspar and illite - are nowhere coarse enough to identify optically. Carbonate minerals where present commonly occur as mircocrystalline crystal aggregates. Coarser, individually recognizable carbonate grains occur but are generally the result of recrystallization and secondary growth.

The results obtained from thin section and hand specimen examination of rock samples from the Adeyton Group are summarized in Table 4.1. The data in this table are briefly discussed below.

4.2.1 Red and Green Mudrocks

These rock types are similar in general composition and texture, the major visually apparent difference being the presence of hematite in the red mudrocks. This mineral occurs as a red-colored, microcrystalline component which is distributed throughout the microcrystalline ('clay size') fraction of the rocks and commonly coats and stains larger crystals. Hematite was not identified in any green-colored mudrock. Both mudrock types contain larger individually recognizable particles of quartz and chlorite, evenly

TABLE 4.1 SUMMARY OF PETROLOGIC OBSERVATIONS ON LITHOLOGICAL GROUPS OF CAMBRIAN SEDIMENTARY ROCKS

SAMPLE GROUP	MACROSCOPIC FEATURES	THIN SECTION FEATURES	
		TEXTURES	STRUCTURES
RED AND GREEN MUDSTONES	Characteristically massive in habit; both red and green mudstones in places contain carbonate nodules. these are commonly concentrated along bedding planes and so mark bedding; cleavage variably developped in mudstones and where present intersects bedding at high angle; some green mudstones contain thin, black lenses and laminae parallel to bedding; pyrite concretions up to several cm + present in some green mudstones; in general, colour contacts are sharp and parallel to bedding, but locally it is apparent that some green mudstone is secondary after red.	Cleavage: variably developped and defined by mineral orientation. differentially developped in samples with resistant carbonate interbeds; grain sizes in general is uniform throughout samples (very fine-grained), but in a few cases thin (1 mm) layers and/or lenses of coarser material are present; quartz and chlorite crystals are characteristically present (to a degree) in larger grains than the remaining mineral species. the larger crystals are evenly distributed throughout the rock.	Bedding: defined by carbonate-rich beds, coarser laminae or chlorite-rich layers (in a minority of samples). fossils: rare in mudstone. where present occur as dispersed shell fragments (carbonate) in argillaceous matrix. abundant in samples with carbonate interbeds.
LIME-STONES	Present in ellipsoidal nodules up to c. 5 cm long and flattened in the bedding plane; also in discrete beds, varying in thickness from less than 1 cm to more than 1 m; colour varies from pink to red to grey;	Cleavage: not well-developped, but can be seen in some samples as shearing at irregular intervals; in some samples, algal texture predominant.	Fossils: fragments common. forms present include trilobites, hyolithes, sponge spicules and several types of algal forms including stromatolites, GIRVANELLA and EPIPHYTON.
MANGANESE HORIZON SAMPLES	Commonly superficially coated with Mn oxides; bedding visible and outlined by carbonate layers, lenses and concentrations of nodules; argillaceous material between carbonate-rich intervals; nodular structures common (especially in Conception Bay exposures); colour varies from pink to grey with argillaceous material green and/or red; fossiliferous.	Cleavage: variably developped. most apparent in argillaceous samples; minerals in shaly material of uniform very fine-grained size; as in red and green mudstone, some quartz and chlorite crystals larger than microcrystalline matrix; patchy textures produced by diagenetic alterations of primary sediments; very rare pelletal textures; large (up to several mm +) authigenic crystals of pyrite, carbonate and barite present in some samples.	Bedding: thin carbonate interbeds occur in some samples. chlorite-rich laminae in some argillaceous samples. colour banding parallel to bedding in some samples. lenticular nodules elongated in bedding direction; nodular structures: carbonate concretions, chloritic nodules and phosphatic nodules all occur. maximum diameter of nodules several cm +. they are generally enclosed in argillaceous matrix and are commonly elongated in the bedding plane; Fossils: present in some samples. shell fragments and algal structures can be recognized in some samples.

TABLE 4.1 SUMMARY OF PETROLOGIC OBSERVATIONS ON LITHOLOGICAL GROUPS OF CAMBRIAN SEDIMENTARY ROCKS

SAMPLE GROUP	MINERALOGY			
	CHLORITE	QUARTZ	CARBONATE	HEMATITE
RED AND GREEN MUDSTONES	Distributed throughout sediment; grain size variable; largest crystals can be seen individually enclosed within argillaceous matrix consisting of a mixture of microcrystalline minerals; larger crystals typically oval in shape and of (relatively) high relief; colourless to green; slightly pleochroic; some crystals in graditional contact with matrix; some crystals shaped like mica flakes; locally, crystals concentrated in bands.	crystals evenly spread out through samples; variable grain size, largest about equal in size to largest chlorite crystals; colourless; generally fresh in appearance, but local coating corrosion by carbonate; individual crystals set in microcrystalline matrix; larger crystals (silt) in rare, coarser bands.	Not common in red and green mudstones; generally present in sparse fossil material, but in a few 'limy' mudstone samples, carbonate crystals occur spread throughout the sediment.	Present in red mudstone, only, as extremely fine-grained 'dust' associated with the microcrystalline argillaceous matrix; does not generally coat the larger quartz and chlorite crystals; responsible for colour difference between red and green mudstone.
LIMESTONES	As in mudstones, less common and restricted to argillaceous fraction of samples.	As in mudstones; again restricted to argillaceous fraction of samples.	Dominant mineral component; carbonate dispersed throughout samples; grain size varies widely: commonly present in very fine-grained micritic patches, but larger crystals also occur (these are commonly twinned); colourless to brown; some carbonate as fossil fragments; crystals in argillaceous matrix.	Present in argillaceous matrix as in mudstones; also coats carbonate crystals in some samples.
MANGANESE HORIZON SAMPLES	Individual chlorite crystals occur dispersed throughout finer matrix as in mudstones; in green samples, large (up to 1 cm + in diameter), bulbous 'nodules' composed mainly of chlorite are present: these are not, however, monomineralic, and other minerals can most often be seen within them. the nodules are commonly in graditional contact with surrounding matrix; rarely larger crystals form incomplete spherulites, with crystals radiating out from one or several centres.	Crystals generally dispersed evenly throughout argillaceous fraction of samples; grain size varies with largest crystals set in finer matrix; some crystals coated by carbonate.	Commonly present in microcrystalline ('micritic') aggregates, though crystal size varies and much larger (sometimes twinned) crystals occur in some samples; euhedral carbonate crystals abundant in some samples and are disseminated through sediment or concentrated in carbonate concretions; some carbonate also present in fossil fragments; colour varies from transparent to brown to red; carbonate concretions commonly elliptical, with long axis parallel to bedding plane; Some spherical 'nodules' occur; nodules may or may not possess a recognizable core.	Present in some samples and absent in others; in some samples, hematite bearing material seems to be replaced by (and is surrounded by) green material with ho hematite; where present occurs in microcrystalline form in argillaceous portion of sample; also coats carbonate in some samples.

TABLE 4.1 SUMMARY OF PETROLOGIC OBSERVATIONS ON LITHOLOGICAL GROUPS OF CAMBRIAN SEDIMENTARY ROCKS

SAMPLE GROUP	OTHER	DIAGENETIC FEATURES
RED AND GREEN MUDSTONES	Opaque mineral(s) typically evely dispersed throughout red and green mudstones; individual grains very small (< 1 mm) and for this reason not identifiable optically; in some green mudstones, authigenic pyrite crystals can be recognized by crystal form; likewise, occasional grains shaped like octagedra suggest the presence of magnetite.	(1) Chlorite crystals range gradationally from large to submicroscopic in the argillaceous matrix; chlorite also rims and replaces the carbonate of some of the scattered fossil fragments in some mudstone samples; in several samples from a volcanic unit within the sequence, chlorite has replaced ferromagnesian crystals, preserving the original euhedral outlines; these features suggest a diagenetic origin for much of the chlorite. (2) Carbonate coating, corroding individual quartz grains, indicates replacement of latter. (3) Alignment of some of the microcrystalline grains in the sediments parallel to the cleavage plane suggests that (at least in part) the minerals have formed during or subsequent to the deformation of the rocks. (4) Spherulitic carbonate crystal aggregates occur in the above-mentioned volcanic rock samples. these also are attributed to diagenesis. (5) euhedral pyrite crystals.
LIME-STONES	Opaque mineral(s) disseminated throughout argillaceous part of samples as in mudstones.	(1) Secondary carbonate crystals commonly fringe fossil fragments; as in mudstones, carbonate coats and corrodes quartz grains. (2) Chlorite crystals in the argillaceous matrix of the limestone samples are similar to those in red and green mudstones are assumed to share a similar diagenetic origin.
MANGANESE HORIZON SAMPLES	Large (up to several mm + in diameter), euhedral crystals of pyrite and barite occur in some samples. phosphatic nodules, brown in colour and opaque, are present in some material; some black opaque patches contain magnetite; amorphous silica present in some samples (as indicated by electron probe analyses).	(1) Diagenetic formation of chlorite widespread; in addition to crystals similar to ones in red and green mudstones, chlorite-rich nodular forms (in gradational contact with adjacent matrix material) occur; rare spherulitic aggregates of chlorite have also formed during diagenesis; chlorite crystals replace earlier authigenic barite crystals in some samples. (2) Secondary carbonate crystals, as in limestone samples, commonly fringe shell fragments; in some samples, euhedral carbonate crystals are abundant; spherulitic carbonate crystal aggregates rarely observed. (3) Carbonate concretions, chloritic nodules and phosphatic nodules are considered to have formed during diagenesis. (4) Fractures resembling shrinkage or dessication cracks formed during early diagenesis, (5) Euhedral crystals of pyrite, barite and carbonate have grown authigenically. (6) Probably magnetite has also formed authigenically, but this mineral is now partially altered in turn to hematite. (7) Late stage veinlets, commonly filled with carbonate and rarely with barite and pyrite, transect all other textural and structural features of sediments.

dispersed throughout a microcrystalline matrix. Red and green mudrocks are only rarely fossiliferous. Laminations or other manifestations of bedding are not commonly visible, though some green mudrocks do contain thin, chlorite-rich lenses lying in the bedding plane. Thin laminae of coarser-grained material, commonly quartz-rich, occur occasionally in both red and green mudrocks.

4.2.2 Limestones

Limestones are usually impure, containing a variable amount of argillaceous material which occurs dispersed throughout the rock as matrix to the carbonate or concentrated in argillaceous laminae. The argillaceous fraction of the limestone samples contains the same identifiable minerals that occur in red and green mudrocks (e.g., quartz, chlorite, hematite). Limestones containing a high proportion of argillaceous material are gradational to limy red and green mudrocks. The distinction between the two rock types was arbitrarily defined on a chemical basis, with samples in which CaO exceeds SiO_2 classed as limestones. Most limestones are fossiliferous, with some dominated by algally-produced textures (see 4.2.6).

4.2.3 Manganese-Rich Rocks

Manganese horizon samples consist of a mixture of argillaceous material and of carbonate minerals. Some contain euhedral crystals of pyrite, barite and magnetite, and phosphatic nodules also occur in some samples. Identifiable minerals in the argillaceous portion of these rocks include chlorite, quartz, and in some samples hematite. Some manganese horizon rocks contain numerous concretionary structures, in which the dominant minerals are chlorite and/or carbonate (See Section 4.2.7). Carbonate minerals also occur disseminated throughout the argillaceous fraction of the rocks and in massive beds and lenses. Fossils are commonly associated with the carbonate minerals, with the same forms present as in limestone samples elsewhere in the Lower and Lower Middle Cambrian portion of the succession. Stromatolite-like nodules are present in the manganese horizon (Dale, 1915) and algally-produced textures can be seen in thin section view (see Section 4.2.7).

4.2.4 General Observations

Several of the dark grey to black mudstones typical of the Upper Middle through Upper Cambrian Harcourt Group were examined in thin section for comparative purposes. These mudstones are much darker in plain light than the red and green mudstones of the Adeyton Group, due to the presence of very fine-grained opaque iron oxides. These rocks are typically well-laminated on a millimeter to centimeter scale, again in contrast to the Adeyton Group rocks. The banding consists of alternating carbonate-rich and argillaceous bands; some of the carbonate bands are abundantly fossiliferous.

Clasts in the limy basal Cambrian conglomerate are mostly composed of quartz, though rock fragments of similar lithology to underlying Precambrian rocks and red, limy mudrock clasts also occur. The red mudrock clasts are identical to Lower Cambrian sediments elsewhere and are presumed to have been derived from erosion of penecontemporaneous material. Some of the clasts are concentrically laminated and resemble stromatolites. The limy cement in the conglomerate is also fossiliferous and contains algally produced textures which suggest that the initial transgression must have taken place gradually in a low-energy environment. Several quartz pebbles in a thin section of the conglomerate from the Brigus, Conception Bay section were composed of aggregates of smaller quartz crystals whose long axes were aligned parallel to each other, producing a lineation in the clasts. This suggests that some deformed rocks were exposed to erosion in that area during the initial Cambrian transgression, though it is emphasized that such clasts form only a minor proportion of the conglomerate. Corroded albite crystals are present in some thin sections of the basal conglomerate - the only samples in which this mineral was positively identified optically.

4.2.5 Diagenesis

Evidence of diagenetic alteration is present in all of the above rock groups. Individual chlorite crystals in the mudrocks are much larger than the average crystal size in the adjacent matrix and moreover possess gradational contacts with this matrix, suggesting that the mineral has formed during diagenesis. Larger carbonate crystals, commonly twinned, are believed to have formed by the recrystallization of originally micritic material, and secondary carbonate crystals usually coat the fossil fragments in the rocks.

Chlorite formation during diagenesis is widespread. Chlorite has replaced, wholly or in part, a variety of minerals, including carbonate (some initially carbonate-bearing fossil fragments have been entirely replaced by chlorite), and barite. In limy mudrock samples, carbonate crystals surround, embay, and coat quartz crystals, features suggesting that the carbonate has replaced the latter mineral.

The manganese horizon has been considerably altered by diagenesis (Table 4.1). Most of the diagenetic features present in the horizon are believed to have been produced during early diagenesis, although several later stages can also be recognized. Concretions produced during diagenesis are present in all manganese horizon exposures and are predominant in some (e.g. Manuel's River, Conception Bay). The concretions are frequently flattened in the bedding plane and hence may have formed before compaction in the primary sediment had been completed. In thin sections, the nodules often possess extremely sharp boundaries (Figure 4.1); nodules are commonly distinctly zoned and adjacent nodules coalesce and form lemniscae. Concentric sets of carbonate-filled dessication cracks are also present in some nodules. These features are consistent with an early diagenetic origin for the concretions. In addition, delicate primary algal textures have been preserved in finely crystalline carbonate material (Figures 4.7, 4.8) in the manganese horizon, which suggests that extensive secondary diagenesis cannot have taken place.

Later-stage diagenetic features in the manganese horizon include authigenic crystals of barite, pyrite, and carbonate which transect earleir textures. Some of these crystals are themselves replaced by chlorite. Thin carbonate-filled fractures which cut all other textures are the latest diagenetic feature observed in manganese horizon thin sections.

The fact that most of the alteration in the manganese horizon in considered to have occurred during early diagenesis is important as such early processes may reflect on the process by which the horizon was formed (Chapter 7). Furthermore, the absence of extensive later diagenetic changes suggests that the bulk composition of the horizon has essentially remained unchanged since deposition and that chemical trends which may be identified in it (Chapter 5) reflect original conditions related to its formation.

4.2.6 Fossils

The Cambrian rocks are fossiliferous, and trilobite fragments, Hyolithes, and sponge spicules can be seen in thin section. Several types of algal remains are present in the rocks. Textures attributed to Girvanella and Epiphyton have been identified (M. M. Anderson, pers. comm., 1975) and stromatolites also occur. The mat-like and radial algal textures and other fossil forms are illustrated in photomicrographs in below.

4.2.7 Thin Section Photomicrographs

Information obtained from thin section study of samples of the Cambrian sequence has been summarized in Table 4.1. In general, the rocks are not well-suited for thin section examination because of their extremely fine-grained nature. Carbonates - in particular manganese horizon carbonates - yielded the most petrographic information. Primary and especially diagenetic features typical of the manganese horizon and other carbonates in the sequence are illustrated below in Figures 4-1 through 4-8.

Sample KE-2. Manganese carbonate nodule (x 80). Plane light. From massive, banded carbonate bed. Note sharp boundary and hematite-stained spots in surrounding matrix. The latter produces a characteristic speckled or mottled appearance in many manganese horizon samples.

Figure 4.1. Photomicrograph of Sample KE-2.

Sample M-96-C. Massive Mn-carbonate bed, Manuel's River exposure (x 20). Plane light. Euhedral pyrite crystal (opaque) in fossiliferous carbonate matrix. Darker tones due to hematite staining. Section contains 1-2% pyrite.

Figure 4.2 Photomicrograph of Sample M-96-C.

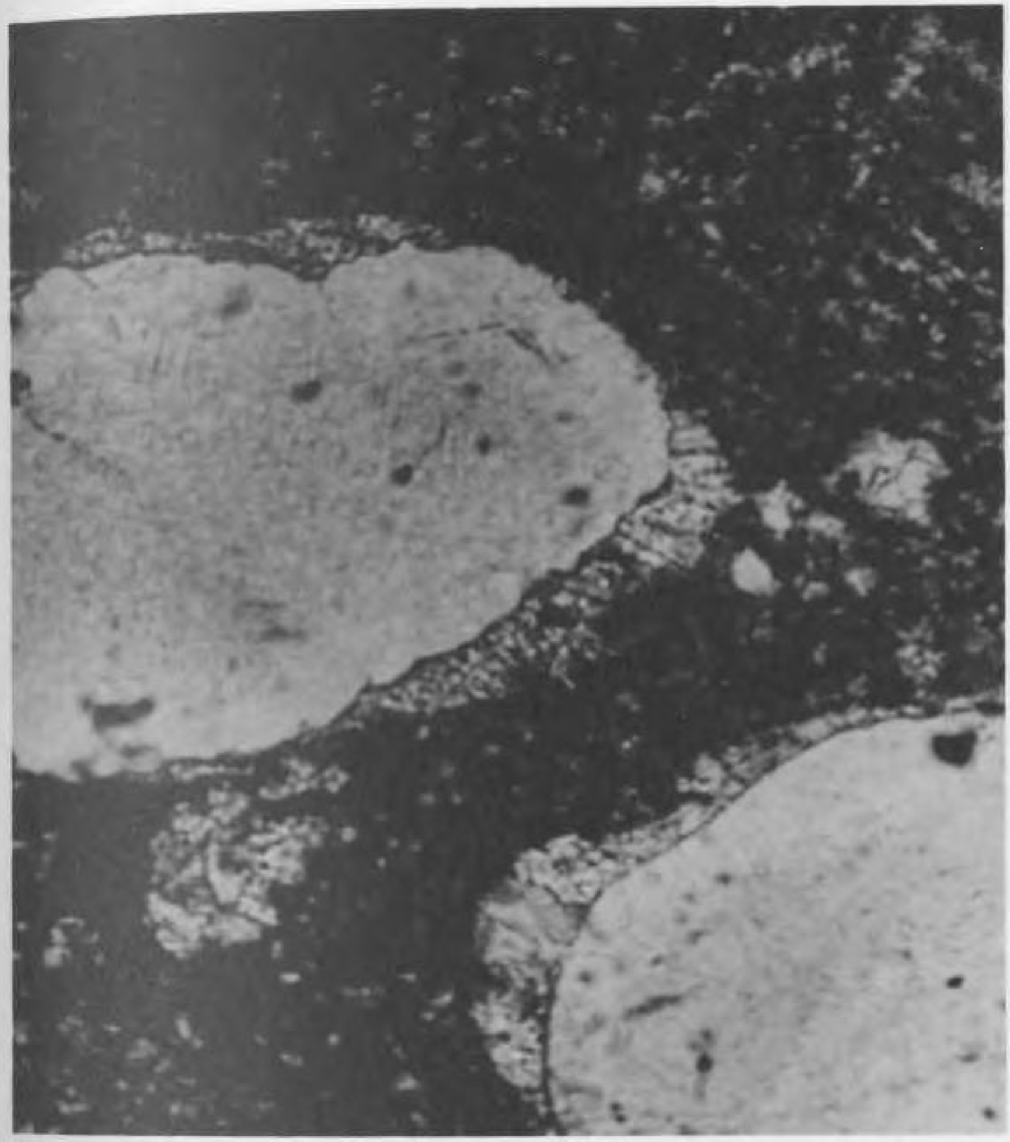

Sample BC-2. Bacon Cove, Conception Bay. From near the basal Cambrian conglomerate; hence the sub-rounded quartz grains. Note secondary carbonate crystals attached to quartz grains. Plane light (x 80).

Figure 4.3. Photomicrograph of Sample BC-2.

Sample HH-44. Manganese horizon, Hopeall Head. Plane light (x 80). Euhedral (rhombic), hematite-stained crystals in chloritic nodule. Note thin carbonate veins cutting nodule. Crystals are similar to $MnCO_3$ crystals detected with electron probe in other samples.

Figure 4.4. Photomicrograph of Sample HH-44.

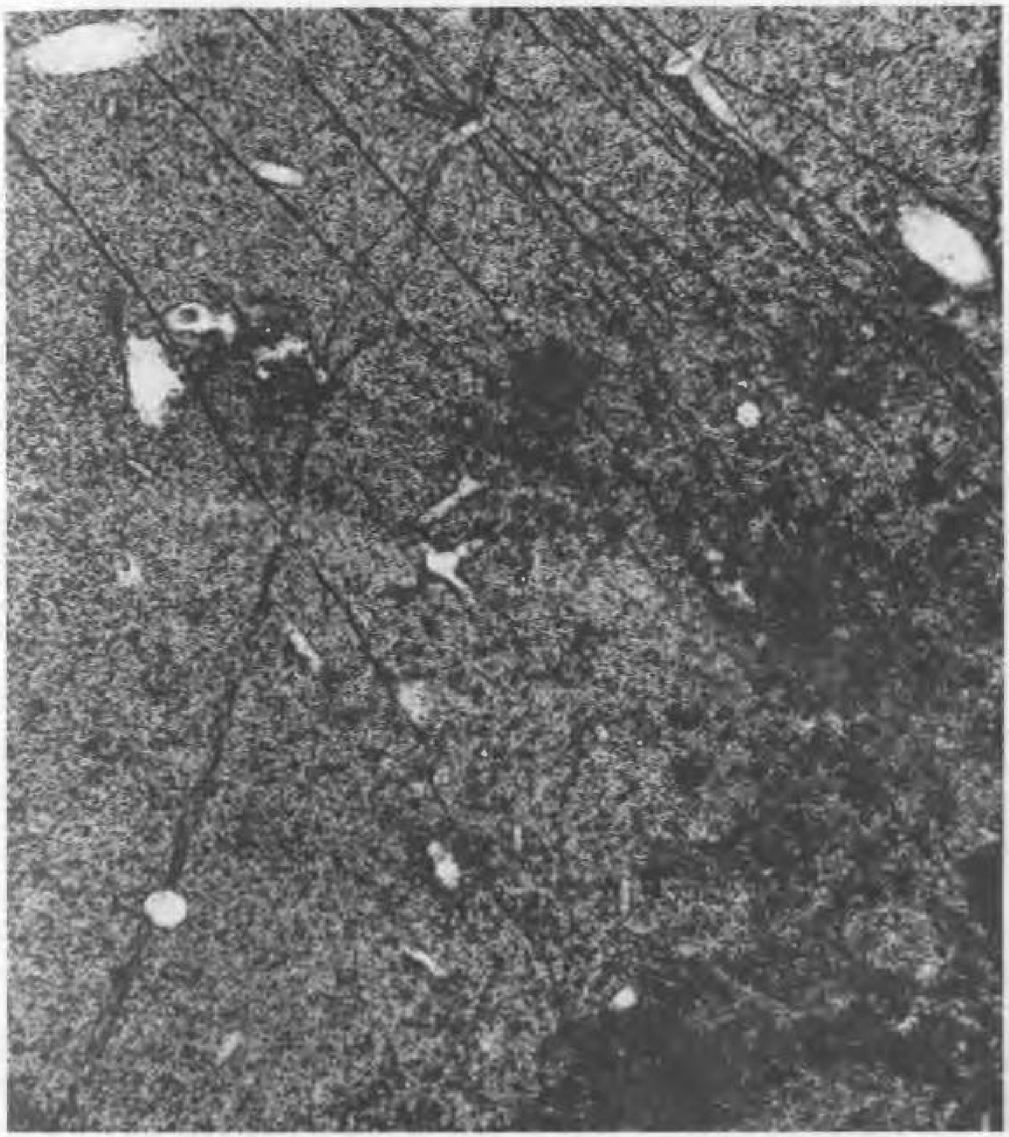

Sample BE-7. Phosphatic nodule in manganese horizon, Brigus. Plane light (x 80). Note fossil fragments, including sponge spicules in center.

Figure 4.5. Photomicrograph of Sample BE-7.

Sample HH-20. Black mudrock, Manuel's River Fm., Hopeall Head. Plane light (x 20). Typical of thin, highly fossilferous layers present in sequence. Note thin, secondary carbonate vein in center of photo.

Figure 4.6. Photomicrograph of Sample HH-20.

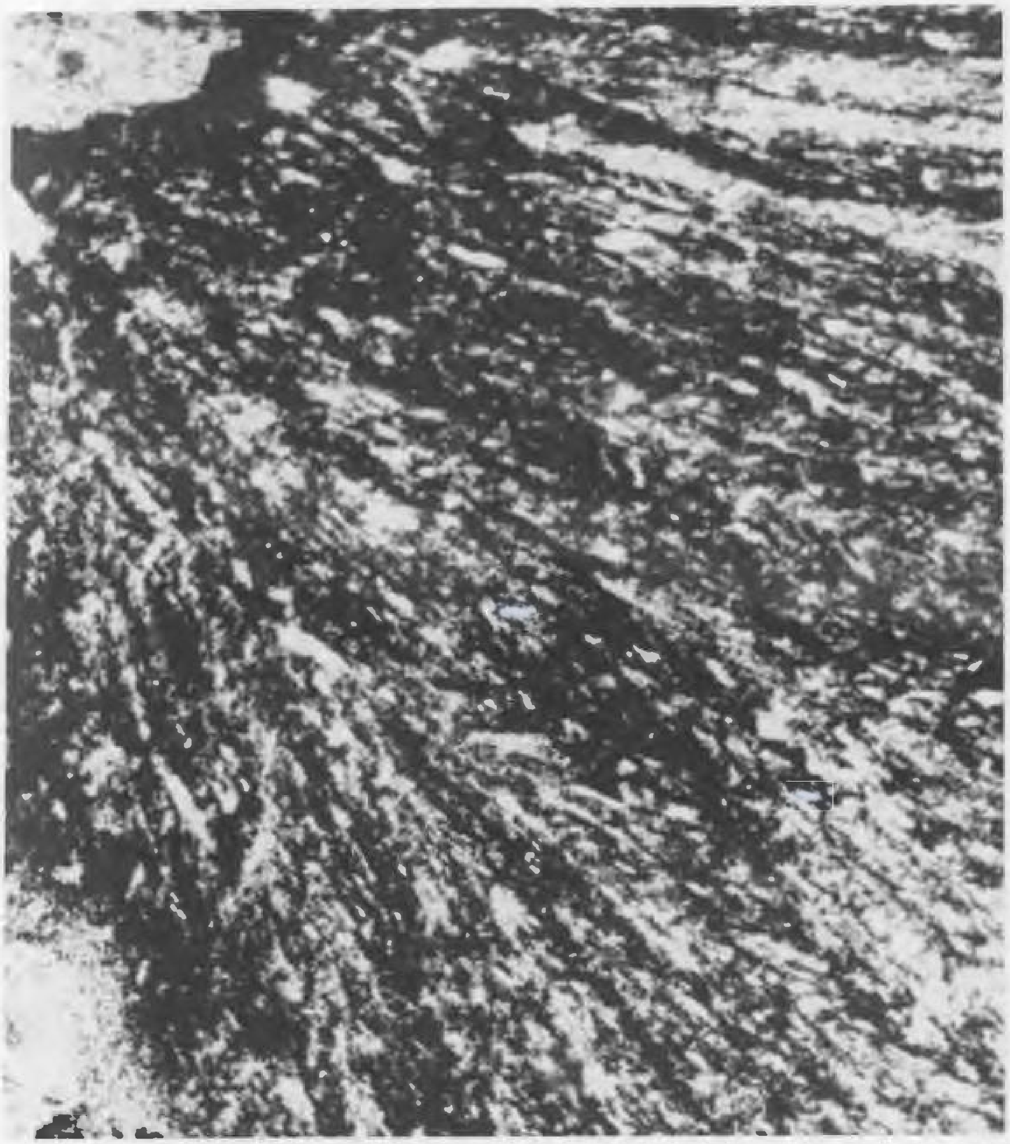

Sample M-88A. Manganese horizon, Manuel's River. Plane light (x 80). Radial, sheaf-like texture produced by algae (M.M. Anderson, pers. comm., 1975).

Figure 4.7 Photomicrograph of Sample M-88A.

Sample BW-1. Manganese horizon, Brigus. Plane light (x 80). Secondary carbonate crystals flanking fossil fragment. Rod-like carbonate crystals intermesh to form matlike texture typical of algal structures.

Figure 4-8. Photomicrograph of Sample BW-1.

4.3 Calculation of Mineral Proportions

The fine-grained nature of the sedimentary rocks comprising the Adeyton Group prevented direct (i.e., petrographic) measurement of their mineralogical composition. It was therefore decided to attempt to obtain mineralogical compositions for the various lithotypes occurring in the Adeyton Group by indirect means.

Macroscopic examination of the sedimentary rocks suggested that, in general, they were of uniform character throughout the study area. Homogeneity was also suggested by the results obtained from preliminary microscopic examination and X-ray diffraction analyses of the rocks. The number of mineralogical components present in the sedimentary rocks of the Adeyton Group is not great - only six minerals are present in sufficient quantity to be consistently detected on X-ray diffractograms. These minerals occur in all samples, regardless of geographic or stratigraphic position.

The mineralogical simplicity and apparent constancy of the sedimentary rocks made them ideal material to use in evaluating the efficacy of indirect methods for obtaining mineralogical compositions. Two such methods were used: X-ray diffraction analysis and the normative recalculation of whole rock chemical data. The results obtained from this work are presented below.

4.3.1 Mineral Proportions Derived from X-ray Diffractometry

X-ray diffractograms were obtained for 180 of the 375 whole rock powders which had been chemically analyzed. The 180 samples included material from all lithologies and formations in the Adeyton Group, and were selected from most of the sampled stratigraphic exposures in the study area. Sample selection was weighted in favor of the 'key' stratigraphic sections exposed around Trinity and Conception Bays on the Avalon Peninsula, with additional emphasis given the manganese horizon at the base of the Chamberlain's Brook Formation.

The minerals identified on the X-ray diffractograms include chlorite, illite, quartz, feldspar, hematite, and several carbonate minerals, including calcite, rhodochrosite, Mn-bearing calcite, and rarely siderite. Standard chemical and X-ray diffraction tests (e.g., glycolation, heat treatment, acid treatment - see Carroll, 1970) indicated that no additional clay minerals, such as montmorillonite or kaolinite, were present in detectable quantities in the Cambrian rocks. One X-ray diffractogram peak was selected for quantitative work for each mineral species, and the intensities (peak area) of the specified peaks measured on each diffractogram. In general, the most intense diffraction peak was selected for each mineral, so as to produce detection limits as low as possible, but the second most intense quartz peak (at 4.27 Angstroms) was used because of interference from illite with the 3.33 Angstrom quartz peak. The peaks selected for area measurements are listed in Table 4.2. The measured peak areas were used to calculate relative mineral proportions for individual samples. The method is essentially that applied to cores recovered by the Deep Sea Drilling Project (Rex, 1969). It is further described in Appendix I.

The relative mineral proportions obtained for 106 samples

Table 4.2: SUMMARY OF XRD-DERIVED MINERALOGICAL OBSERVATIONS.

	Mineral	Peak Used in Peak Area Measurements	Other Remarks
	Chlorite	7 angstrom peak	7 angstrom peak much stronger than 14 angstrom peak, suggesting that mineral is iron-rich. Acid and heat treatments indicate that no kaolinite is present, i.e. that all of 7 Angstrom peak produced by chlorite. Heat treatment (c. 550°C/ 1 hr.) collapses 7 ang. pk., enhances 14 ang. pk. Position of 060 reflection suggests trioctahedral structure.
	Illite	10 angstrom peak	Generally peak is symmetrical and sharply centered, suggesting mineral is well-crystallized.
	Quartz	4.27 angstrom peak	Principal peak at 3.33 angstroms not used because of interfering illite peak. Peaks always symmetrical, sharply centered.
	Feldspar	peak near 3.17 angstroms (near 28° two-theta)	Oligoclase composition assigned on basis of CaO: Na_2O in carbonate-free red and green mudrock samples.
	Hematite	2.71 angstrom peak (near 33.25° two-theta)	Relative intensity in argillaceous samples less than for quartz, fspar., and generally chlorite. Peak symmetrical and sharply centered.
CARBONATE	Calcite	3.03 angstrom peak	Peak intensities vary in relative sense - carbonate peaks in samples from manganese horizon are not as intense as calcite peaks in samples from outside this horizon. Peak shape also varies, in general limestone carb. peaks (calcite) more symmetrical, sharply centered.
	Rhodochrosite	2.84 angstrom peak	
	Manganiferous calcite	Variable; between calcite and rhodochrosite; generally closer to calcite	

are listed in Appendix III. The results obtained are compared with normative estimates of mineralogical composition obtained from chemical analyses and with chemical data in Sections 4.3.3 and 4.4 respectively.

4.3.2 Normative Mineral Proportion Calculations

Quantitative estimates of the abundances of the minerals detected on X-ray diffractograms (see Table 4.2) were calculated for most of the 381 samples which had been chemically analyzed. The computational procedure used is comparable to that employed by other workers (Shaw & Weaver, 1965; Schultz, 1964; Nicholls, 1962), except that the method used simultaneously recalculates the input bulk compositions for the mudrocks in terms of a number of mineral species of prespecified composition, whereas the traditional normative calculation involves the consecutive, one at a time computation of the concentrations of minerals in specified sequence. Thus, the method used herein calculates the mineral proportions in a rock in a single step, rather than in a series of steps as is generally the case, a rapid and time-saving procedure.

The mineral compositions used to obtain the normative mineral proportions are listed in Table 4.3. The compositions were derived in part from electron probe analyses and in part (e.g., feldspar composition) from X-ray diffraction data. Note that two chlorite compositions were used for most samples, one Fe-rich and the other relatively Mg-rich, becuase of the wide variation in chlorite compositions obtained from electron probe analyses (Chapter 5). For calculation purposes, it was assumed that green-colored

TABLE 4.3 MINERAL COMPOSITIONS USED IN QUANTITATIVE ESTIMATION OF MINERAL PROPORTIONS

	MINERAL	% Fe_2O_3	% MgO	% SiO_2	% Al_2O_3	% Na_2O	% K_2O	% CaO	% MnO	Comments
CHLORITE	Iron-rich	36.44	3.16	23.85	20.25				1.5	Two* chlorite compositions used to allow for the known variation in Fe and Mg content. Compositions determined by combined consideration of whole-rock chemistry and electron probe analyses.
	Mg-rich	20.59	19.0	23.85	20.25				1.5	
	Illite			45.0	38.0		12.0			Assigned the composition of sericite.
	Feldspar			64.71	22.15	9.95		3.18		Assigned composition of oligoclase on basis of diffractogram peak positions.
	Quartz			100.0						
	Hematite	100.0								
	'Excess' MnO								100.0	Assumed to occur in carbonate minerals.
	'Excess' CaO							100.0		Assumed to occur in carbonate minerals.

---

* A third chlorite composition was used in the computation of the mineralogical composition of limestone samples. This composition differed in that it contains intermediate amounts of iron (25.06% Fe_2O_3) and magnesium (11.6% MgO). Slightly more MnO was called for (2.8%), while the proportions of SiO_2 and Al_2O_3 remain the same.

samples contain no hematite and that MnO and CaO present in amounts greater than required for other minerals in the rocks occur as carbonate minerals. A maximum of 7 mineral phases were used in the normative calculations; however, the computer program used could be expanded to handle a greater number of components if desired. The method used to obtain the mineralogical proportions is described in Appendix I.

Discussion of Results

Normative mineral proportions were obtained for most of the available whole rock sample powders. The results for representative groups of samples are presented in tabular form in Appendix III. The normative mineral proportions obtained for those samples which had also been analyzed by X-ray diffraction are further considered in sections 4.3.3 and 4.3.4.

The normative mineral proportions obtained for the rocks are believed to be semi-quantitative. They cannot be considered precise duplications of the actual mineralogical compositions of the rocks, as minerals present in minor amounts (e.g., pyrite, barite, magnetite, collophane) are not included in the calculations. The SiO_2, Na_2O, MgO, etc., contained in these minerals are forced into the defined mineral components by the calculation process, lowering the accuracy of the results.

The normative mineral proportion estimates are for the most part consistent with information available from petrographic examination of the rocks. Thus, mudrock samples contain little calculated 'excess' CaO and MnO, as should be the case for these carbonate-poor rocks, samples containing abundant chlorite as estimated from thin section examination contain higher calculated chlorite proportions, and so on. However, the normative mineral proportion estimates are not as satisfactory for red mudrock samples, where about half of the calculated results are unacceptable, producing considerable (to -10%) negative calculated proportions for one of the iron-bearing mineral components. The poor results for such samples are thought to be related to the specified compositions for the chlorite mineral components. When the chlorite component compositions are made more magnesian and the mineralogical composition recalculated, the calculated normative concentrations of other mineral components do not much vary with only the proportions of the chlorite and hematite components changing. It is assumed that the true chlorite compositions of the red mudrock samples yielding the poor results do not correspond as well to the defined compositions as do other rock samples. Because of this discrepancy in chlorite composition, the calculating program produces solutions with negative mineral compositions. The program as written does not reject such 'impossible' solutions.

4.3.3 Comparison of Mineral Proportions Obtained from X-Ray Diffraction and Normative Recalculations

The relative mineral proportions obtained from X-ray diffractogram peak area measurements and the semi-quantitative estimates of mineralogical composition obtained for the same samples by normative recalculation of their chemical composition were compared by means of step-wise multiple regression analysis.

The purpose of doing this was to determine how well the two methods of obtaining estimates of mineralogical composition correspond. As the two methods are independent, a high degree of correspondence in the two sets of results would indicate that both were detecting actual changes in the proportions of the minerals in the rocks. If, however, the two sets of mineral proportion estimates are poorly correlated, it would suggest that one or possibly both methods were not satisfactorily detecting changes in mineral concentrations.

A secondary objective behind the comparison of the two sets of results was to use the semi-quantitative estimates of mineral composition derived from normative recalculation to establish 'correction factors' (regression equations) which would then permit semi-quantitative estimates of mineral composition for the rocks to be made directly from the results of X-ray diffraction analysis, a much more rapid and lower cost procedure.

The results obtained from the regression analysis, presented in Table 4.4, show that there is a strong positive correlation between the two sets of mineral estimates, with the X-ray diffraction relative mineral proportions explaining over 75% of the variance in the corresponding normative mineral proportions for each mineral. This in turn indicates that both methods of obtaining estimates of the mineral proportions of the Cambrian rocks are effective. The regression equations presented in Table 4.4 can be used to convert relative mineral proportions derived from X-ray diffraction peak area measurements into semi-quantitative estimates of the mineralogical composition of the samples, with the standard error in so doing being less than 6% for all minerals.

TABLE 4.4 REGRESSION EQUATIONS RELATING X-RAY DETERMINED RELATIVE MINERAL PROPORTIONS TO CHEMICALLY DERIVED ESTIMATES OF MINERAL PROPORTIONS IN CAMBRIAN SEDIMENTS

REGRESSION EQUATIONS**			
Dependent Variables ESTIMATES OF MINERAL PROPORTIONS DERIVED FROM SAMPLE CHEMISTRY	Independent Variables RELATIVE MINERAL PROPORTIONS DERIVED FROM X-RAY DIFFRACTOGRAMS	Percent of Variance of Left-hand Side of Eq'n Explained by Regression	Standard Error of Estimate of Independent Variable (on left side of equation)
PROPORTION OF CHLORITE	= 0.596*(XRDchlorite) - 0.735*(XRDillite) + 13.851	78%	5.82%
PERCENTAGE ILLITE	= 1.788*(XRDillite) + 4.937	78%	4.93%
PERCENTAGE FELDSPAR	= 0.513*(XRDfeldspar) + 1.989	81%	2.37%
PERCENTAGE QUARTZ	= 0.644*(XRDquartz) + 0.121*(XRDfeldspar) + 0.137*(XRDchlor.) + 5.362	84%	3.12%
PERCENTAGE HEMATITE*	= 0.357*(XRDhematite) + 0.399	93%	0.39%

* Red mudstone samples only inlcuded in this regression (30 cases).

** Number of samples used = 106. Includes red mudstones, green mudstones, and manganese horizon samples.

The mineralogical compositions obtained from the chemical compositions of the samples are believed more accurate than those obtained from X-ray diffraction, principally becuase of absorption errors in the X-ray data. Such errors are believed to be considerable in the case of iron or manganese-enriched samples. Figure 4.9 shows the relationship between the Fe_2O_3 content and chlorite peak area size in the rocks. At low Fe_2O_3 concentrations, the relationship between the two variables is approximately linear. However, as the Fe_2O_3 content increases, absorption errors increase and only small increases in the chlorite peak area are recorded. The iron-rich samples plotted in Figure 4.9 do not contain hematite or any other identifiable iron-bearing minerals, so that the change in behavior between the two variables is not caused by the presence of other minerals.

Mineralogical compositions obtained from normative recalculation of chemical data are limited in accuracy only by the accuracy of the chemical data and the compositions assigned the minerals in the rocks. The fact that the average mudrock composition obtained from the normative recalculations is similar to independently-determined estimates of mudrock mineralogical composition (Table 4.5) indicates that, at least for mudrocks, the compositions given minerals are close to the true compositions.

4.3.4 Average Mineralogical Composition of Major Rock Groups

The average mineralogical compositions of the principal rock types present in the Adeyton Group, as derived from normative recalculation from chemical analyses, are presented in Table 4.5,

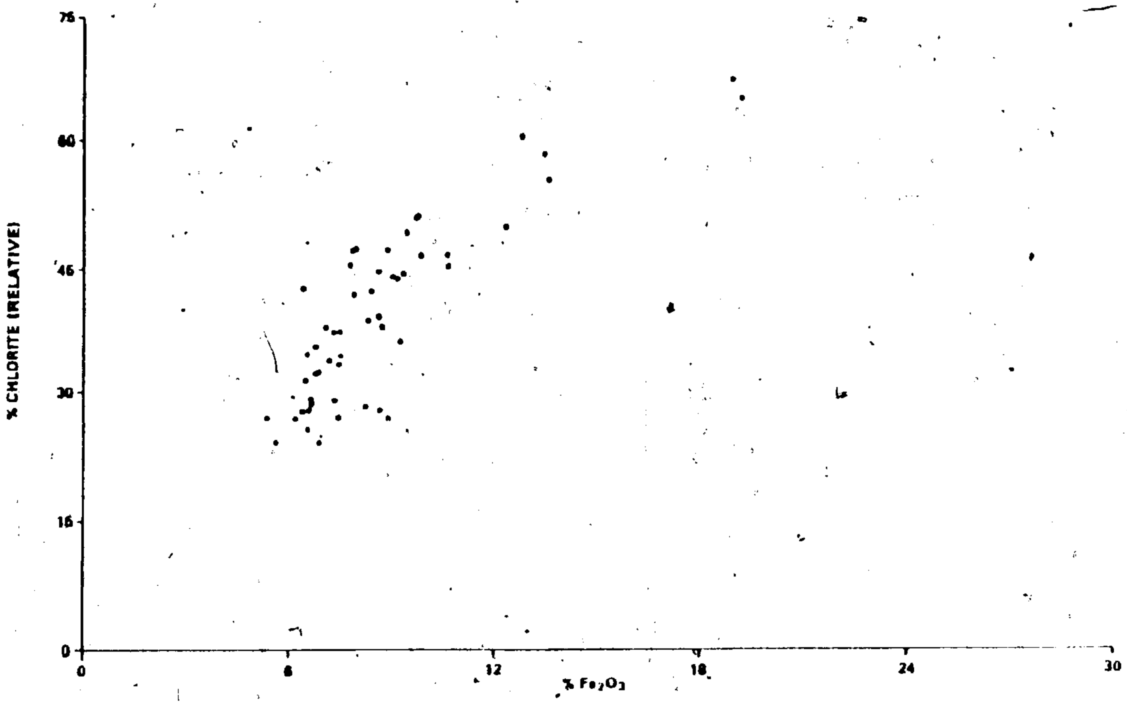

FIG. 4.9 PLOT OF Fe CONTENT AGAINST RELATIVE CHLORITE MINERAL PROPORTION FOR 52 GREEN MUDSTONES

TABLE 4.5: MEAN MINERALOGICAL COMPOSITION OF PRINCIPAL ROCK SAMPLE GROUPS*

	Chlorite	Illite	Quartz	Feldspar	Hematite	"EXCESS"		
						CaO	MnO	
GREEN MUDSTONE	27.16% avg. 92 spls.	28.26% avg. 92 spls.	29.21% avg. 92 spls.	12.52% avg. 92 spls.	none --	0.99% avg. 30 spls.	0.71% avg. 23 spls.	- Calculated on the assumption that the green mudstones are hematite-free. Two 'end-member' chlorite compositions (one rich in iron and the other relatively enriched in magnesium) used in the calculations.
RED MUDSTONE	16.21% avg. 30 spls.	32.70% avg. 30 spls.	29.07% avg. 30 spls.	15.24% avg. 30 spls.	4.55% avg. 30 spls.	0.36% avg. 23 spls.	not calculated	Selected mudstone samples - only those red mudstone samples yielding geologically logical results (i.e., no large negative mineral proportions calculated) were used in the calculation of the 'average' red mudstone--about half of the total no. of red mudstone samples that had been chemically analyzed. Same mineral comp. used as above.
LIMESTONE	7.60% avg. 41 spls.	7.60% avg. 41 spls.	11.81% avg. 41 spls.	5.22% avg. 41 spls.	2.56% avg. 41 spls.	31.66% avg. 41 spls.	1.46% avg. 41 spls.	Limestone samples were calculated on the assumption that both chlorite and hematite were present in the samples. One chlorite composition (relatively Mg-rich used in calculations. Excess CaO and MnO are assumed present in carbonate minerals; small amounts may be in other minerals (Ca in fsp; Mn as oxide).
MANG. HORIZON SPLS.	30.49% avg. 48 spls.	15.98% avg. 47 spls.	21.72% avg. 48 spls.	6.17% avg. 46 spls.	not calculated	5.59% avg. 48 spls.	9.74% avg. 48 spls.	Only samples judged not to contain hematite (i.e., only green colored samples) included in the calculations. The same two chlorite compositions used in green mudstone and red mudstone mineral proportion calculations were used in these calculations. Excess CaO, MgO in carb.
ALL NFLD. SAMPLES	26.17% avg. 170 spls.	25.63% avg. 169 spls.	27.40% avg. 170 spls.	11.27% avg. 168 spls.	4.55%† avg. 30 spls.	6.82% avg. 71 spls.	2.38% avg. 149 spls.	
AVERAGE** SHALE	60.9%		30.8%	4.5%	< 0.5%	3.6%		

*As obtained from chemical bulk composition of samples.
**Shaw & Weaver, 1965. †NOTE: Avg. for red mudrocks only.

together with the average shale composition calculated by Shaw and Weaver (1965). The Cambrian mudrocks in southeastern Newfoundland are similar in overall mineralogical composition to the average shale and the rocks comprising the Adeyton Group, the manganese horizon excepted, are not mineralogically distinct from mudrock successions elsewhere. The red and green mudrocks both contain appreciably higher feldspar concentrations than the average shale, and also contain less carbonate, though the latter trend is in accord with the general behavior of mudrocks through geologic time with respect to carbonate content, as Paleozoic rocks in general tend to contain less carbonate than younger mudrocks (Garrels & MacKenzie, 1971).

Table 4.5 shows that red and green mudrock contain similar concentrations of quartz and feldspar, and approximately the same proportion of chlorite + illite. The major differences between the two lithologies is in the proportions of chlorite and illite, with chlorite relatively more abundant in green and illite in red mudrock samples respectively.

The X-ray diffractograms indicate that red mudrocks are also enriched in hematite. Relative to mudrock samples, the limestones are enriched, as expected, in calcite ('excess' CaO) and to a lesser extent in Mn-bearing carbonate minerals ('excess' MnO). All silicate mineral contents and the concentration of hematite are reduced in limestone samples relative to the mudrock samples. Samples from the manganese horizon contain, on average, more chlorite than do other rock types. These rocks also contain higher proportions of Mn-bearing carbonate and calcite ('excess' MnO and

CaO), as expected on the basis of the abundance of those minerals in thin section and on X-ray diffractograms.

4.4 Relationship Between Rock Mineralogy and Rock Chemistry

Several different methods (e.g. Pearson-type correlation matrix, scattergram plots, etc.) were used to compare the relative mineral proportions obtained from X-ray diffraction to whole rock chemical data for the same samples. As might be expected, these two variables are strongly correlated. A Pearson-type correlation matrix relating these two properties is given in Table 4.6.

The numerous highly significant correlations present in the matrix demonstrate the intimate association between the chemical and mineralogical composition of the sedimentary rocks as determined by independent techniques. The correlations present in the matrix indicate that there is a strong control exerted by the proportions of the minerals present in a sample upon the concentration of the major elements in that sample. Each of the relative mineral proportions is highly correlated (at the 0.001 significance level) with one or several major elements, indicating that the mineral in question controls to a significant degree the concentration of those elements in the rocks. Elements not directly associated with the mineral possess lower correlations with it. This type of association can be seen in the horizontal rows of the matrix presented in Table 4.6. The correlations suggest that the mineral hematite is associated with the Fe_2O_3 content of the rocks in which it occurs, illite with the concentrations of K_2O and Al_2O_3, quartz with SiO_2, feldspar with Na_2O and Al_xO_3, chlorite

TABLE 4.6 CORRELATION MATRIX RELATING RELATIVE MINERAL PROPORTIONS TO MAJOR ELEMENT CHEMISTRY

	Fe_2O_3	TiO_2	P_2O_5	SiO_2	CaO	K_2O	MgO	Al_2O_3	MnO	Na_2O
Illite	-0.0239 n* = 165 s** = 0.380	0.7534 n = 165 s = 0.001	-0.3667 n = 114 s = 0.001	0.6844 n = 165 s = 0.001	-0.6004 n = 165 s = 0.001	0.8970 n = 164 s = 0.001	-0.2107 n = 153 s = 0.004	0.7983 n = 165 s = 0.001	-0.4670 n = 164 s = 0.001	0.4530 n = 165 s = 0.001
Chlorite	0.6956 n = 180 s = 0.001	0.4106 n = 180 s = 0.001	0.0166 n = 122 s = 0.428	0.4331 n = 180 s = 0.001	-0.4587 n = 180 s = 0.001	0.2030 n = 177 s = 0.003	0.4769 n = 169 s = 0.001	0.5529 n = 180 s = 0.001	-0.4061 n = 179 s = 0.001	-0.0104 n = 180 s = 0.445
Quartz	0.0745 n = 178 s = 0.161	0.7722 n = 178 s = 0.001	-0.3766 n = 120 s = 0.001	0.9322 n = 178 s = 0.001	-0.7461 n = 178 s = 0.001	0.6964 n = 175 s = 0.001	-0.1009 n = 165 s = 0.099	0.7898 n = 178 s = 0.001	-0.6023 n = 177 s = 0.001	0.6936 n = 178 s = 0.001
Feldspar	-0.1837 n = 160 s = 0.010	0.5735 n = 160 s = 0.001	-0.2841 n = 114 s = 0.001	0.7535 n = 160 s = 0.001	-0.6215 n = 160 s = 0.001	0.5765 n = 160 s = 0.001	-0.2320 n = 149 s = 0.002	0.5419 n = 160 s = 0.001	-0.4636 n = 159 s = 0.001	0.9371 n = 160 s = 0.001
Hematite	0.7508 n = 44 s = 0.001	0.4640 n = 44 s = 0.001	-0.3373 n = 30 s = 0.034	0.4884 n = 44 s = 0.001	-0.5404 n = 44 s = 0.001	0.5345 n = 44 s = 0.001	-0.2300 n = 44 s = 0.079	0.5406 n = 39 s = 0.001	-0.3421 n = 44 s = 0.012	0.2711 n = 44 s = 0.038
Carbonate***	-0.6107 n = 100 s = 0.001	-0.8224 n = 100 s = 0.001	0.1832 n = 45 s = 0.114	-0.9429 n = 100 s = 0.001	0.7203 n = 100 s = 0.001	-0.6668 n = 97 s = 0.001	-0.2723 n = 87 s = 0.005	-0.9318 n = 100 s = 0.001	0.5285 n = 99 s = 0.001	-0.5811 n = 100 s = 0.001

n* = number of cases upon which calculated value of r is based.
s** = significance of correlation.
*** = total proportion of all carbonate minerals.

with Fe_2O_3, MgO, and Al_2O_3, and the carbonate fraction with the concentrations of CaO and MnO." Some elements - Al for one - are genetically linked in this way with more than one mineral.

Other statistical comparisons yeild similar results to those summarized above and so are not included here.

4.5 Other Aspects of Petrology

4.5.1 Magnetic Minerals

The Curie Point of the magnetic fraction of one sample from the manganese horizon in the Conception Bay area was investigated by heating the material and recording the deflection produced at various temperatures on a Curie Balance, with the measurements made both during heating and cooling of the sample. The results of this examination indicated that two magnetic minerals were present in the sample. One of these minerals is magnetite, and the second most probably the manganese-bearing mineral jacobsite, with pyrrhotite a less likely alternative (in view of the low S content of the Cambrian rocks - see Chapter 5). Neither of the magnetic minerals is very abundant in the sample, with less than 1% of each present (J.P. Hodych, pers. comm., 1974). The magnetite is visible in some samples in the thin sections, occasionally occurring in crystals with characteristic octahedral outline. Larger, irregularly outlined opaque patches visible in the thin sections in some of the manganese horizon samples probably consist of a mixture of one or both magnetic components. Some of these patches contain fossil fragments. suggesting that the opaque oxices have been formed during diagenesis. The patches are difficult to examine due to the presence of a masking coating of hematite.

4.5.2 Manganese Oxides

Manganese oxide minerals in the manganese horizon occur on the surface of the rocks and as coatings on cleavage planes and along fractures. The distribution of the manganese oxide minerals indicates that they have formed in place by superficial alteration during weathering of Mn-bearing carbonate minerals. The presence of these manganese oxides gives the manganese horizon its dark color in field exposures in the Trinity-Conception Bay region on the Avalon Peninsula.

In some localities, loose blocks of material from the horizon have been almost entirely oxidized. X-ray diffraction of a sample of the oxides showed that both pyrolusite and birnessite (Sabina, 1975) are present.

4.5.3 Phosphatic Nodules

Some of the material in the manganese horizon is enriched in phosphorus, which is concentrated in bluish-black nodules visible in some hand specimens. Nodules collected from the manganese horizon exposure at Manuel's River, Conception Bay were analyzed for phosphorus by X-ray fluorescence, confirming their phosphatic nature. However, analysis of the same material by X-ray diffraction did not produce any peaks which could be attributed to a phosphorus-bearing mineral. Together, the results of these tests suggests that the phosphorus is present in amorphous form, i.e., as collophane.

4.6 Summary of Results

The petrographic data presented in this chapter show that:

(1) The Cambrian sedimentary rocks comprising the Adeyton Group are uniform in mineral composition. Only six minerals are abundant enough to be consistently identified on X-ray diffractograms. Two inversely-related mineral groups are present in the rocks: a silicate mineral group (mudrocks) containing quartz, illite, feldspar, hematite, and chlorite and a carbonate mineral group containing calcite, Mn-bearing calcite, rhodochrosite, and in some samples chlorite.

(2) Mineralogical proportions for samples of the Adeyton Group were obtained from X-ray diffraction data and by normative recalculation of whole rock analytical data. The results suggest that both methods can be successfully used to obtain data on mineralogical composition. The red and green mudrocks which make up the bulk of the Adeyton Group are similar in mineralogical composition to estimates for the composition of the average shale.

(3) The manganese horizon contains more carbonate (especially Mn-carbonates) and chlorite than the mudrocks in which it occurs.

CHAPTER 5

CHEMISTRY OF SEDIMENTARY ROCKS

5.1 Introduction

The major and trace element concentrations of 381 rock samples were determined by means of a combination of X-ray fluorescence and atomic absorption spectroscopy. The weight percent loss on ignition was also determined for these samples. Almost all samples were taken from the Lower and Lower Middle Cambrian sedimentary rocks which comprise the Adeyton Group; about one-third were from sampled exposures of the basal Middle Cambrian manganese horizon. A few samples of Precambrian volcanic and sedimentary rocks and of Upper Cambrian sedimentary rocks were analyzed for comparative purposes.

In addition, mineral compositions in 10 samples were investigated by means of electron probe analysis. Total C and S contents were also measured for selected sample groups. Sample preparation methodology and analytical precision and accuracy for these analyses are given in Appendix II.

The results obtained from whole-rock analyses were subjected to statistical analysis in order to determine the average chemical composition of the principal rock groups and to identify regional and/or stratigraphically controlled trends in the data. Particular emphasis was placed on determining the chemical differences characterizing the manganese horizon.

5.2 Results

The analytical results of major and trace element analyses for individual samples are presented in tabular form in Appendix III.

The average concentrations of major and trace elements in the principal rock types present in the Adeyton Group are presented in Table 5.1, together with the standard deviations from the mean concentrations for the analyzed elements in these groups.

The major element concentrations presented in Table 5.1 indicate that:

(1) The manganese horizon is enriched, relative to the average mudrock and average limestone, in Fe_2O_3, MnO, and MgO. The CaO content is higher than that of the average mudrock but is lower than that of the limestones elsewhere in the succession. Other major elements (e.g., Na_2O, K_2O, etc.) are present in lesser concentrations in the manganese horizon. The horizon is enriched relative to mudrocks in Ba and in P_2O_5.

(2) Red and green mudrocks are of similar overall chemical composition. The green mudrocks are enriched in MgO and depleted in K_2O relative to red mudrocks, though the difference is less than 1% for both elements. These changes reflect the changes in proportion of chlorite and illite in the red and green mudrock groups (Chapter 4).

The total iron content of red and green mudrocks (given as Fe_2O_3) is about equal. The latter are believed to contain a higher proportion of ferrous iron. Though the ferric/ferrous iron contents of the samples were not separately analyzed due to time limi-

TABLE 3.1:

MEAN CONCENTRATIONS, MAJOR AND TRACE ELEMENTS, PRINCIPAL CAMBRIAN ROCK TYPES OF AVALON PENINSULA

MAJOR ELEMENTS IN PERCENT, TRACE ELEMENTS IN PPM

* Ba run on major element program (XRF)
** Ba run on trace element program (XRF)

	All Samples Max 174 Cases	All Mudstones Max 155 Cases	All Green Mudstones	All Red Mudstones	All Limestones Max 48 Cases	All Mn Horizon Max 133 Cases
Fe_2O_3	8.28% (S.D.=3.81%)	8.39% (S.D.=1.65%)	8.32% (S.D.=1.70%)	8.40% (S.D.=1.49%)	4.27% (S.D.=3.57%)	9.55% (S.D.=4.58%)
TiO_2	0.70% (S.D.=0.33%)	0.89% (S.D.=0.09%)	0.88% (S.D.=0.09%)	0.91% (S.D.=0.08%)	0.25% (S.D.=0.11%)	0.56% (S.D.=0.23%)
P_2O_5	0.21% (S.D.=0.41%)	0.20% (S.D.=0.24%)	0.22% (S.D.=0.12%)	0.23% (S.D.=0.38%)	0.80% (S.D.=1.02%)	0.56% (S.D.=0.69%)
SiO_2	48.25% (S.D.=18.92%)	57.76% (S.D.=3.60%)	57.17% (S.D.=4.41%)	58.67% (S.D.=3.70%)	20.33% (S.D.=8.70%)	37.24% (S.D.=15.01%)
CaO	7.81% (S.D.=11.89%)	1.18% (S.D.=11.48%)	1.22% (S.D.=1.64%)	1.07% (S.D.=1.18%)	34.68% (S.D.=10.06%)	6.78% (S.D.=5.18%)
K_2O	2.62% (S.D.=1.49%)	3.75% (S.D.=0.74%)	3.56% (S.D.=0.69%)	4.05% (S.D.=0.71%)	0.97% (S.D.=0.60%)	1.92% (S.D.=1.24%)
MgO	2.17% (S.D.=1.57%)	2.18% (S.D.=0.80%)	2.47% (S.D.=0.77%)	1.75% (S.D.=0.80%)	1.69% (S.D.=1.08%)	2.55% (S.D.=1.25%)
Al_2O_3	14.27% (S.D.=5.60%)	18.50% (S.D.=2.41%)	18.99% (S.D.=1.82%)	18.11% (S.D.=1.96%)	5.63% (S.D.=2.99%)	12.14% (S.D.=4.71%)
MnO	4.61% (S.D.=8.84%)	0.37% (S.D.=0.62%)	0.47% (S.D.=0.64%)	0.21% (S.D.=0.16%)	1.95% (S.D.=2.30%)	11.80% (S.D.=11.72%)
Na_2O	1.05% (S.D.=0.73%)	1.46% (S.D.=0.42%)	1.40% (S.D.=0.38%)	1.59% (S.D.=0.36%)	0.49% (S.D.=0.27%)	0.60% (S.D.=0.42%)
Ba*	0.27% (S.D.=0.64%)	0.12% (S.D.=0.28%)	0.14% (S.D.=0.38%)	0.09% (S.D.=0.03%)	0.12% (S.D.=0.30%)	0.53% (S.D.=0.94%)
Ba**	0.27% (S.D.=0.62%)	0.10% (S.D.=0.06%)	0.11% (S.D.=0.08%)	0.09% (S.D.=0.03%)	0.09% (S.D.=0.06%)	0.54% (S.D.=0.98%)
Zr	106 (S.D.=47)	119 (S.D.=37)	116 (S.D.=29)	134 (S.D.=31)	72 (S.D.=66)	87 (S.D.=31)
Sr	112 (S.D.=319)	27 (S.D.=13)	39 (S.D.=30)	33 (S.D.=30)	341 (S.D.=423)	138 (S.D.=118)
Rb	72 (S.D.=46)	109 (S.D.=25)	104 (S.D.=24)	118 (S.D.=30)	19 (S.D.=12)	49 (S.D.=34)
Zn	93 (S.D.=30)	100 (S.D.=14)	102 (S.D.=13)	97 (S.D.=9)	70 (S.D.=26)	94 (S.D.=14)
Cu	33 (S.D.=91)	25 (S.D.=66)	71 (S.D.=183)	25 (S.D.=30)	99 (S.D.=128)	114 (S.D.=182)
[illegible]	2 (S.D.=9)	N.D.	N.D.	N.D.	13 (S.D.=7)	22 (S.D.=24)
Ce	112 (S.D.=63)	100 (S.D.=72)	100 (S.D.=26)	92 (S.D.=31)	40 (S.D.=30)	164 (S.D.=52)
La	23 (S.D.=30)	29 (S.D.=40)	34 (S.D.=35)	37 (S.D.=56)	60 (S.D.=61)	42 (S.D.=41)
Ni	58 (S.D.=25)	68 (S.D.=12)	70 (S.D.=10)	66 (S.D.=12)	27 (S.D.=20)	52 (S.D.=19)
Cr	78 (S.D.=38)	99 (S.D.=10)	104 (S.D.=14)	92 (S.D.=19)	19 (S.D.=18)	78 (S.D.=23)
Y	78 (S.D.=60)	112 (S.D.=22)	113 (S.D.=19)	112 (S.D.=31)	36 (S.D.=15)	64 (S.D.=40)

tations, the results of X-ray diffraction analyses indicate that the chlorite in the rocks is a ferrous iron variety (i.e., 060 peak position on diffractograms at about 1.56 Angstroms; see ASTM cards 7-339, 7-329). The higher chlorite content and absence of detectable hematite (see Chapter 4) suggests that the greem mudrocks contain a higher proportion of ferrous iron.

Fe^{++} determinations on two anomalously chlorite-rich samples from the manganese horizon (see below) confirm that most of the iron in these green mudrock samples is present in the ferrous state.

Sample	% FeO	FeO as % Fe_2O_3	Total Fe in sample as Fe_2O_3
Ch-7-1	15.22	16.74	18.98
Ch-7-2*	22.27	24.49	27.12

*Average, two titrations.

(3) Limestones are enriched, relative to the mudrock samples, in CaO, P_2O_5, and MnO. The higher MnO content suggests that the processes which led to the formation of the manganese horizon were active to some extent during deposition of other carbonate beds in the Adeyton Group.

(4) The red and green mudrock groups are much more uniform in chemical composition than the limestone and manganese horizon groups, as indicated by the size of the standard deviations of the element concentrations. The greater variability in the latter two groups is in response to the wide range in carbonate mineral content in them (see Chapter 4).

The trace element concentrations presented in Table 5.1

indicate that:

(1) in general, the Cambrian rocks are characterized by low trace element contents, with only Ba present in concentrations much above 100 ppm;

(2) red and green mudrocks contain more Zr, Rb, Cr, V, and Ni than the carbonate-mineral bearing limestone and manganese horizon groups;

(3) the limestone samples are enriched in Sr and possibly also Cu, though this element was not detected in the majority of samples;

(4) the manganese horizon contains higher Ce, Cu, Nb, and Sr concentrations than mudrock samples.

Nb is present in low concentrations and was detected in very few (27) manganese horizon samples, and the enrichment mentioned above is not considered significant. Cu concentrations in manganese horizon samples are erratic; though concentrations of several hundred ppm occur in some samples, it has not been detected in the majority of cases. Pyrite is visible in hand specimen in some of the Cu-rich manganese horizon samples and this suggests the Cu may be present in a sulphide phase. Trace amounts of chalcopyrite have been recorded from the manganese horizon exposure at Brigus, Conception Bay (Mines Branch Investigation No. 1249, 1942).

Zn is the least variable trace element, averaging about 100 ppm in all but the limestone rock group where its concentration is lower.

5.2.1 Statistical Examination of Chemical Data

The chemical data obtained from analysis of the Cambrian sedimentary rocks was examined statistically to determine the nature of the trends and elemental relationships present in the rocks. Several methods were used, each of which is discussed below.

Two factors control the distribution of elements in the Cambrian rocks (Sec. 4.4). These are:

(1) a mineralogical association factor, in which the concentrations of specific elements are related to the concentrations of specific minerals in the rocks, and

(2) a mineral grouping factor, in which the elements associated with minerals comprising one of two gradational mineral groups tend to be mutually positively correlated, and negatively correlated with elements in the opposing mineral group.

Influence of Mineral Grouping on Correlations

The minerals which comprise the Adeyton Group (Chapter 4) form two gradational and inversely correlated mineral groups: a silicate mineral group including quartz, feldspar, illite, chlorite and hematite, and a carbonate mineral group including calcite and rhodochrosite.

The concentrations of Fe_2O_3, TiO_2, SiO_2, K_2O, Al_2O_3, and Na_2O are influenced by the concentration of minerals of the silicate group. Each of these elements is positively correlated with all or most of the others in the group, and all are negatively correlated with the concentrations of CaO and MnO, which are associated with the carbonate mineral group. The behavior of MgO is ambiguous, probably because it occurs (see electron probe data) in minerals associated with both the silicate (i.e., in chlorite) and carbonate mineral groups. The correlations are not clear for the concentrations of Ba and P_2O_5, but average chemical concentration data (Table 5.1) indicate that these elements are primarily associated with the carbonate-bearing limestone and manganese horizon groups (particularly the latter). The chemical differentiation brought about in the rocks by the association of the elements with the two gradational mineral groups is shown in the scattergram plots of elemental concentration presented later in this section.

Influence of Mineralogy on Correlations

In an attempt to minimize the influence of mineral grouping upon inter-elemental correlations, Pearson correlation matrices were calculated for three mudrock groupings (i.e. carbonate concentrations low): (1) 61 red mudrock analyses; (2) 93 green mudrock analyses; and (3) a larger group including the above and siliceous manganese horizon samples. The results obtained for the largest grouping are discussed below. Correlation matrices for the other two mudrock groups are included in Appendix III. Correlations for Cu, Nb, and La are not included as they possess no significant correlations.

Major element correlations are given in Table 5.2. The data in this table indicates that the influence of mineral grouping, as described above, remains prominent. Thus, for example, CaO and MnO (carbonate group) are strongly negatively correlated with SiO_2, Al_2O_3, TiO_2, and other elements of the silicate mineral group. Some evidence of mineralogical partitioning of major elements can, however, also be seen in Table 5.2.

(1) The positive correlation between Fe_2O_3 and MgO reflects the association of the two in the mineral chlorite (see Section

TABLE 5.2

CORRELATION COEFFICIENTS FOR 170 SAMPLES COMBINING RED MUDROCK, GREEN MUDROCK, AND MANGANESE HORIZON SAMPLES

	Fe_2O_3	TiO_2	P_2O_5	SiO_2	CaO	K_2O	MgO	Al_2O_3	MnO	Na_2O	Ba
Fe_2O_3	1	-0.0251 s=0.373	0.1028 s=0.117	-0.0376 s=0.313	0.0481 s=0.267	-0.3018 s=0.001	0.4455 s=0.001	0.0659 s=0.196	-0.2531 s=0.001	-0.3182 s=0.001	-0.0979 s=0.103
TiO_2		1	-0.4492 s=0.001	0.8373 s=0.001	-0.7383 s=0.001	0.7765 s=0.001	-0.1151 s=0.067	0.8533 s=0.001	-0.7878 s=0.001	0.660 s=0.001	-0.5395 s=0.001
P_2O_5			1	-0.4935 s=0.001	0.5071 s=0.001	-0.4188 s=0.001	0.1507 s=0.040	-0.4856 s=0.001	0.5542 s=0.001	-0.3407 s=0.001	0.1635 s=0.029
SiO_2				1	-0.8027 s=0.001	0.7263 s=0.001	-0.1286 s=0.047	0.8261 s=0.001	-0.8847 s=0.001	0.7843 s=0.001	-0.6219 s=0.001
CaO					1	-0.6972 s=0.001	0.1990 s=0.005	-0.8021 s=0.001	0.5605 s=0.001	-0.6450 s=0.001	0.3750 s=0.001
K_2O						1	-0.3679 s=0.001	0.8572 s=0.001	-0.6435 s=0.001	0.5584 s=0.001	-0.4377 s=0.001
MgO							1	-0.0706 s=0.180	-0.0880 s=0.127	-0.1769 s=0.011	-0.0332 s=0.334
Al_2O_3								1	-0.8271 s=0.001	0.5691 s=0.001	-0.5215 s=0.001
MnO									1	-0.6069 s=0.001	0.6308 s=0.001
Na_2O										1	-0.4661 s=0.001
Ba											1

5.2.2).

(2) The negative correlation of Fe_2O_3 and MgO with K_2O suggests that the contents of the minerals chlorite and illite are inversely related within the mudrock group.

(3) The strong correlation (+0.85) between K_2O and Al_2O_3 is suggestive of their association in illite.

Trace element correlations between samples of this mudrock group are presented in Table 5.3. Again, the effect of the inversely related carbonate and silicate mineral groups upon the correlations is apparent. The elements Zr, Rb, Zn, Ni, Cr, and V are positively correlated with one another, and inversely correlated with Sr and Ba. These two groups of elements are therefore considered associated with minerals of the silicate and carbonate groups, respectively. The negative correlations of Ce with Zr, Rb, and V suggest, by exclusion, that this element may be associated with the carbonate group.

Correlations between major and trace element concentrations in the mudrock group are presented in Table 5.4. Overall, the correlations again reflect the inverse carbonate-silicate relationship present in mudrocks of the Cambrian sequence. Thus, as suggested by the data in Table 5.3, the trace element group Zr-Rb-Zn-Ni-Cr-V is negatively correlated with the CaO and MnO of the carbonate mineral group. The extreme (+0.95) correlation present between K_2O and Rb demonstrates their presence in the mineral illite. Similarly, the positive correlations between Zn, Fe_2O_3, and MgO suggests that the former may be present in mudrocks in chlorite. Sr and Ba are positively correlated with CaO and

TABLE 5.3

CORRELATION COEFFICIENTS FOR TRACE ELEMENT COMPOSITIONS OF 170 SAMPLES, INCLUDING RED MUDROCK, GREEN MUDROCK AND MANGANESE HORIZON SAMPLES

	Zr	Sr	Rb	Zn	Ce	Ni	Cr	V	Ba
Zr	1	-0.0923 s = 0.142	0.3951 s = 0.001	0.3031 s = 0.001	-0.4560 s = 0.001	0.1369 s = 0.040	-0.0419 s = 0.297	0.3842 s = 0.001	-0.0247 s = 0.377
Sr		1	-0.5524 s = 0.001	-0.2398 s = 0.002	0.1117 s = 0.096	-0.5390 s = 0.001	-0.6317 s = 0.001	-0.5179 s = 0.001	0.7731 s = 0.001
Rb			1	0.0998 s = 0.098	-0.4814 s = 0.001	0.5535 s = 0.001	0.5459 s = 0.001	0.4791 s = 0.001	-0.3942 s = 0.001
Zn				1	-0.0448 s = 0.282	0.3857 s = 0.001	0.2894 s = 0.001	0.2564 s = 0.001	-0.2395 s = 0.001
Ce					1	-0.0557 s = 0.237	-0.0404 s = 0.302	-0.3640 s = 0.001	0.1311 s = 0.046
Ni						1	0.6333 s = 0.001	0.2330 s = 0.002	-0.4693 s = 0.001
Cr							1	0.4536 s = 0.001	-0.4938 s = 0.001
V								1	-0.4131 s = 0.001
Ba									1

TABLE 5.4

CORRELATION COEFFICIENTS BETWEEN MAJOR AND TRACE ELEMENT CONTENTS OF 170 SAMPLES INCLUDING RED MUDROCKS, GREEN MUDROCKS, AND MANGANESE HORIZON SAMPLES

	Zr	Sr	Rb	Zn	Ce	Ni	Cr	V	Ba2*
Fe_2O_3	-0.2356 s=0.001	-0.0498 s=0.279	-0.3046 s=0.001	0.3937 s=0.001	0.4290 s=0.001	0.2407 s=0.001	0.2055 s=0.004	-0.2270 s=0.002	-0.1501 s=0.026
TiO_2	0.6024 s=0.001	-0.6282 s=0.001	0.7389 s=0.001	0.3455 s=0.001	-0.4417 s=0.001	0.5845 s=0.001	0.5507 s=0.001	0.5963 s=0.001	-0.5925 s=0.001
P_2O_5	-0.2662 s=0.001	0.2725 s=0.002	-0.4195 s=0.001	-0.0665 s=0.222	0.3335 s=0.001	-0.2469 s=0.002	-0.3056 s=0.001	-0.3087 s=0.001	0.1697 s=0.025
SiO_2	0.4456 s=0.001	-0.7165 s=0.001	0.6957 s=0.001	0.2910 s=0.001	-0.4726 s=0.001	0.6373 s=0.001	0.5673 s=0.001	0.6126 s=0.001	-0.6362 s=0.001
CaO	-0.3384 s=0.001	0.6942 s=0.001	-0.7138 s=0.001	-0.2384 s=0.001	0.2378 s=0.001	-0.6051 s=0.001	-0.7344 s=0.001	-0.5618 s=0.001	0.4206 s=0.001
K_2O	0.4137 s=0.001	-0.5525 s=0.001	0.9511 s=0.001	0.0573 s=0.230	-0.4978 s=0.001	0.5026 s=0.001	0.5030 s=0.001	0.4281 s=0.001	-0.4390 s=0.001
MgO	-0.1131 s=0.075	0.0132 s=0.439	-0.3569 s=0.001	0.4381 s=0.001	0.2653 s=0.001	0.0903 s=0.122	-0.0040 s=0.479	-0.0150 s=0.426	-0.0539 s=0.243
Al_2O_3	0.3726 s=0.001	-0.6604 s=0.001	0.8411 s=0.001	0.3437 s=0.001	-0.3413 s=0.001	0.6974 s=0.001	0.7117 s=0.001	0.5764 s=0.001	-0.5591 s=0.001
MnO	-0.3826 s=0.001	0.5995 s=0.001	-0.5988 s=0.001	-0.4208 s=0.001	0.3926 s=0.001	-0.6556 s=0.001	-0.5024 s=0.001	-0.6815 s=0.001	0.6629 s=0.001
Na_2O	0.5148 s=0.001	-0.5730 s=0.001	0.5881 s=0.001	0.2817 s=0.001	-0.5072 s=0.001	0.3907 s=0.001	0.4038 s=0.001	0.5221 s=0.001	-0.4705 s=0.001
Ba1*	-0.0433 s=0.291	0.6128 s=0.001	-0.3421 s=0.001	-0.2267 s=0.002	0.1457 s=0.030	-0.4156 s=0.001	-0.3949 s=0.001	-0.1751 s=0.014	0.7926

* Ba1 = barium analyses with barium treated as major element.

Ba2 = barium analyzed as for other trace elements.

MnO and therefore appear to be related to the carbonate mineral group.

Scattergram Plots

Major element concentrations were plotted against Al_2O_3 to visually examine the trends present in the chemical data. The scattergram plots show that the Cambrian rocks fall along a single chemical trend, with carbonate-rich samples at one end (carbonate mineral group predominant) and mudrocks at the other (silicate mineral group predominant). The two groups are gradational, and single linear trends are developed in the scattergrams. Several sets of scattergram plots were made, one involving all analyzed samples and others using specified lithological subgroupings. The chemical trends illustrated by the scattergrams are discussed below, using representative scattergrams as examples, while the remaining scattergrams are separately presented in Appendix III.

The carbonate/silicate trend is shown in Figure 5.1, where mudrock samples cluster at the high Al_2O_3 - SiO_2 end of the trend. Similar scattergrams are obtained for most other major elements, though naturally the MnO and CaO associated with carbonate minerals yield negative correlations when plotted against Al_2O_3. Fe_2O_3, however, behaves in a different manner (Figure 5.2) and can be seen to form two separate trends. Mudrock samples cluster to the right of the scattergram in the high Al_2O_3 range. The carbonate group trend is extended in linear fashion to produce a second group of samples characterized by high Fe_2O_3 - moderate Al_2O_3 contents. These samples are chlorite-rich material from the manganese horizon.

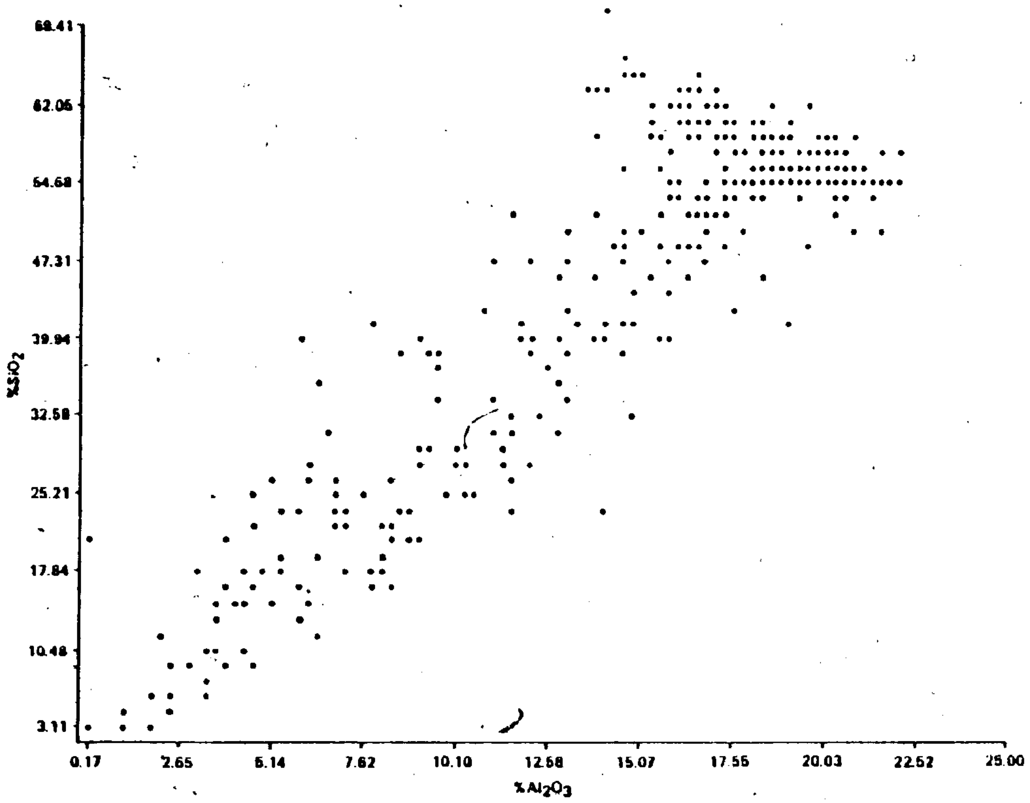

FIG. 5.1 SCATTERGRAM RELATING % SiO_2 TO % Al_2O_3 (ALL SAMPLES)

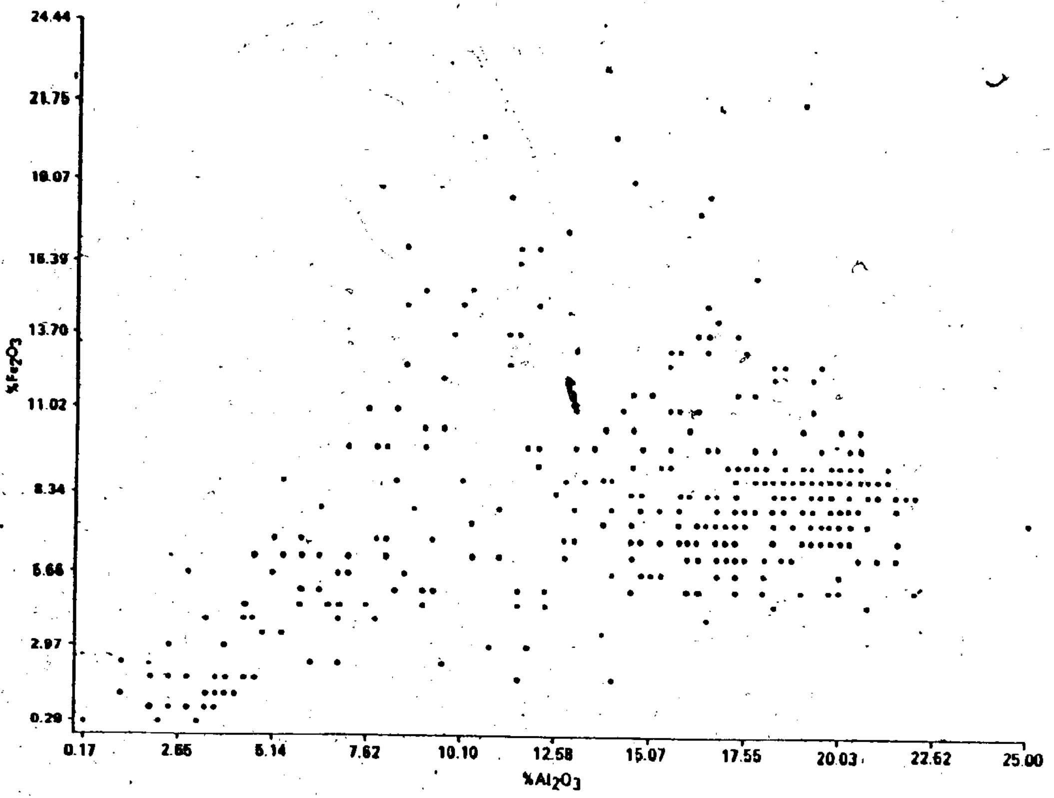

FIG. 5.2 SCATTERGRAM RELATING % Fe_2O_3 TO % Al_2O_3 (ALL SAMPLES)

Other Tests

The results of major and trace element analyses of Cambrian rocks were subjected to several other forms of statistical analysis, including multiple regression analysis, cluster analysis, and discriminant function analysis. In general, these statistical methods produced similar results to those described above though for some, the results were not as complete. Thus, for example, the clusters obtained from cluster analysis were primarily lithological (e.g., limestone, mudrock clusters), but were not as consistently defined as visually determined sample groupings based on color, etc. As none of these methods gave any additional information on the relationships between the analyzed chemical variables in the Cambrian rocks, they are not further discussed here.

5.2.2 Electron Probe Analyses

A number of chemical analyses of minerals in ten rock samples were made using a Cambridge Microscan V electron probe at the Dalhousie University geology department. The results of these analyses are presented in Table 5.5 and are discussed below.

The analyses indicate that the chlorite present in the rocks is enriched in iron, as in every case the chlorite crystals contain more Fe_2O_3 than MgO. The range in concentration of Fe and Mg in the chlorite analyses further indicates that the Fe/Mg ratio in the chlorite in the rocks varies appreciably from sample to sample. The chlorite also contains a variable amount of MnO, with up to 5% calculated for one analysis in a manganese horizon sample, indicating that some of the manganese in the horizon occurs in this

TABLE 5.5 ELECTRON PROBE ANALYSES OF SELECTED CAMBRIAN SAMPLES

9.

	M-96-1A	DI-3 (1)	DI-3 (2)	NM-10 (1)	NM-10 (2)	HH-10 (1)	HH-10 (3)	HH-10 (4)	LZ-8 (1)	LZ-8 (2)	LZ-8 (3)	LZ-8 (4)	KE-3 (1)	KE-3 (2)	KE-3 (4)	KE-3 (6)	KE-3 (9)	KE-3 (10)	KE-3 (12)
Fe_2O_3	-	24.85	25.50	31.68	28.07	0.42	32.37	0.39	0.69	0.71	0.70	71.71	35.13	1.80	0.93	35.91	0.20	0.17	0.43
MgO	-	10.95	11.23	5.46	6.12	0.02	6.70	6.92	8.27	7.89	9.20	0.23	6.77	0.59	0.35	6.31	0.56	0.65	0.70
MnO	7.54	2.84	2.78	3.75	5.29	0.06	1.60	29.00	15.02	14.75	14.96	0.55	0.73	45.12	25.78	0.58	52.94	46.32	44.52
Al_2O_3	-	20.58	19.91	24.07	19.76	1.02	18.44	0.02	0.01	0.05	0.01	7.86	20.11	1.84	0.65	21.49	0.24	0.35	0.92
CaO	9.43	-	-	0.04	0.08	0.01	0.07	7.98	31.22	30.80	29.12	0.21	0.07	4.91	4.35	0.08	5.10	8.15	10.98
SiO_2	20.90	23.68	24.02	26.69	22.94	134.86	36.11	0.00	0.02	0.02	0.00	16.54	23.34	6.48	4.71	24.34	0.31	0.17	1.10
K_2O	-	-	-	0.73	0.24	0.04	0.06	0.04	-	-	-	-	-	-	-	-	-	-	-
Na_2O	-	-	-	0.04	0.03	0.02	0.03	0.04	-	-	-	-	-	-	-	-	-	-	-

mineral. Manganese present in chlorite probably accounts for much of the manganese content of mudrock samples from outside of the manganese horizon.

A number of analyses made of carbonate minerals indicate that the carbonate minerals present in the manganese horizon are Mn-Ca-Mg varieties, with Mg present in subordinate amounts in all analyses. The richest Mn-carbonates can be considered rhodochrosite, and none of the analyzed carbonates were iron-rich, containing under 2% Fe_2O_3. Several of the carbonate analyses from sample LZ-8 were of fossil shell fragments. As it is not probable that the original biogenic carbonate was rich in Mn, it seems likely that the Mn-carbonate analyzed in this sample is of secondary origin.

Several euhedral crystal forms in a diagenetic chloritic nodule in sample HH-10 from the manganese horizon were analyzed. One was a barite crystal (yielding a response for only Ba) formed during diagenesis. Several opaque, hematite-stained patches contain iron contents of approximately 70% Fe_2O_3, suggesting that the mineral phase involved was hematite or some other iron oxide (e.g. magnetite - see Sec. 4.5.1).

A carbonate concretion enclosed in an argillaceous matrix in sample HH-10 was selected for further chemical analyses on the electron probe. The outer rim of the nodule, which consists in sectional view of a carbonate shell enclosed within and infilled with argillaceous material, was traversed. The carbonate shell of the concretion was analyzed along the length of the traverse line (about 1 mm long) for 8 major elements, to determine the nature of the contact with the adjacent argillaceous matrix and to visually examine (on a fine scale) the distribution of the elements in the rock. The results of the analytical traverse are presented in Figure 5.3, which shows that the transition between the Mn and Ca-bearing carbonate comprising the carbonate ring and argillaceous matrix is abrupt. No gradation into the matrix material on either side of the carbonate ring is apparent, though the analyses suggest that a thin Fe-Mg rich zone (chlorite) separates the carbonate from the matrix proper. Figure 5.3 illustrates the negative correlations between the Ca and Mn associated with the carbonate mineral group and the K-Na-Si-Al-Fe-Mg rich argillaceous material on a crystal-to-crystal scale. The irregular distribution of Na along the length of the traverse is interpreted to indicate the discrete distribution of the element in scattered feldspar crystals. The low K content within the nodule suggests that the concentration of illite is low. The positive correlation between the Fe and Mg associated with the chlorite in the sample can also be seen in Figure 5.3.

5.2.3 Additional Chemical Data

Carbon Content of Samples

The C content of a group of 24 samples was determined with a Leco induction furnace, and the results of these determinations are given in Table 5.6. Also included in the table are the calculated amounts of C necessary to place all analyzed CaO and MnO in carbonate minerals, and a third column listing the differences between the analyzed C and the amount needed to place the MnO and CaO in carbonate minerals. The results of Table 5.6 indicate that

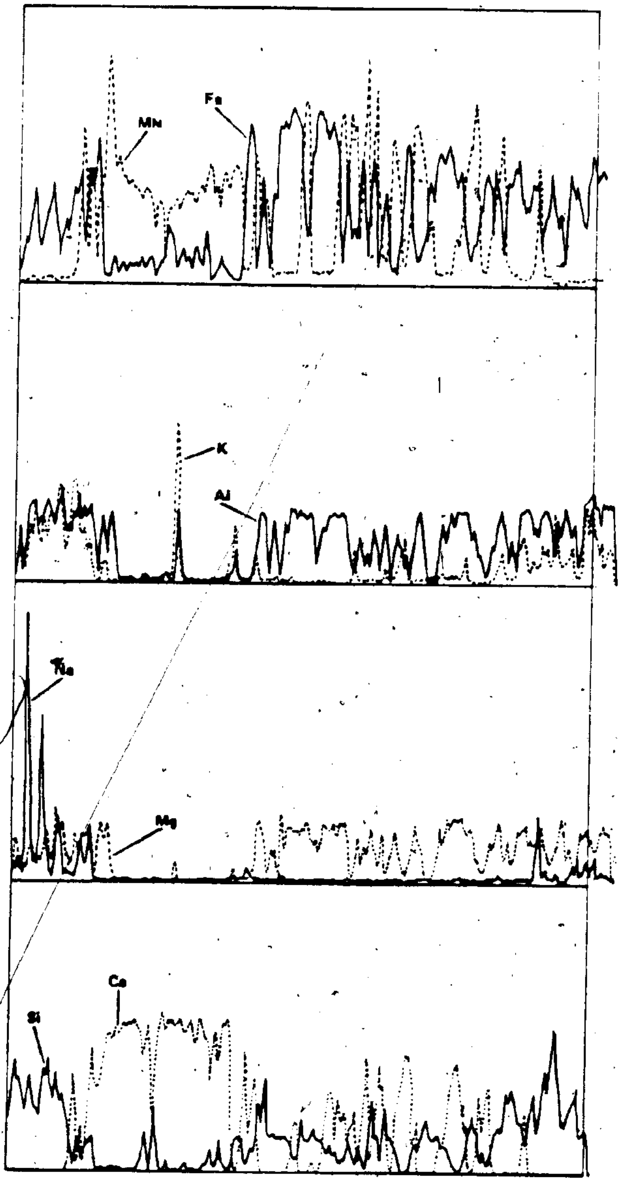

FIG. 5.3 RESULTS OF ELECTRON MICROSCOPE SCAN ACROSS CARBONATE CONCRETION

TABLE 5.6 SAMPLE ANALYSES FOR TOTAL CARBON
(as weight percent C)

Sample	Percent Analyzed Carbon	Percent Calculated Carbon in Carbonate*	Difference From Anal. C
**M-110	0.62%	0.28%	+ 0.34%
**SP-55	0.34%	0.22%	+ 0.12%
Red and Green Mudstones			
M-107	0.05%	0.11%	- 0.06%
CH-1	-	0.18%	-
HH-26	-	0.09%	-
40205	0.09%	0.21%	- 0.12%
M-18	0.04%	0.13%	- 0.09%
SP-735	-	0.19%	-
HH-47	-	0.10%	-
HH-54	-	0.11%	-
OP-57	0.12%	0.12%	0.00%
SP-73-6	n.d.	0.15%	-
Carbonate-rich Samples***			
M-101top	3.14%	3.51%	- 0.37%
M-88-A	2.65%	3.59%	- 0.94%
NC-20-2	9.81%	10.14%	- 0.33%
HH-39b	5.44%	5.30%	+ 0.13%
CC-13	9.39%	9.34%	+ 0.05%
SP-33b	4.91%	4.83%	+ 0.08%
M-90bot	6.32%	7.91%	- 1.59%
M-96bot	4.64%	4.98%	- 0.34%
HH-34A	7.60%	6.76%	+ 0.94%
HH-38	3.98%	4.34%	- 0.36%
LZ-6A	2.56%	2.70%	- 0.14%
LY-14A	3.93%	3.80%	+ 0.13%

n.d. = none detected.

* assuming that all analyzed CaO is present as $CaCO_3$, and all MnO as $MnCO_3$.

** these two samples are black mudstone samples from the Middle Cambrian.

*** all of these samples are from the manganese horizon, except for sample NC-20-2, which is a sample of the Smith Point Limestone Formation.

the bulk of the MnO and CaO are present in the rocks in the form of carbonate minerals, as in most cases there is little difference between the analyzed and calculated C totals. Two samples from the manganese horizon contain more MnO + CaO than can be accommodated in carbonate minerals by the analytically determined C content, and hence probably contain some of these elements in other mineral phases (e.g., Mn-oxides).

Sulphur Content of Samples

The S content of 17 samples was determined with a Leco induction furnace. The results of these analyses, presented in Table 5.7, indicate that, in general, the rocks are not enriched in S. No S was detected in over half of the samples, and in only one sample did the amount exceed 0.5%. The sulphur present in the rocks can be accommodated in the pyrite and barite known from thin section examination to be present in some samples.

Relationship Between Loss on Ignition and Carbonate Mineral Content

Figure 5.4 is a plot of the analyzed total of CaO + MnO against the weight loss on ignition (LOI). The high positive correlation suggests that, as the CaO and MnO largely occur in carbonate minerals, the LOI total is essentially an indication of the amount of CO_2 in the rock samples. The trend intersects the vertical axis at several percent LOI, which is interpreted to be the average amount of LOI in argillaceous samples due to H_2O.

5.3 Chemical Composition Within Stratigraphic Sections

The results of the major element analyses of Cambrian rock

TABLE 5.7 RESULTS OF S ANALYSES FOR SELECTED CAMBRIAN SAMPLES

Sample Number	Weight % S
CH-7-2	n.d.
NM-10	n.d.
BE-8	0.30
NC-20-1	n.d.
WB-40	n.d.
DB-96	n.d.
CH-29	0.015
LY-22	0.055
SP-12-1	trace
W-10top	1.65
HH-38	0.10
HH-14	n.d.
4127	n.d.
SP-40	less than 0.005%
CH-1	n.d.
NC-17	n.d.
HH-55	n.d.

n.d. = none detected

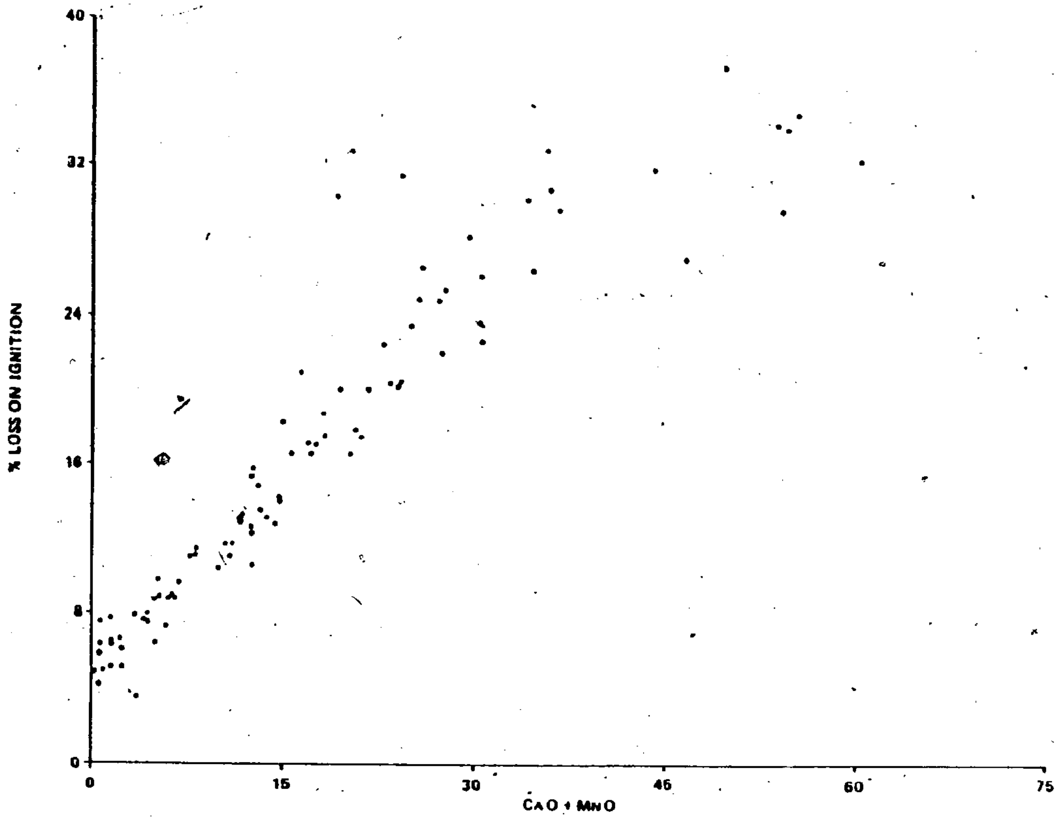

FIG. 5.4 RELATIONSHIP BETWEEN Σ (CAO + MNO) AND LOSS ON IGNITION (93 SAMPLES)

samples were examined to determine what, if any, spatial changes take place in chemical composition, whether these be related to stratigraphic position (i.e., changes in composition of rocks through time) or to geographic position (i.e., regional chemical differences within the basin at any particular time). The results of this examination are discussed in the remainder of this section.

5.3.1 Mudrocks

The red and green mudrocks comprising the bulk of the Adeyton Group are of uniform chemical composition throughout the study area, and no pronounced compositional trends are apparent through the various sampled stratigraphic sections. Table 5.8 presents the average major element compositions of all green mudrock samples from the Chamberlain's Brook and Brigus Formations (with the average composition of all green mudrocks added for comparative purposes). The table shows that green mudrocks from the two formations are of similar composition, and that no large shifts in composition occur in the younger Chamberlain's Brook mudrocks. The increase in K_2O in the Chamberlain's Brook Formation, coupled with the small decreases in SiO_2 and Na_2O, may indicate that the proportions of quartz and feldspar are somewhat reduced while that of illite is increased in the younger rocks.

Chemical variation diagrams were plotted for the 'key' sections around Trinity and Conception Bays (see Sec. 3.2) in order to further examine the nature of spatial changes in chemical composition in the section. The variation diagrams are presented in Figures 5.5.1 through 5.5.5. These diagrams suggest that the red and green

7

TABLE 5.8 VARIATION IN MAJOR ELEMENT COMPOSITION OF GREEN MUDSTONES WITH POSITION IN STRATIGRAPHIC SEQUENCE.

No. Chamberlain's Brook Formation Samples = 37.
No. Brigus Formation Samples = 42.

	All Green Mudstones	All Green Mudstones, Chamberlain's Brook Formation	All Green Mudstones, Brigus Formation
Fe_2O_3	8.32% s.d. = 1.76%	8.97% (s.d. = 1.96%)	8.14% s.d. = 1.51%
TiO_2	0.88% s.d. = 0.09%	0.85% (s.d. = 0.07%)	0.87% s.d. = 0.09%
P_2O_5	0.22% s.d. = 0.12%	0.23% (s.d. = 0.14%)	0.20% s.d. = 0.07%
SiO_2	57.17% s.d. = 3.41%	56.18% (s.d. = 2.67%)	57.27% s.d. = 3.56%
CaO	1.22% s.d. = 1.65%	1.22% (s.d. = 1.24%)	1.21% s.d. = 2.12%
K_2O	3.56% s.d. = 0.69%	3.74% (s.d. = 0.67%)	3.46% s.d. = 0.68%
MgO	2.47% s.d. = 0.77%	2.19% s.d. = 0.71%	2.72% s.d. = 0.72%
Al_2O_3	18.95% s.d. = 1.82%	19.20% s.d. = 1.60%	19.00% s.d. = 1.91%
MnO	0.47% s.d. = 0.64%	0.61% s.d. = 0.94%	0.34% s.d. = 0.22%
Na_2O	1.40% s.d. = 0.38%	1.13% s.d. = 0.29%	1.54% s.d. = 0.27%
Ba	0.14% s.d. = 0.36%	0.15% s.d. = 0.69%	0.17% s.d. = 0.53%

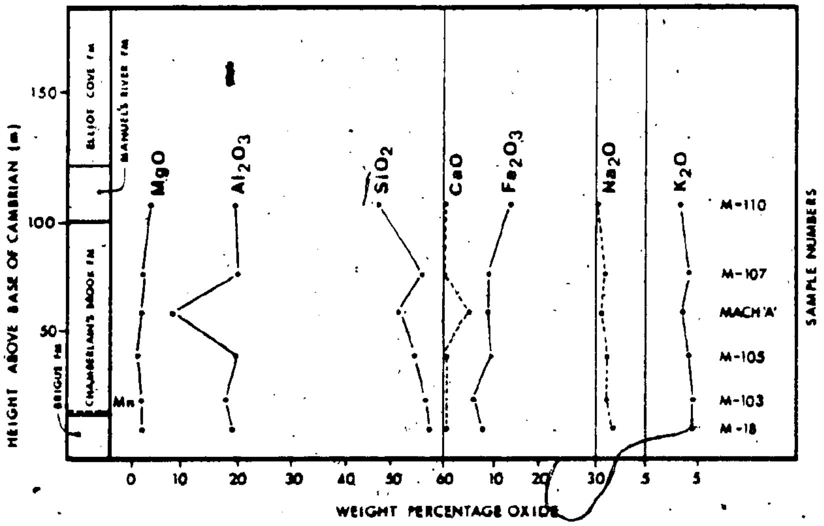

FIGURE 5·5·1
CHEMICAL VARIATION DIAGRAM THROUGH MANUEL'S RIVER SECTION

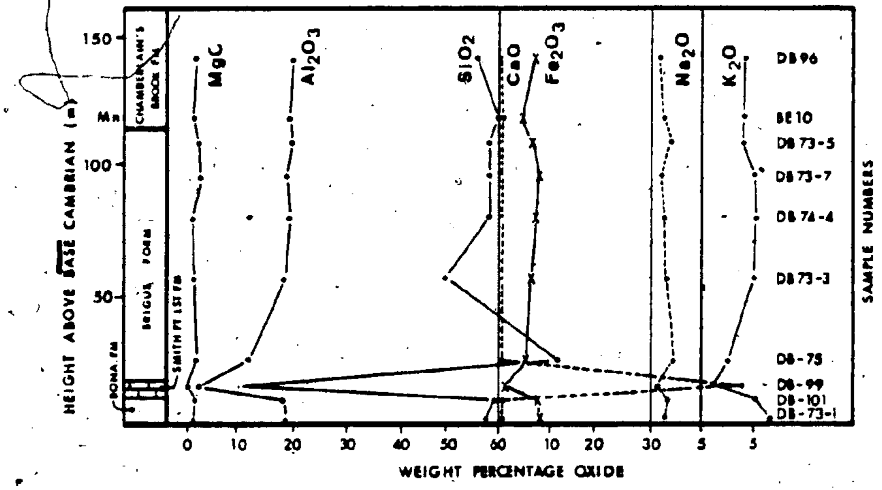

FIGURE 5·5·2
CHEMICAL VARIATION DIAGRAM THROUGH BRIGUS SECTION

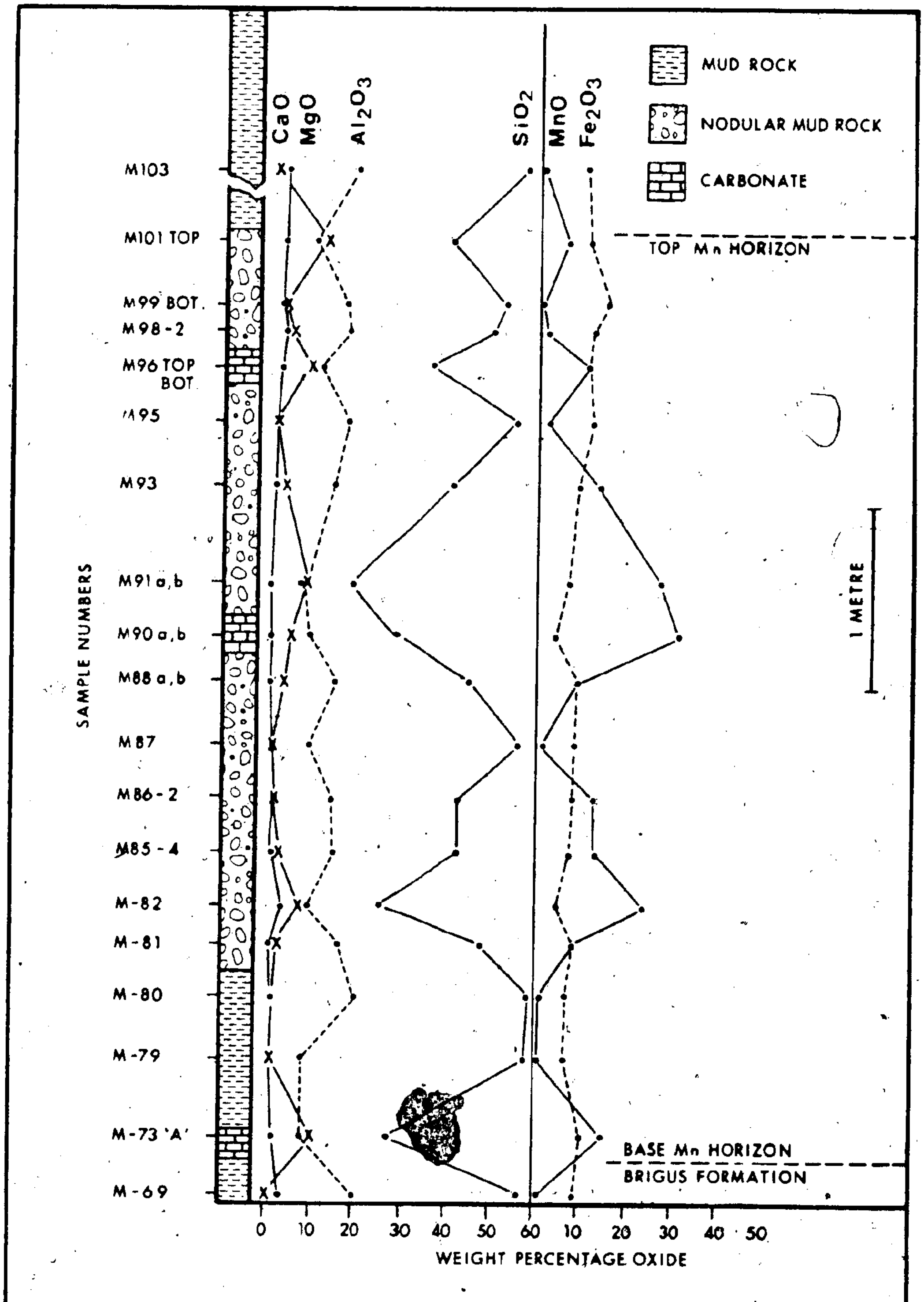

FIGURE 5·5·1a
CHEMICAL VARIATION THROUGH MANGANESE HORIZON, MANUEL'S RIVER

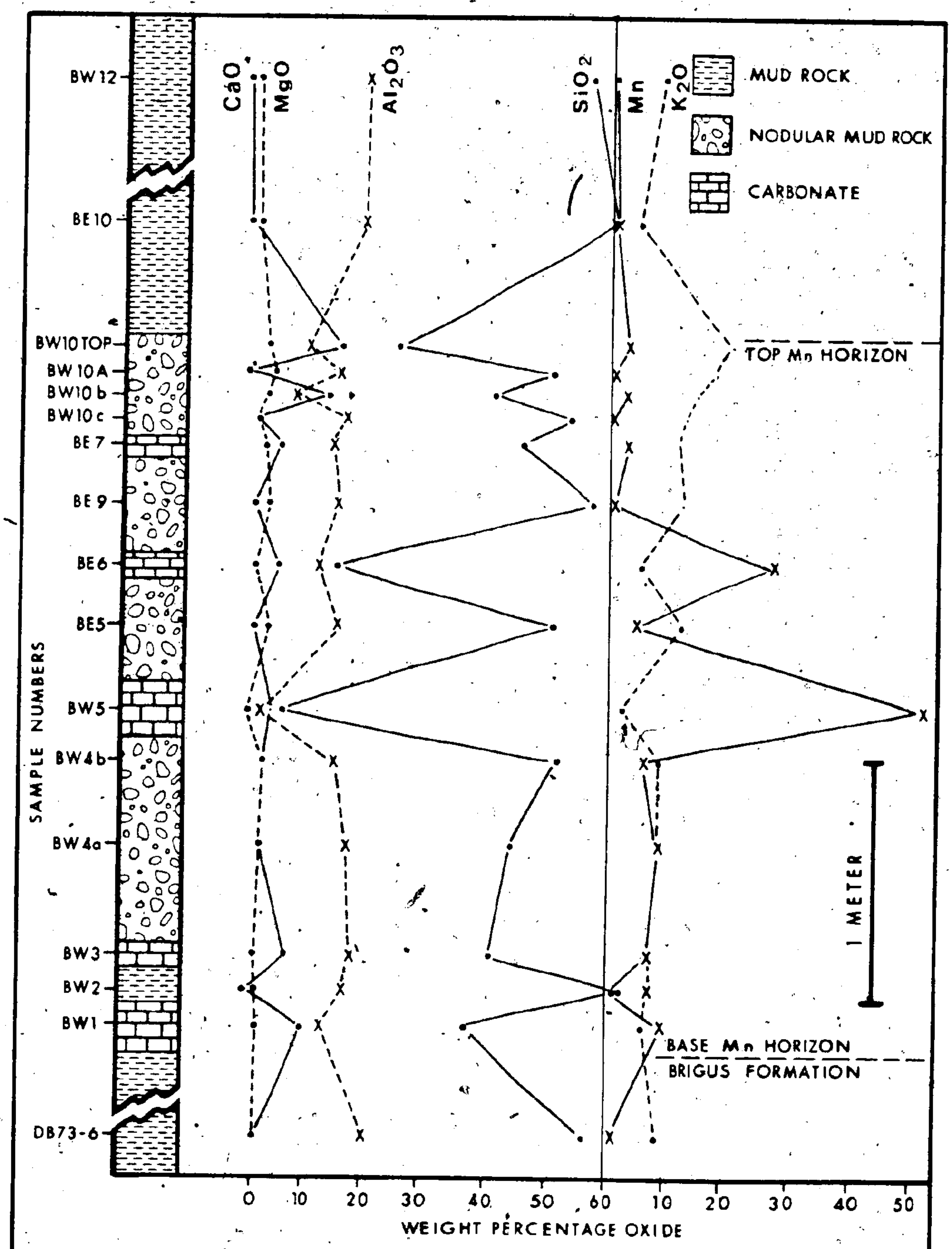

FIGURE 5·5·2a
CHEMICAL VARIATION THROUGH MANGANESE HORIZON, BRIGUS

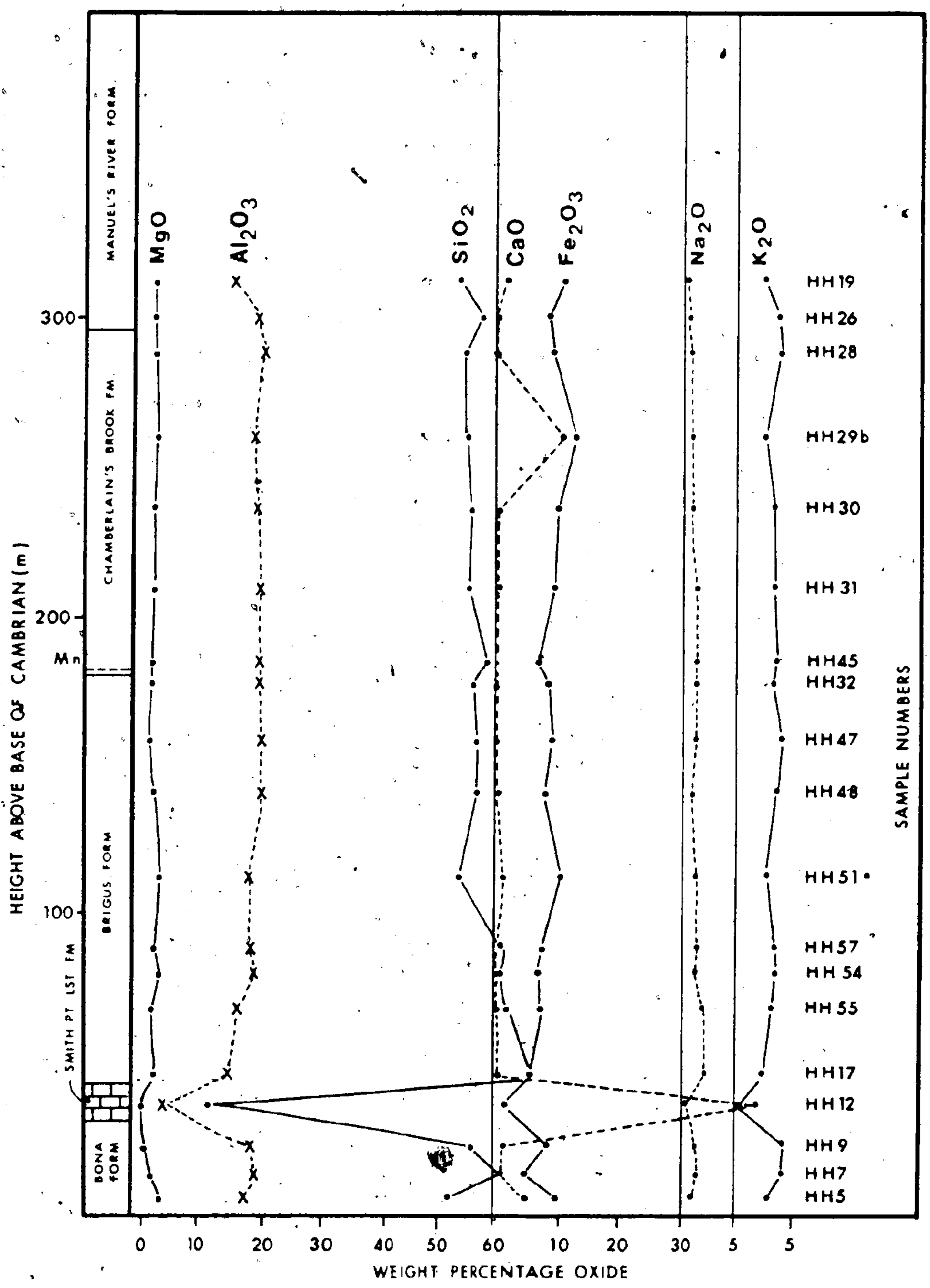

FIGURE 5·5·3
CHEMICAL VARIATION THROUGH HOPEALL HEAD SECTION

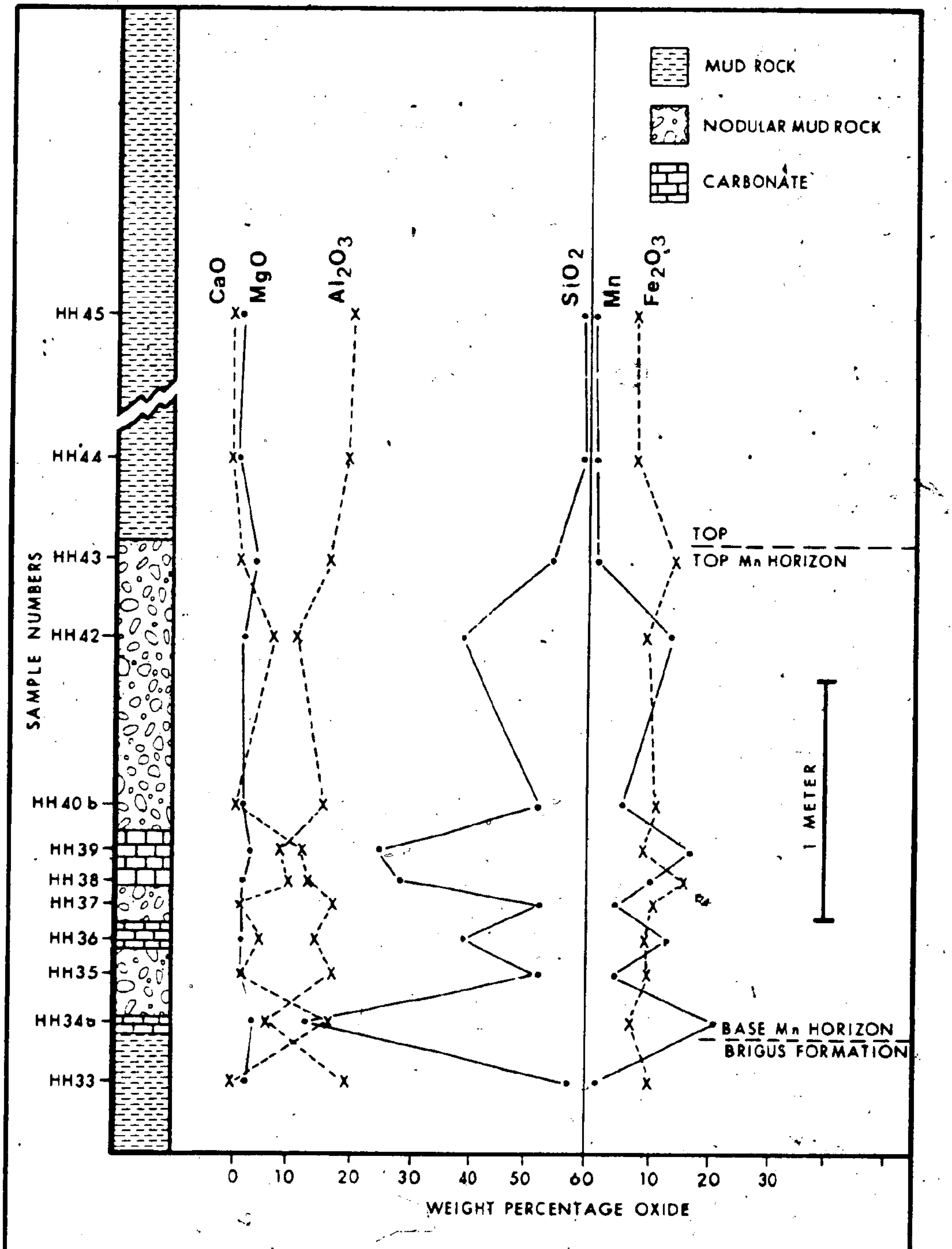

FIGURE 5·5·3a
CHEMICAL VARIATION THROUGH MANGANESE HORIZON, HOPEALL HEAD

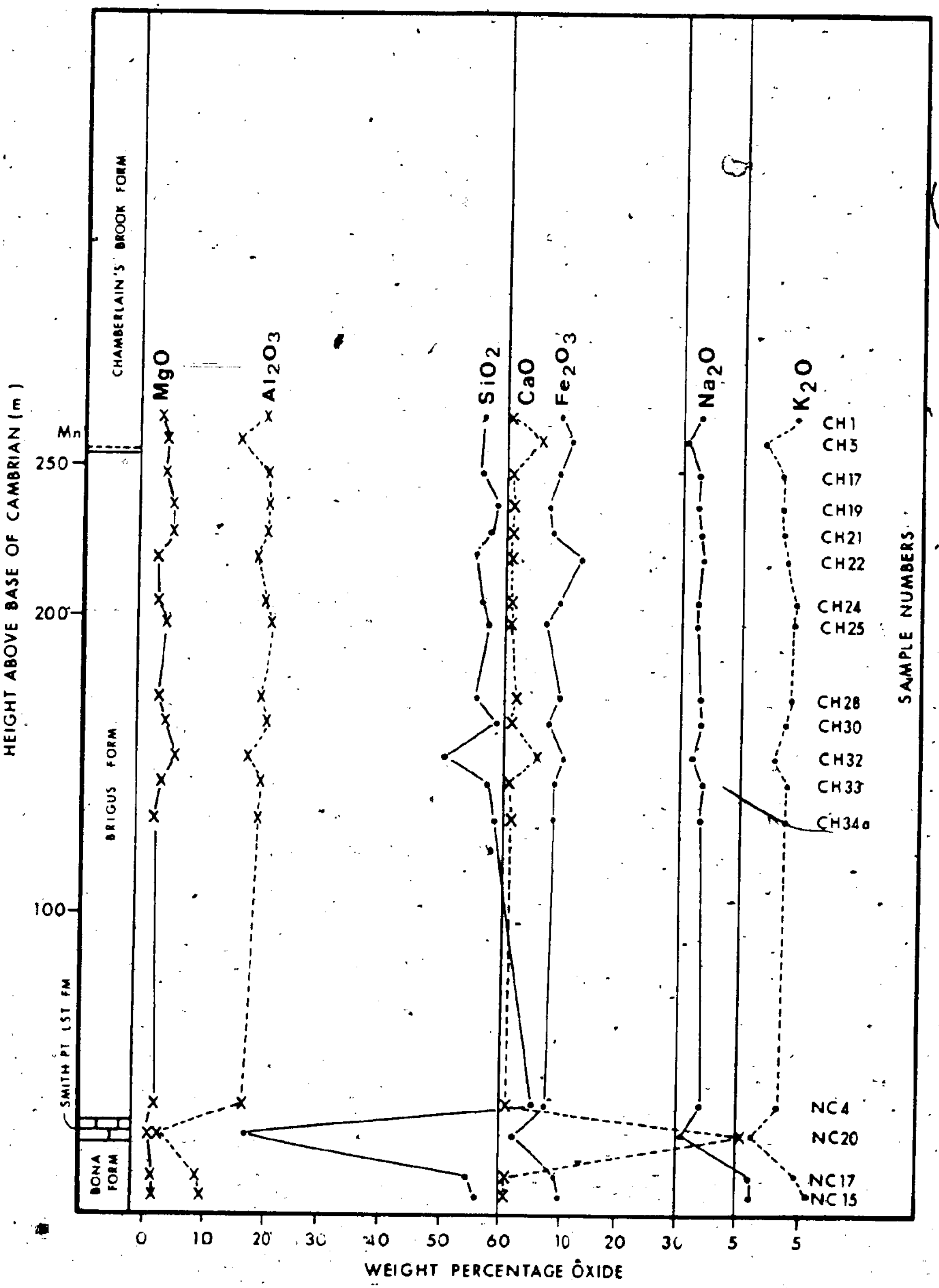

FIGURE 5·5·4
CHEMICAL VARIATION THROUGH CHAPEL HEAD SECTION

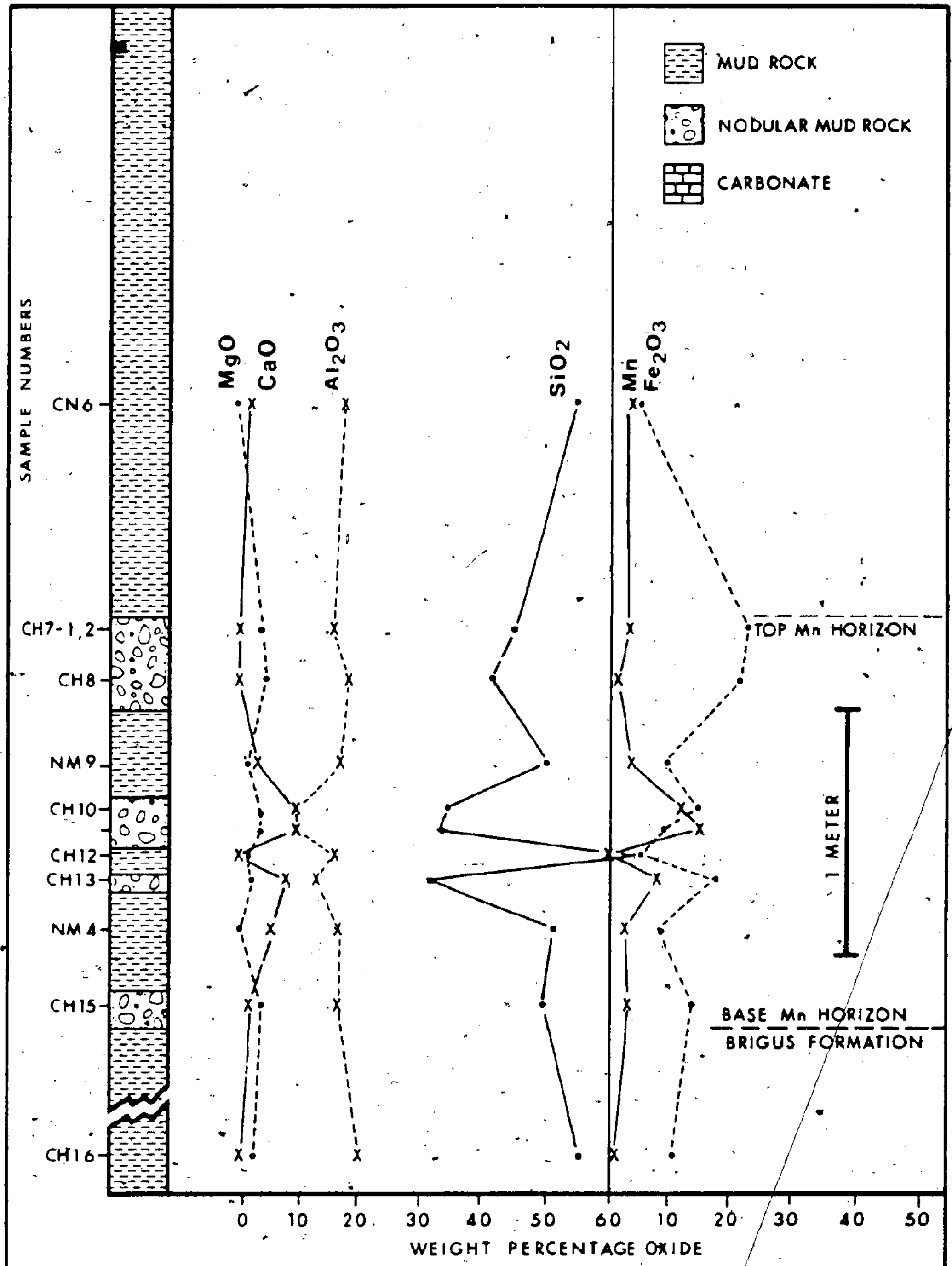

FIGURE 5·5·4a
CHEMICAL VARIATION THROUGH MANGANESE HORIZON, CHAPEL HEAD

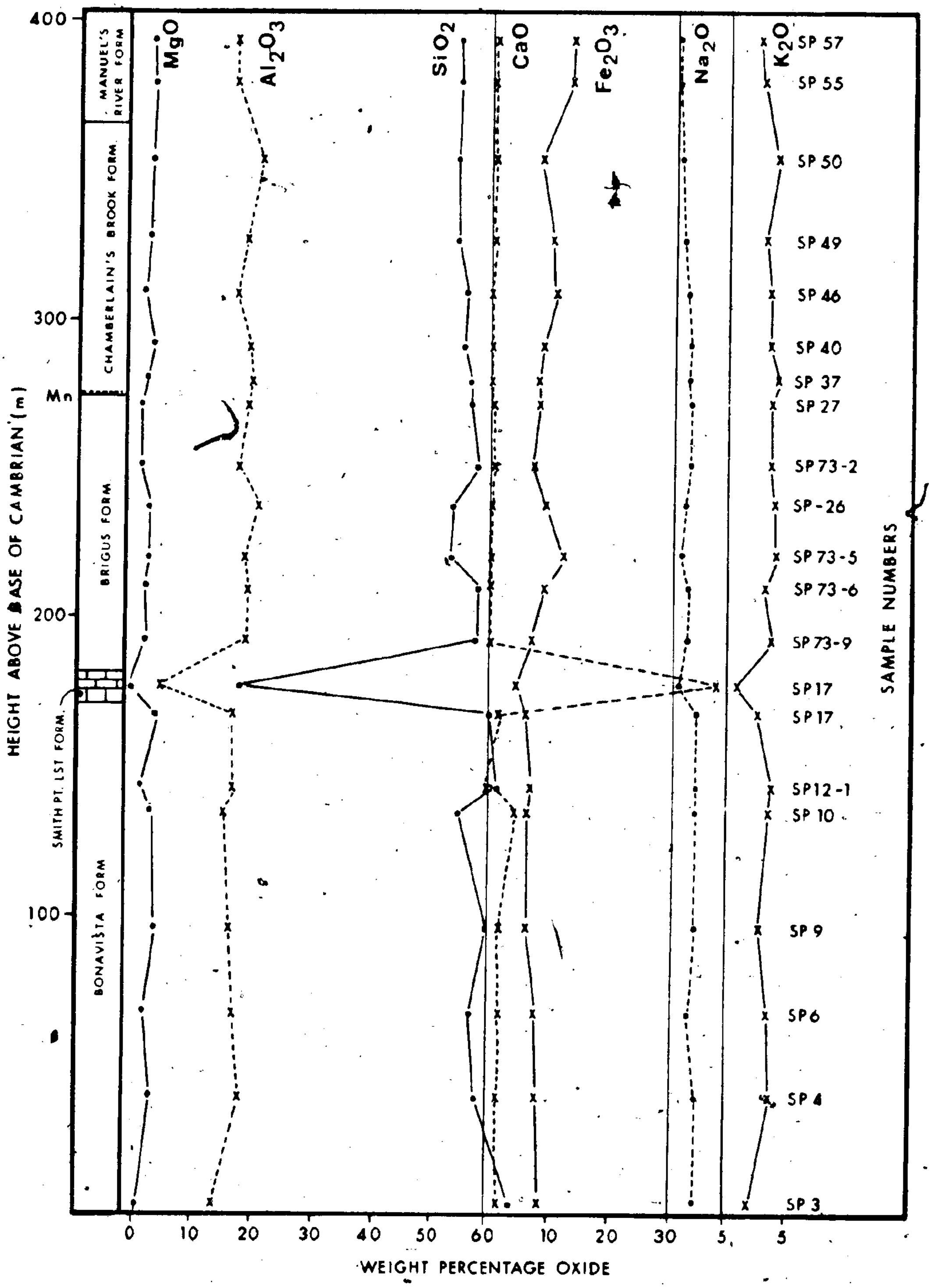

FIGURE 5·5·5
CHEMICAL VARIATION THROUGH SMITH POINT SECTION

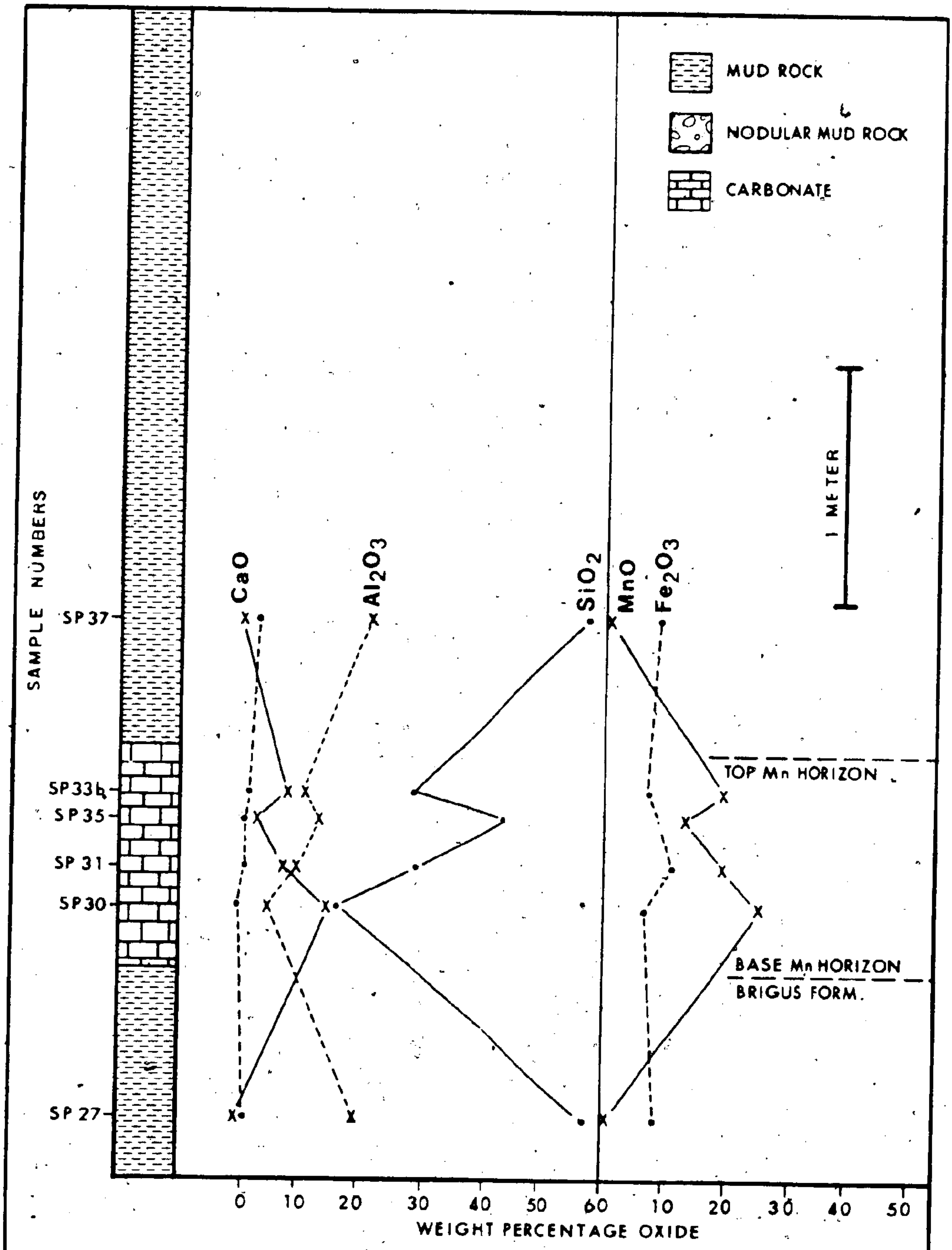

FIGURE 5·5·5a
CHEMICAL VARIATION THROUGH MANGANESE HORIZON, SMLTH POINT

mudrocks in the Adeyton Group are chemically homogeneous throughout the section in the study area. The chemical trends are the same in all diagrams, with a tendency towards a reduction in younger rocks of the SiO_2 and Na_2O contents, suggesting, as do the data in Table 5.8, that there may be a progressive reduction in the proportions of quartz and feldspar through time. These trends are most apparent in the sections in which the Lower Cambrian Bonavista and Brigus Formations are well-developed. The older mudrocks not uncommonly attain Na_2O contents of about 2%, which is considerably higher than that of younger (e.g., Chamberlain's Brook) mudrocks. The upwards decrease in quartz and feldspar (and concomitant increase in 'clay-size' mineral components such as illite) may reflect the development of progressively more quiescent conditions in the basin, the gradual increase in distance of the sections from land areas due to continued Lower Cambrian transgression, or the gradual erosional levelling of the source regions through time.

5.3.2 Manganese Horizon

The average major element concentrations of the analyzed samples from the manganese horizon exposures at Manuel's River, Conception Bay and Chapel Head, Trinity Bay (Table 5.9) serve to illustrate that the average composition of the manganese horizon is quite variable regionally. However, it is likely that a portion of the apparent chemical differences is due to sampling bias in favor of either the carbonate or argillaceous fractions of the manganese horizon. Such sampling bias could enhance the differences between the average horizon compositions in two localities, creating arti-

TABLE 5.9 AVERAGE MAJOR ELEMENT CONTENT OF MANGANESE HORIZON SAMPLES, FOR ALL ANALYZED SAMPLES AND FOR TWO SELECTED STRATIGRAPHIC SECTIONS.

Average concentration of all samples included for comparison.

	All Samples max. no. cases = 374	All Manganese Horizon Samples max. no. cases = 133	Manuel's River Manganese Horizon Samples	Chapel Head Manganese Horizon Samples
Fe_2O_3	8.26% (s.d. = 3.81%)	9.55% (s.d. = 4.58%)	8.74% s.d. = 2.59%	12.88% s.d. = 5.80%
TiO_2	0.70% (s.d. = 0.33%)	0.56% (s.d. = 0.23%)	0.61% s.d. = 0.19%	0.63% s.d. = 0.17%
P_2O_5	0.33% (s.d. = 0.46%)	0.56% (s.d. = 0.69%)	0.66% s.d. = 0.74%	0.22% s.d. = 0.16%
SiO_2	45.25% (s.d. = 16.92%)	37.24% (s.d. = 15.01%)	40.17% s.d. = 13.56%	43.14% s.d. = 12.4%
CaO	7.83% (s.d. = 11.90%)	6.78% (s.d. = 5.18%)	4.64% s.d. = 3.56%	5.42% s.d. = 4.7%
K_2O	2.67% (s.d. = 1.46%)	1.92% (s.d. = 1.24%)	2.53% s.d. = 1.17%	1.81% s.d. = 1.18%
MgO	2.38% (s.d. = 1.48%)	2.55% (s.d. = 1.25%)	1.94% s.d. = 0.91%	3.04% s.d. = 1.44%
Al_2O_3	14.31% (s.d. = 5.62%)	12.14% (s.d. = 4.71%)	13.31% s.d. = 4.12%	14.68% s.d. = 3.44%
MnO	4.62% (s.d. = 8.85%)	11.80% (s.d. = 11.72%)	11.55% s.d. = 10.91%	6.00% s.d. = 6.02%
Na_2O	1.07% (s.d. = 0.72%)	0.62% (s.d. = 0.42%)	0.81% s.d. = 0.45%	0.65% s.d. = 0.45%
Ba	0.27% (s.d. = 0.64%)	0.53% (s.d. = 0.94%)	0.66% s.d. = 0.86%	0.15% s.d. = 0.45%

ficial variations in composition.

The average Mn/Fe ratio in the manganese horizon increases in a south to north direction on the Avalon Peninsula (Figure 5.6). Note that the weighted Fe values used to calculate the ratios in Figure 5.6 are "excess' Fe values. For all analyzed mudrocks (Table 5.1), the ratio $(Fe_2O_3/Al_2O_3) \times 10 = 4.5$. It is assumed that this value of 4.5 reflects the Fe_2O_3/Al_2O_3 ratio in normal clastic sedimentation (i.e. Fe present in minerals of the silicate mineral group). Ratios greater than 4.5 occur in the manganese horizon (Figure 5.8) and the Fe responsible for the increase is taken as Fe associated with Mn during manganese horizon deposition. This 'excess' Fe was used to calculate the Mn/Fe values in Figure 5.6.

The values shown on Figure 5.6 are weighted averages and include both carbonate and argillaceous beds within the horizon. The Mn/Fe ratio in southern Avalon Peninsula exposures (not calculated) must approach that of the average mudstone (0.05) as most of the horizon in these exposures consists of normal red and green mudstone. Proceeding north, the Mn/Fe ratio increases to about 2.0+ in exposures about the heads of Trinity and Conception Bays, and to about seven in the northernmost exposures on Trinity Bay.

The axis of sedimentation in the Cambrian basin during the lowermost Middle Cambrian and the approximate transition from the massive manganiferous limestone comprising the manganese horizon in northernmost Avalon Peninsula exposures to a mixed carbonate/shale facies are also shown on Figure 5.6. Paleontological data suggests (Fletcher, 1972) that the basal Middle Cambrian transgression with

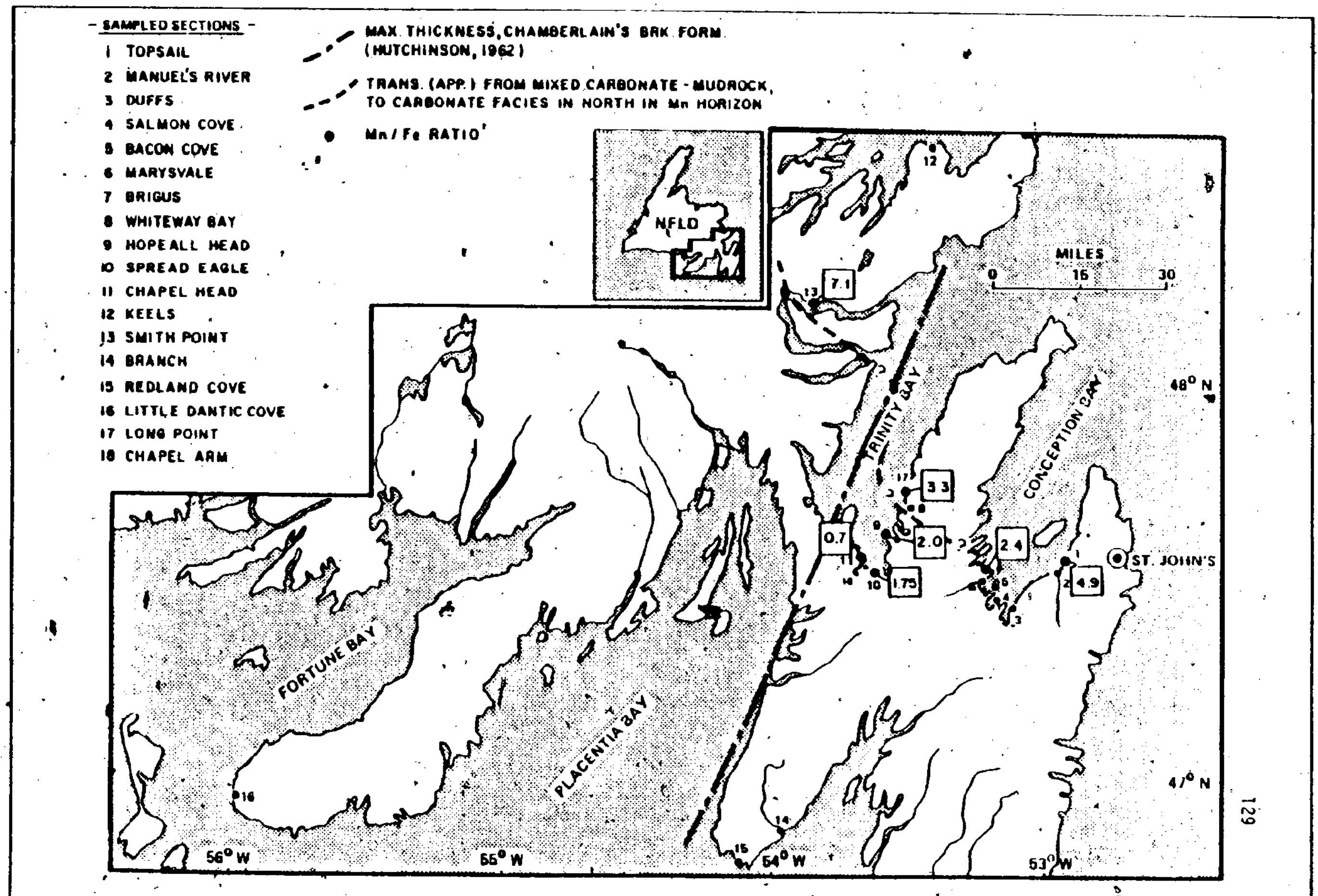

FIGURE 5.6
AVERAGE Mn / Fe RATIOS IN MANGANESE HORIZON SECTIONS, SOUTHEASTERN NEWFOUNDLAND.

which the manganese horizon is associated proceeded from south to north, i.e., at about right angles to the axis of sedimentation shown for the Chamberlain's Brook Formation as a whole. It can be seen, then, that the bulk of the horizon exposures available for sampling around the heads of Trinity and Conception Bays are near-parallel to depositional strike. This unfortunately restricts opportunity to sample the manganese horizon across strike so as to systematically record changes in thickness/chemistry, etc.

Major element variation through the manganese horizon in 'key' sections is shown in Figures 5.5.1a - 5.5.5a. Examination of these indicates that: (1) MnO and SiO_2 are strongly negatively correlated. The same is true for MnO and other elements controlled by the silicate mineral group (Al_2O_3, K_2O, etc.); and (2) the horizon becomes increasingly rich in Fe_2O_3 from bottom up and the uppermost portion is anomalously rich in this element relative to enclosing mudrocks.

Examination of Ba and P_2O_5 data for these sections indicates that anomalous Ba is associated with MnO in the lower portions of the horizon and anomalous P_2O_5 with Fe_2O_3 at or near the top.

~~Figure 5~~.7 shows major element variation through the Brigus exposure of the manganese horizon with the elements ratioed against Al_2O_3 (on the assumption this element is most indicative of silicate or 'detrital' sedimentation). The same relationships present in Figures 5.5.1a - 5.5.5a can be seen here, though the anomalous behavior and concentrations of Fe_2O_3 are more evident. Note also how high Fe_2O_3 contents are maintained at the top of the horizon after MnO values have returned to normal or near-normal levels (i.e., mudrock

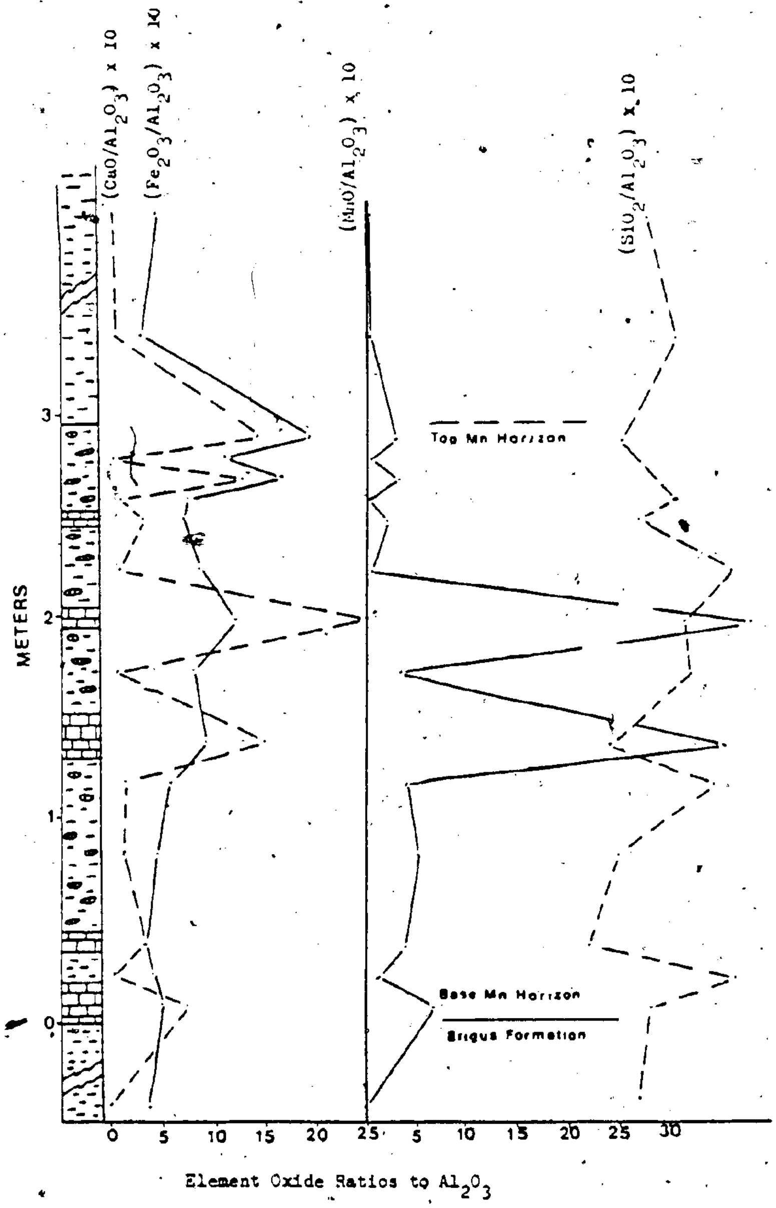

Figure 5.7
Chemical Variation through Manganese Horizon Relative to Al_2O_3 Content in Brigus Section

concentration). This behavior is present also in other exposures located at the heads of Trinity and Conception Bays (Figure 5.8). Note also in Figure 5.7 that the ratio (SiO_2/Al_2O_3) x 10 does not change appreciably from its average value of 30 within the manganese horizon at Brigus. This is interpreted as being due to the association of SiO_2 in the manganese horizon with anomalous Fe_2O_3 concentrations (Figure 5.8) as the mineral chlorite; the iron carbonate only rarely occurs and iron is not abundant in manganese carbonate (Section 5.2.2).

The significance of these chemical variations within the manganese horizon as concerns its origins is considered in Chapter 8.

5.4 Comparison of Newfoundland Mudrocks to Other Mudrocks

The average major element chemical compositions of 155 red and green mudrock analyses is presented in Table 5.10, together with several other estimates of the average chemical composition of mudrocks. Table 5.10 indicates that the Newfoundland mudrocks are of similar chemical composition to these estimates of mudrock composition (e.g., Clarke, 1924). The average CaO content of the Newfoundland rocks most closely parallels the estimated composition for the average Paleozoic shale and average slate compositions, with the Al_2O_3 content also closest to the latter. The MnO content of the average Newfoundland mudrock is greater than that reported for any of the other average rock compositions. The higher MnO content is more characteristic of the green mudrocks, as red mudrocks alone average only 0.21% MnO.

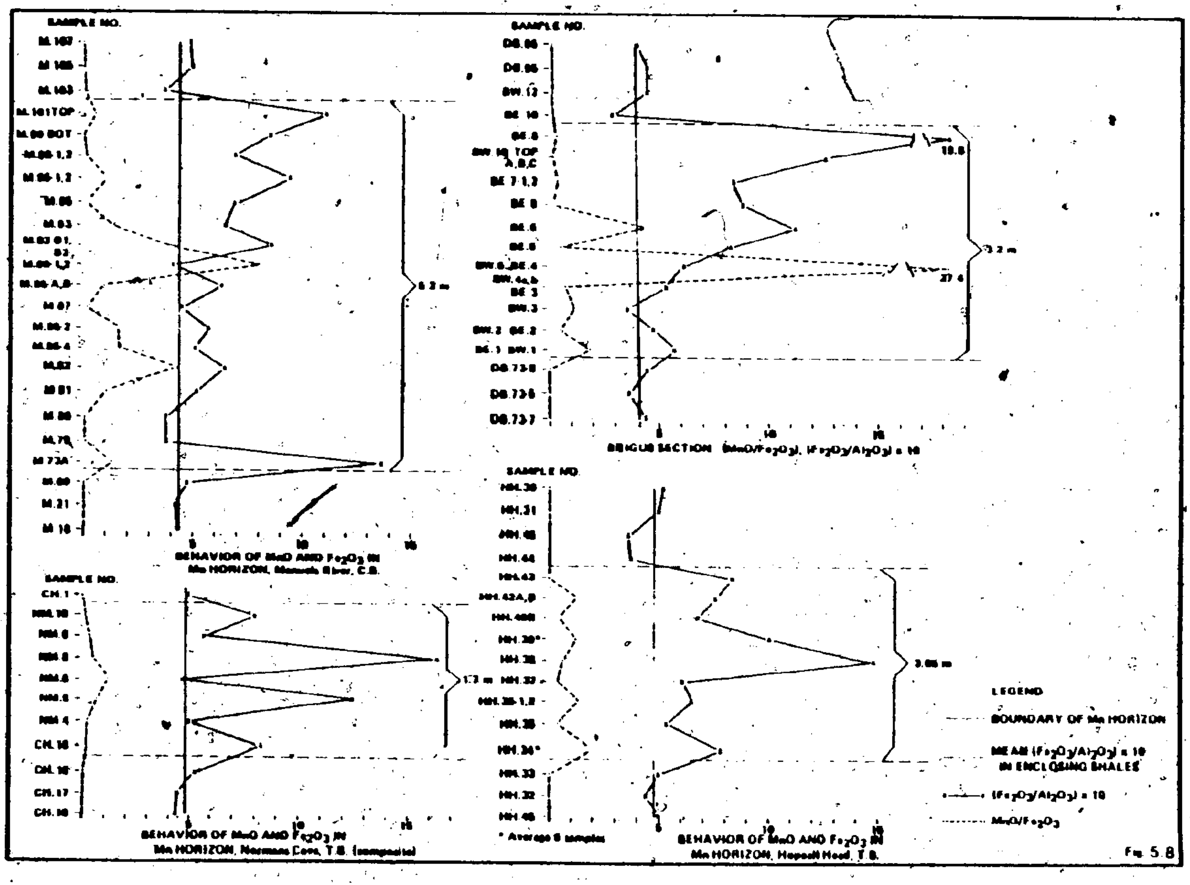
SAMPLE NO.
M.107
M.105
M.103
M.101TOP
M.99 BOT
M.99-1,2
M.98-1,2
M.95
M.93
M.93 B1, B2,
M.90-1,2
M.96-A,B
M.87
M.86-2
M.86-4
M.82
M.81
M.80
M.79
M.73A
M.80
M.21
M.18
5
10
15
6.2 m
BEHAVIOR OF MnO AND Fe2O3 IN Mn HORIZON, Mosquito River, C.B.
SAMPLE NO.
DB.86
DB.85
BW.12
BE.10
BE.8
BW.10 TOP A,B,C
BE 7-1,2
BE 8
BE.6
BE.5
BW.6, BE.4
BW.4a,b
BE 3
BW.3
BW.2 BE.2
BE.1 BW.1
DB.73-8
DB.73-6
DB.73-7
5
10
15
18.8
27.4
3.2 m
BRIGUS SECTION (MnO/Fe2O3), (Fe2O3/Al2O3) x 10
SAMPLE NO.
CH.1
NM.10
NM.6
NM.8
NM.6
NM.5
NM.4
CH.18
CH.16
CH.17
CH.10
5
10
15
1.7 m
BEHAVIOR OF MnO AND Fe2O3 IN Mn HORIZON, Normans Cove, T.B. (composite)
SAMPLE NO.
HH.30
HH.31
HH.46
HH.44
HH.43
HH.42A,B
HH.40B
HH.39*
HH.38
HH.37
HH.35-1,2
HH.35
HH.34*
HH.33
HH.32
HH.45
* Average 8 samples
5
10
15
3.05 m
BEHAVIOR OF MnO AND Fe2O3 IN Mn HORIZON, Hopeall Head, T.B.
LEGEND
BOUNDARY OF Mn HORIZON
MEAN (Fe2O3/Al2O3) x 10 IN ENCLOSING SHALES
(Fe2O3/Al2O3) x 10
MnO/Fe2O3

Fig. 5.8

TABLE 5.10 COMPARISON OF MEAN MUDSTONE COMPOSITION WITH OTHER PUBLISHED AVERAGE COMPOSITIONS FOR FINE-GRAINED SEDIMENTARY ROCKS.

	Average Mudstone, this study. (155 samples)	Average Shale[1]	Average Paleozoic Shale[2]	Average Slate[3]	Mudrocks of Russian Platform[4]
Fe_2O_3	8.35% (includes FeO)	4.0%	4.0%	3.0%	3.4%
FeO	-	2.4%	2.9%	4.4%	2.3%
TiO_2	0.89%	0.6%	0.8%	0.8%	0.8%
P_2O_5	0.20%	0.2%	0.2%	0.1%	0.1%
SiO_2	57.76%	58.1%	60.2%	58.5%	56.2%
CaO	1.16%	3.1%	1.4%	1.3%	4.4%
K_2O	3.75%	3.2%	3.6%	3.7%	2.6%
MgO	2.18%	2.4%	2.3%	2.6%	2.1%
Al_2O_3	18.50%	15.4%	16.4%	17.3%	15.1%
MnO	0.37%	trace	trace	0.1%	0.1%
Na_2O	1.46%	1.3%	1.0%	1.2%	1.1%

1. 78 samples; Clarke, 1924.
2. 51 samples; Clarke, 1924.
3. 69 samples; Pettijohn, 1957.
4. 290 analyses; Ronov et al., 1966.

The chemical similarity of the Newfoundland mudrocks to other mudrocks is illustrated in Figure 5.9 which compares the Na_2O and K_2O content of lutites through time. The average Newfoundland mudrock composition plots close to the variation trend line near the point representing the average shale composition of Clarke (1924).

Figure 5.10 presents the results for the scattergram plot of K_2O against Al_2O_3 for all analyzed samples. Clarke's average shale and limestone and Pettijohn's (1975) average slate have been plotted on the diagram, as have the average Newfoundland mudrock and limestone compositions. It is apparent that the principal chemical variation trend exhibited by the Newfoundland rocks ranges from approximately the average limestone to the average shale compositions.

5.5 Summary of Results

5.5.1 Chemical Trends

Statistical examination of the results of major and trace element analyses shows that two mineral groups are developed in the Adeyton Group in Newfoundland. The concentrations of SiO_2, Al_2O_3, K_2O, Na_2O, TiO_2, Fe_2O_3, and MgO are related to a silicate mineral group, dominant in mudrock samples, while the content of CaO and MnO are associated with a carbonate mineral group. Elements contained in one group are negatively correlated with those present in the other. Trace element relationships are in turn influenced by the concentration of the major elements, and some specific major-trace element associations can be seen.

The major chemical trend displayed by the rocks is a grada-

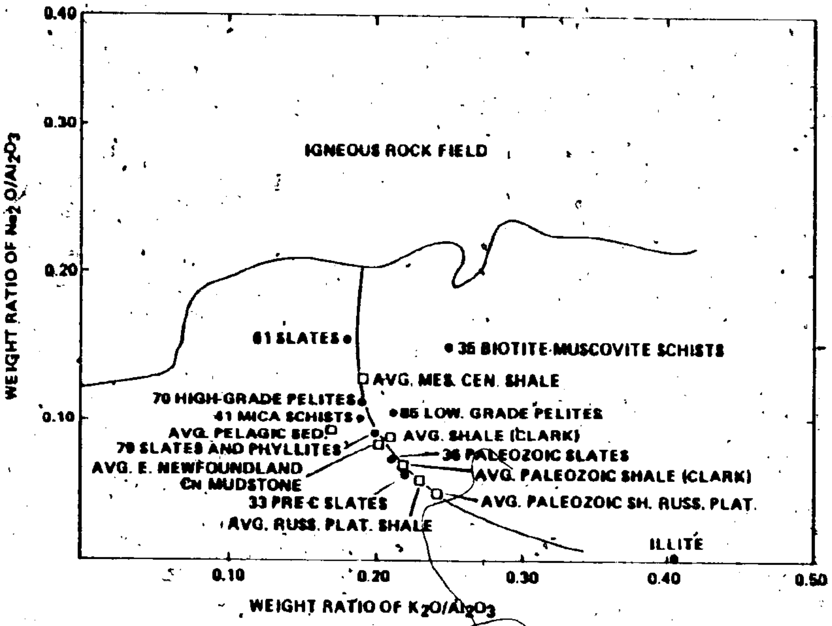

FIG. 5.9 COMPARISON OF E. NEWFOUNDLAND MUDSTONES WITH OTHER LUTITES

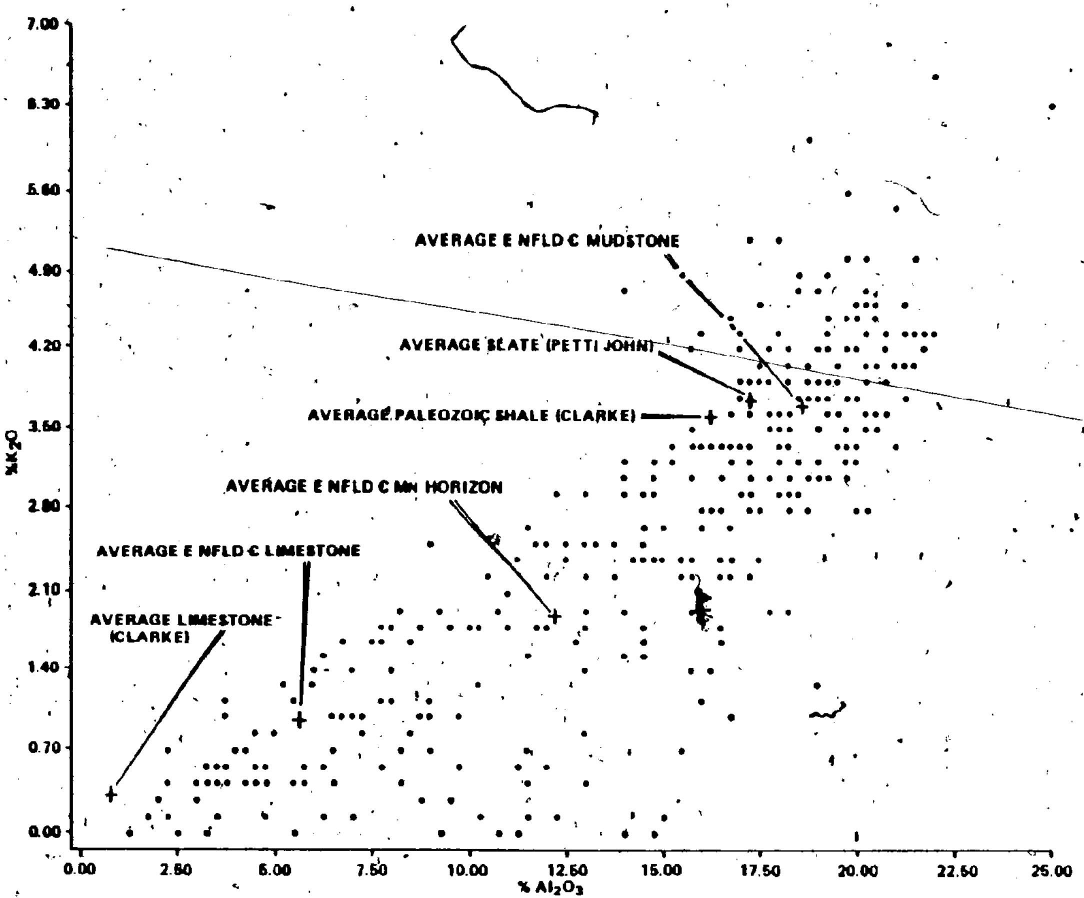

FIG. 5.10 COMPARISON OF E. NEWFOUNDLAND Є ROCKS TO AVERAGE LUTITE AND LIMESTONE

tion from rocks dominated by the carbonate group minerals (limestones, manganese horizon samples) to red and green mudrocks dominated by the silicate mineral group. This chemical variation is visually displayed in scattergram plots of major element concentrations in the rock samples. Electron probe analyses indicate that the chlorite present in the rocks is rich in Fe, and that the carbonates in the manganese horizon contain variable amounts of Mn, with the carbonates most enriched in this element close in composition to rhodochrosite.

5.5.2 Mudrock Composition

The red and green mudrocks comprising the bulk of the Lower and Middle Cambrian Adeyton Group form chemically homogeneous groups, with no pronounced regional variations in composition in the Avalon Peninsula region. Upwards decreases in the contents of SiO_2 and Na_2O probably reflect a gradual decrease in the concentration of quartz and feldspar in the mudrocks through time, possibly due to increasing distance of the depositional sites from the source regions because of continued gradual transgression, or from the gradual erosional beveling of the source areas through time. In terms of chemical composition, red and green mudrocks form similar groups. Green mudrocks are enriched in MgO and depleted in K_2O relative to red mudrocks.

The Newfoundland mudrocks are similar in chemical composition to other published estimates for the composition of fine-grained sedimentary rocks, suggesting that no special processes, conditions or sources were required for their deposition. Analytical data indicate that the mudrocks (in particular green mudrocks) are somewhat enriched in MnO relative to other analyzed groups of fine-grained sedimentary rock.

5.5.3 Manganese Horizon Composition

Chemical analyses indicate that the manganese horizon is characterized by increased concentrations of Fe_2O_3, MgO, CaO and MnO. Some samples from the horizon also contain anomalously high concentrations of Ba and P_2O_5, while trace element analyses suggest that it is enriched, relative to the enclosing mudrock sequence, in Sr, Ce, and possibly Nb. Regionally, the average manganese horizon concentrations of major elements exhibit considerable changes, particularly with respect to Fe_2O_3 and MnO, with the latter enriched in northernmost exposures of the manganese horizon in the Trinity-Conception Bay region on the Avalon Peninsula. The proportion of Fe in the horizon in exposures about the heads of Trinity and Conception Bays increases from the base towards the top. The distribution of Ba and P_2O_5 is spatially irregular, both between localities and within individual localities.

Major element chemical trends within the manganese horizon are summarized, in schematic fashion, in Figure 5.11. Note that increases in the Mn/Al, Ca/Al, and Fe/Al ratios occur in all limestones, not only the manganese horizon. It would appear that the processes which led to deposition of the manganese horizon were operative to a degree throughout deposition of the Adeyton Group.

The data presented in this chapter is further considered in Chapter 8.

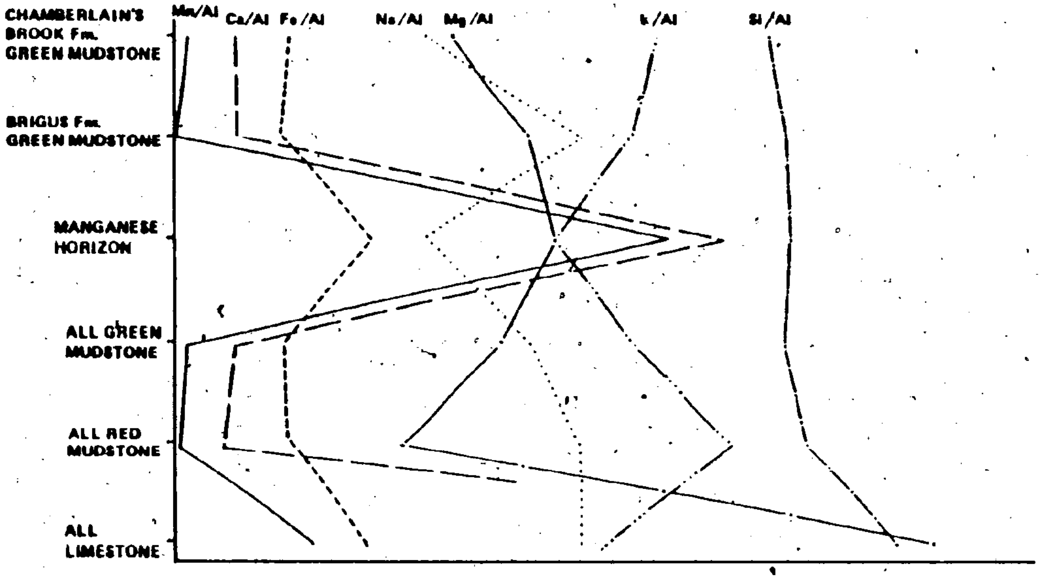

FIG. 5.11 MAJOR ELEMENT CONCENTRATIONS vs. Al_2O_3 FOR MAIN ROCK GROUPS (HORIZONTAL SCALE VARIES FOR DIFFERENT RATIOS)

CHAPTER 6

ECONOMIC POTENTIAL OF CAMBRIAN SEDIMENTARY ROCKS

6.1 Manganese Horizon

Previous Work

In 1900, the Dominion Steel Company began its investigation of the manganese horizon exposure at Kelligrews River, Conception Bay. Additional work was carried out in this area between 1900 and 1910, and in 1909 an attempt was made at mining the ore (Howley & Murray, 1918).

During the Second World War, a number of economically oriented geological surveys of the manganese horizon were conducted at the Brigus, Kelligrews River, and Manuel's River exposures in Conception Bay (Spearman, 1941; Wiseman, 1942; Macaulay, 1944). Several attempts were made during this period to concentrate the manganese ores in these localities (Mines Branch, Ottawa, Investigations No. 1249, 1350 and 1511).

One further beneficiation test was later carried out on material from Brigus (Campbell, 1956), but until recently there has been no further economically oriented work on the manganese horizon.

Results

Grade and Reserves

The results of a limited number of bulk chemical analyses of the material from the Conception Bay manganese horizon exposures indicate that it constitutes a low-grade source of manganese. The highest reported manganese content is 33.35% Mn over a thickness of approximately 0.5 meters for material from Brigus, where the greater detree of oxidation of the horizon probably accounts for the high content (McCartney, 1967). Bulk chemical analyses of material from several other Conception Bay exposures yield lower grades for the horizon - 16.1% Mn over a thickness of about 1.2 meters at Kelligrews River and 10.69% Mn over 1.3 meters at Manuel's River. These grade determinations are more fully discussed by McCartney.

No additional bulk analyses have been made for the present study. The average manganese content (as MnO) of 133 analyzed samples from a number of exposures is 11.8%. A partial listing of the average composition of the manganese horizon samples is given by Table 6.1, while a complete average composition is included in Chapter 5.

TABLE 6.1: AVERAGE CONCENTRATIONS OF SELECTED ELEMENTS IN 133 ANALYZED MANGANESE HORIZON SAMPLES

MnO	11.8%
Fe_2O_3	9.55%
SiO_2	37.24%
CaO	6.78%

Surficial oxidation of the primary manganese carbonate minerals enhances the grade of the horizon to some extent (Wiseman, 1942), so that the grade concentrations given above are somewhat in excess of what is to be expected at depth below the zone of surficial weathering.

The potential reserves of ore at Brigus, where the manganese content of the horizon is greatest, are not believed large, due to truncation of the manganese horizon by faulting no more than 0.4 km offshore of Conception Bay (McCartney, 1967). If it is assumed that the grade of the horizon between Duffs and Topsail along the southeastern margin of Conception Bay remains equal to or better than the grades determined by bulk analysis at Manuel's River and Kelligrews River, there are very large reserves of material 1 meter thick and grading 10% manganese available. The assumptions of uniform grade within this area cannot, however, be accepted without reservation, in view of the pronounced regional variations in thickness and in manganese content elsewhere in the study area (present study; McCartney, 1967; Fletcher, 1972).

Results of Beneficiation Tests

The low grade of the manganese horizon precludes its economic exploitation in the absence of a suitable concentration process. Several series of concentration tests have been made on samples from the manganese horizon exposures at Brigus, Kelligrews River, and Manuel's River (see Mines Branch reports listed above and Campbell, 1956). A variety of techniques were applied to the material; of these, the only one to give encouraging results was a combination sink-float process, which produced a roasted sink product containing 57.06% manganese. However, recovery of manganese with this method was low, due to the complex admixture of carbonate and argillaceous material on a very fine scale and the consequent difficulties in mechanically separating the manganese carbonates. Encouraging results were obtained from material at Brigus, which produced commercially acceptable silicomanganese upon treatment by a single stage electric smelting technique. Whether or not the process would be equally effective with the lower grade material in southeastern Conception Bay exposures remains unknown.

Trace Element Concentrations

Recent oceanic accumulations of ferromanganese nodules and encrustations contain appreciable amounts of Cu, Ni, Pb, and Co in addition to the Mn (up to 1% in some cases), and this fact is responsible for much of the current interest in these deposits as potential economic sources for these metals and manganese (Mero, 1972). One of the objectives of the present study was to determine the trace metal concentrations in the manganese horizon, to ascertain if it too is characterized by anomalously high trace metal contents, which would increase the economic potential of the horizon. However, as reported in Chapter 5, the manganese horizon is not enriched in Cu, Ni, or any other trace element to any marked degree. This is assumed to be due to variations in mineralogy, with the carbonate minerals comprising the manganese-bearing component in the Newfoundland horizon not being capable of accepting trace element substitutes in its structure, in contrast to the manganese oxide deposits which 'scavenge' trace metals from sea water.

Summary of Economic Potential

The manganese horizon is not considered amenable to beneficiation by conventional processes. Several factors contribute to this conclusion.

(1) The low grade of the horizon. To this can be added the difficulties in beneficiating the ore, with the fine-grained nature of the host rocks making it difficult to mechanically separate the manganese carbonate minerals from the barren argillaceous matrix. The present of P in these rocks is also deleterious, as this represents an objectionable impurity in the ore.

(2) At the present time, there is no shortage of lower cost conventional (i.e., oxide) manganese ores; reserves on land are currently believed adequate to meet demand until the turn of the century (Drechsler, 1972). In addition, oceanic ferromanganese deposits constitute a very large potential reserve of Mn, Ni, Cu, and Co. The economic potential of such deposits is presently under active investigation.

However, the manganese horizon is currently being evaluated by the L & M Trading Company. This German concern is testing the hypothesis that they will be able to recover manganese economically by means of a new processing technique which they have devised, provided that sufficient reserves can be established (pers. comm. M. Gordon, 1979). The results of this ongoing work may upgrade the economic potential of the manganese horizon.

CHAPTER 7

COMPARISON OF MANGANESE HORIZON WITH OTHER SEDIMENTARY MANGANESE DEPOSITS

7.1 Introduction

Data pertaining to the chemical and mineralogical composition and the geological setting of the manganese-rich sedimentary rocks exposed in southeastern Newfoundland are compared with data on recent and ancient sedimentary manganese deposits. The comparisons indicate that the Newfoundland deposits are similar to manganese accumulations characterized by deposition in shallow marine waters in which the influence of diagenesis is pronounced.

7.1.1 Recent Deposits

The principal types of recent ferromanganese deposits are described in Chapter 1. The principal chemical, mineralogical, and environmental attributes of oceanic ferromanganese deposits are summarized in Table 7.1, together with comparable information on the Newfoundland manganese horizon. The data presented in Table 7.1 suggest that the Newfoundland deposit most closely resembles the diagenetic class of recent ferromanganese deposit, with which it shares the following characteristics:

(1) The presente of manganese in carbonate minerals formed during early diagenesis (Section 4.2.5); manganese carbonate minerals are rare in other types of modern deposits.

(2) Deposition in shallow marine waters.

TABLE 7.1 COMPARISON OF NEWFOUNDLAND MANGANESE HORIZON TO RECENT SEDIMENTARY MANGANESE DEPOSITS

TYPE OF DEPOSIT	CHEMISTRY		MINERALOGY AND FORM OF DEPOSITS	DEPOSITIONAL ENVIRONMENT AND DEPOSITIONAL PROCESS	SOURCE OF MANGANESE	RATE OF SEDIMENTATION; FORMATION
	MAJOR ELEMENTS	TRACE ELEMENTS				
HYDROGENOUS	Enriched in Mn, Fe; Mn/Fe between 0.5 - 5.	Enriched in trace elements - Cu, Ni, Co; shallower water deposits tend to contain more Ba, P; REE: Ce enrichment.	Mn present in oxides, hydroxides; two common minerals are Birnessite, Todorokite; deposits form nodules of variable size and crusts with latter more prevalent in shallower water deposits.	Depth of water variable, from abyssal plains to continental shelf; shallower types often in association with phosphorite deposits; form in oxidizing environment; form by slow, direct precipitation from sea water.	Sea water	Rate of accumulation of associated pelagic/terrigenous sediment very low: radiometric estimates on nodules indicate growth rate of between 1mm/10^3 - 1mm/10^5 years; shallow water growth faster.
HYDROTHERMAL (oxidizing)	Enriched in Mn, Fe; commonly more Fe, but Mn/Fe increases with distance from source.	Low trace metal concentrations; some deposits enriched in Ba and (relatively) in P; REE: Ce depletion	Fe and Mn hydroxides, oxides; as small spherules in sediment; small amounts of Mn-carbonate (rare).	Depth of water variable; most modern examples in deep sea regions; close spatial relationship to synchronous volcanic activity: deposits located in areas with active oceanic ridges, incipient rifting; deposits formed in oxidizing condition.	Hydrothermal solutions emanating from submarine volcanic activity.	Form more rapidly than hydrogenous type.
HYDROTHERMAL (reducing)	Enriched in Mn, Fe.	Enriched in trace metals but generally less so than hydrogenous type.	No deposition of Mn due to reducing environment; deposits form metalliferous brines in stagnant basins; sulphide deposition in the brine basins.	Modern examples (e.g. Red Sea brines) restricted to isolated marine basins on sea floor; these are stagnant (reducing), located in close proximity to an active rifting centre, and contain sulphides within the sediments collecting at the base of the basins; Fe-silicates precipitate from within brine pools.	Hydrothermal solutions from volcanic activity associated with rifting process.	Similar to hydrogenous type.
DIAGENETIC	Mn, Fe rich; Mn/Fe relatively higher than for hydrogenous deposits.	Low trace metal content.	Mn oxides, hydroxides dominant mineral containing Mn, but Mn-carbonate developed in favourable circumstances.	Deposits form in shallower water environment, in hemipelagic regions and in marginal and enclosed seas; high accumulation rate of organic C in associated sediments; formed by diagenetic remobilization of Mn within the sediment pile, with Mn reduction caused by organic matter decay. subsequent upward migration of Mn^{++} along concentration gradient is followed by precipitation at or near oxidizing/reducing interface, commonly at or near sediment surface. given favourable conditions (high concentration of carbonate ion in pore water), $MnCO_3$ forms in sediment.	Mn derived from underlying sediments by diagenetic activity.	Accumulate in areas where sedimentation rate exceeds the low values characterizing hydrogenous deposits; deposits themselves accrete more rapidly than hydrogenous forms.
HALMYROLYTIC	Enriched in Mn, Fe.	————	MnO_2 microparticles in sediments.	As for hydrogenous deposits, but Mn supplied by submarine weathering of volcanic debris in sediments.	Volcanic material (glass) in sediments.	————
NEWFOUNDLAND DEPOSIT	Enriched in Mn, Ca, Fe; Mn/Fe varies from less than to more than 40, averaging 1.2 for all analyzed samples.	No trace metal enrichment.	Mn occurs as carbonates, rhodochrosite and Mn-calcites; most Fe occurs in chlorite; associated Ba and P occur in discrete phases (collophane, barite); form: concretions of variable shape, size; lenses of Mn-carbonate rich material elongated parallel to bedding	Deposited in shallow-marine waters under neutral to slightly reducing conditions; extensive post-depositional diagenetic changes indicative of reducing condition; Mn supplied by deeper water parts of basin and precipitated in shallower inshore regions.	Mn transported to depositional site in solution in sea water; ultimate source from continental weathering, with volcanic contribution a possibility.	Associated with very slow rates of clastic sedimentation.

(3) Low concentrations of such base metals as Cu and Ni which are present in anomalous concentrations in hyrogenous and, to a lesser degree, in hydrothermal ferromanganese deposits.

(4) The importance of diagenesis. In the case of recent ferromanganese deposits, diagenetic remobilization of manganese in the sediment pile as Mn^{2+} is directly related to their formation (e.g. Lynn and Bonatti, 1965; Calvery and Price, 1972; Klinkhammer, 1980). In the Newfoundland deposit also, early diagenetic alteration of the primary sediment is widespread and the products of such diagenesis are the most important factor in controlling the present mineralogy and texture of the rocks (Section 4.2.5). The relationship between early diagenesis and manganese carbonate formation in recent sediments is discussed in Section 7.2.

The Newfoundland manganese horizon contains anomalous concentrations of Ba and P_2O_5 (Table 5.1). Hydrothermal ferromanganese deposits of recent origin are enriched to a degree in these elements relative to other types of deposit (Bonatti, et al., 1972), which suggests the possibility that the Newfoundland deposit may have been influenced by hydrothermal processes. However, the evidence on this point is unclear, as there is some analytical data suggesting that in general shallow water deposits are enriched in Ba and in P relative to deeper water deposits (Manheim, 1965). Thus, the presence of Ba, and P in anomalous amounts in the Newfoundland manganese horizon may reflect the depth of water during deposition rather than linkage with hydrothermal processes.

7.1.2 Ancient Deposits

More than 90% of the lithified manganese deposits of the world are sedimentary in origin (Wissink, 1972). These sedimentary manganese deposits have been classified by several authors on the basis of their tectonic setting, composition, associated sedimentary rocks, and source of the manganese (Varentsov, 1964; Wissink, 1972). Quantitatively, the most important of these classes is the Nicopol' Formation type (see Table 7.2) described by Varentsov. This type of deposit is widely developed in sediments of Lower Oligocene age in the southern Ukraine in the U.S.S.R., which collectively contain more than 800 million tons of Mn and constitute the largest economic reserve of land-based manganese ores in the world. Wissink (1972) estimated that deposits of this nature contain more than 65% of the total world manganese ore reserves.

Information on the chemical and mineralogical composition and on various other aspects of the Newfoundland manganese horizon is summarized in Table 7.2, together with similar information for the manganese horizon of equivalent age present in the North Wales region and for the Oligocene/Nicopol' deposits in the U.S.S.R. Examination of Table 7.2 shows that all three of these deposits are similar in many respects:

(1) All are deposited on or adjacent to a stable cratonic block, i.e., in a stable tectonic regime. The Newfoundland and Russian deposits were formed in stable platformal regions, whereas the Welsh deposit formed in a more unstable tectonic environment.

(2) All deposits are considered to be the product of deposition in shallow marine waters.

TABLE 7.2 COMPARISON OF NEWFOUNDLAND MANGANESE HORIZON WITH SEDIMENTARY DEPOSITS OF THE NICOPOL' TYPE AND THE MANGANESE HORIZON IN THE HARLECH BASIN, NORTH WALES.

Data from present study, Fletcher (1972); Wissink (1972); Varentsov (1964); Sapozhnikov (1970); Mohr (1966); and Woodland (1939).

	CHEMISTRY		MINERALOGY OF DEPOSITS AND NATURE OF ASSOCIATED SEDIMENTS	TECTONIC SETTING OF DEPOSITS	DEPOSITIONAL ENVIRONMENT	RELATIONSHIP TO STRATIGRAPHIC SUCCESSION	IMPORTANCE OF DIAGENESIS	SUGGESTED SOURCE(S) OF MN
	MAJOR ELEMENT	TRACE ELEMENT						
NICOPOL' TYPE DEPOSIT	Principal major element enrichment is Mn; Fe content in general low, (several percent or less). Inverse correlation between Mn, Fe.	Low absolute content of trace metals (Cu, Ni, Co), less than clarke contents. Some material relatively enriched in Ba. P content is generally low, 0.5% or less.	Both oxide, carbonate facies present; latter towards deeper water portions of basin; some oxide secondary (supergene), but some considered primary. Carbonate facies consists of Mn-carbonates: rhodochrosite, Mn-calcites. Ore developed within sequence of sands, silts, and clays; argillaceous sediments are prominent in ore zone, with clay minerals characteristic of carbonate facies. Carbonate facies contains greater than average terrigenous material.	Deposits form in stable regions: on Russian Platform, in stable marginal regions of geosynclines. Deposits related to marine transgression which immediately follows regression. Deposits occur around the margin of a deeper water basin (Maikop Basin), in which reducing conditions are known to have existed during ore deposition.	Deposits laid down in shallow marine waters of normal salinity, water circulation pattern. Depth water considered in part littoral, and only occasionally to exceed 30 m. Low rate of terrigenous sedimentation associated with ore deposition. Climate: deposition considered to occur in humid environment; ore deposition coincident with climatic changes, cooler from tropical to subtropical or temperate.	Ore horizon continuously located at same stratigraphic position. Lower Oligocene, over strike length of 250 km. Horizon varies in thickness, but average thickness is in order of several metres. Width of development of ore zone varies up to c. 20 km.; ore zone disappears via facies changes in either direction: to sands in shorewards direction, and to a thicker sequence of clays seawards.	Diagenesis very important in ore horizon; is considered to have resulted in concentration of original Mn in ore zone sediments. Wide variety of concretionary forms produced by diagenesis; considerable supergene oxidation of carbonate ores has occurred.	Ultimate source from continental weathering; volcanic source not considered. Immediate source of Mn not agreed upon; either by separation of Mn from Fe in weathering crust, followed by transport and deposition, or by transport of both Mn, Fe into deeper water portions of Maikop Basin, where reducing conditions result in separation of Mn from Fe (the latter remaining in the deeper water sediment) followed by lateral transport, deposition in shallower, more oxidised water.
WELSH MANGANESE HORIZON	Enriched in Mn; basal part of horizon with Fe in excess of Mn, but main Mn-bed with reverse situation; average Mn/Fe of 1.7, as compared to average of 1.2 for Nfld. deposit; Ca-rich relative to enclosing rocks, due to carb. mineralogy.	Low concentrations of Cu, Ni in ore horizon; Mn-carbonate samples enriched in Ba, but not to the degree that are some of Nfld. samples; ore horizon also enriched in P, Sr.	Mixed carbonate-silicate-oxide mineralogy; primary minerals considered to be mainly Mn-carb. minerals, lesser primary oxide; Mn-silicate minerals (spessartite and rarely rhodonite) considered to be secondarily formed during metamorphism. Deposit contains very fine grained argillaceous matrix in addition to these minerals; ore horizon is enclosed in shale.	Deposited in marginal basin to main Dalradian geosynclinal trough; thicker sequence and turbiditic nature of sediments suggest relatively more unstable environment than for Nfld. horizon. Deposit associated with depositional break in normal clastic sedimentation. Fe-rich basal portion of horizon (pyrite) suggests reducing conditions at beginning of deposition.	Considered to have formed in shallow marine waters; restricted or partially restricted basinal conditions postulated. Hot, arid climate postulated during ore accumulation. Lack of detrital minerals in ore horizon indicates that terrigenous sedimentation was restricted during ore formation.	Horizon present at same stratigraphic position throughout exposure area in Harlech Basin areas, at or near base of Middle Cambrian; averages in order of 3 metres thick; ore deposition confined to central portions of basin, with facies changes into more terrigenous material to east and west.	Deposits strongly influenced by low-grade metamorphism; this has resulted in the widespread development of spessartite in the horizon. Numerous nodular, banded features in ore are considered to predate metamorphism and reflect either primary or early diagenetic features of ore.	Composite source for Mn has been proposed, with some Mn originating from continental weathering of older rocks and some from the weathering of older and synchronous volcanic rocks. Direct hydrothermal/volcanic source not postulated; Mn-derived from weathering of such rocks; separation of Mn from Fe proposed at source, under severe weathering conditions; subsequent transport to (partially) restricted shallow water basin, where deposition, chiefly in carbonate form, occurred, possibly by flocculation of ore constituents in gel form in basin waters.
NEWFOUNDLAND MANGANESE HORIZON	Major elements enriched are: Mn, Fe, Ca; latter due to carbonate mineralogy; relatively richer in Fe than Nicopol' type; inverse correlation between Mn, Fe.	No trace metal enrichment in horizon, with low mean Cu, Ni, Zn contents; horizon is relatively enriched in P, Ba, more so on average than for Nicopol' type; distribution of these elements very irregular.	Carbonate facies; bulk of Mn in all horizons contained in Mn-carbonate minerals (rhodochrosite, Mn-calcites); minor amounts of oxide minerals, largely due to weathering of primary carbonate. Ore horizon developed within sequence of mudrocks; the horizon itself contains the same suite of minerals as the enclosing mudrocks, hence consists essentially of a dilution of the mudrock lithology; no arenaceous rocks above base of Cambrian sequence.	Deposit formed in stable platformal Avalon zone. Deposit related to hiatus in clastic sedimentation; with accumulation of horizon during the early stages of a renewed marine incursion following the Lower-Middle Cambrian break in sedimentation.	Formed in shallow, marine waters; presence of algal structures within horizon indicate that depth of water could not have been great; basinal environment could not have been greatly different from normal, as trilobite fauna is present within horizon as in enclosing sediments. Paleontological data indicates that ore deposition related to slow rates of terrigenous sedimentation.	Horizon everywhere developed at same stratigraphic position: Lower-Middle Cambrian transition. Equivalent strata enriched to some degree in Mn throughout Cambrian exposures on Avalon Peninsula in SE Nfld., but more manganiferous exposures restricted to smaller area located around Trinity and Conception Bays; strike 'length' unknown. Where most strongly manganiferous, the horizon is between 1 to 5 metres thick; the horizon is greatly diminished in Mn-concentration to the south of the exposure area due to the progressive increase in argillaceous material.	Diagenetic changes within original sediments of ore horizon very widespread and largely responsible for present textural, mineralogical character of the horizon; secondary alteration of carbonate ores is not widespread, though enough oxide minerals have been formed to black on surface exposures of the horizon.	Ultimate source of Mn believed from continental weathering; Mn believed to have been transported in solution from deeper water portions to where deposited; volcanic contribution to sediments of horizon a possibility in view of the spatial association with volcanic rocks, but no contemporaneous volcanic source can be proved in the basin.

(3) All are associated with low rates of clastic sedimentation.

(4) Mineralogically, the deposits are characterized by the Mn-carbonate minerals. The Russian deposits in addition contain an oxide facies which is lacking or unexposed in southeastern Newfoundland. In the Russian Nicopol'-type deposits, the mineralogical sequence oxide facies - mixed manganese oxide/carbonate facies - manganese carbonate facies is observed from shallow through intermediate to deeper water portions of the depositional basin (Sapozhnikov, 1970). Most Russian authors regard the manganese oxide zone as being primary, and some also consider the manganese-carbonate zones to be primary; others, however, regard the carbonates as being formed during diagenesis after deposition (Sapozhnikov, 1970). All agree that diagenetic production of manganese carbonates in this deposit type is widespread (see below). The Newfoundland (Dale, 1915) and Welsh (Mohr, 1964, 1966) manganese carbonates have been classified as primary sediments by earlier workers, though again the importance of diagenesis in producing carbonate minerals has been recognized.

(5) Chemically, the deposits are enriched in manganese; no other element is enriched to anywhere near the same extent. The Newfoundland and Welsh deposits contain higher average iron contents than the Russian deposits; in part, this may be the result of a higher average content of Fe-bearing terrigenous impurities in the analyzed material from the former two regions. Samples from the manganese horizon in Newfoundland which contain

little or no terrigenous impurities (i.e., consist of 'pure' carbonate) are characterized by high MnO contents (to 50% plus) and low Fe_2O_3 contents (less than 2%), and are similar to the Russian deposits in this respect.

All three deposits contain low concentrations of trace metals such as Cu and Ni that are enriched to varying degrees in modern oceanic and lacustrine ferromanganese deposits. All are enriched to a degree in Ba and P, with the Newfoundland manganese horizon seemingly more enriched than the others.

(6) Diagenesis plays an important role in all three deposits. A variety of nodular and concretionary carbonate structures formed during early diagenesis is widespread in all deposits; such nodular and lenticular forms have effected the concentration of Mn initially more dispersed in the sediments.

The Welsh deposit has been metamorphosed and this has replaced in part manganese carbonate with the manganese garnet, spessartine.

The data presented in Tables 7.1 and 7.2 indicate that the Newfoundland horizon can be correlated with recent diageletic ferromanganese deposits and with ancient stratified deposits of the Nicopol' type. The genetic implications of these correlations are discussed in the next chapter.

The Newfoundland deposit is also similar in age, in chemistry, and in tectonic setting to a deposit of manganese carbonates in North Wales. During early Middle Cambrian time, both areas were located on the European margin of the proto-Atlantic Ocean (Section 2.1), and it has been suggested (Mohr and Allen, 1965) that the two areas may have been contiguous and the manganese horizons genetically linked. However, the fact that the Newfoundland deposit was formed in shallow water whereas the Welsh deposit may have been associated with a deep water sequence of turbidites (Crimes, 1970; Hager, 1980) mitigates against the hypothesis of Mohr and Allen; a single deposit is unlikely to span such an environmental range.

7.2 Formation of Manganese Carbonates in Recent Sediments

Manganese oxide minerals are stable relative to manganese carbonate in oxic ocean waters; consequently, primary manganese carbonates have not been detected in modern sediments. Manganese carbonates are known to form during diagenesis within marine sediments in a variety of environments (Manheim, 1961; Rex, 1970; Calvert and Price, 1970; Hein *et al.*, 1979), and have also been recorded in freshwater, lacustrine environments (Callender, 1973). Manganese oxides buried in marine sediments are dissolved at depth in the anoxic environments produced by organic reduction during diagenesis (Lynn and Bonatti, 1975; Calvert and Price, 1972); the Mn^{2+} released by this process generally migrates upwards to the oxic/anoxic interface (commonly situated at or near the sediment surface) to be reprecipitated as manganese oxides. At depth in such sediments, the Mn^{2+} concentration can reach saturation with respect to the manganese carbonate, and precipitation take place (Klinkhammer, 1980; Pederson and Price, ms). Carbonate precipitation in the anoxic zone of marine sediments appears to occur preferentially in coarser grained zones with greater porosity.

(Hein et al., 1979), perhaps because such zones favor crystal growth (Pederson and Price, ms). Some authigenic marine manganese carbonates may be related to hydrothermal activity (Rex, 1970) and the Mn source in some cases appears to be from the alteration of buried volcanic ash and tuff beds (Hein et al., 1979).

The carbonates are formed according to the reaction: $MnCO_3 \rightleftharpoons Mn^{2+} + CO_3^{=}$. Note than an increase of either Mn^{2+} or alkalinity (e.g. $CO_3^{=}$) will favor the production of carbonate, i.e. high alkalinities are not necessarily required if high concentrations of Mn^{2+} are available in the anoxic zone (Pederson and Price, ms). The formation of authigenic manganese carbonates in Mn^{2+} rich solutions has been demonstrated by the experimental work of Häger (1980). In complex natural systems, ions other than Mn^{2+} are present and are involved in manganese carbonate precipitation; most authigenic carbonates are mixed Mn - Ca (-Mg) phases (Pederson and Price, ms).

The above synopsis suggests that manganese carbonate minerals are produced in anoxic environments during diagenesis of recent sediments and that the formation of primary manganese carbonates in oxic sediments is improbable. Manganese carbonates therefore serve as indicators of anoxic environments during early diagenesis (Krumbein and Garrels, 1952; Berner, 1981), and is likely that the manganese horizon in southeastern Newfoundland, as now constituted, formed in such an environment.

CHAPTER 8

ORIGIN OF MANGANESE HORIZON

Previous researchers (Dale, 1915; Mohr, 1964, 1966) have concluded that the manganese horizon in southeastern Newfoundland is a chemically precipitated stratiform deposit, and that the manganese carbonate which comprises the horizon is an original or primary component of the deposit. Data presented in the previous chapter suggest that it is unlikely that manganese carbonates would precipitate in the normal (i.e. oxic) conditions in which the horizon was formed (see below).

The geochemical, mineralogical, and geological data contained in the present study are used to construct an alternative mechanism for its deposition.

8.1 Geological Setting

Lower Paleozoic sedimentary rocks present in the Avalon Zone in southeastern Newfoundland were deposited in a stable tectonic environment (Williams, 1979). The Late Precambrian history of the Avalon Zone is unclear. The history may indicate rifting associated with the formation of Iapetus (Strong, 1979) or may alternatively reflect the development of an island-arc complex connected to a late Precambrian (pre-Iapetus) subduction zone (Rast et al., 1976).

The former interpretation is favored here as it can accommodate:

(1) the linear nature of the Cambrian basin during the Lower Cambrian, when sedimentation was limited to a north-south trending trough bounded east and west by positive (land) areas (Hutchinson, 1962).

(2) a mechanism by which continued subsidence of this trough during the Lower Cambrian along this north-south trending zone of instability (i.e. rift) culminated in Middle Cambrian time with the extrusion of tholeitic basaltic lavas (Papezik, 1980).

The Cambrian basin in southeastern Newfoundland is believed to have been partially restricted; that is, not in direct contact with the main body of Iapetus. The absence of the oldest known Acado-Baltic trilobite species in the Avalon Zone (i.e. the pre-trilobite zone of Fletcher, 1972) is believed to be a consequence of the restricted nature of the basin (Anderson, 1981). However, the very presence of the trilobite fauna suggests that the degree of restriction could not have been great, as a normal fauna is maintained.

The mudrocks which comprise the bulk of the Lower and Middle Cambrian succession are similar in composition to the average shale (Chapter 5), which suggests that conditions present during their deposition were not radically different from the norm. Note, however, that the average mudrock MnO content of 0.37% (Table 5.10) is more than double that of other shales. This suggests that anomalous concentrations of Mn were present in the sedimentary basin throughout deposition of the Adeyton Group.

The Lower-Middle and Middle-Upper Cambrian boundaries in the Avalon Zone are disconformable and mark significant regressions

(Hutchinson, 1962; Poulson and Anderson, 1975). The Lower-Middle Cambrian non-sequence is marked by deposition of the manganese-rich sedimentary rocks which this study treats. The manganese horizon is characterized mineralogically by manganese carbonates. It differs only in degree, however, from other carbonates in the Adeyton Group; limestones as a group contain anomalous MnO concentrations (Table 5.1, Fig. 5.11). This suggests that the chemical/depositional processes responsible for the manganese horizon were active throughout the Lower and Middle Cambrian.

8.1.1 The Manganese Horizon

As mentioned above, the manganese horizon in southeastern Newfoundland is associated with a regression at the Lower-Middle Cambrian boundary. Correlative Acado-Baltic sequences also reflect this regressive event (Table 2.2), and it may possibly have been extensive enough to effect both sides of the Iapetus Ocean (Palmer and James, 1980). In southeastern Newfoundland, the regression is most pronounced in northern Avalon Peninsula exposures and the manganese horizon is best developed in this region. Southwards from this area, the effects of the event lessen and paleontological data (Fletcher, 1972) suggests that in southernmost Avalon Peninsula exposures sedimentation across the Lower-Middle Cambrian boundary was essentially uninterrupted. The following salient features apply to the manganese horizon (see also Figure 8.1 and 8.2):

(1) in thickness, the horizon varies from 25m in southernmost Avalon Peninsula exposures, to 5 m about the heads of Trinity and Conception Bays, to only 1 m in northernmost Trinity Bay exposures;

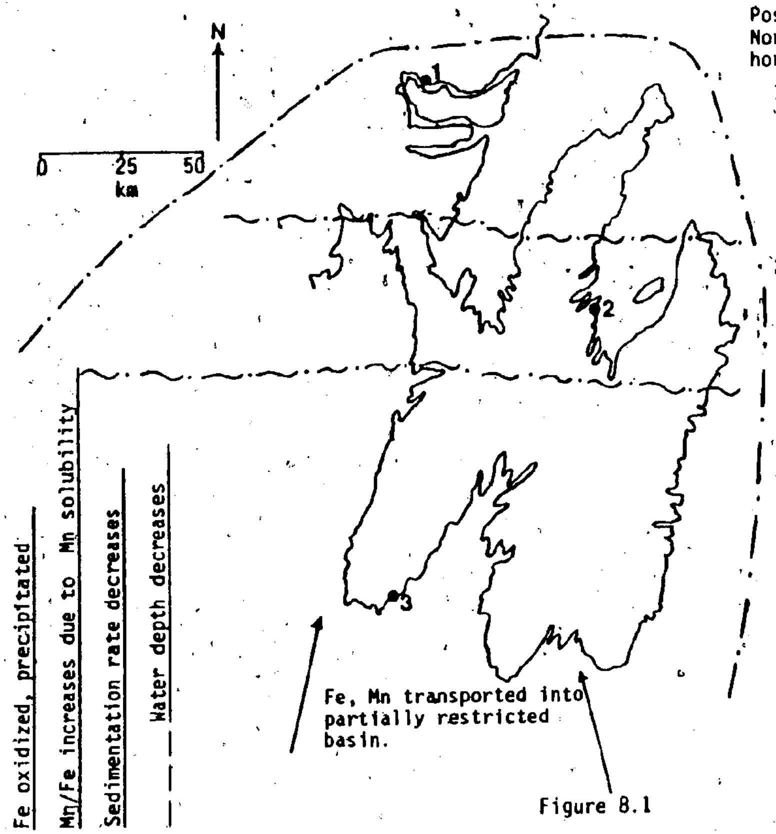

Possible Exposure and Erosion in North During Deposition of Mn horizon.

1. Smith Point, Massive Mn-rich carbonate bed deposited

2. Brigus. Mn-rich carbonates in thin beds, lenses, nodules intercalated with argillaceous sediments. Carbonate wedgeout towards South.

3. Essentially uninterrupted sedimentation; red and green mudrocks deposited, Mn present only in scattered, thin, nodular horizons.

Fe, Mn transported into partially restricted basin.

Figure 8.1

Schematic Plan View of Cambrian Basin During Deposition of Manganese Horizon

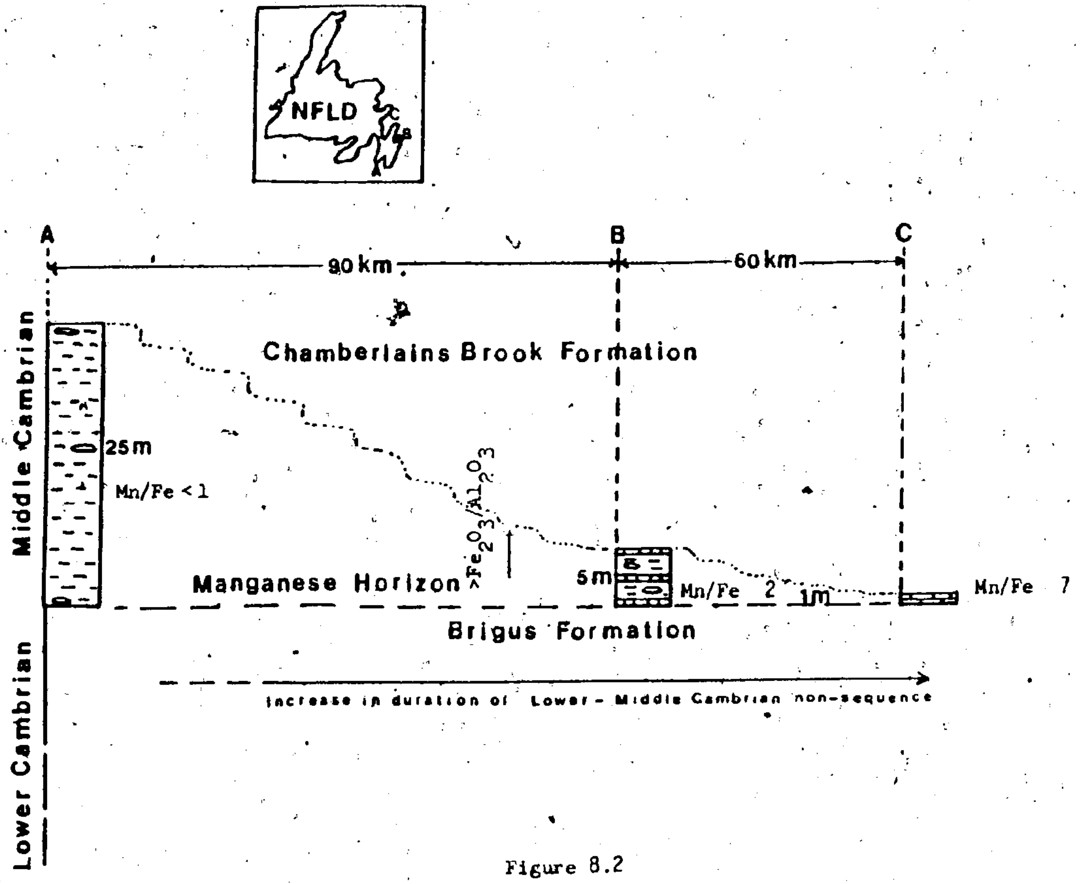

Figure 8.2

Schematic Sectional View of Cambrian Basin During Deposition of Manganese Horizon.

(2) thickness changes are accompanied south to north by a progressive increase in the proportion of manganese carbonate in the horizon, such that a complete gradation from mudrock in southern exposures to carbonate in northern Trinity Bay exposures is effected;

(3) the horizon contains anomalous concentrations of Mn, Fe, Ca, and Mg. Areally, the Mn/Fe ratio increases from south to north from less than one in southern Avalon Peninsula exposures to more than 5 in northernmost exposures;

(4) within individual manganese horizon exposures around the heads of Trinity and Conception Bays, the proportion of Fe relative to Mn increases towards the top (Fig. 5.8);

(5) mineralogically, the manganese horizon is characterized by the presence of manganese carbonates. Analytical data (Section 5.2.2) indicates that mixed Mn-Ca-Mg carbonates and rhodochrosite both occur. Manganese oxide minerals are restricted to late-stage alteration (along fracture surfaces, etc. Anomalous Fe present in the manganese horizon is primarily present in chlorite (Figure 5.2);

(6) early diagenetic formation of manganese carbonate nodules, lenses, and concretions is widespread and is responsible for most of the sedimentary textures present in the horizon (Chapter 4). Authigenic minerals include rhodochrosite, pyrite, and barite. The diagenetic formation of chlorite is also widespread.

8.1.2 Formation of Manganese Horizon

The data on the nature and setting of the manganese horizon given above suggest that it was formed during the Lower-Middle Cambrian regression as follows:

(1) during the regression, sedimentation continued in the southern regions of the Cambrian basin (e.g. Cape St. Mary's area; Fletcher, 1972), whereas the northern Avalon Peninsula was subject to uplift, shallowing, and the cessation of normal clastic sedimentation. The fauna preserved in the manganese horizon (especially the presence of algae; Section 3.4.3.4) suggest that water depths remained shallow during deposition of the Mn-rich sediments. The basin waters are believed to have remained normal (oxic) during the regression; no indications of euxinic, salinie or other unusual depositional environments are present.

(2) Mn entering into southern portions of the basin where sedimentation continued was transported northwards into shallow waters in the north, concentrated over time, and precipitated as manganese oxide. The manganese oxide accumulated slowly during the hiatus in clastic sedimentation.

(3) Renewed transgression led to the burial of the manganese oxides and associated biogenic debris.

(4) Following burial, decomposition of organic matter resulted in the establishment of anoxic conditions within the sediments. These conditions in turn caused ~~the dis~~solution of the manganese oxides and the subsequent re-precipitation of the Mn++ in manganese carbonates produced during early diagenesis.

(5) Steps two and three may have been repeated at a given site in the Cambrian basin as minor fluctuations in sea level

during the regression caused the zones of sediment deposition and non-deposition to move back and forth.

(6) Note that step two of the process leads to the establishment of high Mn++ concentrations in the buried sediment, which in turn suggests that high alkalinities are not required to produce the manganese carbonates (Pederson and Price, ms). The presence of high Mn++ concentrations together with $CaCO_3$ (in shell fragments, etc.) is likely to result in the replacement of $CaCO_3$ by manganese carbonates (Hager, 1980), as is the case in the Newfoundland deposit (Chapter 4).

8.1.3 Separation of Mn and Fe

The bulk of the Fe accompanying Mn into the southern reaches of the Cambrian basin is believed to have remained fixed in the sediments accumulating in that part of the basin during deposition of the manganese horizon. The southern part of the depositional basin is believed to have acted as an iron 'sink' during formation of the horizon. Mn was further separated from Fe during migration from the deeper, southern portion of the basin to the Trinity-Conception Bay area, with less soluble iron being oxidized and precipitated basinwards relative to the manganese. Evidence suggesting the latter process can be seen in the chemical variation diagrams prepared for various Trinity-Conception Bay sections (Fig. 5.7, 5.8), which show that the upper part of the horizon becomes enriched in Fe relative to Mn.

Given the marine transgression which restored normal conditions of sedimentation to the northern Avalon Peninsula, the Fe-rich tops are regarded as a basinwards (i.e. southern), relatively Fe-rich 'facies' which overstepped older Mn-rich sediments as the transgression moved north.

8.1.4 Source of Manganese

The Mn and Fe present in the horizon are believed to have been ultimately derived from erosion of Precambrian rocks adjacent to the depositional basin. Though volcanic rocks of Middle Cambrian age occur in the succession, the oldest known are situated some 60 m above the manganese horizon, so that a contemporaneous volcanic source for the Mn and Fe cannot be demonstrated. It is of course possible that time-equivalent volcanism was occurring in deeper portions of the Cambrian basin to the south of the Avalon Peninsula, but this postulate cannot be proved given the present-day limitations of exposure of the Cambrian sequence. Dale (1915) has also concluded that the Mn in the horizon was derived from the erosion of Precambrian rocks exposed around the basinal margins.

8.2 Summary

The manganese horizon of basal Middle Cambrian age present in southeastern Newfoundland is genetically linked to a regression of that age. Mn derived from sediments accumulating in the southern portion of the depositional basin (e.g. southern Avalon Peninsula and areas south of this) was transported northwards into the restricted Trinity-Conception Bay area, concentrated over time, and precipitated as manganese oxides.

Subsequent early diagenetic alteration of the manganese horizon produced the manganese carbonates and associated mineral components (e.g. chlorite, pyrite) which now dominate the horizon. The process of manganese carbonate formation is viewed as being analogous to that occurring during diagenesis in some recent marine sediments (e.g. Klinkhammer, 1980; Pederson and Price, ms).

The presence of manganese carbonate and iron silicate (chlorite) minerals in the manganese horizon suggest that it falls within the post-oxic category of Berner's (1981) classification of sedimentary environments.

CHAPTER 9

CONCLUSIONS

The results of the present study of manganese-rich sedimentary rocks exposed in southeastern Newfoundland indicate that:

(1) the red and green mudrocks comprising the Adeyton Group, in which the manganese horizon is developed, are chemically and mineralogically homogenous throughout the study area;

(2) the single major trend exhibited by the Cambrian rocks is that of dilution by carbonate minerals of the dominant mudrock lithotype. Two carbonate dilution trends are present, a CaO-rich trend characteristic of limestone samples outside of the manganese horizon, and an MnO-rich trend produced by the Mn-carbonate bearing rocks of the manganese horizon. These trends are apparent in the results of statistical examination of both chemical and mineralogical data;

(3) the manganese horizon is enriched, relative to the enclosing mudrocks, in Mn, Fe, Mg, Ba, P, Sr, and Ce. Manganese is much more enriched than any other of these elements. Mineralogically, the horizon is characterized by the presence of Mn-carbonate minerals (rhodochrosite and Mn-bearing calcite). Some exposures of the horizon contain abundant chlorite, and the mean content of this mineral in analyzed horizon samples is greater than that of the enclosing mudrock sequence.

The red and green mudrocks present over and below the manganese horizon are chemically similar to other published estimates of the average composition of fine-grained sedimentary rock groups, though the average MnO content is greater in the Newfoundland sequence;

(4) the manganese horizon has been considerably altered by diagenesis. Carbonate nodules and lensese formed during early diagenesis are predominant in the manganese rich rocks. Diagenetically-formed chlorite contains most of the Fe in the horizon;

(5) the chemical and mineralogical composition of the Newfoundland horizon, the associated stable tectonic and shallow marine environment of deposition, and the strong influence of diagenesis on the rocks suggest that the Newfoundland deposit is correlated with diagenetic oceanic ferromanganese deposits and with the Nicopol' Formation type of ancient deposit;

(6) the manganese horizon was deposited during a regression which defines the Lower/Middle Cambrian boundary and which interrupted sedimentation in correlative areas on the eastern margin of the proto-Atlantic ocean. The horizon is best-developed in the Trinity-Conception Bay portion of the Avalon Peninsula. The manganese was originally precipitated as oxide minerals in this area; subsequent diagenetic alteration produced the manganese carbonates and allied minerals which now typify the horizon.

(7) the Mn is believed to have been ullimately derived from Late Precambrian rock assemblages exposed around the depositional basin.

No synchronous volcanic activity is known in the Cambrian sequence in southeastern Newfoundland.

(8) The bulk of the Fe associated with the Mn contained in the horizon is believed to have been retained in sediments which were accumulating in the depositional basin south of the Avalon Peninsula area during deposition of the manganese-rich sediments in the north. Fe was also separated from Mn during transportation to the Trinity-Conception Bay area.

(9) due to the low grade,unfavorable mineralogical composition, presence of the undesirably high concentrations of P, and existence of abundant supplies of conventional manganese oxide ores, the Newfoundland manganese horizon is not considered an economically viable deposit at present.

LIST OF REFERENCES

LIST OF REFERENCES

ABBEY, S.

1968 Analysis of rocks and minerals by Atomic Absorption Spectroscopy. Part 2. Determination of total iron, magnesium, calcium, sodium and potassium. Geol. Surv. Can. Paper 68-20.

ANDERSON M.M.

1972 A possible time span for the Precambrian of the Avalon Peninsula, southeastern Newfoundland, in the light of worldwide correlation of fossils, tillites, and rock units within the succession. Can. J. Earth Sci., v. 9, p. 1710-1726.

______

1981 The Random Formation of southeastern Newfoundland: a discussion aimed at establishing its age and relationship to bounding formations. Am. J. Sci., v. 281, p. 807-830.

ANDERSON, M.M. and MISRA, S.B.

1968 Fossils found in the Precambrian Conception Group of southeastern Newfoundland. Nature, v. 220, p. 680-681.

BENGSTON, S. and FLETCHER, T.P.

(unpub. Manu.) The succession of skeletal fossils in the basal Lower Cambrian of southeastern Newfoundland.

BERNER, R.A.

1981 A new geochemical classification of sedimentary environments. Journal of Sedimentary Petrology, v. 51, p. 0359-0365.

BIRD, J.M. and DEWEY, J.F.

1970 Lithosphere plate-continental margin tectonics and the evolution of the appalachian Orogen. Geol. Soc. Amer. Bull., v. 81, p. 1031-1060.

BJORLYKKE, K.

1974 Depositional history and geochemical composition of Lower Palaeozoic epicontinental sediments from the Oslo region. Norges Geol. Unders., No. 305.

BJORLYKKE, K.

______

1978 The eastern marginal zone of the Caledonide Origin in Norway. In: Caledonian-Appalachian Origin of the North Atlantic Region, IGCP Project 27, Caledonide Origin, Geol. Surv. Can. Paper 78-13, p. 49-55.

BONATTI, E., KRAEMER, T. and RYDELL, H.

1972 Classification and genesis of submarine iron-manganese deposits. In: Ferromanganese Deposits on the Ocean Floor, D.R. Horn, ed., p. 149-166, the office for the International Decade of Ocean Exploration, National Sci. Foundation, Washington, D.C.

BORELLA, P.E. and C. ADELSECK

1980 Manganese micronodules in sediments: a subsurface in situ origin; Leg 51, Deep Sea Drilling Project In: Donnelly, T., Francheteau, J., Bryan, W., Robinson, P., Flower, M. and Salisbury, M.; Initial reports of the Deep Sea Drilling Projects, v. 51,52,53, Part 2 Washington (U.S. Gov't. Printing Office), p. 771-776.

BOSTROM, K. and PETERSON, M.

1969 Precipitates from hydrothermal exhalations on the East Pacific Rise. Econ. Geol., v. 61 p. 1258-1265.

BRUECKNER, W.D.

1969 Geology of eastern part of Avalon Peninsula - a summary. In: North Atlantic - Geology and Continental Drift, A.A.P.G. Mem. 12, p. 130-138.

BRUECKNER, W.D. and ANDERSON M.M.

1971 Late Precambrian glacial deposits in southeastern Newfoundland - a preliminary note. Geol. Assoc. Can., Proc., v. 24 p. 95-102.

BUDDINGTON, A.F.

1916 Pyrophyllitization, pinitization, and silicification of rocks around Conception Bay, Newfoundland. J. Geol., v. 24, p. 130-152.

BUDDINGTON, A.F.

____

1919 Precambrian rocks of southeast Newfoundland. J. Geol., v. 27, p. 449-479.

BULLARD, E.C., EVERETT, J.E. and SMITH, A.G.

1965 The fit of the continents around the Atlantic. In: Symposium on Continental Drift, Philos. Trans. R. Soc. Lond., Ser. A., v. 258 p. 41-51.

BURNS, R.G. and BROWN, R.A.

1972 Nucleation and mineralogical controls on the composition of manganese nodules. In: Ferromanganese Deposits on the Ocean Floor, D.R. Horn, ed., p.51-62, the office for the International Decade of Ocean Exploration, Nat. Sci. Foundation, Washington, D.C.

BUTLER, A.J. and BARTLETT, G.

1967 Silica assessment - southeastern Newfoundland. Unpub. rept., Min. Res. Div., Dept. Mines, Agric. and Resources, St. John's, Newfoundland.

CALLENDER, E.

1973 Geochemistry of ferromanganese crusts, manganese carbonate crusts, and associated ferromanganese nodules from Green Bay, Lake Michigan. In: Inter-University Program of Research on Ferromanganese Deposits of the Ocean Floor, Phase 1 Rept., p. 105-120 (unpub.).

CALVERT, S.E. and PRICE, N.B.

1970 Composition of manganese nodules and manganese carbonates from Loch Fyne, Scotland. Contr. Mineral. and Petrol., v. 29, p. 215-233.

____

1972 Diffusion and reaction profiles of dissolved Mn in the pore waters of marine sediments. Earth Planet. Sci. Lett., v. 16, p. 245.

CAMPBELL, R.A., VIENS, G.E. and ROGERS, R.R.

1956 Experimental electric smelting of manganese ores. Bull. Can. Inst. Min. Met., v. 49, p. 274-280.

CARROLL, D.

1970 Clay minerals; a guide to their x-ray identification. Geol. Soc. Amer., Spec. Paper 126.

CHURCH, W.R. and STEVENS R.K.

1971 Early Paleozoic aphiolite complexes of the Newfoundland Appalachians as mantle-oceanic crust sequences. Journal of Geophysical Research, v. 76, p. 1460-1466.

CLARKE, F.W.

1924 Data of Geochemistry, 5th ed. U.S. Geol. Sur. Bull. 770, 841p.

COWIE, J.W.

1971 Lower Cambrian Faunal Provinces in space and time. In; Middlemiss, F.A., Rawson, P.F., and Newall, G. (eds.), Faunal provinces in space and time, Jour. Geol., Spec. Issue No. 4 p. 31-46.

COWIE, J.W. and RUSHTON, A.W.A.

1974 Palaeogeography of the Cambrian of the British Isles. In: 'Cambrian of the British Isles, Norden and Spitsbergen' Lower Palaeozoic Rocks of the World, v. 2, p. 177-183, John Wiley & Sons, London.

CRERAR, D.A. and BARNES, H.L.

1974 Deposition of deep-sea manganese nodules. Geochim. Cosmochim. Acta, v. 38, p. 279-300.

CRIMES, T.P.

1970 A facies analysis of the Cambrian of Wales. Palaeogeog., Palaeoclim., Palaeoecol., v. 7, p. 113-170.

CRONAN, D.S.

1972 Regional geochemistry of ferromanganese nodules in the world ocean. In: Ferromanganese Deposits on the Ocean Floor, D.R. Horn, ed., p. 19-30, the office for the International Decade of Ocean Exploration, Nat. Sci. Foundation, Washington, D.C.

DALE, N.C.

1915 The Cambrian manganese deposits of Conception and Trinity Bays, Newfoundland. Proc. Amer. Philos. Soc., v. 54, p. 371-456.

DE GRACE, J.R.

1974 Limestone Resources of Newfoundland and Labrador. Dept. Mines and Energy, Min. Dev. Div., Newfoundland, rept. 74-2.

DEWEY, J.F. and BIRD, J.M.

1971 Origin and emplacement of the ophiolite suite: Appalachian ophiolites in Newfoundland. J. Geophys. Res., v. 76, p. 3179-3206.

DYMOND, J., CORLISS, J.B., HEATH, G.R., FIELD, C.W., DASCH, E.J. and VEHN, H.

1973 Origin of metalliferous sediments from the Pacific Ocean. Geol. Soc. Amer. Bull., v. 84, p. 3355-3372.

ERLICH, H.L.

1972 The role of microbes in manganese nodule formation and degradation. In: Ferromanganese Deposits on the Ocean Floor, D.R. Horn, ed., p. 63-72, the office for the International Decade of Ocean Exploration, Nat. Sci. Foundation, Washington, D.C.

FLETCHER, T.P.

1972 Geology and Lower to Middle Cambrian trilobite faunas of southwest Avalon, Newfoundland. Unpub. Ph. D. thesis, Univ. Cambridge, England.

GARRELS, R.M. and MACKENZIE, F.T.

1971 Evolution of Sedimentary Rocks. W.W. Norton and Co., Inc.

GEE, D.G.

1972 The regional context of the Tasjö Uranium Project, Caledonian Front, central Sweden. Sveriges Geol. Undersökning, Ser. C. NR671, Arsbok 66, Nr. 2, Stockholm.

GOLDBERG, E.D.

1954 Chemical seavengers of the sea. J. Geol. and Geophys., v. 62, p. 249-265.

GREENE, B.A.

1962 Geology of the Branch-Point Lance area. Unpub. M. Sc. thesis, Memorial University of Newfoundland.

GREENE, B.A. and WILLIAMS, H.

1974 New fossil localities and the base of the Cambrian in southeastern Newfoundland. Can. J. Earth Sci., v. 11, p. 319-323.

HAGER, J.L.

1980 Sorption of manganese and silica by clay and carbonate. Mar. Chem., v. 9, p. 199-209.

HAYES, A.O.

1915 Wabana iron ore of Newfoundland. Geol. Surv. Can. Mem. 78.

____

1929 Further studies of the origin of the Wabana iron ore of Newfoundland. Econ. Geol., v. 24, p. 687-690.

HEIN, J.R., O'NEIL, J.R., and JONES, M.G.

1979 Origin of authigenic carbonates in sediment from the deep Bering Sea, Sedimentology, v. 26, p. 681-705.

HENDERSON, E.P.

1960 Surficial Deposits, St. John's, Newfoundland. Geol. Surv. Can., Map 35-1959.

____

1972 Surficial Geology of Avalon Peninsula, Newfoundland. Geol. Surv. Can. Mem. 368.

HORN, D.R., HORN, B.M. and DELACH, M.N.

1972 Distribution of ferromanganese deposits in the world ocean. In: Ferromanganese Deposits on the Ocean Floor, D.R. Horn, ed., p. 9-17, the office for the International Decade of Ocean Exploration, Nat. Sci. Foundation, Washington, D.C.

HOWELL, B.F.

1925 The faunas of the Cambrian Paradoxides beds at Manuels, Newfoundland. Bull. Amer. Paleontology, v. 11, p. 9-140.

HSU, E.Y.C.

1972 The stratigraphy and sedimentology of the Late Precambrian St. John's and Gibbet Hill Formations and the upper part of the Conception Group in the Torbay map-area, Avalon Peninsula, Newfoundland. Unpub. M.Sc. thesis, Memorial University of Newfoundland.

HUGHES, C.J.

1970 The Late Precambrian Avalonian Orogeny in Avalon, southeast Newfoundland. Amer. J. Sci., v. 269, p. 183-190.

____

1973 Late Precambrian volcanic rocks of Avalon, Newfoundland - a spilite/keratophyne province: recognition and implications. Can. J. Earth Sci., v. 10, p. 272-282.

HUGHES, C.J. and BRUECKNER, W.D.

1971 Late Precambrian rocks of eastern Avalon Peninsula, Newfoundland - a volcanic island complex. Can. J. Earth Sci., v. 8, p. 899-915.

HURLEY, P.M., BOUDA, A., KANES, W.H. and NAIRN, A.

1974 A plate tectonics origin for the Late Precambrian-Paleozoic orogenic belt in Morocco. Geol., v. 2, p. 343-344.

HUTCHINSON, R.D.

1953 Geology of Harbour Grace map-area, Newfoundland. Geol. Surv. Can. Mem. 275.

____

1962 Cambrian stratigraphy and trilobite faunas of southeastern Newfoundland. Geol. Surv. Can. Bull. 88.

JENESS, S.E.

1963 Terra Nova and Bonavista map-areas, Newfoundland (2D, E½ and 2C). Geol. Surv. Can. Mem. 327.

JUKES, J.B.

1843 General Report of the Geological Survey of Newfoundland, during the years 1839 and 1840. London, England, John Murray, vols. I and II, 160p.

KEATS, H.F.

1970 Geology and mineralogy of the pyrophyllite deposits south of Manuels, Avalon Peninsula, Newfoundland. Unpub. M. Sc. thesis, Memorial University of Newfoundland.

KING, A.F.

1972 Late Precambrian molasse of the Avalon Platform, Newfoundland. Geol. Soc. Amer., Abstracts with programs, v. 4, no. 1, p. 26.

____

1980 The birth of the Caledonides: Late Precambrian rocks of the Avalon Peninsula, Newfoundland, and their correlatives in the Appalachian Orogen. In: Proc., the Caledonides in the U.S.A., IGCP Project 27, Caledonide Orogen, D.R. Wones, ed., p. 3-8; Dept. of Geol. Sci., Virginia Polytechnic Inst. and State Univ., Mem No. 2.

KING, A.F., BRUECKNER, W.D., ANDERSON, M.M. and FLETCHER, T.P.

1974 Late Precambrian and Cambrian sedimentary sequences of eastern Newfoundland. Fieldtrip Manual B-6, Ann. Meet., Geol. Min. Assoc., Canada, St. John's, Newfoundland.

KLINKHAMMER, G.P.

1980 Early diagenesis in sediments from the eastern equatorial Pacific: II. Pore water metal results. Earth Planet. Sci. Lett., v. 49, p. 81-101.

KRAUSKOPH, K.

1967 Introduction to Geochemistry. McGraw-Hill, Inc., 721p.

KRUMBEIN, W.C. and GARRELS, R.M.

1952 Origin and classification of chemical sediments in terms of pH and oxidation-reduction potentials. J. Geol., v. 60, p.1-39.

KUENVOLDEN, K.A., and BLUNT, D.J.

1979 Amino acid dating of bond nuclei in manganese nodules from the North Pacific. In: Marine Geology and Oceanography of the Pacific Ocean Manganese Nodule Province, Bishop, J.L. and Piper, D.Z. eds., Plenum Press, New York, p. 763-773.

LANGYMHYR, F.J. and PAUS, P.E.

1968 Analysis of silicate rocks. Anal. Chem. Acta, v.43, p. 397-408.

LYNN, D.C. and BONATTI, E.

1965 Mobility of Mn in diagenesis of deep-sea sediments. Mar. Geol., v. 3, p. 457-474.

MACAULAY, R.M.

1944 Brigus Manganese. Private rept. from Brigus Manganese Ltd., in files Geol. Surv. Can.

MAHER, J.B.

1972 Stratigraphy and petrology of the Pouch Cove-Cape St. Francis area. Unpub. M.Sc. thesis, Memorial University of Newfoundland.

MALPAS, J.G.

1972 The petrochemistry of the Bull Arm Formation near Rantem Station, southeast Newfoundland. Unpub. M.Sc. thesis, Memorial University of Newfoundland.

MANHEIM, F.T.

1961 A geochemical profile in the Baltic Sea. Geochim. Cosmochim. Act., v. 25, p. 52-71.

____

1965 Manganese-iron accumulations in the shallow marine environment. Narragansett Mar. Lab., Univ. Rhode Island, Occ. Pub. No. 3, p. 217-275.

MARTINSSON, A.

1974 The Cambrian of Norden. In: 'Cambrian of the British Isles, Norden and Spitsbergen, Lower Palaeozoic Rocks of the World', v. 2, C.H. Holland, ed., p. 185-259, John Wiley & Sons, London.

MATTHEW, G.F.

1887 On the Cambrian faunas of Cape Breton and Newfoundland. Proc. and Trans., Roy Soc. Can., Sec. 4, p. 147-157.

1896 Faunas of the Paradoxides beds in eastern North America. Trans. New York Acad. Sci., v. 15, p. 192-247.

MERO, J.L.

1972 Potential economic value of ocean-floor manganese nodule deposits. In: Ferromanganese Deposits on the Ocean Floor, D.R. Horn, ed., p. 191-204, the office for the International Decade of Ocean Exploration, Nat. Sci. Foundation, Washington, D.C.

MCCARTNEY, W.D.

1959 Manganese localities in Conception and Trinity Bays, Newfoundland. Excerpt from 'Geology of the North-Central Avalon Peninsula, Newfoundland', unpub. Ph. D. thesis, Harvard University.

1967 Whitbourne Map-area, Newfoundland. Geol. Surv. Can. Mem. 341.

MCKELVEY, V.E., WRIGHT, N.A., and ROWLAND, R.W.

1979 Manganese nodule resources in the Northeastern Equatorial Pacific. In: Marine Geology and Oceanography of the Pacific Manganese Nodule Province, Bischoff, J.L. and Piper, D.Z., eds., Plenum, Press, New York, p. 747-762.

MCKERROW, W.S., and COCKS, L.R.M.

1976 Progressive faunal migration across the Iapetus Ocean. Nature, v. 263, p. 304-306.

MINES BRANCH, OTTAWA

1942 Flotation concentration of manganese ore from the Manuel's manganese deposit of Canception Bay, Newfoundland. Ore Dressing and Metallurgical Lab., Invest No. 1249.

1943 Concentration of manganese ore from Brigus, Newfoundland, Ore Dressing and Metallurgical Lab., Invest No. 1350. Sink-and-float tests on a sample of manganese ore from Brigus, Newfoundland. Ore Dressing and Metallurgical Lab., Invest No. 1511.

MISRA, S.B.

1969 Geology of the Biscay Bay-Cape Race area, Alalon Peninsula, Newfoundland. Unpub. M.Sc. thesis, Memorial University of Newfoundland.

MOHR, P.A.

1964 Genesis of the Cambrian manganese carbonate rocks of North Wales. J. Sed. Pet., v. 34, p. 819-829.

____

1966 Genetic problems of some sedimentary manganese carbonate ores. Contr. from the Geophysical Observatory, Faculty of Science, Haile Sellassie I University, Addis Ababa, Ethiopa.

MOHR, P.A. and ALLEN, R.

1965 Further considerations on the deposition of the Middle Cambrian manganese carbonate beds of Wales and Newfoundland. Geol. Man., v. 102, p. 328-337.

MURRAY, A. and HOWLEY, J.P.

1881a Geological Survey of Newfoundland (from 1864 - 1880) London, Edward Stanford.

____

1881b Map of the Peninsula of Avalon. Geol. Surv. Nfld.

MURRAY, J. and IRVINE, R.

1895 On the manganese oxides and manganese nodules in marine deposits. Trans. Roy. Soc. Edinburgh, v. 37 p. 721-742.

NAUTIYAL, A.C.

1966 The Cambro-Ordovician sequence in the southeastern part of the Conception Bay area, Newfoundland. unpub. M.Sc. thesis, Memorial University of Newfoundland.

NICHOLLS, G.D.

1962 A scheme for recalculating the chemical analyses of argillaceous rocks for comparative purposes. Amer. Mineral., v.47, p. 34-46.

O'BRIEN, S.E., STRONG, P.G. and EVANS, J.L.

1977 The geology of the Grand Bank (1M/4) and Lamaline (1L/13) map-areas, Burin Peninsula, Newfoundland. Newfoundland Dept. Mines. Agric. and Resources, Min. Dev. Div., Report 77-7.

PALMER, A.R. and JAMES, N.P.

1980 The Hawke Bay Event; a circum-Iapetus Regression near the lower-Middle Cambrian boundary. In: Proc., the Caledonides in the USA, IGCP Project 27, Caledonide Orogen, D.R. Wones, ed., p. 15-18, Dept. Geol. Sci., Virginia Polytechnic Inst. and State Univ., Mem. No. 2

PAPEZIK, V.S.

1970 Petrochemistry of volcanic rocks of the Harbour Main Group, Avalon Peninsula, Newfoundland. Can. J. Earth Sci., v. 7, p. 1485-1498.

____

1972 Late Precambrian ignimbrites in eastern Newfoundland and their tectonic significance. In: 24th Int. Geol. Cong. (Montreal), Sect. 1, p. 147-152.

____

1973 Detrital garnet and muscovite in Late Precambrian sandstone near St. John's, Newfoundland, and their significance. Can. J. Earth Sci., v. 10, p. 430-432.

____

1980 Volcanic rocks in Newfoundland: a review. In: Proc., the Caledonides in the USA, IGCP Project 27, Caledonide Orogen, D.R. Wones, ed., p. 245-248, Dept. of Geol. Sci., Virginia Polytechnic Inst. and State Univ., Mem. No. 2.

PEARSON, M.J.

1978 Quantitative clay mineralogical analyses from the bulk chemistry of sedimentary rocks. Clays and Clay Minerals, v. 26, p. 423-432.

PEDERSON, T.F. and PRICE, N.B.

(unpub. manuscript.) The geochemistry of manganese carbonate in Panama Basin sediments.

PETTIJOHN, F.J.

1957 Sedimentary Rocks, 2nd ed. New York: Harper & Bros., 718p

POULSON, V. and ANDERSON, M.M.

1975 The Middle-Upper Cambrian transition in southeastern Newfoundland, Canada. Can. J. Earth Sci., v. 12, p. 2065-2079.

RAST, N., KENNEDY, M.J. and BLACKWOOD, R.F.

1976 Comparison of some tectono-stratigraphic zones in the Appalachians of Newfoundland and New Brunswick. Can. J. Earth Sci., v. 13, p. 868-875.

RAST, N., O'BRIEN, B.H. and WARDLE, R.J.

1976 Relationships between Precambrian and Lower Paleozoic rocks of the 'Avalon Platform' in New Brunswick, the Northeast Appalachians, and the British Isles. Tectonophysics, v. 30, p. 315-338.

REX, R.W.

1969 X-ray mineralogy studies--Leg 1. In: Peterson <u>et al.</u>, Initial Reports of the Deep Sea Drilling Project, v. 1, U.S. Gov't. Printing Office, p. 354-367.

———

1970 X-ray mineralogy studies, Leg 2. In: Peterson, M.N.A. <u>et al.</u>, Initial reports of the Deep Sea Drilling Project, v. 2. Washington (U.S. Gov't. Printing Office), p. 329-346.

REX, R.W. and MURRAY, B.

1970 X-ray mineralogy studies. In: McManus <u>et al.</u>, Initial Reports of the Deep Sea Drilling Project., v. V, U.S. Gov't Printing Office, p. 441-482.

RONA, R.A.

1978 Criteria for recognition of hydrothermal mineral deposits in oceanic crust. Econ. Geol., v. 73, p. 135-160.

ROSE, E.R.

1948 Geology of the area between Bonavista, Trinity, and Placentia Bays, Eastern Newfoundland. Geol. Surv. Nfld., Bull. 32, pt. 2, p. 39-49.

———

1952 Torbay map-area, Newfoundland. Geol. Surv. Can. Mem. 265.

ROSE, H.J., JR., ADLER, I. and FLANAGAN, F.J.

1962 Use of La_2O_3 as a heavy absorber in the x-ray analysis of silicate rocks. U.S.G.S. Prof. Papers 450-R, B-80-B-82.

SABINA, A.P.

1975 Rocks and minerals for the collector, the Magdalen Islands Quebec and the Island of Newfoundland. Geol. Surv. Can. Paper 75-36.

SAPOZHNIKOW, D.G. (ed.)

1970 Manganese Deposits of the Soviet Union. Trans. by Israel Program for Scientific Trans., Jerusalem, 1970.

SCHENK, P.E.

1971 Southeastern Atlantic Canada, Northwestern Africa and continental drift. Can. J. Earth Sci., v. 8, p. 1218-1251.

SCHULTZ, L.G.

1964 Quantitative Interpretation of mineralogical composition from x-ray and chemical data for the Pierre Shale. U.S.G.S. Prof. Paper 391-C.

SHAW, D.B. and WEAVER, C.E.

1965 The mineralogical composition of shales. J. Sed. Pet., v. 35, p. 213-222.

SHERIDAN, R.E. and DRAKE, C.L.

1968 Seaward extension of the Canadian Appalachians. Can. J. Earth Sci., v. 5, p. 373.

SPEARMAN, C.

1941 Report on manganese deposit near Brigus, Conception Bay, Newfoundland. Private rept. in files, Geol. Surv. Can.

STRONG, D.F.

1979 Proterozoic tectonics of northwestern Gondwanaland: new evidence from eastern Newfoundland. Tectonophysics, v. 54, p. 81-101.

STRONG, D.F., DICKSON, W.L., O'DRISCOLL, C.F., KEAN, B.F. and STEVENS, R.K.

1974 Geochemical evidence for eastward Appalachian subduction in Newfoundland. Nature, v. 248, p. 37-39.

STRONG, D.F., O'BRIEN, S.J., STRONG, P.G., EVANS, J.L. and SWINDEN, H.S.

1978a Geology of the Grand Bank (1M/4) and Lamaline (1L/13) map-areas, Newfoundland. Unpub. rept., Dept. Mines and Energy, Govt. of Newfoundland and Labrador.

STRONG, D.F., O'BRIEN, S.J., TAYLOR, S.W., STRONG, P.G., and WILTON, D.H.

1978b Aborted Proterozoic rifting in eastern Newfoundland. Can. J. Earth Sci., v. 15, p. 117-131.

TRAILL, R.J. and LACHANCE, G.R.

1965 A new approach to x-ray spectrochemical analysis. Geol. Surv. Can. Paper 64-57.

VAN ALSTINE, R.E.

1948 Geology and mineral deposits of St. Lawrence area, Burin Peninsula, Geol. Surv. Nfld., Bull. 23.

VAN INGEN, G.

1914 Table of geological formations of the Cambrian and Ordovician Systems about Conception and Trinity Bays, Newfoundland. Princeton Univ. Contr. to Geol. of Newfoundland, No. 4.

VARENTSOV, I.M.

1964 Sedimentary manganese ores. Elsevier Publishing Co., Amsterdam.

WALCOTT, C.D.

1900 Lower Cambrian terrane in the Atlantic Provinces. Proc. Wash. Acad. Sci., v. 1, p. 301-399.

WHITE, D.E.

1939 Geology and molybdenite deposits of the Rencontre East area, Fortune Bay, Newfoundland, Ph.D. thesis, Princeton University.

WIDMER, K.

1952 The geology of the Hermitage Bay area, Newfoundland. Unpub. Ph.D. theiss, Princeton University.

WILLIAMS, H.

1964 The Appalachians in northeastern Newfoundland--a two-sided symmetrical system. Amer. J. Si., v. 262, p. 1137-1158.

———

1971 Geology of Belleoram map-area, Newfoundland (1M/11). Geol. Surv. Can. Paper 70-65.

———

1979 Appalachian Orogen in Canada. Can. J. Earth Sci., v. 16, p. 792-807.

WILLIAMS, H.

1980 Structural telescoping across the Appalachian Orogen and the minimum width of the Iapetus Ocean. In: The Continental Crust and its Mineral Deposits, D.W. Strangway, ed., G.S.C. Special Paper 20, p. 421-440.

WILLIAMS, H., KENNEDY, M.J. and NEALE, E.R.W.

1972 The Appalachian Structural Province. In: Variations in Tectonic Styles in Canada, R.A. Price and R.J.W. Douglas eds., p. 181-261, Geol. Assoc. Can. Spec. Paper no. 11.

1974 The northeastward termination of the Appalachian Orogen. In: The Ocean Basins and Margins, A.E.M. Nairn and F.G. Stehli, eds., p. 79-123, Plenum Press, New York.

WILLIAMS, H. and KING, A.F.

1976 Southern Avalon Peninsula, Newfoundland. Trepassey map-area. Geol. Surv. Can., Paper 76-1A, p. 179-182.

WILSON, J.T.

1966 Did the Atlantic close--then re-open? Nature, v. 211, p. 676-681.

WISEMAN, R.

1942 Manuels and Kelligrews manganese deposits. Geol. Surv. Newfoundland, unpub. rept., in files of Geol. Surv. Can.

WISSINK, A.

1972 Les gisement de manganese du monde, conditions de depot, typologie et metal contenu. Bull du. B.R.G.M. (deuxieme serie), Sect. II, 33-48.

WOODLAND, A.W.

1939 The petrography and petrology of the Lower Cambrian manganese ore of West Merionethshire. Quart. J. Geol. Soc., London, v. 95, p. 1-36.

APPENDICES

APPENDIX 1-1 X-RAY DIFFRACTION DATA

All x-ray diffractograms were obtained using unorientated powder mounts contained in aluminum holders. A Norelco generator with a Phillips PW1050 goniometer and Phillips electronic panel was used to obtain the diffractograms. Cu radiation, Ni-filtered, was used throughout. Other operating parameters were as follows: mA = 20; kV = 20; chart speed 1^0/minute; range 4×10^2; and time constant = 4.

Calculation of Relative Mineral Proportions

The method employed is essentially that used on cores recovered by the Deep Sea Drilling Project (Rex, 1969). Peak areas (see Table 4.2) for chlorite, illite, quartz, feldspar, hematite (when present), and carbonate minerals (when present) were measured as follows: a) baselines were drawn for each peak from background count levels on either side; b) peak areas were computed by overlaying a 1 mm^2 grid and counting the number of squares contained within the peaks (half-squares were counted as such, while > half squares were counted as units and ≥ half squares not counted); the total area of all peaks measured in a sample obtained by addition; and relative proportion percentages obtained for each mineral by division against the total peak area.

The relative proportions obtained in this way were stored on computer cards and used statistically as discussed in Chapter 4. The results obtained for 106 samples are listed in Table III-1.

1-2 Calculation of Normative Mineral Proportions

The results obtained from major element analyses of Cambrian rock samples were used to obtain these normative estimates. Insofar as chlorite, illite, quartz, feldspar, hematite and carbonates were the only mineral species detected on x-ray diffractograms, it was assumed that these minerals contained all of the major element concentrations obtained from analysis. Mineral compositions were assigned each species as discussed in Chapter 4 (Table 4.2). Then, for each element, an equation of the type

$$C_1 \times xi + C_2 \times yi + C_3 \times zi + \ldots\ldots = Ri$$

can be formulated, where C_1 represents the proportion of mineral C_1 in the rock; xi, yi, and zi represent the percentage of element i present in minerals C_1, C_2 and C_3; and Ri represents the total concentration of element i in the rock as determined by chemical analysis. Similar equations can be set up for other elements, and the equations solved simultaneously, using matrices, to obtain percentage values for C_1, C_2, C_3, etc.

The computer program used for these calculations could solve for up to seven mineral components. It is available from the Department of Geology, Memorial University of Newfoundland. The method used is similar to that employed by Pearson (1978) to calculate clay mineral proportions in sedimentary rocks. Because of the mineralogical simplicity and constancy of the sedimentary rocks in SE Newfoundland, proportions for all mineral species could be obtained.

The normative proportions calculated in this way were compared with relative mineral proportions obtained from x-ray diffraction as discussed in Chapter 4. The results obtained for 106 green mudrocks, manganese horizon samples, and limestones are listed in Table III-1.

Additional normative proportions calculated for red mudrocks and limestones are given in Table III-2 and Table III-3 respectively.

APPENDIX II. CHEMICAL DATA

Chemical data were obtained from lower and middle Cambrian rocks by means of X-ray fluorescence and atomic absorption spectroscopy. All trace element and most major element data were obtained from X-ray fluorescence (XRF) analysis. Atomic absorption spectroscopy (AA) was used to measure MnO and Na_2O contents in the samples, because of a problem with Cr interference in the case of the former and the lack of the appropriate X-ray tube for the latter. A small group of samples were analyzed for all major elements by AA so as to allow comparison of the two methods.

The results obtained for major and trace element analysis are listed in Table III-4. Analytical techniques and sample preparation are discussed below.

II-1. X-Ray Fluorescence (XRF)

Sample Preparation

Samples were crushed with a hammer into pieces approximately 0.5 cm diameter. This material was then further crushed in a swing mill utilizing a tungsten-carbide bowl and rings for a period of one minute, which was sufficient time to reduce the sample to a powder passing through a 100 mesh nylon screen. The tungsten-carbide bowl and rings were first scoured with quartz sand and then cleaned by hand with detergent. Sample powders were stored in labelled glass bottles.

The analytical method used for XRF analyses is essentially that described by Rose (1962). Samples were prepared for major element analysis as follows: The fusion mixture was composed of 0.750 gm sample, 0.750 gm Lanthanum oxide, and 7.500 gm lithium tetraborate. The samples were fused in batches of 12 in a muffle furnace at 1050°C, where they were held for 20 minutes. They were then allowed to cool, the fusion beads weighed, and sugar added to bring the weight to a constant 9.000 gm. The fusion beads were then crushed in a Spex ball mill for 20 minutes, following which 1.5 gm of the mixture was weighed and placed in a 32 mm die on top of Boric acid (used for disc backing). The mixture was then subjected to 20 tons p.s.i. pressure for 1 minute in a Hertzog press to prepare the discs used for major element determinations.

In the case of trace element analyses, 1.5 gm of rock powder was mixed with 2% wt/vol solution of polyvinyl alcohol cement. The mixture was placed in a 32 mm die with Boric acid and pressed as above to create discs.

The analyses were conducted using a Phillips Model 1220 System with a Honeywell computer used for calculations.

Accuracy of Data

The calculated accuracy of XRF major and trace element analyses, as derived from the calibration curves used to control the analytical programs, is given in Table II-1. The number of standards used to construct the calibration curves, and the range in elemental concentration of these standards, are also shown. The figures for MnO are misleading, in view of the Cr interference problem mentioned earlier; also the majority of Manganese Horizon samples fall well beyond the high end of the standard range (0.73%). However, the correspondence

TABLE II-1. ACCURACY* FOR XRF CHEMICAL DATA

Element	No. Standards	Standard Deviation**	Range
SiO_2	22	0.58%	0.07-75.8%
TiO_2	22	0.046%	0.02-4.6%
Al_2O_3	22	0.313%	0.19-23.58%
Fe_2O_3	23	0.198%	0.05-28.00%
MnO	--	---	----
MgO	20	0.69%	0.36-43.3%
CaO	18	0.348%	0.15-30.15%
Na_2O	--	---	----
K_2O	21	0.128%	0.01-15.34%
P_2O_5	19	0.11%	0.01-1.00%
Ba^+	18	0.008%	0.10-0.25%
Ba^{++}	18	0.0025%	8-358 ppm
MnO^{++}	17	0.016%	0.01-0.73%
Zr	18	0.0016%	17-507 ppm
Sr	16	0.0018%	3-4482 ppm
Rb	18	0.0006%	5-531 ppm
Zn	19	0.0008%	32-197 ppm
Cu	20	0.0005%	4-536 ppm
Nb	11	0.0013%	12-964 ppm
Ce	13	0.0016%	2-1897 ppm
La	12	0.0016%	2-1699 ppm
Ni	18	0.008%	4-2120 ppm
Cr	19	0.0014%	5-2729 ppm
V	14	0.0025%	8-358 ppm

* derived from calibration curves

** ~ standard error of estimate

\+ run as major element

++ run as trace element

between XRF major element data and AA data obtained for the same samples (see below) suggest that the values given for major elements in Table II-1 are acceptable.

Precision of Data

The precision for XRF major element analyses is summarized in Table II-2. Data obtained from multiple analyses of three rock standard powders and from an "in house" bulk sample (MACH A) are included in the table. It can be seen that with the exception of MgO, precision levels are good, < 0.25%. The precision achieved on multiple runs of the bulk sample MACH A (a limy green mudrock) further suggests that the Cambrian mudrocks which dominate the stratigraphic section are homogenous, at least on the scale of a hand specimen.

Trace element precision for the XRF data is shown in Table II-3. Standard deviations from the mean concentrations are <10 ppm, except for Sr, Ce, La and Ba (the latter with a much higher mean). Nb was not detected in bulk sample MACH 1-B.

II-2. Atomic Absorption Spectroscopy (AA)

Rock powders used in AA analyses were those used in XRF work (described above). The analytical method employed has been adapted from the work of Langymhyr and Paus (1968), and Abbey (1968). All analyses were made with a Perkin-Elmer Model 303 instrument.

Sample preparation and standard preparation are described below.

TABLE II-2. XRF MAJOR ELEMENT PRECISION

	Pcc-1 (N=15)		GSP-1 (N=17)		NBS-88a (N=15)		MACH 'A' (N=27)	
	Mean	S.D.	Mean	S.D.	Mean	S.D.	Mean	S.D.
Fe_2O_3	8.51	0.087	4.46	0.091	0.49	0.047	9.39	0.09
TiO_2	0.03	0.003	0.66	0.007	0.03	0.003	0.78	0.03
BaO	--	---	0.13	0.003	--	---	0.129	0.002
P_2O_5	0.26	0.13	0.27	0.141	0.04	0.146	0.15	0.109
SiO_2	41.08	0.22	66.57	0.418	0.71	0.18	58.68	0.50
CaO	1.02	0.034	2.02	0.074	30.86	0.43	5.34	0.132
k_2O	--	--	5.65	0.065	0.10	0.009	3.65	0.039
MgO	70.15	15.31	0.54	0.593	31.26	0.095	1.53	0.71
Al_2O_3	0.59	0.092	15.25	0.182	0.21	0.104	18.02	0.282

N = nd. runs. Pcc-1, GSP-2, NBS-88a = rock standard powders

MACH 'A' = bulk sample, Chamberlains Brook Formation, Manuel's, Conception Bay

TABLE II-3. XRF TRACE ELEMENT PRECISION, SAMPLE MACH 1-8

Element	No. Runs	Mean (ppm)	Standard Deviation (ppm)
Zr	16	100	5
Sr	16	41	13
Rb	16	103	4
Zn	16	85	2
Cu	10	4	3
Ni	16	68	1
MnO*	16	0.31	0.01
Cr	16	83	7
V	16	92	5
Ce	16	96	14
La	15	57	48
Ba	16	1337	27

* in percent

The weights and dilutions for the analyses of major elements are made to simplify final calculations.

The sample weight of 0.2000 gm is made up to 200 ml, thus giving 100 mg per 100 ml of solution. In this way, if a solution contains 100 ppm of Fe_2O_3, the percentage Fe_2O_3 in the actual sample is 10%.

E.g. 1 ppm = 1 mg/ml or 1 mg/1 litre

100 ppm = 100 mg/1

Above we have 200 ml of solution and each ml contains the equivalent of 100 mg/litre; therefore in the total solution (200 ml) there are 20 mg Fe_2O_3.

Since this came from 0.2000 gm

$$\therefore 1 \text{ gm of sample would contain } \frac{.020}{.2000} = 0.1 \text{ gm}$$

$$+ \frac{0.1}{1} \times 100 = 10\%$$

This is the basis for the calculations and the making up of standard solutions.

Making Standard Blends

The standards are really artificially made rock samples. All the elements are added in proportions to resemble rock types.

The basic standard solutions are solutions made from 'spetpure' elements or salts of the elements to give 1000 ppm of the oxide of the element.

E.g. 0.26463 gm of pure aluminium is dissolved using 25 ml conc. HCl and the final volume is made to 500 ml with H_2O, then this solution contains the equivalent of 0.5000 gm of Al_2O_3 = 1000 ppm.

The 'specpure' compounds and elements used are SiO_2, Ti, Al, Fe_2O_3, KCl, $CaCO_3$, MgO, Na_2CO_3 and Mn.

To make a standard blend to correspond with definite percentages as in a typical rock:

	% oxide in rock	ml of 1000 ppm Sol'n	ppm of oxides in sol'n
SiO_2	51.5	103.0*	515
TiO_2	1.0	2.0	10
Al_2O_3	18.0	36.0	180
Fe_2O_3	9.5	19.0	95
MnO	0.15	0.3	1.5
MgO	6.0	12.0	60.0
CaO	10.0	20.0	100
Na_2O	3.0	6.0	30
K_2O	0.7	1.4	7
P_2O_5	0.15	0.3	1.5
	100.00%	200 ml	10000 ppm

* In order to have the same amount of HF and saturated Boric acid in the standards as in the sample the SiO_2 is weighed exactly: i.e. 0.1030 gm in this case, 5 ml HF is added and 50 ml of saturated Boric acid is added. Hence 48 ml of H_2O must be added to make total to 200 ml.

Using this as a guide a series of blends can be made up giving a range of values for each oxide to be determined.

The results obtained from duplicate analyses of a number of samples for MnO are given in Table II-4. It is evident that AA analysis for MnO yields reproducable results.

II-3. Comparison of XRF and AA Analytical Data

The results obtained from AA analysis of a small group of samples for major elements are compared with the results obtained by XRF analysis for those samples in Table II-5. The data in this table show that the two methods yield equivalent results. The correspondence is, in general, good; excellent for some elements (e.g. K_2O, Fe_2O_3) and suspect only for MgO determinations.

Table II-2 shows that MgO determinations by XRF are the least precise for any major element. The anomalously low MgO determinations (by XRF) in Table II-5 occur in Ca- or Mn-rich carbonate samples; presumably, some matrix or mass absorption effect in such samples is responsible for the low XRF values.

Loss on Ignition

Weight percent loss on ignition (L.O.I.) was determined by heating sample powders in a muffle furnace at 1000°C for 90 minutes, then weighing and measuring weight loss. Duplicate L.O.I. determinations, shown in Table II-6, are in close agreement.

TABLE II-4. DUPLICATE MnO ANALYSES BY AA

Sample No.	1st (%)	2nd (%)
BE-1	1.22	1.32
DB-99	0.56	0.61
DB-105	0.16	0.12
M-98	1.61	1.85
DB-94	3.41	3.31
M-91-b	26.66	27.24
M-93	13.30	12.55
Bw-4b	6.90	6.24
M-73A	15.73	15.74
CC-13	48.56	49.50
BE-0	26.24	27.04
BE-4	48.12	50.49
LZ-6-A	11.90	11.70
LY-2	0.22	0.21
HH-36-1	14.11	14.06

TABLE II-5. COMPARISON OF XRF TO AA MAJOR ELEMENT DATA

Sample No.	SiO_2	TiO_2	Al_2O_3	Fe_2O_3	MgO	CaO	K_2O	P_2O_5
DB-99	9.91	0.11	2.33	1.22	---	47.07	0.75	--
	11.51^{+}	<0.1	2.93	1.13	0.60	44.85	0.61	0.30^{++}
DB-62	6.39	0.09	1.88	0.91	---	49.85	0.29	--
	7.32	<0.1	2.40	0.74	0.75	47.25	0.26	--
DB-63	59.01	0.96	18.43	6.43	3.84	0.98	3.83	0.25
	58.49	0.70	16.95	6.44	3.46	0.75	3.93	0.25
DB-101	59.24	1.10	18.45	8.12	2.03	0.44	5.00	0.18
	58.23	0.89	16.91	8.11	2.17	0.45	5.16	0.10
CC-16	6.28	0.09	2.37	3.37	---	9.10	0.17	--
	5.34	0.15	2.33	3.21	1.70	8.62	0.21	0.18
HH-39-2	15.75	0.30	5.79	6.08	3.11	13.86	0.51	--
	14.88	0.25	5.87	6.42	3.54	13.45	0.51	0.60
HH-34001	22.16	0.31	10.99	8.13	2.75	9.63	0.96	--
	21.87	0.36	8.75	7.98	3.34	9.67	0.99	0.10
LZ-8	24.00	0.30	9.89	9.79	2.10	9.19	1.86	--
	23.60	0.32	8.07	10.17	2.90	9.50	1.83	0.40
M-96BOT	24.03	0.38	9.55	10.78	1.16	13.17	0.80	--
	23.47	0.41	8.33	11.11	2.54	13.19	0.82	0.29
WB-10	48.54	0.59	12.05	6.62	---	4.32	2.36	--
	48.13	0.52	11.20	6.65	2.17	4.14	2.40	0.07
SE-5-1	19.30	0.34	5.10	6.30	1.59	9.72	0.42	--
	18.56	0.22	5.43	6.26	2.50	10.22	0.42	0.28
MACH A*	50.68	0.78	18.02	9.39	1.53	5.34	3.65	0.15
	51.70	0.80	17.81	9.45	1.96	5.51	3.51	--

All data in weight percent oxide.

+ second line = AA values
++ P_2O_5 colorometrically analyzed
* XRF data average of 27 analyses.

TABLE II-6. DUPLICATE L.O.I. DETERMINATIONS

Sample No.	First Determination	Second Determination
CC-16	30.61	30.56
NC-3	4.02	3.87
CH-11b	28.39	28.35
Sc-9	25.11	24.84
BE-6	27.13	26.73
WB-51	23.94	23.69
HH-39-2	26.19	25.97
HH-34-A	27.47	27.14
SP-33-b	19.20	19.00
RL-11	19.26	18.95
M-73'A'	18.31	17.91
LZ-8	19.17	18.90
BW-HA	6.13	6.05
C-19	10.87	10.88
BW-5	28.58	28.31

All values in weight percent loss on ignition

APPENDIX III. TABLES AND DIAGRAMS

Tables III-1 through III-4 have been discussed in earlier appendices. The key to locating the samples listed in Table III-4 is given below (see Fig. 1.1 for geographic location).

TABLE III-1

Normative and X-ray Diffraction-Derived Estimates of Mineralogical Composition of Cambrian Rock Samples

Sample No.	Relative Mineral Proportions (in percent). Results from X-ray Diffraction Analysis. Blanks = none detected.						Normative Mineral Proportions (in percent). From Major Element Chemical Analysis. Blanks = not calculated.						
	Illite	Chlorite	Quartz	Feldspar	Hematite	Total Carbonate	Chlorite	Illite	Feldspar	Amount CaO in carbonate minerals	Amount MgO in carbonate minerals	Quartz	Hematite
CW-6	8.26	34.86	27.52	29.36			25.32	25.66	17.98	0.21	-0.11	29.47	
LY-8	8.87	47.58	24.19	19.35			29.35	27.16	15.82	-0.00	-0.17	29.80	
MP-1	17.39	53.26	21.74	7.61			29.25	32.75	10.89	1.31	1.26	21.92	
KEEL-1	16.34	45.75	22.22	15.69			23.71	27.38	14.45	0.07	-0.18	32.54	
LY-17	6.90	45.69	30.17	17.24			23.89	22.67	14.01	0.63	-0.01	38.60	
WB-1	7.14	34.92	27.78	30.16			20.28	23.11	19.96	0.22	-0.06	35.17	
CAV-3	11.11	37.78	31.11	20.00			22.62	30.43	9.78	1.34	1.10	32.29	
SE-1	10.23	44.32	26.14	19.32			31.75	31.78	12.81	0.05	-0.05	24.03	
436	13.98	26.88	30.11	29.03			17.13	35.36	14.67	-0.25	-0.13	29.58	
SP-9	11.50	25.66	27.43	35.40			25.04	19.43	18.53	1.44	-0.23	32.74	
SP-25	6.48	50.00	14.81	9.26		19.44	40.94	19.44	11.68	2.33	-0.27	20.29	

9.

TABLE III-1 (continued)

Sample No.	Relative Mineral Proportions (in percent). Results from X-ray Diffraction Analysis. Blanks = none detected.						Normative Mineral Proportions (in percent). From Major Element Chemical Analysis. Blanks = not calculated.						
	Illite	Chlorite	Quartz	Feldspar	Hematite	Total Carbonate	Chlorite*	Illite	Feldspar	Amount CaO in carbonate minerals	Amount MnO in carbonate minerals	Quartz	Hematite
SP-17	9.52	27.78	30.95	31.75			25.66	19.88	18.96	0.61	-0.18	35.09	
OP-6	7.92	29.71	29.70	33.66			23.72	24.67	19.78	-0.01	-0.11	32.97	
SP-73-9	12.05	32.53	30.12	25.30			22.71	32.14	12.40	0.23	-0.17	30.16	
SP-73-6	13.10	44.05	26.19	16.67			29.66	27.57	13.29	0.14	-0.23	29.95	
SP-3	7.83	26.96	35.65	29.57			25.20	13.65	16.87	0.73	-0.21	40.73	
SP-50	12.05	44.58	26.30	18.07			30.97	34.03	9.31	0.27	-0.27	25.76	
SP-25	16.50	45.63	20.39	17.48			34.63	29.20	11.28	0.21	-0.25	25.45	
OP-27	13.27	39.80	24.49	14.29			25.19	37.88	11.70	0.05	-0.16	24.54	
JW-5	12.36	26.97	28.09	32.58			22.88	30.96	18.64	-0.04	-0.13	27.22	
DC-3	13.24	29.41	39.71	17.65			25.93	31.46	7.85	0.43	-0.05	34.20	
BR-3	10.13	39.24	27.85	22.78			28.12	25.35	14.33	1.95	-0.03	27,94	
CH-25	21.43	31.63	24.49	22.45			23.00	33.85	15.41	0.02	-0.11	26.31	
CH-19	10.47	36.05	30.23	23.26			26.75	29.41	15.45	-0.03	-0.04	29.02	
CH-29	8.91	32.67	26.73	31.68			24.01	27.81	19.44	-0.09	-0.13	28.99	
CH-16	9.38	46.88	25.00	18.75			33.59	25.67	15.06	-0.03	0.07	25.98	

TABLE III-1 (continued)

Sample No.	Relative Mineral Proportions (in percent). Results from X-ray Diffraction Analysis. Blanks = none detected.						Normative Mineral Proportions (in percent). From Major Element Chemical Analysis. Blanks = not calculated.						
	Illite	Chlorite	Quartz	Feldspar	Hematite	Total Carbonate	Chlorite*	Illite	Feldspar	Amount CaO in carbonate minerals	Amount MnO in carbonate minerals	Quartz	Hematite
M-103	15.19	29.11	34.18	21.52			22.32	31.78	7.63	0.66	0.51	31.96	
M-107	17.70	46.90	23.89	11.50			29.92	32.99	0.01	0.18	-0.29	28.41	
M-69	16.33	36.73	22.45	24.49			30.12	29.15	11.22	0.15	-0.26	29.64	
M-21	19.75	28.40	25.93	25.93			25.79	32.24	10.99	0.32	-0.14	28.31	
BE-9	5.13	54.70	24.79	11.97		3.42	42.74	14.76	6.56	1.36	0.44	35.44	
DB-95	6.67	57.14	21.90	14.29			28.12	33.68	10.00	0.04	-0.09	28.16	
DB-73-5	9.01	37.84	24.32	28.83			25.03	30.88	16.04	-0.15	-0.13	28.74	
DB-96	16.94	47.58	20.97	14.52			25.51	35.26	9.75	0.43	-0.11	28.23	
HH-45	14.91	39.60	22.81	23.68			23.24	30.83	15.24	0.08	0.25	29.59	
HH-28	11.93	49.54	25.69	12.84			29.61	33.07	8.44	0.06	-0.34	27.36	
HH-26	16.52	42.61	24.35	16.52			26.55	31.88	8.73	0.10	-0.31	33.90	
HH-43	6.84	55.56	23.03	14.53			45.36	14.34	9.14	1.63	-0.16	31.13	
HH-32	11.86	44.92	22.03	21.19			27.22	28.64	15.16	-0.04	-0.11	27.49	
HH-31	13.95	51.16	17.05	17.83			30.96	28.30	12.25	0.06	-0.19	27.84	

TABLE III-1 (continued)

Sample No.	Relative Mineral Proportions (in percent). Results from X-ray Diffraction Analysis. Blanks = none detected.						Normative Mineral Proportions (in percent). From Major Element Chemical Analysis. Blanks = not calculated.						
	Illite	Chlorite	Quartz	Feldspar	Hematite	Total Carbonate	Chlorite*	Illite	Feldspar	Amount CaO in carbonate minerals	Amount MnO in carbonate minerals	Quartz	Hematite
HH-296	9.17	60.55	22.02	8.26			40.22	23.10	7.91	0.23	-0.37	30.34	
HH-48	12.82	47.86	21.37	17.95			31.03	29.75	11.19	0.15	-0.31	29.19	
HH-5	10.40	40.00	16.80	14.40		18.40	32.98	22.08	9.75	4.34	0.24	27.87	
HH-51	10.00	41.67	20.83	20.00		7.50	35.10	21.94	13.41	1.10	-0.18	27.71	
CW-5	13.76	20.18	25.69	33.03	7.34		14.20	32.71	18.62	-0.23		31.95	3.42
LY-6	15.60	33.03	19.27	21.10	11.01		12.88	37.77	15.96	-0.09		27.44	5.46
OP-37	9.89	27.47	34.07	10.68	9.89		18.15	28.60	11.59	1.10		34.67	4.59
OP-18	17.95	28.21	25.64	17.95	10.26		22.73	36.71	12.21	0.07		25.24	3.40
SP-37	14.67	14.67	32.00	26.67	12.00		15.03	36.44	15.22	0.06		27.14	4.21
SP-73-2	14.29	9.09	38.96	27.27	10.39		15.82	32.38	14.71	0.24		31.24	2.74
SP-46	12.33	13.70	34.25	21.92	17.81		19.64	31.91	19.03	0.25		28.96	5.19
BR-11-2	10.53	14.47	28.95	28.95	17.11		18.48	24.04	13.59	0.67		33.89	5.57
CH-28	10.81	12.16	28.38	28.38	20.57		10.29	32.96	19.54	1.00		25.64	6.53
CH-20	12.35	17.28	30.86	27.16	12.35		16.59	33.11	19.08	-0.16		26.21	3.73
CH-1	14.12	17.65	25.88	30.59	11.76		15.70	34.76	16.51	0.03		26.36	5.27

TABLE III-1 (continued)

Sample No.	Relative Mineral Proportions (in percent). Results from X-ray Diffraction Analysis. Blanks = none detected.						Normative Mineral Proportions (in percent). From Major Element Chemical Analysis. Blanks = not calculated.						
	Illite	Chlorite	Quartz	Felspar	Hematite	Total Carbonate	Chlorite*	Illite	Feldspar	Amount CaO in carbonate minerals	Amount MgO in carbonate minerals	Quartz	Hematite
CH-34A	14.00	16.00	29.00	27.00	14.00		12.98	30.06	17.83	0.09		30.42	5.42
HH-47	18.02	33.33	22.52	18.92	7.21		12.91	35.68	15.69	-0.12		27.94	5.34
NM-6	8.65	22.12	17.31	10.58		41.35	21.51	24.25	5.90	6.46	7.39	24.99	
NM-9	6.82	46.59	21.59	6.82		18.18	30.58	25.60	6.01	3.23	3.11	27.29	
NM-8	1.77	53.98	7.08	3.54		33.63	55.44	-0.01	0.56	10.34	7.25	17.18	
NM-4	8.74	31.08	22.33	9.71		28.16	22.81	27.45	7.76	5.41	1.66	28.68	
NM-15	9.35	45.79	20.56	14.02		10.28	39.37	22.26	8.02	0.29	1.31	29.24	
CH-8	4.63	77.78	14.81	2.78			68.25	10.61	4.81	1.09	0.42	18.23	
CH-13	2.36	56.69	10.34			30.71	52.98	4.19	2.65	8.08	7.62	15.41	
CH-10	1.91	31.85	12.10			54.14	41.78	1.59	2.19	9.56	10.82	23.16	
CH-12	10.28	24.30	42.06	23.36			18.99	22.67	16.30	0.49	0.54	39.22	
CH-15	5.69	47.97	18.70	8.94		18.70	44.90	14.67	8.63	2.58	1.51	26.51	
CH-11-B		15.56	2.96			81.48	20.83	0.96	0.84	17.33	26.89	4.47	
CH-3	5.36	38.39	16.07	7.14		33.04	37.50	14.50	6.93	5.41	7.74	18.96	
CH-5		41.84	11.22	7.14		39.80	37.38	11.30	5.66	9.03	7.96	16.44	

TABLE III-1 (continued)

Sample No.	Relative Mineral Proportions (in percent). Results from X-ray Diffraction Analysis. Blanks = none detected.						Normative Mineral Proportions (in percent). From Major Element Chemical Analysis. Blanks = not calculated.						
	Illite	Chlorite	Quartz	Feldspar	Hematite	Total Carbonate	Chlorite	Illite	Feldspar	Amount CaO in carbonate minerals	Amount MnO in carbonate minerals	Quartz	Hematite
CH-11-A	6.38	42.55	29.79	11.70		9.57	42.50	11.29	8.07	1.92	1.73	35.47	
CH-6	14.15	15.09	26.42	19.81		24.53	16.40	28.54	17.36	1.50	3.51	27.11	
CH-7-T	1.03	67.01	22.68	3.09		6.19	57.51	9.58	6.09	0.41	0.30	26.01	
M-90-BOT		9.68	4.84			85.48	9.77	8.18	4.23	5.75	40.94	6.46	
M-95	8.57	47.62	22.86	13.33		7.62	34.47	23.58	6.59	0.90	1.38	31.45	
M-85-4	10.71	28.57	14.29	13.10		33.33	21.52	23.06	7.57	2.06	12.62	21.98	
M-73-A		31.03	8.05	3.45		57.47	35.31	2.48	1.57	9.86	15.21	16.51	
M-80	18.52	27.16	25.93	28.40			22.28	31.35	13.85	0.14	0.12	30.61	
M-79	16.84	24.21	29.47	29.47			20.44	29.62	13.34	0.30	0.49	31.22	
M-96-BOT	5.08	27.97	6.78	3.39		56.78	34.21	4.13	-0.28	13.30	12.80	13.64	
M-62-TOP	4.67	11.21	5.61	8.41		70.09	23.57	10.01	1.44	7.04	23.65	14.07	
BE-7-TOP	4.13	39.67	18.53	8.26		31.40	32.77	13.92	5.58	7.58	5.02	26.26	
BW-4A-TOP	12.73	35.45	12.73	6.36		32.73	26.17	30.26	3.76	2.16	8.79	21.61	
BW-3-2	23.16	33.68	11.58	14.74		16.84	23.30	50.20	5.86	0.39	1.15	15.97	
BW-1BOT	5.06	20.25	13.92	6.33		54.43	20.56	21.98	2.48	9.56	8.67	20.05	

TABLE III-1 (continued)

Sample No.	Relative Mineral Proportions (in percent). Results from X-ray Diffraction Analysis. Blanks = none detected.						Normative Mineral Proportions (in percent). From Major Element Chemical Analysis. Blanks = not calculated.						
	Illite	Chlorite	Quartz	Feldspar	Hematite	Total Carbonate	Chlorite*	Illite	Feldspar	Amount CaO in carbonate minerals	Amount MnO in carbonate minerals	Quartz	Hematite
BW-10C	6.06	53.59	25.25	10.10			37.95	20.66	9.05	1.51	0.05	29.33	
BW-5		7.20				92.80	7.03	1.44	1.94	3.62	51.05	2.33	
BW-3-1	8.00	17.60	10.40	4.00		60.00	17.12	20.28	2.05	11.90	12.56	18.38	
BW-15TOP	14.95	42.99	25.23	16.82			21.99	31.90	10.11	1.19	1.31	31.09	
BW-2TOP	9.52	34.29	38.10	18.10			22.72	29.02	7.08	0.36	0.26	39.57	
BE-4	0.71	8.57				90.71	4.78	4.10	3.24	3.43	50.42	1.51	
BE-3TOP	10.13	45.57	26.58	17.72			27.33	26.24	6.00	1.61	2.59	32.60	
BE-7BOT	4.88	51.22	17.07	3.25		23.58	45.75	16.74	5.49	3.40	1.05	25.89	
402002	3.39	14.41	7.63	2.54		72.03	16.78	11.57	-0.48	17.46	13.07	16.74	
HH-38	1.54	40.77	6.92			50.77	45.72	1.74	1.22	13.11	8.69	15.94	
HH-39A	2.84	27.66	4.96	2.13		62.41	28.34	6.19	3.82	10.09	17.15	12.91	
HH-36-1	3.65	29.93	8.76	8.03		49.64	34.04	12.59	4.93	7.67	13.55	14.60	
HH-39B		20.12	4.73			75.15	35.53	2.46	8.91	13.58	14.17	12.71	
HH-40S	6.61	41.32	18.18	9.92		23.97	32.76	17.78	9.66	1.0[illegible]	4.26	30.14	
HH-42B	6.61	19.01	15.70	15.70		42.93	23.40	19.13	8.[illegible]	3.72	8.18	26.70	

TABLE III-1 (continued)

Sample No.	Relative Mineral Proportions (in percent). Results from X-ray Diffraction Analysis. Blanks = none detected.						Normative Mineral Proportions (in percent). From Major Element Chemical Analysis. Blanks = not calculated.						
	Illite	Chlorite	Quartz	Feldspar	Hematite	Total Carbonate	Chlorite*	Illite	Feldspar	Amount CaO in carbonate minerals	Amount MnO in carbonate minerals	Quartz	Hematite
HH-37	7.56	41.18	20.17	15.13		15.97	30.94	20.45	12.78	1.07	3.58	27.49	
HH-36-2	9.02	34.59	15.79	9.02		31.58	26.89	19.18	9.82	2.80	9.80	23.23	
HH-35	6.11	35.14	20.72	21.62		14.41	29.19	22.57	12.44	1.60	3.43	27.02	
HH-42A	5.32	31.91	12.77	6.38		43.62	31.99	5.90	2.11	9.82	13.67	17.94	
HH-39-1	6.00	54.00	29.00	11.00			45.26	12.68	8.38	1.52	0.69	31.69	
HH-34A	0.09	5.55	2.78	1.85		89.73	27.09	2.38	0.63	16.71	10.17	5.01	

* Arithmetic Sum of Calculated Proportions of Two End-Member Chlorite Minerals

TABLE III-2

Results of Normative Mineralogical Composition Calculations for 60 Red Mudrock Samples*

Sample No.	Calculations based on one chlorite component (in percent).							Calculations based on two chlorite components - one Fe-rich, one Mg-rich (in percent). Excess MnO in carbonate minerals not computed.						
	Chlorite	Illite	Feldspar	Excess MnO**	Excess CaO**	Quartz	Hematite	Fe-rich Chlorite	Mg-rich Chlorite	Illite	Feldspar	Hematite	Excess CaO**	Quartz
CW-5	10.63	31.50	21.40	-0.10	-0.71	32.12	5.06	8.76	5.44	32.71	18.62	3.42	-0.23	31.95
LY-6	12.97	35.93	17.15	-0.22	-0.44	27.95	5.69	5.22	7.66	37.72	15.96	5.46	-0.09	27.44
CC-10	2.25	34.13	13.88	0.08	0.57	36.75	6.69	-6.57	3.58	37.05	14.76	8.84	0.79	35.69
SG-26	11.28	23.81	19.81	-0.06	-0.49	37.49	4.34	-6.51	9.66	28.27	21.37	7.55	-0.18	35.88
FCJ-4	15.23	26.09	15.01	-0.05	-0.01	37.12	4.71	5.00	9.22	27.95	14.41	4.81	0.28	36.54
LY-3	10.43	30.04	14.49	0.02	-0.16	32.74	5.06	-3.93	8.23	33.37	15.67	7.42	0.25	31.54
LD-13	4.23	41.86	17.12	0.25	-0.39	24.72	8.32	20.14	-1.56	39.38	10.89	2.36	0.12	25.98
OP-37	18.60	27.22	12.22	-0.09	0.86	35.11	4.85	7.45	10.70	23.60	11.59	4.59	1.10	34.67
OP-18	22.90	35.27	13.18	-0.46	-0.20	25.61	3.97	10.10	12.63	35.71	12.21	3.40	0.07	25.24
SP-10	17.84	21.64	16.61	-0.42	3.96	30.93	2.31	-15.70	15.98	20.00	21.68	9.21	4.10	28.25
SP-6	16.66	27.39	14.66	-0.39	1.47	31.53	4.23	-4.82	12.43	31.63	16.83	7.61	1.66	29.93
OP-10	7.49	31.15	20.15	-0.09	-0.40	31.16	5.98	-1.70	5.96	34.22	19.90	7.25	-0.02	30.17
SP-37	17.23	34.11	15.59	-0.36	-0.24	27.84	3.70	4.53	10.50	36.44	15.22	4.21	0.06	27.14
SP-73-2	12.19	31.64	17.21	-0.14	-0.15	31.29	4.49	9.77	6.05	32.38	14.71	2.74	0.24	31.24

TABLE III-2 (continued)

Sample No.	Calculations based on one chlorite component (in percent).							Calculations based on two chlorite components - one Fe-rich, one Mg-rich (in percent). Excess MnO in carbonate minerals not computed.						
	Chlorite	Illite	Feldspar	Excess MnO**	Excess CaO**	Quartz	Hematite	Fe-rich Chlorite	Mg-rich Chlorite	Illite	Feldspar	Hematite	Excess CaO**	Quartz
SP-46	17.45	30.98	14.87	-0.23	-0.03	29.11	6.51	10.42	9.22	31.91	13.03	5.19	0.25	28.96
OP-38	20.93	25.34	11.42	-0.19	0.24	36.28	4.90	6.59	12.38	27.11	11.37	5.20	0.45	35.68
OP-14	9.84	27.84	20.48	-0.16	0.70	31.15	5.08	-7.46	8.92	32.47	22.04	8.43	1.02	29.50
OP-19	20.36	35.62	15.21	-0.25	-0.21	26.03	5.11	11.94	10.75	33.54	13.31	3.64	0.13	25.38
SP-73-5	20.76	33.63	9.44	-0.33	0.25	27.78	7.12	13.52	10.38	33.72	7.62	5.25	0.48	27.91
SP-4	20.99	25.48	16.34	-0.43	1.15	31.27	2.81	-7.56	15.99	30.93	19.64	7.53	1.34	[illegible].23
SP-27	14.88	31.25	19.89	-0.21	-0.19	27.21	4.55	12.63	7.16	31.91	15.71	2.20	0.27	27.26
SP-12-1	12.15	25.70	19.04	-0.26	-0.33	35.15	4.62	-10.04	10.98	31.03	21.69	9.06	-0.07	33.20
JH-1	14.43	31.18	20.09	-0.22	-0.28	26.60	5.35	9.76	7.58	32.47	17.81	3.85	0.16	26.38
BR-11-2	12.92	24.15	16.38	0.75	0.28	33.82	8.05	12.07	6.41	24.04	13.59	5.57	0.67	33.89
BR-26	14.40	31.62	18.94	-0.31	-0.43	27.79	5.39	8.29	7.83	33.13	16.94	4.36	-0.02	27.48
DC-7-A	11.67	33.83	7.27	-0.21	1.26	37.43	4.36	0.68	7.62	35.60	7.94	5.47	1.37	36.81
JB-27	18.04	32.98	20.98	-0.43	-0.61	22.85	3.93	11.90	9.33	34.29	19.28	2.24	-0.14	22.67
BR-30	13.95	18.07	19.93	-0.11	-0.07	43.32	2.13	-2.81	10.47	22.00	20.92	4.50	0.27	41.93
RL-12	23.89	31.39	16.75	-0.50	-0.36	25.70	1.83	9.39	13.49	33.44	15.78	1.57	-0.02	25.14
CH-28	12.72	30.12	20.10	-0.23	0.61	26.52	5.75	1.86	8.43	32.96	19.54	6.53	1.00	25.64

TABLE III-2 (continued)

Sample No.	Calculations based on one chlorite component (in percent).							Calculations based on two chlorite components - one Fe-rich, one Mg-rich (in percent). Excess MnO in carbonate minerals not computed.						
	Chlorite	Illite	Feldspar	Excess MnO**	Excess CaO**	Quartz	Hematite	Fe-rich Chlorite	Mg-rich Chlorite	Illite	Feldspar	Hematite	Excess CaO**	Quartz
CH-20	13.41	31.74	21.75	-0.18	-0.64	26.44	5.30	9.54	7.05	33.11	19.08	3.73	-0.16	26.21
CH-1	14.62	33.20	18.09	-0.01	-0.34	26.78	6.00	7.34	8.36	34.76	16.51	5.27	0.03	26.36
CH-34A	19.03	26.34	16.70	-0.38	-0.17	31.71	3.14	-0.51	12.98	30.06	17.83	5.42	0.09	30.42
NC-19	13.74	33.45	9.03	-0.19	0.88	35.41	4.66	-15.41	13.08	39.12	14.18	11.02	0.88	33.11
NC-4	11.51	23.24	20.95	-0.05	-0.44	38.27	4.16	-5.42	9.58	27.59	22.16	7.05	-0.09	36.71
NC-15-1	5.71	43.94	8.23	-0.01	-0.04	29.44	8.14	-9.09	6.30	47.29	10.74	11.53	0.03	22.12
CH-24	12.57	34.10	18.66	-0.19	-0.40	26.10	6.14	10.99	6.01	34.77	15.74	4.05	0.03	26.12
CH-18	9.66	31.49	19.53	-0.03	-0.14	26.56	6.55	6.63	5.31	32.87	17.37	5.46	0.29	26.27
NC-17	12.14	36.49	9.68	-0.02	0.18	29.82	6.30	-4.10	9.31	39.51	11.55	8.92	0.29	28.64
NC-3	11.10	37.37	7.44	-0.16	0.73	30.51	6.56	-18.34	12.05	43.28	13.17	13.54	0.68	29.09
NC-2	9.98	23.22	18.67	0.11	-0.10	39.06	4.57	-9.67	9.66	28.07	21.05	8.61	0.16	37.22
CH-33	20.39	28.55	17.30	-0.40	-0.17	28.88	3.21	0.87	13.54	32.18	18.37	5.21	0.12	27.63
CH-22	12.76	28.90	19.30	-0.14	-0.32	27.40	9.92	10.53	6.30	23.72	16.33	7.93	0.12	27.36
DB-101	13.64	34.90	10.73	-0.10	-0.21	33.63	4.70	-17.60	13.61	41.22	16.30	11.73	-0.08	31.09
DB-73-4	9.27	39.58	12.05	-0.10	-0.22	30.96	5.70	-3.60	7.34	42.47	13.19	7.82	-0.04	29.91

TABLE III-2 (continued)

Sample No.	Calculations based on one chlorite component (in percent).							Calculations based on two chlorite components - one Fe-rich, one Mg-rich (in percent). Excess MnO in carbonate minerals not computed.						
	Chlorite	Illite	Feldspar	Excess MnO**	Excess CaO**	Quartz	Hematite	Fe-rich Chlorite	Mg-rich Chlorite	Illite	Feldspar	Hematite	Excess CaO**	Quartz
DB-73-1	8.14	42.93	4.68	-0.06	0.07	33.83	6.82	-28.02	12.50	50.37	12.89	16.50	-0.10	30.69
DB-75	13.59	14.70	17.27	-0.23	-0.04	51.90	2.05	-10.55	12.02	20.09	20.39	6.83	0.17	49.87
DB-73-7	22.88	35.58	5.48	-0.47	0.08	33.56	2.75	-11.67	17.89	41.09	11.02	9.05	-0.00	31.32
DB-73-3	13.13	35.71	11.65	-0.25	-0.20	33.73	3.80	-9.55	11.27	40.31	14.90	8.25	-0.09	31.95
DB-73-2	2.22	37.44	11.02	0.14	0.60	36.01	7.20	-19.98	6.90	43.06	15.82	13.62	0.65	33.72
DB-1	1.07	36.47	6.04	-0.19	4.26	38.72	5.52	-14.90	4.74	40.36	9.73	10.24	4.25	37.09
DB-105	10.00	30.25	9.96	-0.16	0.98	40.37	5.45	-12.29	9.89	34.95	13.71	10.40	1.04	38.51
HH-17	16.97	17.50	20.84	-0.29	0.06	41.13	1.85	-5.72	13.11	22.53	22.79	5.48	0.37	39.32
HH-9	7.01	36.47	13.37	0.02	0.81	30.10	6.72	-4.27	6.13	39.36	14.35	8.77	1.02	29.03
HH-55	17.83	21.94	16.46	-0.37	-0.06	36.50	2.80	-3.43	12.99	26.35	20.10	5.85	0.22	34.94
HH-47	12.35	34.04	17.09	-0.18	-0.47	28.36	5.81	5.77	7.14	35.63	15.69	5.34	-0.12	27.94
HH-49	10.12	37.82	15.39	-0.11	0.34	26.97	6.33	4.27	6.03	39.39	14.25	6.12	0.66	26.54
HH-57	21.95	27.85	13.78	-0.48	-0.18	35.37	2.21	2.28	14.04	30.97	14.76	3.99	0.04	34.29
HH-53B	7.09	29.43	18.55	-0.08	0.14	35.53	5.11	4.57	4.08	30.93	16.68	4.38	0.54	35.18

*Samples yielding illogical results (i.e., negative iron-bearing mineral proportions) not included.
**Assumed present in carbonates.

TABLE III-3

Normative Mineralogical Compositions of 49 Limestone Samples (Mineral Proportions in Weight Percent)

Sample	Chlorite	Illite	Feldspar	Excess CaO*	Excess MnO*	Quartz	Hematite
LY-23	9.86	8.63	0.84	34.45	1.34	12.99	1.55
CW-2	-0.52	4.42	12.77	40.06	0.88	6.96	2.42
SE-19	11.51	12.64	2.74	23.69	3.06	15.21	8.44
SE-27	8.34	12.18	8.93	26.25	1.77	15.04	3.03
WB-40	8.56	1.87	6.13	36.89	0.70	9.93	0.90
CA-5	0.04	0.08	0.50	42.05	1.52	21.73	0.28
GH-1	0.20	5.00	6.50	43.71	0.64	5.36	1.67
DI-2	9.51	13.33	3.92	33.58	0.63	8.34	1.88
431	-0.14	14.25	5.88	31.11	0.86	17.69	2.93
999	-0.86	9.32	10.88	31.65	0.95	16.71	3.11
CC-4C	-0.06	-0.12	1.20	53.53	0.89	2.43	0.38
CC-4B	-0.79	11.87	7.45	28.86	0.42	18.55	3.12
XY-2	0.00	8.16	2.24	42.28	1.86	5.68	2.40
OP-24	19.58	16.80	6.79	19.23	1.85	13.16	4.94
SP-23	14[illegible]	3.43	2.77	35.52	0.85	11.33	0.09
OP-17B	19.53	8.19	5.14	27.51	1.94	9.32	4.00
SP-51	1.53	6.59	5.46	37.19	5.02	3.99	4.44
SP-21	-0.02	7.62	6.44	38.24	0.60	10.95	4.47
OP-7	10.42	0.16	6.42	40.57	0.45	7.92	-0.74
OP-32	14.58	8.37	2.83	31.13	1.46	14.00	0.84

TABLE III-3 (continued)

Sample	Chlorite	Illite	Feldspar	Excess CaO*	Excess MnO*	Quartz	Hematite
OP-36	14.93	7.99	3.61	29.88	1.01	16.41	1.27
OP-34	10.96	15.44	4.43	24.28	2.03	17.93	2.48
OP-16	3.69	0.99	4.04	43.55	0.68	9.42	-0.26
SP-8	9.45	0.00	7.46	40.66	0.17	8.42	-1.26
SP-54	31.75	9.21	5.91	5.56	15.02	8.62	8.65
BR-28	0.28	12.49	4.72	32.79	0.99	15.38	4.62
NC-20-1	5.62	4.62	3.56	41.21	0.30	10.97	0.37
CH-34B	1.49	4.46	9.30	41.54	2.85	2.59	1.81
CH-31	35.44	6.06	8.17	16.62	0.73	15.09	4.86
NC-20-2	0.13	4.48	4.97	46.50	0.62	5.06	1.23
NC-15-2	37.55	4.73	-4.43	32.05	0.05	10.69	-2.77
M-16	24.86	1.39	3.21	21.18	1.36	27.58	1.65
DB-100	11.93	17.16	1.32	31.01	0.38	9.54	1.87
DB-106	0.07	4.14	11.71	35.77	0.54	16.21	1.88
DB-99	-0.27	5.79	0.81	47.23	0.57	6.87	1.29
40201	-0.45	5.88	7.07	38.68	0.58	14.23	2.01
DB-40	-0.36	3.36	8.19	39.99	0.72	12.79	0.89
DB-6-2	-0.06	2.31	4.08	49.65	0.61	2.84	0.93
DB-73-9	4.29	7.74	0.16	44.25	0.32	5.80	0.44
DB-103	8.93	8.92	0.19	29.90	0.71	21.45	4.73
HH-13	-0.49	5.88	8.47	40.28	0.41	8.14	1.97
HH-11	0.65	5.16	8.85	42.53	0.69	8.12	1.88
HH-50	0.94	8.40	12.69	26.65	1.08	20.23	4.41
HH-218	22.45	6.24	3.60	15.65	1.22	31.41	4.77

TABLE III-3 (continued)

Sample	Chlorite	Illite	Feldspar	Excess CaO*	Excess MnO*	Quartz	Hematite
HH-22	6.56	22.74	11.34	16.27	0.38	21.75	5.41
HH-12	0.28	4.50	6.85	43.97	0.51	5.27	1.69
HH-14	0.04	5.24	10.10	33.21	1.44	14.28	4.25
HH-29	9.20	15.85	9.89	26.18	0.59	10.44	4.35
HH-53A	-0.21	3.13	4.83	48.67	1.02	2.82	1.14

* Presumed to occur in rocks in carbonate minerals.

KEY TO SAMPLE CODE NUMBERS USED IN TABLE III-4

1. Conception Bay Samples

Manuel's River Section: M- , MACH- , HGR- (granite)
Brigus Section: DB- , 40-
BE- , BW- } manganese horizon
Chapel Cove: CC- , 42-
Salmon Cove: SC- , 43-

Miscellaneous:

Kelligrews: KE-
999, RECK- : grab samples

2. Trinity Bay Samples

Hopeall Head: HH-
Chapel Head: CC- , NC-
Norman's Cove: NM- , CAV- , CA-
Smith Point: SP-
Burgoyne's Cove: OP-
Long Point: LY- , LZ-
Whiteway Bay: WB- , C-
Spread Eagle: SE- , LD- , 41-
Chapel Arm West: CW-
TransCanada Highway: TCH- , TCJ-
Dildo Island: DI-
Green's Harbour: GH-

Miscellaneous samples: KEEL- , MP- , RECK- , XY-

3. St. Mary's Bay Samples

Jigging Head Cove: JH- , JB-
Branch Cove: BC-
Redland Cove: RL-

4. Burin Peninsula Samples

Little Dantzic Cove: DC-

TABLE III-4

LISTING OF MAJOR AND TRACE ELEMENT CONCENTRATIONS IN ANALYZED CAMBRIAN ROCK SAMPLES, SOUTHEASTERN NEWFOUNDLAND

GREEN MUDSTONE

MAJOR ELEMENTS (WT%)

SAMPLE	TCJ-1	CAV-3	DI-3	MP-1	KEEL-1
SiO_2	56.46	57.71	59.49	50.68	59.87
Al_2O_3	20.97	18.30	19.97	20.84	18.30
Fe_2O_3	8.85	7.51	5.75	8.80	8.00
MnO	.47	1.44	.33	1.70	.18
CaO	.56	1.65	.48	1.66	.53
MgO	3.45	1.46	1.89	2.72	1.50
Na_2O	1.50	1.00	1.50	.95	1.68
K_2O	3.37	3.69	4.53	3.74	3.63
TiO_2	.86	.78	1.10	.99	1.06
P_2O_5	.18	.22	.05	.32	.10
Ba	.08	.10	.08	.13	.05
H_2O	4.55	5.97	4.20	0.00	0.00
TOTAL	101.30	99.83	99.37	92.53	94.90

TRACE ELEMENTS (PPM)

Zr	123	55	166	116	174
Sr	72	0	0	86	20
Rb	111	86	117	102	104
Zn	113	70	106	96	110
Cu	0	0	118	38	0
Nb	0	0	0	0	0
Ce	109	123	114	142	112
La	14	85	9	27	0
Ni	87	64	55	56	62
Cr	111	106	82	122	94
V	118	103	121	119	145

TABLE III-4 (Cont'd)

GREEN MUDSTONE

MAJOR ELEMENTS (WT%)

SAMPLE	LD-14	411	4120	CW-6	TCH-8
SiO_2	54.89	54.24	58.38	58.65	58.50
Al_2O_3	21.84	21.33	19.47	18.83	19.83
Fe_2O_3	8.58	9.05	6.73	7.55	7.26
MnO	.26	.43	.19	.27	.71
CaO	.48	.47	.50	.78	1.11
MgO	1.28	3.53	2.13	2.49	2.81
Na_2O	1.18	1.30	1.79	1.82	1.99
K_2O	4.27	3.85	3.72	3.13	3.20
TiO_2	.89	.94	1.01	.92	.86
P_2O_5	0.00	.34	0.00	.26	.22
Ba	.62	.08	.06	.05	.07
H_2O	4.57	4.69	4.11	4.35	5.17
TOTAL	98.86	100.25	98.09	99.10	101.73

TRACE ELEMENTS (PPM)

	LD-14	411	4120	CW-6	TCH-8
Zr	124	105	145	0	123
Sr	174	108	30	0	96
Rb	139	98	124	88	110
Zn	97	80	102	114	111
Cu	0	17	6	36	21
Nb	0	0	0	0	0
Ce	120	156	121	115	115
La	9	47	35	91	44
Ni	76	66	65	67	72
Cr	121	103	97	107	115
V	127	96	99	104	120

TABLE III-4 (Cont'd)

GREEN MUDSTONE

MAJOR ELEMENTS (WT%)

SAMPLE	WB-91	C-17	LD-001	LD-3	LD-12
SiO_2	61.35	55.68	59.02	59.74	59.77
Al_2O_3	17.37	19.34	18.27	18.24	19.07
Fe_2O_3	8.02	11.32	9.23	8.63	7.11
MnO	.41	.40	.46	.47	.65
CaO	.70	.82	.58	.75	1.30
MgO	1.70	1.92	3.08	2.03	.47
Na_2O	1.33	.85	1.50	1.51	1.50
K_2O	3.32	3.19	2.83	2.89	3.34
TiO_2	.74	.89	.87	.85	.87
P_2O_5	.13	.19	.16	.20	.20
Ba	.22	.13	.07	.07	.09
H_2O	4.13	4.95	4.24	3.92	5.17
TOTAL	99.42	99.68	100.31	99.30	99.54

TRACE ELEMENTS (PPM)

Zr	81	97	107	106	114
Sr	10	6	42	0	32
Rb	96	86	92	8	105
Zn	73	107	102	1009	95
Cu	0	0	0	0	57
Nb	0	0	0	0	0
Ce	103	129	96	11	106
La	44	0	10	6001	26
Ni	60	74	81	9008	85
Cr	102	130	96	7010	103
V	65	122	86	1008	108

TABLE III-4 (Cont'd)

GREEN MUDSTONE

MAJOR ELEMENTS (WT%)

SAMPLE	LY-19	LZ-1	WB-1	WB-6	WB-9
SiO2	59.21	59.18	63.32	65.81	55.80
Al2O3	17.96	20.22	17.23	14.81	21.63
Fe2O3	9.80	7.34	6.53	6.11	8.22
MnO	.29	.26	.24	.20	.20
CaO	.52	.40	.85	1.48	.42
MgO	1.90	1.85	1.58	1.23	2.66
Na2O	1.30	1.71	2.16	2.48	1.35
K2O	3.07	3.72	3.02	2.44	4.37
TiO2	.88	.96	1.07	.83	.94
P2O5	.16	0.00	.12	.07	.20
Ba	.12	.11	.07	.05	.15
H2O	3.91	4.18	3.57	3.69	4.46
TOTAL	99.12	99.93	99.76	99.20	100.40

TRACE ELEMENTS (PPM)

Zr	110	113	198	155	127
Sr	43	41	28	52	40
Rb	101	122	79	74	143
Zn	94	122	115	97	111
Cu	0	26	583	1	13
Nb	0	0	0	0	0
Ce	114	90	108	85	113
La	34	26	0	0	22
Ni	70	74	76	61	74
Cr	108	106	88	90	120
V	160	106	154	112	131

TABLE III-4 (Cont'd)

GREEN MUDSTONE

MAJOR ELEMENTS (WT%)

SAMPLE	OP-17-A	OP-6	LY-2	LY-8	LY-17
SiO2	60.43	62.53	65.34	59.26	63.57
Al2O3	18.23	18.54	14.62	19.76	16.51
Fe2O3	7.98	6.69	6.75	8.90	7.80
MnO	.21	.25	.22	.27	.35
CaO	.56	.62	1.95	.50	1.08
MgO	1.87	2.72	1.57	2.73	1.71
Na2O	1.64	2.01	1.52	1.59	1.50
K2O	3.10	3.02	2.60	3.28	2.87
TiO2	.93	.97	.78	.76	.67
P2O5	.21	.20	.14	.18	.47
Ba	.05	.06	.08	.11	.34
H2O	3.94	3.47	4.48	3.98	3.61
TOTAL	99.15	101.08	100.05	101.32	100.48

TRACE ELEMENTS (PPM)

Zr	139	162	123	106	104
Sr	32	47	51	20	76
Rb	92	82	82	107	94
Zn	108	111	92	108	97
Cu	20	47	0	0	0
Nb	0	0	0	0	0
Ce	137	73	73	131	95
La	0	0	0	103	0
Ni	60	74	57	76	67
Cr	101	81	79	99	93
V	111	127	94	101	92

TABLE III-4 (Cont'd)

GREEN MUDSTONE

MAJOR ELEMENTS (WT%)

SAMPLE	OP-44	OP-30	OP-27	OP-26	OP-25
SiO_2	53.32	55.09	55.17	54.77	58.03
Al_2O_3	18.00	19.07	22.12	21.67	21.46
Fe_2O_3	9.01	9.34	8.69	8.44	6.75
MnO	.50	.35	.22	.23	.15
CaO	4.01	2.20	.43	.49	.46
MgO	2.27	2.17	1.25	2.01	2.13
Na_2O	.93	1.09	1.09	.97	1.07
K_2O	3.35	3.51	4.44	4.43	4.38
TiO_2	.87	.88	.92	.91	.92
P_2O_5	0.00	.31	.45	.11	.40
Ba	.14	.14	.14	.12	.17
H_2O	6.86	5.44	4.20	4.60	0.00
TOTAL	99.26	99.59	99.12	98.75	95.92

TRACE ELEMENTS (PPM)

Zr	109	100	104	100	95
Sr	107	70	15	0	0
Rb	96	109	129	124	134
Zn	87	91	105	94	69
Cu	0	0	0	0	0
Nb	0	0	0	0	0
Ce	97	92	125	121	148
La	38	27	1	14	29
Ni	66	71	85	77	72
Cr	101	110	117	110	109
V	141	164	113	107	123

TABLE III-4 (Cont'd)

GREEN MUDSTONE

MAJOR ELEMENTS (WT%)

SAMPLE	SP-17	SP-12-2	SP-9	SP-3	SP-2
SiO_2	62.42	61.57	59.51	63.80	64.12
Al_2O_3	16.83	16.21	16.43	13.92	13.66
Fe_2O_3	6.45	6.35	6.59	8.90	10.26
MnO	.20	.16	.15	.17	.23
CaO	1.21	1.39	2.03	1.27	.57
MgO	3.83	2.27	3.49	1.19	2.15
Na_2O	2.15	2.23	2.21	1.92	1.30
K_2O	2.76	2.91	2.85	1.98	2.28
TiO_2	.96	1.00	.94	.77	.81
P_2O_5	.62	.28	.20	.29	.31
Ba	.03	.03	.04	.02	.04
H_2O	3.43	4.28	4.77	4.48	3.72
TOTAL	100.89	98.68	99.21	98.71	99.45

TRACE ELEMENTS (PPM)

Zr	134	186	170	145	166
Sr	17	0	27	22	10
Rb	80	78	84	52	59
Zn	107	98	109	118	134
Cu	42	12	111	0	13
Nb	0	0	0	0	0
Ce	67	72	79	82	143
La	0	0	0	6	32
Ni	54	52	56	49	56
Cr	90	92	83	66	71
V	123	125	122	96	102

TABLE III-4 (Cont'd)

GREEN MUDSTONE

MAJOR ELEMENTS (WT%)

SAMPLE	SP-26	SP-25	SP-73-6	SP-7371	SP-73-9
SiO2	54.16	46.36	58.03	49.44	58.07
Al2O3	20.60	18.35	19.40	16.12	19.53
Fe2O3	10.67	12.36	9.18	8.59	6.84
MnO	.26	.34	.21	.92	.17
CaO	.57	2.75	.56	7.12	.62
MgO	3.05	3.76	2.59	2.52	2.18
Na2O	1.14	.97	1.38	1.25	1.30
K2O	3.53	2.06	3.39	2.74	3.95
TiO2	.96	.86	.96	.77	.91
P2O5	.35	0.00	.21	0.00	.19
Ba	.07	3.55	.07	.04	.05
H2O	5.31	7.09	4.99	10.02	5.31
TOTAL	100.67	98.45	100.97	99.53	99.12

TRACE ELEMENTS (PPM)

	SP-26	SP-25	SP-73-6	SP-7371	SP-73-9
Zr	129	112	137	112	125
Sr	53	7	20	45	0
Rb	109	108	97	66	115
Zn	118	104	100	101	108
Cu	0	0	0	9	48
Nb	0	0	0	0	0
Ce	122	139	119	68	144
La	19	33	56	19	20
Ni	66	76	65	54	69
Cr	116	120	106	79	112
V	131	117	115	100	156

TABLE III-4 (Cont'd)

GREEN MUDSTONE

MAJOR ELEMENTS (WT%)

SAMPLE	CH-32	NC-12	SP-50	SP-49	SP-40
SiO2	49.98	61.00	54.51	55.25	55.80
Al2O3	16.49	17.64	21.28	19.66	19.85
Fe2O3	9.97	6.58	9.39	10.47	9.31
MnO	.70	.26	.19	.19	.30
CaO	5.48	.72	.57	.75	.53
MgO	3.98	1.34	2.88	2.69	3.54
Na2O	1.27	1.54	.94	.98	0.00
K2O	2.40	4.27	4.11	3.43	3.49
TiO2	.78	1.11	.89	.86	.89
P2O5	.32	.26	.19	.21	.25
Ba	0.00	.06	.14	.11	.14
H2O	9.12	3.56	5.60	5.23	5.49
TOTAL	100.49	98.34	100.69	99.83	99.59

TRACE ELEMENTS (PPM)

Zr	119	199	116	90	110
Sr	61	4	61	31	11
Rb	56	115	129	104	109
Zn	120	97	116	121	110
Cu	187	4	93	0	12
Nb	0	0	0	0	0
Ce	89	142	99	117	105
La	0	20	174	12	27
Ni	60	80	81	77	81
Cr	93	78	119	117	113
V	108	141	106	104	122

TABLE III-4 (Cont'd)

GREEN MUDSTONE

MAJOR ELEMENTS (WT%)

SAMPLE	CH-19	CH-21	CH-25	CH-29	CH-30
SiO_2	58.64	57.47	57.00	59.73	58.26
Al_2O_3	20.03	19.98	20.92	19.71	19.84
Fe_2O_3	6.83	7.58	6.52	6.88	7.36
MnO	.36	.45	.23	.23	.26
CaO	.41	.50	.51	.53	.53
MgO	3.75	3.59	2.60	2.66	2.69
Na_2O	1.51	1.64	1.56	2.00	1.81
K_2O	3.49	3.32	4.10	3.43	3.44
TiO_2	.87	.83	.94	.97	.96
P_2O_5	.18	.13	.29	.14	.03
Ba	.08	0.00	.06	0.00	0.00
H_2O	4.56	4.83	4.75	4.23	4.40
TOTAL	100.71	100.32	99.48	100.51	99.58

TRACE ELEMENTS (PPM)

Zr	111	114	127	138	145
Sr	30	59	24	45	69
Rb	122	114	124	100	110
Zn	118	138	107	103	112
Cu	2	298	264	12	26
Nb	0	0	0	0	0
Ce	123	120	125	83	118
La	175	0	28	2	68
Ni	79	82	68	65	66
Cr	129	105	116	110	112
V	126	120	134	122	127

TABLE III-4 (Cont'd)

GREEN MUDSTONE

MAJOR ELEMENTS (WT%)

SAMPLE	HH-54	HH-7	HH-5	CH-16	CH-17
SiO2	60.14	61.01	51.98	55.31	56.25
Al2O3	19.03	18.94	17.11	19.98	19.68
Fe2O3	7.09	5.41	9.75	10.64	8.75
MnO	.18	.25	.73	.58	.41
CaO	.43	.67	4.65	.45	.54
MgO	3.61	2.07	3.43	2.63	2.60
Na2O	1.54	1.70	1.23	1.35	1.40
K2O	3.61	4.32	3.02	2.87	3.37
TiO2	.90	1.03	.96	.86	.86
P2O5	.25	.26	.30	.16	.21
Ba	.06	.08	.09	0.00	0.00
H2O	3.90	4.01	7.38	4.85	4.75
TOTAL	100.74	99.75	100.63	99.68	98.82

TRACE ELEMENTS (PPM)

	HH-54	HH-7	HH-5	CH-16	CH-17
Zr	117	152	132	96	112
Sr	0	0	65	14	48
Rb	90	112	68	80	106
Zn	98	90	131	98	111
Cu	100	186	0	0	7
Nb	0	0	0	0	0
Ce	101	96	91	0	161
La	0	0	0	0	42
Ni	71	50	56	91	76
Cr	100	91	72	127	111
V	111	133	107	106	123

TABLE III-4 (Cont'd)

GREEN MUDSTONE

MAJOR ELEMENTS (WT%)

SAMPLE	HH-33	HH-32	HH-46	HH-48	HH-51
SiO2	56.91	56.68	55.65	57.22	54.63
Al2O3	18.97	19.73	19.31	19.99	18.32
Fe2O3	9.44	8.65	9.77	8.04	10.42
MnO	.76	.30	.25	.16	.35
CaO	.59	.44	.60	.51	1.53
MgO	2.83	2.15	3.41	4.33	3.58
Na2O	1.58	1.56	1.65	1.29	1.55
K2O	3.15	3.51	3.12	3.82	2.94
TiO2	.85	.85	.78	.89	.95
P2O5	.19	.13	.31	.30	.27
Ba	.11	.11	.09	.08	.11
H2O	4.14	4.21	4.24	4.50	4.97
TOTAL	99.52	98.32	99.18	101.13	99.62

TRACE ELEMENTS (PPM)

SAMPLE	HH-33	HH-32	HH-46	HH-48	HH-51
Zr	96	110	0	0	128
Sr	0	24	0	0	28
Rb	85	108	7008	11	70
Zn	97	115	9011	5012	120
Cu	0	0	4027	8000	50
Nb	0	0	9000	0	0
Ce	112	128	11	10	108
La	31	49	3000	4002	21
Ni	80	79	7	2006	58
Cr	120	111	4011	9010	109
V	73	125	11	9011	112

TABLE III-4 (Cont'd)

GREEN MUDSTONE

MAJOR ELEMENTS (WT%)

SAMPLE	HH-30	HH-31	HH-45	HH-44	HH-43
SiO_2	56.43	55.89	58.87	59.04	54.23
Al_2O_3	19.47	19.67	19.77	19.19	16.51
Fe_2O_3	10.12	9.74	7.13	7.04	13.64
MnO	.27	.27	.60	.42	.52
CaO	.71	.45	.57	.49	1.92
MgO	2.69	2.59	2.10	1.63	4.40
Na_2O	1.16	1.37	1.58	1.68	1.08
K_2O	3.49	3.61	3.79	3.72	1.94
TiO_2	.86	.86	.86	.85	.82
P_2O_5	.28	.37	.09	.22	.71
Ba	.11	.13	.14	.14	.07
H_2O	4.72	4.32	4.79	4.28	4.89
TOTAL	100.31	99.27	100.29	98.70	100.73

TRACE ELEMENTS (PPM)

Zr	82	110	121	117	0
Sr	0	34	42	23	49
Rb	87	117	131	126	54
Zn	103	113	102	97	116
Cu	0	4	24	174	0
Nb	0	0	0	0	0
Ce	112	107	119	107	211
La	22	22	36	24	47
Ni	71	74	83	85	80
Cr	112	122	108	109	112
V	114	119	115	114	88

TABLE III-4 (Cont'd)

GREEN MUDSTONE

MAJOR ELEMENTS (WT%)

SAMPLE	DB-61	4063	HH-26	HH-28	HH29B
SiO2	52.35	59.01	58.30	54.81	55.46
Al2O3	11.69	18.43	19.44	20.42	18.63
Fe2O3	4.90	6.43	8.45	9.52	12.85
MnO	.29	.13	.09	.11	.23
CaO	11.78	.98	.38	.33	.48
MgO	2.95	3.84	2.23	2.34	3.13
Na2O	1.49	1.70	.97	.96	.90
K2O	1.94	3.83	3.97	4.14	2.93
TiO2	.51	.96	.82	.85	.82
P2O5	0.00	.25	.18	.06	.09
Ba	.05	.13	.14	.13	.10
H2O	12.16	4.12	4.55	4.65	4.60
TOTAL	100.11	99.81	99.52	98.32	100.22

TRACE ELEMENTS (PPM)

	DB-61	4063	HH-26	HH-28	HH29B
Zr	95	175	89	103	90
Sr	88	1	0	23	0
Rb	32	110	108	125	71
Zn	87	120	83	101	101
Cu	90	39	19	25	0
Nb	0	0	0	0	0
Ce	45	81	89	103	122
La	0	0	15	22	87
Ni	45	73	89	80	67
Cr	50	103	106	118	115
V	102	184	115	112	109

TABLE III-4 (Cont'd)

GREEN MUDSTONE

MAJOR ELEMENTS (WT%)

SAMPLE	4094	DB-73-8	DB-73-5	4095	402001
SiO2	50.44	55.55	58.99	56.58	54.23
Al2O3	21.56	20.13	20.27	20.71	20.20
Fe2O3	6.33	8.95	7.36	9.07	8.03
MnO	3.31	.29	.24	.33	1.22
CaO	1.74	.42	.36	.36	1.47
MgO	2.39	1.83	2.64	2.14	1.45
Na2O	1.02	.88	1.79	1.16	.84
K2O	5.13	4.82	3.98	4.30	5.04
TiO2	.93	.85	.80	.83	.83
P2O5	.11	.26	.04	.19	.10
Ba	.19	.19	.12	.15	.21
H2O	6.66	4.10	4.20	3.91	5.40
TOTAL	99.81	98.27	100.79	99.73	99.02

TRACE ELEMENTS (PPM)

	4094	DB-73-8	DB-73-5	4095	402001
Zr	105	108	93	99	104
Sr	8	0	0	0	29
Rb	137	139	107	120	139
Zn	84	81	133	101	82
Cu	0	0	32	0	0
Nb	0	0	0	0	0
Ce	126	91	111	93	123
La	46	46	17	19	214
Ni	73	66	74	75	72
Cr	122	108	108	112	119
V	116	93	108	107	55

TABLE III-4 (Cont'd)

GREEN MUDSTONE

MAJOR ELEMENTS (WT%)

SAMPLE	M-18	M-21	4096	BW15TOP	BW-12
SiO2	57.44	56.08	56.49	57.20	56.60
Al2O3	19.13	19.71	20.65	18.73	20.57
Fe2O3	8.27	8.29	7.93	6.45	9.09
MnO	.29	.25	.27	1.64	.30
CaO	.63	.67	.74	1.51	.47
MgO	2.44	2.12	2.25	2.34	1.53
Na2O	1.60	1.53	1.14	1.19	.95
K2O	4.35	4.49	4.47	4.09	4.72
TiO2	.84	.88	.89	.78	.89
P2O5	0.00	.18	.14	0.00	.47
Ba	.09	.10	.18	.16	.15
H2O	4.62	5.01	4.30	5.48	4.30
TOTAL	99.70	99.31	99.45	99.57	100.04

TRACE ELEMENTS (PPM)

	M-18	M-21	4096	BW15TOP	BW-12
Zr	90	98	104	108	112
Sr	0	11	0	9	0
Rb	131	149	137	120	141
Zn	107	115	101	84	91
Cu	0	112	26	0	0
Nb	0	0	0	0	0
Ce	79	82	75	94	105
La	8	8	0	10	4
Ni	67	75	66	61	69
Cr	104	134	119	111	112
V	91	120	116	118	115

TABLE III-4 (Cont'd)

GREEN MUDSTONE

MAJOR ELEMENTS (WT%)

SAMPLE	M-105	MACHA1	MACHB1	M-103	M-69
SiO2	55.06	51.70	51.01	56.51	57.20
Al2O3	20.54	17.81	17.92	18.11	19.47
Fe2O3	10.25	9.45	9.33	6.69	9.29
MnO	.15	.29	.29	.84	.19
CaO	.59	5.51	5.07	.90	.51
MgO	1.63	1.96	2.11	2.32	2.83
Na2O	.92	.24	0.00	1.13	1.54
K2O	4.06	3.51	3.70	4.34	4.10
TiO2	.99	.80	.76	.89	.89
P2O5	.33	.11	.12	.23	.13
Ba	.13	.13	.13	.14	.12
H2O	5.10	0.00	0.00	5.45	4.52
TOTAL	99.75	91.51	90.44	97.55	100.79

TRACE ELEMENTS (PPM)

Zr	105	106	94	101	96
Sr	7	58	34	0	9
Rb	118	110	100	136	133
Zn	99	89	86	75	104
Cu	3	2	8	8	168
Nb	0	0	0	0	0
Ce	110	94	107	101	89
La	21	29	132	0	3
Ni	67	68	69	72	69
Cr	108	80	87	99	99
V	101	89	88	100	129

TABLE III-4 (Cont'd)

GREEN MUDSTONE

MAJOR ELEMENTS (WT%)

SAMPLE	436	43101	43102	CC-33	M-107
SiO2	59.07	56.06	61.10	59.94	55.57
Al2O3	20.02	17.71	16.88	18.39	20.35
Fe2O3	5.38	11.71	7.00	7.46	9.87
MnO	.13	.48	.16	.23	.16
CaO	.21	.94	.91	.47	.44
MgO	1.54	2.14	1.52	2.52	2.00
Na2O	1.76	1.16	1.71	1.82	.84
K2O	4.67	3.19	4.35	4.79	4.02
TiO2	.97	.78	.92	1.20	.94
P2O5	.21	.35	.04	.26	.26
Ba	.15	.16	.11	.13	.14
H2O	3.78	0.00	4.40	3.93	5.03
TOTAL	97.89	94.68	99.10	101.14	99.62

TRACE ELEMENTS (PPM)

Zr	120	95	128	180	115
Sr	0	25	0	0	20
Rb	145	85	114	160	129
Zn	105	93	88	111	103
Cu	25	0	0	0	0
Nb	0	0	0	0	0
Ce	84	208	79	77	112
La	0	0	0	0	2
Ni	73	73	66	86	71
Cr	107	96	80	72	118
V	120	76	90	91	127

TABLE III-4 (Cont'd)

GREEN MUDSTONE

MAJOR ELEMENTS (WT%)

SAMPLE	BR-3	BR-24	JH-5	DC-3	DC-9-B
SiO2	55.37	55.80	58.67	59.62	58.34
Al2O3	18.44	20.18	20.54	18.84	18.33
Fe2O3	8.37	7.16	6.23	7.35	8.12
MnO	.34	1.25	.21	.34	.84
CaO	2.42	.59	.55	.68	.81
MgO	2.84	2.86	2.82	3.02	1.56
Na2O	1.59	1.60	1.83	1.01	1.10
K2O	3.28	3.51	3.68	4.10	3.76
TiO2	.85	.87	.82	1.09	1.06
P2O5	.38	0.00	.15	.19	.10
Ba	.04	.05	.05	.05	.08
H2O	5.90	5.63	4.99	4.77	5.13
TOTAL	99.82	99.50	100.54	101.06	99.23

TRACE ELEMENTS (PPM)

SAMPLE	BR-3	BR-24	JH-5	DC-3	DC-9-B
Zr	99	92	107	148	150
Sr	10	0	17	20	28
Rb	103	104	131	123	110
Zn	104	102	107	118	109
Cu	52	21	48	54	0
Nb	0	0	0	0	0
Ce	97	121	120	105	131
La	37	32	11	14	28
Ni	80	68	86	99	85
Cr	106	114	107	108	88
V	122	91	121	135	123

TABLE III-4(Cont'd)

MANGANESE HORIZON

MAJOR ELEMENTS (WT%)

SAMPLE	TCJ-13	RL-3	RL-11	BR-11-1	BR-13A
SiO2	49.64	56.87	26.38	43.64	40.28
Al2O3	14.48	18.18	9.81	10.78	11.91
Fe2O3	6.54	4.77	13.72	3.44	3.14
MnO	7.61	3.00	12.91	12.90	3.56
CaO	3.64	1.24	10.76	5.88	16.43
MgO	2.20	2.21	2.95	2.43	1.06
Na2O	1.18	1.58	.20	.85	.80
K2O	2.42	3.43	.62	2.06	2.34
TiO2	.72	.81	.33	.54	.56
P2O5	0.00	0.00	0.00	0.00	0.00
Ba	.05	.15	.36	.03	.06
H2O	10.41	6.95	18.99	15.90	18.22
TOTAL	98.89	99.19	97.03	98.45	98.36

TRACE ELEMENTS (PPM)

Zr	87	118	65	72	84
Sr	81	84	203	55	95
Rb	65	128	22	52	61
Zn	82	105	122	88	81
Cu	193	40	389	216	643
Nb	0	0	0	0	0
Ce	150	129	224	95	111
La	0	12	0	0	8
Ni	64	80	41	53	46
Cr	93	103	74	63	55
V	65	98	54	45	147

TABLE III-4 (Cont'd)

MANGANESE HORIZON

MAJOR ELEMENTS (WT%)

SAMPLE	TCH-2-B	TCH-3	TCH-5	TCJ-9	TCJ-12
SiO2	24.44	27.53	44.54	18.09	56.46
Al2O3	8.71	11.58	15.70	7.03	17.37
Fe2O3	12.79	17.21	7.28	10.31	11.88
MnO	16.15	11.27	6.36	21.69	.70
CaO	11.99	10.26	6.10	13.52	.63
MgO	3.00	3.38	2.81	2.48	3.76
Na2O	.15	.14	1.34	.10	1.17
K2O	.36	.27	2.47	.18	2.32
TiO2	.45	.50	.65	.38	.80
P2O5	0.00	0.00	0.00	0.00	.28
Ba	.20	.03	.05	.01	.05
H2O	20.58	15.35	11.83	23.35	4.34
TOTAL	98.82	97.52	99.13	97.14	99.76

TRACE ELEMENTS (PPM)

Zr	67	78	80	52	107
Sr	151	146	113	147	47
Rb	16	17	64	9	69
Zn	104	113	101	89	99
Cu	0	0	26	22	0
Nb	0	1	0	0	0
Ce	190	285	128	200	201
La	6	75	21	19	50
Ni	40	53	62	35	78
Cr	70	82	91	56	107
V	11	48	79	0	84

TABLE III-4 (Cont'd)

MANGANESE HORIZON

MAJOR ELEMENTS (WT%)

SAMPLE	4111	CW-7	CW-9	CW-12	CW-[illegible]3
SiO2	49.79	38.69	23.80	48.64	40.78
Al2O3	17.24	12.03	8.51	12.17	13.80
Fe2O3	5.98	15.30	15.10	16.99	23.06
MnO	5.84	3.82	5.92	2.10	2.61
CaO	3.18	9.66	20.46	4.08	5.45
MgO	.98	3.35	1.19	5.10	5.01
Na2O	1.33	.32	.04	.22	.04
K2O	3.39	.66	0.00	.20	0.00
TiO2	.80	.51	.31	.67	.79
P2O5	0.00	0.00	0.00	.28	.57
Ba	.08	.02	.02	.01	0.00
H2O	9.65	13.58	21.06	8.80	8.94
TOTAL	98.26	97.94	96.41	99.26	101.05

TRACE ELEMENTS (PPM)

Zr	105	86	64	62	68
Sr	108	200	262	2	35
Rb	98	20	3	0	1
Zn	80	120	126	113	122
Cu	17	0	0	0	0
Nb	0	0	0	0	0
Ce	156	251	139	152	289
La	47	73	0	134	184
Ni	66	60	33	63	55
Cr	103	75	42	104	103
V	96	36	62	72	85

TABLE III-4 (Cont'd)

MANGANESE HORIZON

MAJOR ELEMENTS (WT%)

SAMPLE	C-26	LD-4	LD-5	LD-7	41501
SiO2	31.09	48.63	51.80	52.52	18.56
Al2O3	9.37	13.06	13.93	16.57	5.43
Fe2O3	5.34	8.08	10.62	15.15	6.26
MnO	4.74	9.56	3.33	.82	26.91
CaO	20.90	3.70	4.43	.87	10.22
MgO	1.48	2.90	3.10	4.86	2.50
Na2O	.47	.90	.96	.86	.18
K2O	2.04	1.87	1.67	1.78	.42
TiO2	.56	.71	.59	.71	.22
P2O5	0.00	0.00	.23	.03	.28
Ba	.07	.05	.05	.05	.01
H2O	21.94	10.60	7.73	4.74	25.33
TOTAL	98.00	100.06	98.44	98.96	96.32

TRACE ELEMENTS (PPM)

Zr	74	84	79	81	44
Sr	189	72	114	22	126
Rb	43	48	41	45	16
Zn	78	89	95	111	79
Cu	0	0	0	27	25
Nb	0	0	0	0	0
Ce	45	118	184	163	167
La	0	95	37	63	0
Ni	46	67	75	69	34
Cr	41	88	90	115	58
V	28	48	53	141	0

TABLE III-4 (Cont'd)

MANGANESE HORIZON

MAJOR ELEMENTS (WT%)

SAMPLE	LZ-6A	LZ-8	WB-10	WB-51	C-19
SiO_2	42.59	23.60	48.13	22.62	41.39
Al_2O_3	11.79	8.07	11.20	7.17	12.12
Fe_2O_3	10.46	10.17	6.65	5.91	10.01
MnO	11.90	14.79	8.82	15.98	7.55
CaO	3.64	9.50	4.14	14.07	8.37
MgO	1.63	2.90	2.17	4.53	1.44
Na_2O	.80	.35	.80	.28	.74
K_2O	2.60	1.83	2.40	1.07	2.59
TiO_2	.57	.32	.53	.25	.60
P_2O_5	0.00	.40	.07	0.00	1.51
Ba	.50	4.35	1.20	1.89	.11
H_2O	11.46	19.18	13.12	23.81	10.88
TOTAL	97.94	95.46	99.23	97.58	97.31

TRACE ELEMENTS (PPM)

	LZ-6A	LZ-8	WB-10	WB-51	C-19
Zr	76	145	114	101	69
Sr	113	299	326	272	118
Rb	65	39	63	27	59
Zn	88	67	75	79	80
Cu	0	0	0	0	0
Nb	0	66	0	25	0
Ce	219	132	81	133	193
La	0	0	0	0	8
Ni	72	44	47	45	58
Cr	78	43	61	42	54
V	0	0	0	0	15

TABLE III-4 (Cont'd)

MANGANESE HORIZON

MAJOR ELEMENTS (WT%)

SAMPLE	OP-39	LY-14	LY-14-A	LZ-5	LZ-6
SiO_2	25.09	17.52	29.26	10.84	29.77
Al_2O_3	6.97	8.26	10.46	3.29	10.08
Fe_2O_3	5.94	9.11	15.61	4.12	9.26
MnO	17.73	22.07	10.64	15.88	14.93
CaO	13.80	12.32	9.69	22.75	8.23
MgO	2.50	0.00	1.44	7.20	1.96
Na_2O	.32	.21	.46	.15	.51
K_2O	1.48	1.97	2.29	.58	1.95
TiO_2	.36	.41	.44	.24	.35
P_2O_5	0.00	0.00	.07	0.00	0.00
Ba	.04	.65	1.46	.20	1.94
H_2O	23.19	26.24	15.45	33.05	17.66
TOTAL	97.42	98.76	97.27	98.30	96.64

TRACE ELEMENTS (PPM)

	OP-39	LY-14	LY-14-A	LZ-5	LZ-6
Zr	57	80	99	41	95
Sr	155	272	211	94	204
Rb	32	45	48	18	42
Zn	83	80	75	69	82
Cu	0	0	0	0	0
Nb	0	2	15	0	13
Ce	108	180	158	127	210
La	0	130	0	0	0
Ni	48	59	47	25	68
Cr	40	66	67	23	62
V	0	18	26	0	0

TABLE III-4 (Cont'd)

MANGANESE HORIZON

MAJOR ELEMENTS (WT%)

SAMPLE	SP-30	SP-29	SP-28	OP-42	OP-LOW
SiO_2	16.44	23.94	19.41	39.07	18.31
Al_2O_3	5.76	7.16	6.38	9.48	4.33
Fe_2O_3	7.03	6.35	5.57	7.04	4.84
MnO	24.73	26.17	29.17	12.69	23.67
CaO	14.69	7.90	8.70	8.23	15.35
MgO	0.00	1.75	1.45	2.24	2.71
Na_2O	.33	.52	.40	.50	.14
K_2O	.58	.92	1.01	1.91	.74
TiO_2	.31	.45	.43	.54	.20
P_2O_5	0.00	0.00	0.00	.53	0.00
Ba	.07	.12	.43	.06	.01
H_2O	31.26	22.00	24.44	15.06	27.54
$TOTAL_O$	101.20	97.28	97.39	97.35	97.84

TRACE ELEMENTS (PPM)

Zr	61	58	83	60	44
Sr	205	101	247	81	139
Rb	19	500	26	43	15
Zn	91	240	85	110	84
Cu	8	890	0	0	0
Nb	0	0	6	0	0
Ce	234	0	165	151	73
La	0	2480	0	0	0
Ni	59	0	61	93	46
Cr	54	750	57	59	36
V	0	640	0	14	0

TABLE III-4 (Cont'd)

MANGANESE HORIZON

MAJOR ELEMENTS (WT%)

SAMPLE	NM-13	NM-15	SP-35	SP-33-B	SP-31
SiO2	42.84	53.89	42.63	28.18	28.79
Al2O3	14.84	18.19	13.30	10.26	9.01
Fe2O3	8.28	12.27	9.07	7.59	10.79
MnO	7.96	1.90	12.79	19.40	19.13
CaO	5.84	.55	2.77	7.88	8.30
MgO	2.39	3.46	1.74	2.19	1.91
Na2O	.68	.93	1.03	.62	.57
K2O	3.13	2.86	2.61	1.38	1.19
TiO2	.64	.74	.62	.49	.41
P2O5	0.00	.28	0.00	0.00	0.00
Ba	.06	.05	.09	.08	.08
H2O	12.60	5.03	12.11	18.92	19.51
TOTAL	99.26	100.15	98.76	96.99	99.69

TRACE ELEMENTS (PPM)

	NM-13	NM-15	SP-35	SP-33-B	SP-31
Zr	61	87	75	67	61
Sr	220	0	56	134	121
Rb	8	70	66	35	30
Zn	81	117	98	110	94
Cu	471	12	9	7	0
Nb	0	0	0	0	0
Ce	0	154	173	263	225
La	0	47	110	38	0
Ni	13	61	108	108	88
Cr	9	117	84	71	75
V	32	100	46	0	0

TABLE III-4 (Cont'd)

MANGANESE HORIZON

MAJOR ELEMENTS (WT%)

SAMPLE	NM-5	NM-6	NM-8	NM-9	MN-10
SiO_2	28.23	44.85	30.76	49.99	51.31
Al_2O_3	11.33	14.82	11.34	17.20	17.77
Fe_2O_3	14.15	6.90	18.60	9.86	16.08
MnO	8.98	7.71	8.08	3.57	2.67
CaO	13.24	6.65	10.36	3.47	.68
MgO	.90	1.68	3.36	2.30	2.72
Na_2O	.15	.72	.07	.71	.58
K_2O	.63	3.10	.02	3.23	2.09
TiO_2	.39	.61	.42	.72	.74
P_2O_5	0.00	0.00	0.00	0.00	.09
Ba	1.09	.08	1.03	.07	.04
H_2O	19.49	11.62	13.77	7.79	5.13
TOTAL	98.58	98.74	97.81	98.91	99.90

TRACE ELEMENTS (PPM)

SAMPLE	NM-5	NM-6	NM-8	NM-9	MN-10
Zr	86	88	83	76	87
Sr	180	99	178	9	0
Rb	13	82	4	76	45
Zn	117	86	106	86	101
Cu	0	87	0	118	0
Nb	0	0	0	0	0
Ce	167	106	183	133	219
La	28	6	25	31	19
Ni	63	61	47	61	66
Cr	55	69	66	98	105
V	0	90	35	131	81

TABLE III-4 (Cont'd)

MANGANESE HORIZON

MAJOR ELEMENTS (WT%)

SAMPLE	CH-11-B	CH-12	CH-13	CH-15	NM-4
SiO2	10.42	64.50	31.65	49.40	51.50
Al2O3	4.75	16.08	12.92	16.56	16.71
Fe2O3	6.41	5.62	17.68	13.83	8.28
MnO	27.20	.82	8.42	2.18	2.00
CaO	17.36	1.01	8.16	3.15	5.66
MgO	1.86	1.89	3.29	3.97	.82
Na2O	.13	1.60	.24	.90	.91
K2O	.18	2.69	.47	1.82	3.49
TiO2	.24	.75	.67	.70	.99
P2O5	0.00	.08	.12	.02	.28
Ba	.02	.05	.10	0.00	.08
H2O	28.35	4.15	14.70	7.25	0.00
TOTAL	96.92	99.24	98.42	99.78	90.72

TRACE ELEMENTS (PPM)

	CH-11-B	CH-12	CH-13	CH-15	NM-4
Zr	54	106	80	94	105
Sr	238	29	121	98	31
Rb	12	88	16	49	88
Zn	78	78	120	106	86
Cu	33	0	0	0	0
Nb	0	0	0	0	0
Ce	150	118	236	168	61
La	0	17	58	21	0
Ni	33	73	65	81	82
Cr	48	85	87	95	110
V	0	81	6	47	69

TABLE III-4 (Cont'd)

MANGANESE HORIZON

MAJOR ELEMENTS (WT%)

SAMPLE	CH-7-1	CH-7-2	CH-8	CH-10	CH-11-A
SiO2	49.98	40.88	42.39	35.26	56.91
Al2O3	16.67	15.83	18.92	9.52	14.62
Fe2O3	18.98	27.12	21.95	12.60	14.62
MnO	1.16	1.58	1.45	11.45	10.91
CaO	.60	1.77	1.24	9.63	2.37
MgO	3.76	5.48	5.07	3.97	2.18
Na2O	.53	.09	.47	.28	5.98
K2O	1.04	0.00	1.26	.28	.94
TiO2	.75	.51	.77	.55	1.55
P2O5	.19	.49	.15	0.00	.67
Ba	0.00	.01	0.00	0.00	.23
H2O	5.62	6.02	6.22	14.63	0.00
					3.77
TOTAL	99.28	99.85	99.89	98.17	100.13

TRACE ELEMENTS (PPM)

	CH-7-1	CH-7-2	CH-8	CH-10	CH-11-A
Zr	115	57	76	73	75
Sr	17	31	47	98	39
Rb	24	5	28	10	34
Zn	112	128	124	100	102
Cu	0	0	0	0	0
Nb	0	0	0	0	0
Ce	205	263	208	221	207
La	63	38	50	150	51
Ni	65	45	82	53	82
Cr	111	87	131	78	87
V	65	134	84	74	74

TABLE III-4 (Cont'd)

MANGANESE HORIZON

MAJOR ELEMENTS (WT%)

SAMPLE	HH34003	HH34004	CH-3	CH-5	CH-6
SiO2	32.34	9.29	38.86	34.10	55.10
Al2O3	11.08	2.94	14.58	13.07	18.02
Fe2O3	8.22	6.05	11.69	11.38	5.20
MnO	13.10	23.82	8.30	8.52	3.76
CaO	3.96	17.67	5.63	9.21	2.05
MgO	1.49	3.11	3.16	3.47	1.29
Na2O	.72	.12	.69	.67	1.71
K2O	1.89	.38	1.71	1.51	3.40
TiO2	.52	.30	.66	.45	.79
P2O5	0.00	0.00	0.00	.53	0.00
Ba	5.83	.42	0.00	0.00	.07
H2O	13.47	28.71	12.60	14.31	7.49
TOTAL	92.62	92.81	97.88	97.22	98.88

TRACE ELEMENTS (PPM)

	HH34003	HH34004	CH-3	CH-5	CH-6
Zr	213	50	80	61	104
Sr	347	117	59	110	60
Rb	38	14	35	34	103
Zn	92	92	110	121	80
Cu	0	0	898	0	46
Nb	93	0	0	0	0
Ce	75	171	149	178	122
La	0	0	14	30	21
Ni	49	27	57	50	78
Cr	55	41	98	67	104
V	0	0	123	51	95

TABLE III-4 (Cont'd)

MANGANESE HORIZON

MAJOR ELEMENTS (WT%)

SAMPLE	HH-36-2	HH-35	HH-34-A	HH34001	HH34002
SiO2	44.63	52.19	12.95	21.87	52.74
Al2O3	14.85	17.20	6.47	8.75	20.22
Fe2O3	8.58	9.16	6.23	7.98	10.07
MnO	10.20	3.87	19.58	15.24	3.25
CaO	3.11	2.00	16.73	9.67	1.28
MgO	2.13	2.44	4.56	3.34	2.85
Na2O	1.11	1.33	.20	.40	1.42
K2O	2.49	2.84	.48	.99	2.89
TiO2	.80	.81	.18	.36	.73
P2O5	0.00	.41	0.00	.10	0.00
Ba	.08	.10	1.97	5.12	.16
H2O	10.93	6.82	27.14	20.88	6.62
TOTAL	98.91	99.17	96.49	94.70	102.23

TRACE ELEMENTS (PPM)

	HH-36-2	HH-35	HH-34-A	HH34001	HH34002
Zr	94	103	91	176	85
Sr	67	65	200	356	30
Rb	64	81	17	19	74
Zn	93	100	97	87	102
Cu	0	0	0	0	0
Nb	0	0	31	69	0
Ce	233	136	159	82	124
La	37	24	0	0	18
Ni	67	80	32	45	76
Cr	90	88	35	40	86
V	48	61	0	0	50

TABLE III-4 (Cont'd)

MANGANESE HORIZON

MAJOR ELEMENTS (WT%)

SAMPLE	HH-39-3	HH-39-4	HH-38	HH-37	HH-36-1
SiO2	39.09	29.10	28.42	52.34	31.61
Al2O3	13.02	11.36	10.19	16.86	12.71
Fe2O3	13.42	13.13	15.11	10.28	9.29
MnO	9.71	11.64	9.38	4.05	14.06
CaO	6.13	8.45	13.15	1.48	7.83
MgO	4.20	4.48	3.00	1.98	4.26
Na2O	.48	.29	.13	1.29	.65
K2O	.94	.57	.22	2.48	1.73
TiO2	.62	.45	.52	.76	.53
P2O5	.15	0.00	0.00	0.00	0.00
Ba	.33	1.68	.46	.08	.23
H2O	13.26	16.14	16.92	6.82	16.63
TOTAL	101.35	97.29	97.50	98.42	99.53

TRACE ELEMENTS (PPM)

SAMPLE	HH-39-3	HH-39-4	HH-38	HH-37	HH-36-1
Zr	90	124	78	102	83
Sr	70	167	175	45	138
Rb	21	18	8	68	42
Zn	105	96	99	107	95
Cu	0	21	17	0	0
Nb	0	24	0	0	0
Ce	268	240	191	171	264
La	54	25	23	34	27
Ni	73	64	45	76	63
Cr	80	67	69	109	81
V	40	0	46	68	0

TABLE III-4 (Cont'd)

MANGANESE HORIZON

MAJOR ELEMENTS (WT%)

SAMPLE	HH-40-B	HH-39-A	HH-39-B	HH-39-1	HH-39-2
SiO2	52.20	24.93	22.88	53.62	14.88
Al2O3	15.48	8.92	8.25	15.87	5.87
Fe2O3	10.46	7.85	9.40	13.60	6.42
MnO	4.75	17.58	14.70	1.37	22.96
CaO	1.38	10.21	13.61	1.79	13.45
MgO	2.56	3.39	4.75	4.29	3.54
Na2O	1.07	.42	.27	.77	.12
K2O	2.29	.80	.55	1.43	.51
TiO2	.80	.35	.39	.86	.25
P2O5	0.00	1.00	0.00	.51	.60
Ba	.08	2.02	.49	.07	.86
H2O	7.28	21.48	21.36	5.18	26.20
TOTAL	98.35	98.95	96.65	99.36	95.66

TRACE ELEMENTS (PPM)

Zr	87	111	86	93	74
Sr	20	188	105	11	125
Rb	60	23	16	42	16
Zn	95	79	93	112	75
Cu	42	17	0	0	0
Nb	0	39	2	0	9
Ce	184	157	245	166	121
La	39	0	0	7	0
Ni	91	46	48	91	35
Cr	116	50	53	99	45
V	113	0	0	90	0

TABLE III-4 (Cont'd)

MANGANESE HORIZON

MAJOR ELEMENTS (WT%)

SAMPLE	BE-2	402002	BW11TOP	HH-42-A	HH-42-B
SiO_2	50.77	25.64	53.80	29.59	46.59
Al_2O_3	13.09	7.57	17.19	9.08	13.79
Fe_2O_3	7.00	5.07	5.53	10.11	7.29
MnO	4.73	13.32	5.06	14.15	8.53
CaO	6.86	17.44	1.99	9.89	3.99
MgO	1.65	1.70	1.94	2.67	2.09
Na_2O	.68	.22	1.13	.45	1.10
K_2O	2.63	1.77	3.97	1.05	2.65
TiO_2	.50	.53	.73	.33	.67
P_2O_5	.52	.85	0.00	2.35	.12
Ba	1.07	.27	.15	.05	.09
H_2O	10.32	22.75	7.92	17.71	11.70
TOTAL	99.82	97.13	99.41	97.43	98.61

TRACE ELEMENTS (PPM)

SAMPLE	BE-2	402002	BW11TOP	HH-42-A	HH-42-B
Zr	125	71	92	52	76
Sr	362	233	43	129	70
Rb	67	35	115	25	67
Zn	87	72	76	97	72
Cu	0	0	1	0	27
Nb	0	0	0	0	0
Ce	90	68	114	219	184
La	190	0	15	16	21
Ni	60	38	63	56	48
Cr	92	28	98	66	96
V	47	2	83	22	71

TABLE III-4 (Cont'd)

MANGANESE HORIZON

MAJOR ELEMENTS (WT%)

SAMPLE	BW-1BOT	BE-8	BE-6	BE-4	BE-3TOP
SiO_2	36.45	39.14	15.92	6.59	54.81
Al_2O_3	12.93	8.63	5.04	3.37	16.73
Fe_2O_3	6.51	17.11	6.15	1.25	8.76
MnO	8.98	3.66	27.04	50.49	3.00
CaO	9.64	11.40	12.60	3.53	1.80
MgO	1.77	3.22	1.77	.51	2.17
Na_2O	.55	.07	.11	.04	.83
K_2O	3.07	0.00	.84	.09	3.48
TiO_2	.91	.42	.33	.10	.66
P_2O_5	.39	1.70	0.00	0.00	.08
Ba	1.14	.22	.05	2.87	.89
H_2O	14.89	11.52	26.73	28.23	5.74
TOTAL	97.23	97.09	96.58	97.07	98.95

TRACE ELEMENTS (PPM)

Zr	143	81	55	86	101
Sr	415	330	293	269	85
Rb	69	2	18	13	85
Zn	91	113	77	63	90
Cu	0	12	22	0	0
Nb	5	0	0	42	0
Ce	93	181	201	207	150
La	0	23	0	0	184
Ni	47	43	29	19	72
Cr	49	76	52	54	88
V	9	168	0	0	58

TABLE III-4 (Cont'd)

MANGANESE HORIZON

MAJOR ELEMENTS (WT%)

SAMPLE	BW4ATOP	BW-3-1	BW-3-2	BW-2TOP	BW-1TOP
SiO2	43.90	32.92	47.91	62.63	39.29
Al2O3	17.49	11.53	25.00	17.08	14.62
Fe2O3	8.30	5.18	7.50	7.24	7.74
MnO	9.18	12.82	1.50	.60	7.25
CaO	2.28	11.97	.58	.59	8.88
MgO	2.21	1.70	1.82	1.88	.50
Na2O	.69	.42	.79	.97	.53
K2O	4.08	2.74	6.32	3.86	3.06
TiO2	.86	.43	.85	.63	1.50
P2O5	0.00	0.00	0.00	.14	.68
Ba	.73	.17	.79	.26	1.79
H2O	9.86	18.74	5.71	3.70	12.66
TOTAL	99.58	98.62	98.77	99.58	98.50

TRACE ELEMENTS (PPM)

	BW4ATOP	BW-3-1	BW-3-2	BW-2TOP	BW-1TOP
Zr	119	74	211	99	205
Sr	86	167	76	15	708
Rb	107	60	167	115	61
Zn	109	80	88	90	77
Cu	0	0	0	0	0
Nb	0	0	0	0	18
Ce	119	138	176	88	131
La	0	0	3	30	33
Ni	71	40	72	69	55
Cr	81	55	62	87	42
V	62	7	28	61	44

TABLE III-4.(Cont'd)

MANGANESE HORIZON

MAJOR ELEMENTS (WT%)

SAMPLE	BE-7BOT	BE-9	BE-5TOP	BW-5	BW-4B
SiO2	47.83	56.52	50.14	5.93	50.74
Al2O3	16.75	15.65	15.55	2.45	14.68
Fe2O3	14.49	13.51	12.77	2.28	8.52
MnO	1.74	1.08	5.35	51.16	6.24
CaO	3.57	1.57	1.33	3.68	2.10
MgO	3.70	3.48	3.86	.45	2.64
Na2O	.70	.80	.58	.08	.61
K2O	2.24	1.98	2.41	.01	3.00
TiO2	.67	.67	.69	.16	.66
P2O5	.27	.38	0.00	0.00	0.00
Ba	.35	.08	.10	2.45	.24
H2O	7.42	4.95	7.45	28.57	8.55
TOTAL	99.73	100.67	100.23	97.22	97.98

TRACE ELEMENTS (PPM)

Zr	96	72	84	41	91
Sr	123	22	40	93	90
Rb	45	42	63	16	77
Zn	112	109	104	68	115
Cu	51	0	0	0	0
Nb	0	0	0	5	0
Ce	134	186	159	208	108
La	0	0	24	0	4
Ni	68	75	67	19	65
Cr	101	130	91	85	81
V	121	101	48	0	44

TABLE III-4 (Cont'd)

MANGANESE HORIZON

MAJOR ELEMENTS (WT%)

SAMPLE	BW10TOP	W-10-A	W-10-B	W-10-C	BE-7TOP
SiO_2	26.58	50.15	40.97	53.53	43.75
Al_2O_3	10.67	16.34	9.22	17.55	13.06
Fe_2O_3	20.79	18.21	15.44	13.50	10.24
MnO	3.30	.77	3.08	.63	5.51
CaO	15.16	.33	11.94	1.80	7.76
MgO	3.83	4.31	3.26	1.52	2.84
Na_2O	.03	.49	0.00	.88	.78
K_2O	.01	1.42	.02	2.45	1.99
TiO_2	.22	.80	.40	.78	.56
P_2O_5	3.15	.17	2.98	.86	1.00
Ba	.01	.07	.01	.10	.25
H_2O	14.86	4.96	9.74	4.34	10.58
TOTAL	98.61	98.02	97.06	97.94	98.32

TRACE ELEMENTS (PPM)

SAMPLE	BW10TOP	W-10-A	W-10-B	W-10-C	BE-7TOP
Zr	65	80	63	88	91
Sr	361	12	193	41	191
Rb	6	28	1	55	39
Zn	111	127	109	110	99
Cu	112	14	480	0	188
Nb	0	0	0	0	0
Ce	177	215	220	281	190
La	14	54	30	88	11
Ni	44	79	49	79	47
Cr	45	114	64	105	81
V	219	93	31	110	107

TABLE III-4 (Cont'd)

MANGANESE HORIZON

MAJOR ELEMENTS (WT%)

SAMPLE	M-81	M-80	M-79	M-73A	BE-10
SiO_2	47.67	59.00	58.16	27.07	60.34
Al_2O_3	15.87	19.35	18.22	8.37	19.90
Fe_2O_3	8.27	7.49	6.92	11.44	5.62
MnO	8.56	.46	.80	15.74	.82
CaO	2.22	.58	.73	9.91	.82
MgO	1.60	1.48	1.31	2.62	1.87
Na_2O	1.31	1.70	1.62	.32	1.45
K_2O	3.37	4.22	3.97	.53	4.26
TiO_2	.71	.85	.80	.27	.87
P_2O_5	.04	0.00	.03	.35	.12
Ba	.12	.14	.11	2.21	.12
H_2O	9.11	4.26	4.75	17.91	4.18
TOTAL	98.85	99.53	97.42	96.74	100.37

TRACE ELEMENTS (PPM)

Zr	81	103	103	112	0
Sr	57	10	12	416	0
Rb	87	141	135	11	0
Zn	99	107	98	111	0
Cu	0	16	0	8	0
Nb	0	0	0	13	0
Ce	111	141	131	57	0
La	7	2	33	0	0
Ni	74	90	81	36	0
Cr	82	101	99	35	0
V	15	124	125	0	0

TABLE III-4 (Cont'd)

MANGANESE HORIZON

MAJOR ELEMENTS (WT%)

SAMPLE	M-88-B	M-87	M-86-2	M-85-4	M-82TOP
SiO2	54.75	55.85	42.37	42.40	25.13
Al2O3	17.78	19.20	13.97	14.64	8.68
Fe2O3	10.07	8.71	8.08	7.55	5.67
MnO	2.30	1.39	12.80	12.94	24.00
CaO	1.17	.88	2.55	2.30	7.09
MgO	.43	.59	1.54	1.13	3.88
Na2O	1.47	1.47	.99	1.10	.62
K2O	4.03	4.49	3.11	3.26	1.88
TiO2	.77	.83	.62	.65	.44
P2O5	.10	.21	0.00	0.00	0.00
Ba	.24	.17	.11	.19	.16
H2O	4.88	5.35	12.17	11.89	21.25
TOTAL	97.99	99.14	98.31	98.05	98.80

TRACE ELEMENTS (PPM)

Zr	77	91	78	81	56
Sr	35	20	84	68	101
Rb	106	134	81	79	43
Zn	100	108	91	89	82
Cu	0	0	0	0	0
Nb	0	0	0	0	0
Ce	155	100	170	156	146
La	38	18	38	0	0
Ni	85	98	62	71	43
Cr	77	118	83	151	82
V	57	72	24	13	0

TABLE III-4 (Cont'd)

MANGANESE HORIZON

MAJOR ELEMENTS (WT%)

SAMPLE	M91B1	M91B2	M-90TOP	M-90BOT	M-88-A
SiO_2	19.62	17.27	33.81	15.21	34.76
Al_2O_3	8.05	7.85	12.32	6.14	11.07
Fe_2O_3	6.74	6.96	4.81	2.75	8.26
MnO	27.24	26.34	20.44	41.09	14.81
CaO	7.60	8.28	3.38	5.89	5.59
MgO	0.00	1.65	1.27	1.00	0.00
Na_2O	.35	.25	.92	.16	.88
K_2O	1.41	1.15	3.00	.61	2.13
TiO_2	.39	.31	.75	.33	.38
P_2O_5	0.00	0.00	0.00	0.00	.22
Ba	.91	2.01	.34	1.77	2.30
H_2O	22.03	25.21	17.41	22.61	13.20
TOTAL	94.34	97.28	98.45	97.56	93.60

TRACE ELEMENTS (PPM)

	M91B1	M91B2	M-90TOP	M-90BOT	M-88-A
Zr	79	112	66	96	125
Sr	184	385	78	339	376
Rb	34	24	62	20	41
Zn	85	83	80	73	81
Cu	0	0	0	0	0
Nb	11	22	0	20	18
Ce	203	104	115	151	192
La	100	0	55	0	0
Ni	44	41	44	24	43
Cr	78	64	69	60	55
V	0	0	20	0	0

TABLE III-4 (Cont'd)

MANGANESE HORIZON

MAJOR ELEMENTS (WT%)

SAMPLE	M-98-2	M-96TOP	M-96BOT	M-95	M-93
SiO_2	47.22	46.43	23.47	54.50	41.36
Al_2O_3	16.36	12.91	8.33	17.25	14.02
Fe_2O_3	11.36	9.11	11.11	11.94	9.03
MnO	1.85	7.68	13.31	1.90	12.55
CaO	5.52	4.56	13.19	1.11	2.69
MgO	2.65	2.43	2.54	1.83	1.89
Na_2O	.63	.62	.20	.91	.70
K_2O	2.81	2.36	.82	3.18	2.97
TiO_2	.78	.77	.41	.80	.68
P_2O_5	2.13	.25	.29	0.00	0.00
Ba	.11	.45	2.68	.13	.12
H_2O	6.72	10.61	19.47	5.78	12.96
TOTAL	98.14	98.18	95.82	99.33	98.97

TRACE ELEMENTS (PPM)

	M-98-2	M-96TOP	M-96BOT	M-95	M-93
Zr	78	99	167	101	71
Sr	97	115	558	48	57
Rb	66	60	23	95	69
Zn	97	87	107	100	85
Cu	179	80	0	0	0
Nb	0	0	59	0	0
Ce	250	150	98	154	174
La	54	3	0	27	0
Ni	67	67	61	73	59
Cr	93	101	46	87	89
V	101	70	0	89	16

TABLE III-4 (Cont'd)

MANGANESE HORIZON

MAJOR ELEMENTS (WT%)

SAMPLE	CC-13	CC-16	M101TOP	M-99BOT	M-98
SiO2	4.46	5.34	39.65	51.93	49.31
Al2O3	1.83	2.33	9.63	16.39	17.22
Fe2O3	1.97	3.21	10.74	14.03	11.75
MnO	49.50	41.26	6.11	.31	1.61
CaO	6.19	8.62	11.73	2.78	4.14
MgO	.98	1.70	2.75	3.00	3.27
Na2O	.08	.04	.41	.72	.66
K2O	.19	.21	1.00	2.32	2.99
TiO2	.15	.15	.39	.82	.80
P2O5	0.00	.18	1.19	1.30	1.84
Ba	.03	.02	.54	.13	.11
H2O	31.47	30.61	13.80	5.01	6.10
TOTAL	96.85	93.67	97.94	98.74	99.80

TRACE ELEMENTS (PPM)

Zr	34	35	68	82	89
Sr	71	85	151	62	94
Rb	16	14	25	59	81
Zn	65	72	107	98	100
Cu	1	0	65	87	276
Nb	1	0	0	0	0
Ce	170	170	130	205	209
La	0	0	0	64	70
Ni	13	22	45	71	70
Cr	78	59	50	113	100
V	0	0	15	79	97

TABLE III-4 (Cont'd)

MANGANESE HORIZON

MAJOR ELEMENTS (WT%)

SAMPLE	4328	4381	4382	439	KE-3
SiO2	8.47	50.85	3.93	4.91	46.01
Al2O3	3.45	15.03	1.26	1.26	15.32
Fe2O3	1.58	11.65	1.41	2.72	8.30
MnO	51.35	4.46	51.74	41.74	10.50
CaO	5.13	2.38	8.82	17.28	1.39
MgO	0.00	2.84	.59	.95	1.20
Na2O	.09	.92	.08	.09	.83
K2O	.27	2.44	0.00	.02	3.26
TiO2	.17	.72	.18	.14	.72
P2O5	0.00	0.00	.30	.46	0.00
Ba	.89	.14	.27	.26	.14
H2O	28.44	7.74	27.28	24.84	10.16
TOTAL	99.84	99.17	95.86	94.67	97.83

TRACE ELEMENTS (PPM)

	4328	4381	4382	439	KE-3
Zr	58	93	39	61	86
Sr	127	90	114	206	42
Rb	13	61	11	14	80
Zn	93	95	69	72	91
Cu	0	0	0	0	0
Nb	0	0	1	5	0
Ce	248	122	182	246	151
La	0	0	0	0	14
Ni	69	66	19	12	73
Cr	65	82	51	32	89
V	0	28	0	0	25

TABLE III-4 (Cont'd)

MANGANESE HORIZON

MAJOR ELEMENTS (WT%)

SAMPLE	BR-13B	JB-23	DC-9-A	DC-9-C	DC-9-D
SiO2	37.94	49.97	54.62	53.25	53.08
Al2O3	9.49	16.41	17.46	15.70	17.21
Fe2O3	2.77	5.21	9.46	8.50	8.44
MnO	16.87	6.21	2.11	3.92	2.63
CaO	7.59	2.70	1.31	2.45	2.51
MgO	2.14	3.02	3.03	2.02	.65
Na2O	.73	1.37	1.01	.92	.97
K2O	1.86	3.36	4.00	3.56	4.00
TiO2	.47	.75	1.01	.91	1.08
P2O5	0.00	0.00	.23	0.00	.20
Ba	.02	.19	.06	.86	.13
H2O	18.76	10.08	6.10	7.85	7.72
TOTAL	98.64	99.27	100.40	99.94	98.62

TRACE ELEMENTS (PPM)

Zr	60	112	139	154	145
Sr	58	179	38	153	54
Rb	47	109	112	91	107
Zn	80	94	103	94	99
Cu	258	48	0	0	0
Nb	0	0	0	0	0
Ce	125	145	150	116	131
La	0	22	16	16	3
Ni	40	73	88	70	75
Cr	67	97	83	77	79
V	50	73	107	67	101

TABLE III-4 (Cont'd)

RED MUDSTONE

MAJOR ELEMENTS (WT%)

SAMPLE	BR-26	BR-30	JH-1	JB-27	DC-7-A
SiO_2	57.20	67.13	56.65	55.00	59.95
Al_2O_3	19.62	14.51	19.80	21.40	16.97
Fe_2O_3	9.00	5.63	8.97	8.50	7.29
MnO	.09	.28	.18	.07	.12
CaO	.52	.93	.73	.44	1.62
MgO	1.75	1.90	1.75	2.15	1.47
Na_2O	1.66	2.10	1.76	1.78	.79
K_2O	3.94	2.68	3.88	4.06	4.27
TiO_2	.90	.90	.92	.88	1.04
P_2O_5	.06	.34	.07	.20	.15
Ba	.06	.05	.05	.08	.07
H_2O	4.28	3.78	4.56	5.16	5.82
TOTAL	99.08	100.23	99.32	99.72	99.56

TRACE ELEMENTS (PPM)

SAMPLE	BR-26	BR-30	JH-1	JB-27	DC-7-A
Zr	112	188	115	97	159
Sr	9	23	34	11	11
Rb	122	86	124	141	94
Zn	100	91	109	108	92
Cu	0	4	0	0	8
Nb	0	0	0	0	0
Ce	125	77	96	123	58
La	3	8	64	25	0
Ni	64	58	73	78	36
Cr	101	74	107	133	55
V	100	102	119	162	112

TABLE III-4 (Cont'd)

RED MUDSTONE

MAJOR ELEMENTS (WT%)

SAMPLE	CW-1	CW-5	TCJ-4	RL-12	BR-11-2
SiO_2	59.87	62.10	61.83	55.86	57.92
Al_2O_3	20.89	19.43	16.68	20.85	15.83
Fe_2O_3	4.77	7.73	8.53	7.77	11.29
MnO	.20	.20	.37	.16	1.11
CaO	0.00	.36	.74	.48	1.10
MgO	1.01	1.31	1.91	2.86	1.60
Na_2O	1.29	1.85	1.46	1.54	1.49
K_2O	5.53	3.92	3.39	3.97	3.08
TiO_2	1.00	1.03	.86	.90	.75
P_2O_5	0.00	.31	.30	.16	.11
Ba	.09	.06	.16	.06	.08
H_2O	4.27	3.65	3.39	5.50	5.03
TOTAL	98.92	101.95	99.62	100.11	99.39

TRACE ELEMENTS (PPM)

Zr	150	0	114	122	85
Sr	0	3	64	46	0
Rb	152	108	112	150	83
Zn	104	100	74	107	86
Cu	159	0	0	85	82
Nb	0	0	0	0	0
Ce	94	106	103	110	133
La	50	93	20	26	55
Ni	56	69	76	84	67
Cr	78	102	91	117	101
V	133	128	106	129	107

TABLE III-4 (Cont'd)

RED MUDSTONE

MAJOR ELEMENTS (WT%)

SAMPLE	LY-6	LD-13	4126	41251	41252
SiO2	57.84	55.18	63.18	61.25	59.85
Al2O3	20.50	21.13	16.10	16.84	13.87
Fe2O3	8.94	9.38	7.17	6.18	3.66
MnO	.14	.37	.25	.29	.60
CaO	.42	.47	.50	.96	5.38
MgO	1.62	.34	1.63	2.81	2.57
Na2O	1.58	1.10	2.16	2.33	2.39
K2O	4.52	4.75	3.44	3.33	2.34
TiO2	.84	.84	.92	1.03	.93
P2O5	.10	.09	.13	.60	.13
Ba	.14	.22	.06	.05	.04
H2O	3.65	5.33	2.47	3.80	5.84
TOTAL	100.29	99.20	98.01	99.47	97.60

TRACE ELEMENTS (PPM)

Zr	109	102	152	191	172
Sr	14	43	4	60	69
Rb	149	159	98	98	59
Zn	100	79	91	95	95
Cu	0	0	0	1	100
Nb	0	0	0	0	0
Ce	120	99	37	66	34
La	113	19	0	0	0
Ni	69	68	54	60	55
Cr	107	118	77	93	119
V	110	106	115	187	152

TABLE III-4 (Cont'd)

RED MUDSTONE

MAJOR ELEMENTS (WT%)

SAMPLE	OP-19	OP-18	OP-14	OP-10	LY-3
SiO_2	55.00	55.09	58.72	59.46	57.73
Al_2O_3	20.29	21.27	17.51	18.27	17.02
Fe_2O_3	10.21	9.68	7.55	7.86	7.68
MnO	.32	.18	.12	.12	.13
CaO	.55	.46	1.72	.61	.75
MgO	2.42	2.72	1.46	1.08	1.44
Na_2O	1.32	1.19	2.21	1.99	1.57
K_2O	4.02	4.37	3.92	4.12	4.02
TiO_2	.94	.98	1.06	1.00	.85
P_2O_5	.35	.24	.14	.16	.26
Ba	.13	.13	.05	.06	.10
H_2O	4.27	4.35	4.62	3.56	3.38
TOTAL	99.82	100.66	99.08	98.29	94.93

TRACE ELEMENTS (PPM)

SAMPLE	OP-19	OP-18	OP-14	OP-10	LY-3
Zr	108	120	159	150	140
Sr	41	28	25	23	23
Rb	125	130	114	125	134
Zn	100	102	94	101	82
Cu	0	0	1	0	0
Nb	0	0	0	0	0
Ce	120	120	66	72	72
La	47	23	8	0	30
Ni	72	64	54	67	62
Cr	102	112	93	86	90
V	98	125	127	110	118

TABLE III-4 (Cont'd)

RED MUDSTONE

MAJOR ELEMENTS (WT%)

SAMPLE	SP-10	SP-6	SP-4	OP-38	OP-37
SiO2	55.22	56.92	57.87	59.76	59.37
Al2O3	15.72	17.29	17.81	16.65	17.10
Fe2O3	6.78	8.41	8.07	10.15	9.51
MnO	.08	.08	.16	.40	.43
CaO	4.79	2.20	1.97	.81	1.47
MgO	2.54	2.21	2.80	2.56	2.27
Na2O	2.17	1.67	1.96	1.15	1.18
K2O	3.45	3.79	3.72	3.28	3.47
TiO2	.93	.88	.90	.78	.77
P2O5	.17	.15	0.00	.31	.16
Ba	.07	.05	.05	.19	.12
H2O	7.11	5.05	5.10	3.73	4.26
TOTAL	99.03	98.70	100.41	99.77	100.11

TRACE ELEMENTS (PPM)

Zr	158	137	136	101	106
Sr	70	17	35	41	54
Rb	99	106	107	104	109
Zn	94	98	104	117	111
Cu	9	0	3	0	0
Nb	0	0	0	0	0
Ce	53	72	69	124	138
La	0	0	0	23	42
Ni	51	60	57	94	101
Cr	70	83	79	146	82
V	105	100	116	77	78

TABLE III-4 (Cont'd)

RED MUDSTONE

MAJOR ELEMENTS (WT%)

SAMPLE	SP-37	SP-27	SP-73-2	SP-73-5	SP-12-1
SiO2	56.97	57.15	59.11	53.72	61.42
Al2O3	20.27	19.84	18.77	19.35	16.78
Fe2O3	8.02	8.28	7.55	12.32	7.66
MnO	.12	.21	.20	.25	.08
CaO	.54	.80	.71	.72	.62
MgO	2.14	1.76	1.46	2.40	1.77
Na2O	1.50	1.65	1.46	.74	2.17
K2O	4.35	3.81	3.88	4.02	3.74
TiO2	.98	.91	.87	.96	.98
P2O5	.17	.38	.17	.16	.32
Ba	.11	.08	.15	.08	.04
H2O	4.89	4.96	4.85	5.30	3.28
TOTAL	100.06	99.83	99.18	100.02	98.86

TRACE ELEMENTS (PPM)

Zr	130	110	119	125	171
Sr	62	23	18	48	2
Rb	140	117	112	114	111
Zn	114	105	96	104	94
Cu	0	0	9	0	13
Nb	0	0	0	0	0
Ce	132	109	136	180	70
La	29	32	28	39	0
Ni	85	69	65	80	57
Cr	110	95	115	109	87
V	181	75	89	116	125

TABLE III-4 (Cont'd)

RED MUDSTONE

MAJOR ELEMENTS (WT%)

SAMPLE	NC-4	NC-15-1	NC-17	NC-19	SP-46
SiO2	64.46	55.68	55.14	59.34	56.43
Al2O3	16.22	19.77	18.61	17.52	18.99
Fe2O3	7.05	9.57	9.34	8.10	10.88
MnO	.27	.15	.32	.19	.26
CaO	.61	.37	.66	1.33	.66
MgO	1.65	.91	1.64	2.00	2.08
Na2O	2.24	1.10	1.19	1.45	1.29
K2O	3.36	5.72	4.80	4.75	3.82
TiO2	.99	1.02	.99	.96	.92
P2O5	.23	.05	.12	0.00	.30
Ba	.06	.08	.09	.07	.13
H2O	2.97	5.56	4.17	4.08	4.89
TOTAL	100.11	99.98	97.07	99.79	100.65

TRACE ELEMENTS (PPM)

	NC-4	NC-15-1	NC-17	NC-19	SP-46
Zr	167	156	154	183	107
Sr	30	4	8	32	32
Rb	97	145	131	129	116
Zn	91	93	119	109	97
Cu	5	0	85	4	0
Nb	0	0	0	0	0
Ce	86	83	38	68	162
La	0	0	0	0	184
Ni	60	51	57	74	77
Cr	84	84	77	71	91
V	114	117	115	163	80

TABLE III-4 (Cont'd)

RED MUDSTONE

MAJOR ELEMENTS (WT%)

SAMPLE	CH-28	CH-33	CH-34-A	NC-2	NC-3
SiO2	55.57	57.44	58.46	63.47	54.59
Al2O3	18.94	19.22	17.90	15.30	18.07
Fe2O3	8.94	8.32	7.91	7.07	9.34
MnO	.13	.17	.15	.39	.15
CaO	1.62	.70	.66	.83	1.10
MgO	1.66	2.60	2.45	1.53	1.71
Na2O	1.94	1.82	1.77	2.16	1.35
K2O	3.95	3.85	3.60	3.46	5.25
TiO2	.93	.92	.87	.90	1.10
P2O5	.15	.20	.24	.16	.27
Ba	.06	0.00	0.00	.07	.08
H2O	4.92	4.33	4.21	3.09	3.87
TOTAL	98.81	99.57	98.22	98.43	96.88

TRACE ELEMENTS (PPM)

Zr	128	132	139	159	164
Sr	51	23	46	0	0
Rb	114	112	114	92	132
Zn	99	100	96	86	89
Cu	0	0	0	0	0
Nb	0	0	0	0	0
Ce	85	96	68	79	73
La	8	0	31	0	0
Ni	65	65	62	102	50
Cr	91	102	92	90	78
V	133	128	120	131	102

TABLE III-4 (Cont'd)

RED MUDSTONE

MAJOR ELEMENTS (WT%)

SAMPLE	CH-1	CH-18	CH-20	CH-22	CH-24
SiO2	56.43	55.15	57.41	55.31	56.01
Al2O3	20.03	18.75	20.17	18.32	20.15
Fe2O3	9.66	8.97	8.66	13.12	9.29
MnO	.40	.24	.20	.22	.16
CaO	.56	.84	.45	.64	.53
MgO	1.82	1.22	1.64	1.53	1.49
Na2O	1.67	1.74	1.89	1.62	1.55
K2O	4.21	3.96	3.96	3.56	4.15
TiO2	.93	.81	.82	.82	.87
P2O5	.07	.14	.13	.16	.09
Ba	.10	.09	.11	0.00	.07
H2O	4.29	4.36	4.11	4.04	4.58
TOTAL	100.17	96.27	99.55	99.34	98.94

TRACE ELEMENTS (PPM)

Zr	108	103	102	97	117
Sr	32	35	35	66	51
Rb	137	126	124	107	130
Zn	98	98	100	90	98
Cu	0	0	0	0	0
Nb	0	0	0	0	0
Ce	110	136	129	0	107
La	25	182	247	0	24
Ni	67	79	76	60	67
Cr	106	125	115	136	114
V	88	112	116	145	131

TABLE III-4 (Cont'd)

RED MUDSTONE

MAJOR ELEMENTS (WT%)

SAMPLE	HH-53-B	HH-57	HH-55	HH-17	HH-9
SiO2	61.96	61.67	62.08	65.97	56.48
Al2O3	17.20	18.35	16.40	15.10	18.50
Fe2O3	6.89	7.71	7.27	6.10	8.48
MnO	.12	.13	.13	.18	.22
CaO	1.07	.51	.86	1.10	1.48
MgO	.92	2.74	2.36	2.31	1.03
Na2O	1.66	1.45	2.00	2.28	1.46
K2O	3.71	3.69	3.16	2.72	4.77
TiO2	.84	.96	.91	.89	.99
P2O5	.22	.18	.24	.23	.13
Ba	.05	.06	.05	.05	.08
H2O	3.79	3.90	3.62	3.40	4.32
TOTAL	98.43	101.35	99.08	100.33	97.94

TRACE ELEMENTS (PPM)

SAMPLE	HH-53-B	HH-57	HH-55	HH-17	HH-9
Zr	128	138	141	163	156
Sr	15	0	5	29	26
Rb	106	106	87	80	124
Zn	91	107	91	93	107
Cu	0	0	0	0	0
Nb	0	0	0	0	0
Ce	102	85	109	67	116
La	0	0	0	0	1
Ni	53	59	65	58	70
Cr	90	113	90	76	71
V	113	127	103	96	120

TABLE III-4 (Cont'd)

RED MUDSTONE

MAJOR ELEMENTS (WT%)

SAMPLE	DB-73-1	4078	401	HH-47	HH-49
SiO2	57.99	41.30	2059.1	57.23	55.95
Al2O3	18.82	5.88	3015.4	19.65	20.21
Fe2O3	8.86	5.26	5.70	8.91	8.92
MnO	.17	.45	1000.2	.17	.17
CaO	.31	22.94	3004.5	.38	1.11
MgO	1.49	0.00	3000.4	1.54	1.28
Na2O	1.35	.86	201.00	1.56	1.42
K2O	6.14	1.41	604.90	4.28	4.73
TiO2	1.03	.20	90.80	.83	.94
P2O5	0.00	.15	300.20	.12	.10
Ba	.11	.04	300.00	.11	.09
H2O	3.26	19.71	0.00	4.01	4.64
TOTAL	99.53	98.20	100.10	98.79	99.56

TRACE ELEMENTS (PPM)

	DB-73-1	4078	401	HH-47	HH-49
Zr	151	62	153	103	116
Sr	0	155	6	18	10
Rb	167	36	143	135	134
Zn	101	59	100	106	102
Cu	0	73	0	0	0
Nb	0	0	0	0	0
Ce	59	15	52	116	117
La	0	0	12	32	68
Ni	63	15	84	71	69
Cr	64	19	73	109	106
V	111	47	93	113	122

TABLE III-4 (Cont'd)

RED MUDSTONE

MAJOR ELEMENTS (WT%)

SAMPLE	4329'	CC-4A	CC-10	DB-73-7	DB-73-4
SiO_2	49.41	64.57	61.25	58.43	58.45
Al_2O_3	0.00	14.02	16.77	19.31	19.81
Fe_2O_3	11.39	6.19	7.26	8.48	8.02
MnO	.74	.20	.14	.17	.16
CaO	7.69	1.84	1.26	.35	.38
MgO	0.00	1.44	.48	3.03	1.28
Na_2O	1.13	1.95	1.50	1.11	1.33
K_2O	3.25	3.31	4.49	4.95	5.12
TiO_2	.60	.80	.95	.77	.92
P_2O_5	2.92	.25	.42	.08	.05
Ba	.16	.11	.10	.14	.14
H_2O	0.00	4.19	4.50	3.97	3.58
TOTAL	77.29	98.87	99.12	100.79	99.24

TRACE ELEMENTS (PPM)

SAMPLE	4329'	CC-4A	CC-10	DB-73-7	DB-73-4
Zr	98	133	131	78	111
Sr	263	38	0	0	0
Rb	80	90	137	134	146
Zn	92	82	90	99	96
Cu	0	0	0	0	0
Nb	0	0	0	0	0
Ce	96	64	75	98	93
La	114	0	4	16	1
Ni	88	53	57	69	62
Cr	51	69	75	100	85
V	57	88	109	134	100

TABLE III-4 (Cont'd)

RED MUDSTONE

MAJOR ELEMENTS (WT%)

SAMPLE	DB-73-3	DB-75	40105	DB-73-2	40101
SiO2	60.15	72.46	62.54	60.22	59.24
Al2O3	18.96	12.44	15.82	17.19	18.45
Fe2O3	7.09	5.46	7.96	7.76	8.12
MnO	.12	.15	.12	.20	.17
CaO	.38	.82	1.48	1.15	.44
MgO	1.84	1.95	1.49	.68	2.03
Na2O	1.50	2.05	1.39	1.64	1.66
K2O	4.86	2.44	4.23	5.26	5.00
TiO2	.96	.85	.98	.98	1.10
P2O5	.15	.23	.17	.13	.18
Ba	.12	.05	.10	.09	.10
H2O	3.51	2.54	3.82	3.84	3.17
TOTAL	99.64	101.44	100.10	99.14	99.66

TRACE ELEMENTS (PPM)

SAMPLE	DB-73-3	DB-75	40105	DB-73-2	40101
Zr	137	237	222	170	171
Sr	0	0	0	0	0
Rb	13	74	109	153	122
Zn	8008	99	80	103	102
Cu	3000	0	0	0	0
Nb	0	0	0	0	0
Ce	4	69	70	51	39
La	5000	0	0	0	0
Ni	5	50	48	78	66
Cr	7008	73	93	61	75
V	5009	87	104	104	130

TABLE III-4 (Cont'd)

LIMESTONE

MAJOR ELEMENTS (WT%)

SAMPLE	DB-100	DB-103	40106	40201	HH-21-B
SiO2	20.93	27.72	25.35	21.15	41.81
Al2O3	9.11	5.16	4.52	3.88	7.85
Fe2O3	4.86	6.97	1.90	1.90	10.40
MnO	.71	.96	.54	.57	1.85
CaO	31.08	29.21	36.36	39.03	15.83
MgO	1.66	1.19	0.00	0.00	2.55
Na2O	.60	.29	.92	.66	1.19
K2O	2.56	1.35	.48	.80	.65
TiO2	.42	.30	.28	.21	.29
P2O5	2.66	0.00	.32	0.00	.97
Ba	.03	.03	0.00	.05	.02
LOI	22.65	24.61	28.89	31.39	14.99
TOTAL	97.27	97.79	99.56	99.64	97.40

TRACE ELEMENTS (PPM)

	DB-100	DB-103	40106	40201	HH-21-B
Zr	76	84	84	73	55
Sr	120	143	156	219	191
Rb	41	19	0	10	11
Zn	82	65	61	55	159
Cu	0	0	220	0	27
Nb	0	0	0	0	0
Ce	38	60	0	0	120
La	0	0	0	45	20
Ni	35	20	12	15	50
Cr	19	10	22	7	35
V	61	38	53	32	44

TABLE III-4 (Cont'd)

LIMESTONE

MAJOR ELEMENTS (WT%)

SAMPLE	HH-29	HH-22	HH-50	HH-53-A	HH-11
SiO2	25.90	40.60	32.11	7.17	16.08
Al2O3	10.37	12.94	6.62	2.34	4.35
Fe2O3	6.66	7.05	4.65	1.09	2.04
MnO	.85	.56	1.11	1.01	.71
CaO	26.67	16.84	27.29	48.91	42.97
MgO	1.05	.55	0.00	0.00	0.00
Na2O	.76	.53	.82	.43	.57
K2O	1.87	2.35	.81	.42	.48
TiO2	.42	.47	.31	.08	.22
P2O5	0.00	0.00	0.00	0.00	0.00
Ba	.05	.06	.01	0.00	0.00
LOI	23.93	17.32	22.98	38.45	34.14
TOTAL	98.53	99.27	96.71	99.90	101.56

TRACE ELEMENTS (PPM)

Zr	71	75	74	50	48
Sr	248	236	211	276	188
Rb	42	50	15	6	6
Zn	76	78	72	50	63
Cu	0	0	38	0	78
Nb	0	0	0	0	0
Ce	33	40	18	0	0
La	96	0	0	0	0
Ni	32	45	29	7	14
Cr	33	48	24	2	4
V	65	51	44	27	38

TABLE III-4 (Cont'd)

LIMESTONE

MAJOR ELEMENTS (WT%)

SAMPLE	HH-12	HH-13	HH-14	CH-31	CH-34-B
SiO2	11.61	15.92	22.91	31.34	10.72
Al2O3	3.50	4.22	4.53	11.60	4.36
Fe2O3	1.76	1.85	4.26	13.74	2.18
MnO	.52	.40	1.44	1.72	2.89
CaO	44.31	40.70	33.72	17.03	42.01
MgO	0.00	0.00	0.00	3.98	.11
Na2O	.49	.78	.80	.42	.63
K2O	.48	.81	.62	.49	.42
TiO2	.13	.23	.24	.49	.27
P2O5	0.00	0.00	0.00	0.00	0.00
Ba	0.00	.01	.01	.01	0.00
LOI	35.92	33.58	28.82	17.06	36.18
TOTAL	98.72	98.50	97.35	97.91	99.77

TRACE ELEMENTS (PPM)

Zr	12	63	71	70	84
Sr	237	217	226	132	85
Rb	9	16	7	6	76
Zn	59	57	56	150	100
Cu	294	6	0	17	37
Nb	0	0	0	0	0
Ce	0	0	5	54	158
La	0	0	0	0	26
Ni	12	16	31	31	62
Cr	8	6	15	70	87
V	60	37	29	35	74

TABLE III-4 (Cont'd)

LIMESTONE

MAJOR ELEMENTS (WT%)

SAMPLE	NC-20-1	NC20-2	NC-15-2	SP-54	SP-51
SiO_2	16.60	10.19	19.03	24.00	10.71
Al_2O_3	3.78	2.98	8.09	11.50	4.28
Fe_2O_3	1.78	1.26	6.64	16.61	4.82
MnO	.46	.62	1.10	15.91	5.06
CaO	41.39	46.75	31.83	5.86	37.46
MgO	.66	0.00	4.71	3.52	0.00
Na_2O	.30	.37	.28	.18	.12
K_2O	.57	.51	1.21	.81	.47
TiO_2	.19	.17	.27	.30	.12
P_2O_5	0.00	0.00	0.00	0.00	0.00
Ba	0.00	0.00	.01	.02	.05
LOI	32.54	35.14	27.27	18.31	32.17
TOTAL	98.27	97.99	100.44	97.02	95.26

TRACE ELEMENTS (PPM)

Zr	57	51	57	38	45
Sr	181	199	145	67	247
Rb	11	10	25	21	13
Zn	60	59	155	119	68
Cu	16	150	20	0	0
Nb	0	0	0	0	0
Ce	0	0	0	155	11
La	0	0	0	168	0
Ni	13	11	67	35	20
Cr	6	0	2	53	11
V	39	37	28	0	12

TABLE III-4 (Cont'd)

LIMESTONE

MAJOR ELEMENTS (WT%)

SAMPLE	SP-23	SP-21	SP-8	OP-36	OP-34
SiO2	17.93	18.37	15.30	25.80	30.24
Al2O3	4.83	4.50	3.64	6.95	9.13
Fe2O3	3.60	4.47	1.11	5.01	5.23
MnO	1.24	.60	.43	1.43	2.34
CaO	35.66	38.56	41.03	30.06	24.50
MgO	1.63	0.00	1.34	1.75	1.38
Na2O	.23	.52	1.03	.32	.55
K2O	.42	.92	.44	.99	2.05
TiO2	.18	.31	.16	.27	.33
P2O5	0.00	0.00	0.00	0.00	0.00
Ba	1.44	.12	.04	.03	.07
LOI	30.65	31.06	33.42	25.79	22.23
TOTAL	97.81	99.43	97.94	98.40	98.05

TRACE ELEMENTS (PPM)

Zr	120	60	485	54	60
Sr	325	161	5903	212	190
Rb	12	17	0	22	50
Zn	69	55	58	84	70
Cu	81	0	40	0	0
Nb	8	0	0	0	0
Ce	0	0	0	31	40
La	0	0	0	16	0
Ni	17	36	10	37	38
Cr	5	5	5	20	27
V	3	31	33	50	42

TABLE III-4 (Cont'd)

LIMESTONE

MAJOR ELEMENTS (WT%)

SAMPLE	OP-32	OP-24	OP-17-B	OP-16	OP-7
SiO2	23.00	29.60	20.85	13.25	14.46
Al2O3	6.81	12.10	8.38	2.06	3.65
Fe2O3	4.50	9.85	8.89	.66	1.87
MnO	1.87	2.40	2.49	.78	.74
CaO	31.27	19.57	27.77	43.75	40.89
MgO	1.75	2.18	2.22	.56	1.43
Na2O	.33	.38	.33	.56	.91
K2O	1.11	1.85	.90	.36	.42
TiO2	.24	.45	.32	.10	.21
P2O5	0.00	0.00	.14	0.00	0.00
Ba	.04	.07	0.00	.03	.06
LOI	27.06	20.08	25.60	35.61	34.25
TOTAL	97.98	98.53	97.89	97.72	98.89

TRACE ELEMENTS (PPM)

Zr	53	74	59	43	69
Sr	224	177	172	251	364
Rb	26	36	19	0	5
Zn	79	82	96	48	57
Cu	0	0	9	27	169
Nb	0	0	0	0	0
Ce	8	89	26	0	0
La	0	0	0	0	0
Ni	34	47	33	8	11
Cr	19	51	29	0	3
V	40	45	43	31	15

TABLE III-4 (Cont'd)

LIMESTONE

MAJOR ELEMENTS (WT%)

SAMPLE.	LY-23	WB-40	CA-5	4119	4127
SiO2	19.75	16.61	22.09	25.34	28.05
Al2O3	5.43	3.85	.17	7.74	8.44
Fe2O3	4.02	3.04	.29	11.33	5.12
MnO	1.62	.94	1.52	3.38	2.00
CaO	34.49	37.20	42.08	23.83	26.70
MgO	1.24	1.21	0.00	1.47	1.16
Na2O	.24	.88	.03	.46	1.06
K2O	1.21	.62	0.00	1.76	1.81
TiO2	.25	.20	.05	.28	.48
P2O5	.01	0.00	0.00	.15	0.00
Ba	.03	.02	0.00	.02	.56
LOI	29.46	32.12	33.72	22.61	23.58
TOTAL	97.75	96.69	99.95	98.37	98.96

TRACE ELEMENTS (PPM)

	LY-23	WB-40	CA-5	4119	4127
Zr	71	68	42	71	130
Sr	426	252	345	239	302
Rb	23	10	0	35	33
Zn	61	54	43	85	77
Cu	13	0	0	0	0
Nb	0	0	0	0	0
Ce	21	0	0	18	31
La	0	0	0	0	0
Ni	26	39	3	30	97
Cr	16	4	0	84	38
V	39	29	13	92	22

TABLE III-4 (Cont'd)

LIMESTONE

MAJOR ELEMENTS (WT%)

SAMPLE	CW-2	XY-2(	DI-2	GH-1	BR-28
SiO_2	16.74	10.74	19.04	11.69	23.99
Al_2O_3	4.73	3.66	7.87	3.58	6.00
Fe_2O_3	2.29	2.40	4.26	1.72	4.69
MnO	.87	1.86	.90	.65	1.00
CaO	40.70	42.39	33.78	44.04	33.03
MgO	0.00	0.00	1.28	0.00	0.00
Na_2O	1.13	.18	.63	.48	.32
K_2O	.64	.98	1.92	.56	1.44
TiO_2	.20	.18	.43	.13	.27
P_2O_5	0.00	.08	0.00	0.00	0.00
Ba	.01	.02	.02	.05	.38
LOI	32.44	34.32	28.40	0.00	27.42
TOTAL	99.75	96.81	98.53	62.90	98.54

TRACE ELEMENTS (PPM)

Zr	43	43	78	54	72
Sr	145	314	160	269	173
Rb	4	14	32	4	24
Zn	51	58	85	55	66
Cu	0	18	0	230	3
Nb	0	0	0	0	0
Ce	0	0	6	0	15
La	16	0	0	0	0
Ni	17	13	82	10	66
Cr	9	10	20	5	15
V	31	35	43	53	27

TABLE III-4 (Cont'd)

LIMESTONE

MAJOR ELEMENTS (WT%)

SAMPLE	431	999	CC-4B	CC-4C	M-16
SiO2	27.72	27.45	28.32	3.11	36.13
Al2O3	6.85	6.03	6.16	.24	6.37
Fe2O3	2.90	2.89	2.92	.37	7.88
MnO	.86	.93	.40	.89	2.06
CaO	31.40	32.19	29.23	53.39	21.34
MgO	0.00	0.00	0.00	0.00	2.88
Na2O	.50	1.05	.76	.11	.25
K2O	1.74	1.30	1.59	0.00	.16
TiO2	.29	.28	.39	0.00	.26
P2O5	0.00	0.00	0.00	0.00	2.08
Ba	.03	.06	.06	.11	1.46
LOI	27.88	27.77	26.00	41.85	17.22
TOTAL	100.17	99.95	95.83	100.07	98.09

TRACE ELEMENTS (PPM)

SAMPLE	431	999	CC-4B	CC-4C	M-16
Zr	66	67	63	32	131
Sr	314	186	168	238	440
Rb	30	22	28	0	7
Zn	55	64	60	44	79
Cu	0	0	0	0	27
Nb	0	0	0	0	18
Ce	0	0	4	0	67
La	0	0	0	0	0
Ni	24	20	21	0	28
Cr	13	12	18	0	33
V	44	45	41	12	24

TABLE III-4 (Cont'd)

LIMESTONE

MAJOR ELEMENTS (WT%)

SAMPLE	M-19	DB-73-9	DB-99	4062	DB-40
SiO2	47.64	10.41	9.91	6.39	19.30
Al2O3	14.48	3.78	2.33	1.88	3.23
Fe2O3	19.24	1.52	1.22	.91	.80
MnO	1.57	.44	.56	.61	.71
CaO	1.27	44.26	47.07	49.85	40.40
MgO	2.72	.62	0.00	0.00	0.00
Na2O	.75	.23	.12	.34	.73
K2O	1.90	1.15	.75	.29	.48
TiO2	.62	.22	.11	.09	.16
P2O5	.33	0.00	0.00	0.00	0.00
Ba	.92	.02	.01	0.00	.55
LOI	7.27	35.68	37.01	100196	32.80
TOTAL	98.71	98.33	99.09	100.07	99.16

TRACE ELEMENTS (PPM)

SAMPLE	M-19	DB-73-9	DB-99	4062	DB-40
Zr	99	65	43	42	58
Sr	158	195	202	214	150
Rb	45	22	9	0	0
Zn	124	53	53	48	45
Cu	0	0	0	11	318
Nb	0	0	0	0	0
Ce	171	0	0	0	0
La	41	0	0	0	0
Ni	52	14	13	8	4
Cr	102	3	0	0	2
V	50	37	26	24	44

TABLE III-4 (Cont'd)

BLACK MUDSTONE

MAJOR ELEMENTS (WT%)

SAMPLE	M-110	M-300	M-301	HH-19	HH-20
SiO_2	50.10	56.35	55.15	54.26	49.66
Al_2O_3	19.47	18.90	18.44	16.11	14.48
Fe_2O_3	12.88	9.32	9.49	10.94	9.88
MnO	.94	.16	.25	1.86	2.75
CaO	.64	1.11	1.60	2.17	4.82
MgO	3.79	1.55	3.17	2.70	2.72
Na_2O	.62	.69	.63	.70	.62
K_2O	3.36	4.03	3.90	2.81	2.70
TiO_2	.91	.97	.89	.78	.72
P_2O_5	.27	.22	.04	.23	.28
Ba	.08	.12	.45	.08	.07
LOI	7.10	5.34	5.82	7.29	10.56
TOTAL	100.16	98.76	99.83	99.93	99.26

TRACE ELEMENTS (PPM)

Zr	98	124	129	95	77
Sr	26	20	53	37	41
Rb	85	115	110	70	54
Zn	92	114	118	87	71
Cu	18	138	189	63	57
Nb	0	0	0	0	0
Ce	146	130	107	140	123
La	49	35	4	38	0
Ni	51	102	117	89	65
Cr	120	93	93	96	89
V	119	109	107	103	90

TABLE III-4 (Cont'd)

BLACK MUDSTONE

MAJOR ELEMENTS (WT%)

SAMPLE	HH-21-A	HH-23	SP-57	SP-55	LY-21
SiO2	49.53	55.94	55.39	54.85	59.33
Al2O3	14.35	20.20	17.23	17.57	15.68
Fe2O3	11.51	9.50	13.72	13.47	9.51
MnO	3.96	.13	.31	.26	.43
CaO	3.07	.51	1.01	.84	1.71
MgO	3.21	2.40	2.72	3.43	2.74
Na2O	.65	.97	.55	.61	.83
K2O	2.46	4.04	2.80	2.81	2.26
TiO2	.75	.88	1.05	.90	.62
P2O5	0.00	.08	.10	.04	.10
Ba	.07	.12	.11	.07	1.83
LOI	9.17	5.11	5.01	5.20	5.00
TOTAL	98.73	99.88	100.00	100.05	100.04

TRACE ELEMENTS (PPM)

Zr	101	107	120	117	138
Sr	76	18	68	55	159
Rb	62	114	76	81	63
Zn	86	90	112	115	100
Cu	42	0	13	22	198
Nb	0	0	0	0	12
Ce	169	133	175	171	80
La	0	54	37	41	0
Ni	68	76	99	114	69
Cr	93	112	97	102	67
V	86	118	85	115	112

TABLE III-4 (Cont'd)

BLACK MUDSTONE

MAJOR ELEMENTS (WT%)

SAMPLE	LY-22	RECK-1	DC-2
SiO2	55.36	59.21	53.25
Al2O3	18.12	18.92	16.78
Fe2O3	9.23	7.92	8.01
MnO	.74	.37	.81
CaO	2.29	.49	4.10
MgO	2.33	2.21	4.29
Na2O	.83	1.42	.79
K2O	3.57	4.02	3.27
TiO2	.95	.96	.87
P2O5	.21	.26	.05
Ba	.10	.10	.04
LOI	6.34	4.38	8.35
TOTAL	100.07	100.26	100.61

TRACE ELEMENTS (PPM)

Zr	114	109	120
Sr	67	0	66
Rb	95	102	96
Zn	86	93	91
Cu	70	37	25
Nb	0	0	0
Ce	161	108	93
La	40	0	11
Ni	101	73	53
Cr	106	98	101
V	173	97	94

TABLE III-4 (Cont'd)

PRECAMBIAN SEDIMENTS

MAJOR ELEMENTS (WT%)

SAMPLE	DB-35	DB-58	40204	40205	CC-3
SiO2	76.78	58.64	75.79	65.01	61.54
Al2O3	2.90	22.04	11.54	16.63	18.13
Fe2O3	2.43	5.34	2.22	4.58	6.03
MnO	.99	.06	.13	.15	.24
CaO	8.29	.51	1.26	.90	.55
MgO	0.00	.98	.34	0.00	.29
Na2O	.93	1.84	4.33	4.35	2.72
K2O	.35	6.70	1.58	3.49	4.23
TiO2	.11	.78	.36	.63	.88
P2O5	.46	.34	.28	.27	.28
Ba	.06	.15	.04	.06	.08
LOI	7.24	3.56	1.24	2.12	3.38
TOTAL	100.54	100.94	99.11	98.19	98.35

TRACE ELEMENTS (PPM)

Zr	0	223	206	204	184
Sr	0	0	17	91	23
Rb	0	194	22	100	107
Zn	0	66	60	84	100
Cu	0	0	6	20	19
Nb	0	0	0	0	0
Ce	0	123	58	24	82
La	0	45	8	0	0
Ni	0	6	4	11	22
Cr	0	12	6	26	39
V	0	76	35	79	104

TABLE III-4 (Cont'd)

PRECAMBIAN SEDIMENTS

MAJOR ELEMENTS (WT%)

SAMPLE	XY-1	HA-1
SiO_2	61.14	63.74
Al_2O_3	15.94	17.17
Fe_2O_3	6.62	6.44
MnO	.14	.07
CaO	1.22	1.40
MgO	2.04	.85
Na_2O	2.87	2.50
K_2O	4.34	3.77
TiO_2	.75	1.08
P_2O_5	0.00	.28
Ba	.06	.11
LOI	3.02	3.15
TOTAL	98.14	100.56

TRACE ELEMENTS (PPM)

	XY-1	HA-1
Zr	173	248
Sr	102	70
Rb	98	95
Zn	82	88
Cu	41	4
Nb	0	0
Ce	63	56
La	0	0
Ni	21	27
Cr	47	67
V	104	119

TABLE III-4 (Cont'd)

IGNEOUS ROCKS

MAJOR ELEMENTS (WT%)

SAMPLE	HGR-1	40202	40203	HH-24	SP-39
SiO2	72.31	55.57	61.35	23.85	32.91
Al2O3	14.09	15.96	15.32	5.41	14.89
Fe2O3	2.40	6.43	9.71	9.40	9.97
MnO	.10	.53	.37	.96	1.22
CaO	.53	4.20	1.16	29.82	8.87
MgO	.94	2.90	.94	1.60	6.72
Na2O	3.38	5.45	2.69	.04	1.18
K2O	4.81	1.18	3.35	.01	.21
TiO2	.44	.95	.95	1.64	1.80
P2O5	.23	.29	.41	.23	.95
Ba	.12	.04	.10	.59	.53
LOI	1.57	5.47	3.23	25.11	20.39
TOTAL	100.92	98.97	99.58	98.66	99.64

TRACE ELEMENTS (PPM)

Zr	170	201	112	189	248
Sr	91	200	7	301	723
Rb	136	32	87	6	0
Zn	56	112	101	96	71
Cu	0	0	0	0	14
Nb	0	0	0	38	0
Ce	39	82	70	36	234
La	0	0	0	0	91
Ni	0	26	24	70	44
Cr	15	18	18	95	20
V	41	98	71	74	182

TABLE III-4 (Cont'd)

IGNEOUS ROCKS

MAJOR ELEMENTS (WT%)

SAMPLE	CAV-1	CAV-2	RL-15
SiO2	23.93	45.57	40.06
Al2O3	14.00	14.75	15.55
Fe2O3	21.11	10.21	11.03
MnO	.50	.63	.85
CaO	8.80	5.58	7.64
MgO	17.66	12.45	6.56
Na2O	3.73	0.00	3.53
K2O	.01	.03	.75
TiO2	2.60	2.78	2.22
P2O5	.15	.37	.45
Ba	.03	0.00	.02
LOI	8.24	0.00	11.33
TOTAL	100.76	92.37	99.99

TRACE ELEMENTS (PPM)

Zr	187	140	243
Sr	204	93	111
Rb	0	5	12
Zn	123	129	86
Cu	53	12	22
Nb	7	19	34
Ce	58	87	92
La	0	89	17
Ni	182	212	50
Cr	286	286	100
V	270	295	222

ADDENDUM TO TABLE III-4

MAJOR ELEMENTS (WT%)

SAMPLE	DB 73-6	BW 4'a',bot.	M-302	CA8C
SiO_2	56.01	52.92	38.88	57.18
Al_2O_3	20.62	17.96	11.08	19.97
Fe_2O_3	8.77	9.04	13.66	8.89
MnO	0.32	3.37	2.70	0.52
CaO	0.35	1.09	11.67	0.50
MgO	0.81	2.60	13.86	2.05
Na_2O	0.87	0.84	0.44	1.04
K_2O	5.12	3.97	1.33	3.60
TiO_2	0.82	0.75	0.43	0.90
P_2O_5	0.00	0.05	0.00	0.00
Ba	0.21	0.43	0.04	2.77
LOI	4.36	5.72	14.76	1.68
TOTAL	98.26	98.74	98.76	99.10

TRACE ELEMENTS (PPM)

Zr	95	119	52	359
Sr	0	86	82	2100
Rb	147	107	27	41
Zn	49	109	103	118
Cu	0	0	0	0
Nb	0	0	0	31
Ce	94	119	73	78
La	1	0	0	0
Ni	69	71	55	60
Cr	94	81	63	87
V	72	62	18	282

Tables III-5 through III-10 present correlations matrices between major elements, trace elements, and major and trace elements in two mudrock groups containing 61 red and 93 green mudrock.

Figures III-1 to III-6 are scattergram plots of major element concentrations versus Al_2O_3 for all analyzed samples (III-1, III-2), all red mudrocks (III-3, III-4), and all green mudrocks (III-5, III-6). The detrital-carbonate trend is clearly shown in Fig. III-1 and III-2. The remaining scattergrams illustrate the homogeneity of red and green mudrocks as groups and also the chemical similarity between red and green mudrocks.

TABLE III-5

CORRELATION COEFFICIENTS BETWEEN MAJOR ELEMENT CONTENTS OF 61 RED MUDROCK SAMPLES*

	Fe_2O_3	TiO_2	P_2O_5	SiO_2	CaO	K_2O	MgO	Al_2O_3	MnO	Na_2O	Ba
Fe_2O_3	1	-0.2018 s=0.059	0.2034 s=0.063	-0.7177 s=0.001	-0.0241 s=0.427	0.1529 s=0.120	0.1181 s=0.184	0.5531 s=0.001	0.4400 s=0.001	-0.5122 s=0.001	0.3577 s=0.002
TiO_2		1	-0.4298 s=0.001	0.0850 s=0.2[illegible]	-0.3704 s=0.002	0.4592 s=0.001	-0.0912 s=0.244	0.1425 s=0.139	-0.4971 s=0.001	0.0866 s=0.253	-0.3304 [illegible].005
P_2O_5			1	-0.2443 s=0.032	0.7224 s=0.001	-0.2358 s=0.039	0.1256 s=0.176	-0.3342 s=0.006	0.4020 s=0.001	-0.1298 s=0.166	0.2246 s=0.005
SiO_2				1	-0.2355 s=0.034	-0.4291 s=0.001	-0.0477 s=0.359	-0.7696 s=0.001	-0.1430 s=0.136	0.4906 s=0.001	-0.3012 s=0.009
CaO					1	-0.1709 s=0.094	-0.0957 s=0.234	-0.4553 s=0.001	0.2671 s=0.019	-0.0736 s=0.286	0,0306 s=0.407
K_2O						1	-0.3583 s=0.002	0.5207 s=0.001	-0.2704 s=0.018	-0.5075 s=0.001	0.2703 s=0.018
MgO							1	0.0723 s=0.291	-0.0457 s=0.364	0.0727 s=0.291	-0.1058 s=0.210
Al_2O_3								1	-0.1601 s=0.111	-0.3825 s=0.001	0.3173 s=0.007
MnO									1	-0.2105 s=0.052	0.3217 s=0.006
Na_2O										1	-0.5721 s=0.001
Ba											1

TABLE III-6

CORRELATION COEFFICIENTS BETWEEN MAJOR ELEMENT CONTENTS OF 61 RED MUDROCK SAMPLES

	Zr	Sr	Rb	Zn	Ca	Ni	Cr	V	Ba
Zr	1	-0.3052 s=0.018	-0.2466 s=0.029	-0.1344 s=0.153	-0.6349 s=0.001	-0.4397 s=0.001	-0.5685 s=0.001	0.0486 s=0.356	-0.4934 s=0.001
Sr		1	-0.2715 s=0.031	-0.1096 s=0.229	0.0985 s=0.255	0.3663 s=0.005	-0.1785 s=0.112	-0.2687 s=0.032	0.3204 s=0.013
Rb			1	0.2437 s=0.029	0.0535 s=0.342	0.1601 s=0.109	0.2128 s=0.050	0.2805 s=0.014	0.3691 s=0.002
Zn				1	0.2373 s=0.034	0.3787 s=0.001	0.2196 s=0.045	0.2195 s=0.045	-0.1021 s=0.217
Ca					1	0.5120 s=0.001	0.6485 s=0.001	-0.0342 s=0.398	0.3511 s=0.003
Ni						1	0.3284 s=0.005	-0.0039 s=0.488	0.3432 s=0.003
Cr							1	0.2885 s=0.012	0.2525 s=0.025
V								1	-0.3066 s=0.008
Ba									1

TABLE III-7

CORRELATION COEFFICIENTS BETWEEN MAJOR AND TRACE ELEMENT CONTENTS OF 61 RED MUDROCK SAMPLES

	Zr	Sr	Rb	Zn	Ce	Ni	Cr	V	Ba2*
Fe_2O_3	-0.5898 s=0.001	0.3970 s=0.003	0.1691 s=0.096	0.1716 s=0.093	0.6049 s=0.001	0.3155 s=0.007	0.4219 s=0.001	-0.0075 s=0.477	0.3865 s=0.001
TiO_2	0.5329 s=0.001	-0.5870 s=0.001	0.2643 s=0.020	0.1028 s=0.215	-0.3325 s=0.005	-0.4146 s=0.001	-0.2175 s=0.046	0.3520 s=0.003	-0.3165 s=0.006
P_2O_5	-0.1068 s=0.215	0.8687 s=0.001	-0.3127 s=0.008	-0.1018 s=0.224	-0.0002 s=0.499	0.2111 s=0.056	-0.3125 s=0.008	-0.3895 s=0.001	0.1852 s=0.082
SiO_2	0.6002 s=0.001	-0.4421 s=0.001	-0.4696 s=0.001	-0.2682 s=0.018	-0.3589 s=0.002	-0.2703 s=0.018	-0.2772 s=0.015	-0.1031 s=0.215	-0.3078 s=0.008
CaO	0.0596 s=0.325	0.6883 s=0.001	-0.3116 s=0.007	-0.1011 s=0.219	-0.2054 s=0.058	0.0930 s=0.238	-0.4646 s=0.001	-0.3661 s=0.002	-0.0350 s=0.395
K_2O	-0.0263 s=0.421	-0.2765 s=0.028	0.8471 s=0.001	0.1684 s=0.097	-0.1624 s=0.107	-0.0502 s=0.350	-0.1090 s=0.202	0.2387 s=0.033	0.2790 s=0.015
MgO	-0.1204 s=0.182	0.3388 s=0.010	-0.2952 s=0.011	0.3197 s=0.006	0.1817 s=0.084	0.1154 s=0.190	0.2153 s=0.049	0.1171 s=0.186	-0.0873 s=0.253
Al_2O_3	-0.6119 s=0.001	0.0268 s=0.429	0.7014 s=0.001	0.3772 s=0.001	0.4667 s=0.001	0.2381 s=0.033	0.5467 s=0.001	0.3295 s=0.005	0.3488 s=0.003
MnO	-0.3349 s=0.004	0.6813 s=0.001	-0.2971 s=0.010	-0.1374 s=0.146	0.2578 s=0.023	0.3750 s=0.001	-0.0025 s=0.492	-0.3405 s=0.004	0.3125 s=0.007
Na_2O	0.3248 s=0.006	-0.1870 s=0.102	-0.4032 s=0.001	-0.1694 s=0.096	-0.3039 s=0.009	-0.1975 s=0.064	-0.0813 s=0.267	0.1375 s=0.145	-0.5696 s=0.001
Ba1*	-0.4664 s=0.001	0.3443 s=0.008	0.3415 s=0.004	-0.1073 s=0.205	0.3177 s=0.007	0.3372 s=0.004	0.2136 s=0.049	-0.3365 s=0.004	0.9909 s=0.001

* Ba1 = barium values with Ba analyzed as major element.

Ba2 = barium values with Ba analyzed as trace element.

TABLE III-8

CORRELATION COEFFICIENTS BETWEEN MAJOR ELEMENT CONCENTRATIONS OF 93 GREEN MUDROCK SAMPLES

	Fe_2O_3	TiO_2	P_2O_5	SiO_2	CaO	K_2O	MgO	Al_2O_3	MnO	Na_2O	Ba
Fe_2O_3	1	-0.1914 s=0.032	0.3134 s=0.002	-0.4793 s=0.001	-0.0176 s=0.433	-0.3401 s=0.001	0.2809 s=0.003	0.0441 s=0.336	-0.1503 s=0.074	-0.5390 s=0.001	0.2478 s=0.008
TiO_2		1	-0.0861 s=0.218	0.1972 s=0.028	-0.4520 s=0.001	0.4208 s=0.001	-0.0473 s=0.325	0.3844 [illegible].001	-0.1855 s=0.037	0.1934 s=0.032	-0.0472 s=0.326
P_2O_5			1	-0.1490 s=0.088	0.1041 s=0.173	-0.2310 s=0.017	0.2990 s=0.003	-0.1096 s=0.161	-0.0198 s=0.429	-0.1256 s=0.130	0.0685 s=0.268
SiO_2				1	-0.4572 s=0.001	-0.0473 s=0.325	-0.3261 s=0.001	-0.2278 s=0.014	-0.2994 s=0.002	0.6522 s=0.001	-0.3493 s=0.001
CaO					1	-0.4135 s=0.001	0.1252 s=0.115	-0.6010 s=0.001	0.1386 s=0.091	-0.1427 s=0.087	0.0662 s=0.263
K_2O						1	-0.3191 s=0.001	0.7006 s=0.001	0.0999 s=0.169	-0.2292 s=0.014	-0.1455 s=0.081
MgO							1	-0.0053 s=0.480	-0.0421 s=0.344	0.0260 s=0.403	0.1070 s=0.152
Al_2O_3								1	-0.0374 s=0.360	-0.2702 s=0.005	0.0260 s=0.402
MnO									1	-0.2088 s=0.023	-0.0034 s=0.487
Na_2O										1	-0.1834 s=0.040
Ba											1

TABLE III-9

CORRELATION COEFFICIENTS BETWEEN TRACE ELEMENT CONTENTS OF 93 GREEN MUDROCK SAMPLES

	Zr	Sr	Rb	Zn	Ce	Ni	Cr	V	Ba
Zr	1	0.0090 s=0.472	-0.0189 s=0.430	0.3607 s=0.001	-0.2737 s=0.005	-0.1793 s=0.046	-0.4074 s=0.001	0.4437 s=0.001	-0.2917 s=0.003
Sr		1	-0.0815 s=0.256	-0.1307 s=0.146	-0.0193 s=0.439	-0.1852 s=0.067	-0.1448 s=0.121	-0.0176 s=0.444	0.3719 s=0.001
Rb			1	-0.0832 s=0.214	-0.0603 s=0.284	0.3871 s=0.001	0.3756 s=0.001	0.1953 s=0.030	0.4456 s=0.001
Zn				1	0.0175 s=0.434	0.1697 s=0.052	0.0973 s=0.177	0.2748 s=0.004	-0.3121 s=0.001
Ce					1	0.3045 s=0.002	0.4544 s=0.001	-0.0827 s=0.217	0.1117 s=0.145
Ni						1	0.4655 s=0.001	0.0379 s=0.359	0.1791 s=0.043
Cr							1	0.1883 s=0.035	0.2915 s=0.002
V								1	-0.0803 s=0.222
Ba									1

TABLE III-10

CORRELATION COEFFICIENTS BETWEEN MAJOR AND TRACE ELEMENT CONTENTS OF 93 GREEN MUDROCK SAMPLES

	Zr	Sr	Rb	Zn	Ce	Ni	Cr	V	Ba2*
Fe_2O_3	-0.4003 s=0.001	-0.0755 s=0.272	-0.2794 s=0.003	0.1628 s=0.059	0.4973 s=0.001	0.2119 s=0.024	0.3683 s=0.001	-0.2019 s=0.026	0.1272 s=0.112
TiO_2	0.6711 s=0.001	-0.1128 s=0.182	0.3931 s=0.001	0.2423 s=0.010	-0.0378 s=0.360	0.1100 s=0.163	0.0319 s=0.246	0.4282 s=0.001	-0.1286 s=0.110
P_2O_5	-0.1075 s=0.173	0.0640 s=0.315	-0.2161 s=0.025	0.0181 s=0.435	0.2593 s=0.009	-0.1090 s=0.163	0.0763 s=0.246	-0.0707 s=0.263	0.0555 s=0.309
SiO_2	0.4285 s=0.001	-0.1351 s=0.138	-0.0327 s=0.378	0.0526 s=0.308	-0.2346 s=0.012	-0.0321 s=0.380	-0.2745 s=0.004	0.0873 s=0.203	-0.1809 s=0.041
CaO	-0.0955 s=0.187	0.2597 s=0.017	-0.4887 s=0.001	-0.1448 s=0.083	-0.2853 s=0.003	-0.4224 s=0.001	-0.5300 s=0.001	-0.1434 s=0.085	-0.1647 s=0.057
K_2O	-0.0470 s=0.331	-0.0705 s=0.285	0.8822 s=0.001	-0.2093 s=0.022	-0.0895 s=0.198	0.2164 s=0.019	0.2715 s=0.004	0.1407 s=0.089	-0.4065 s=0.001
MgO	-0.0109 s=0.460	-0.0183 s=0.442	-0.2592 s=0.006	0.4418 s=0.001	0.1357 s=0.099	0.0412 s=0.347	0.1418 s=0.088	0.0700 s=0.253	-0.3344 s=0.001
Al_2O_3	-0.1815 s=0.044	0.0032 s=0.490	0.7239 s=0.001	0.0796 s=0.224	0.2764 s=0.004	0.4740 s=0.001	0.6866 s=0.001	0.2175 s=0.018	0.3426 s=0.001
MnO	-0.2332 s=0.014	0.0141 s=0.455	0.0060 s=0.498	-0.3177 s=0.001	0.1536 s=0.072	-0.0850 s=0.211	0.0750 s=0.238	-0.2136 s=0.020	0.1020 s=0.165
Na_2O	0.5729 s=0.001	-0.0604 s=0.316	-0.1578 s=0.068	0.3035 s=0.002	-0.3430 s=0.001	-0.1836 s=0.041	-0.3429 s=0.001	0.1370 s=0.098	-0.4100 s=0.001
Ba1*	-0.0661 s=0.269	-0.0496 s=0.345	0.0922 s=0.190	-0.0504 s=0.316	0.1273 s=0.113	0.0766 s=0.233	0.1531 s=0.071	0.0059 s=0.478	0.2619 s=0.006

* Ba1 = samples analyzed as with major elements.

Ba2 = barium analyzed as trace element.

SCATTERGRAMS OF MAJOR ELEMENT CONCENTRATIONS VERSUS Al_2O_3,
ALL ANALYZED SAMPLES

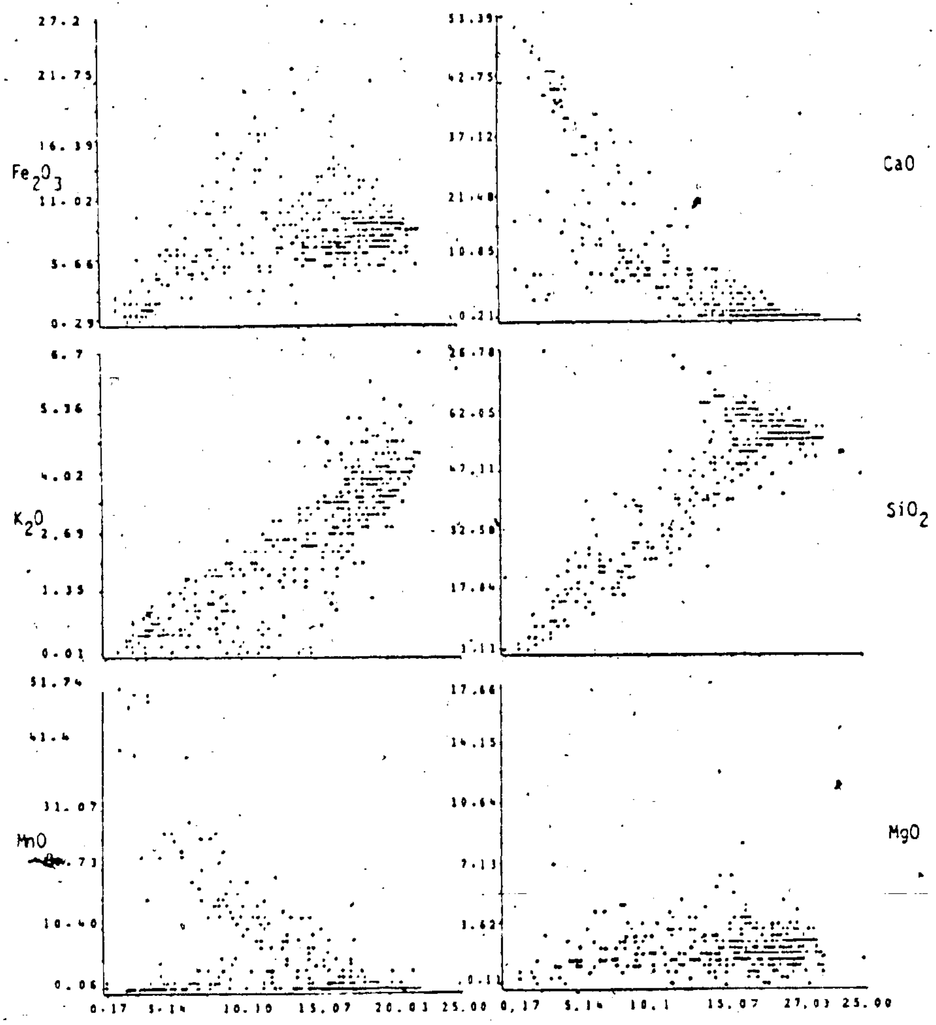

Figure III-1

SCATTERGRAM OF Na_2O CONCENTRATIONS VERSUS Al_2O_3,
ALL ANALYZED SAMPLES

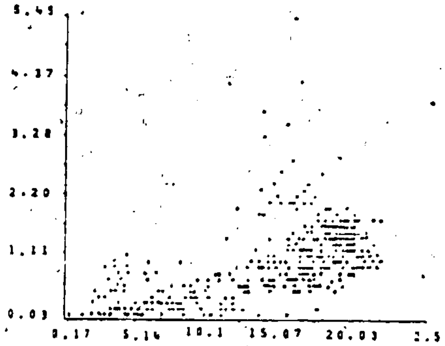

Figure III-2.

SCATTERGRAMS OF MAJOR ELEMENT CONCENTRATIONS VERSUS Al_2O_3,
ALL ANALYZED RED MUDROCK SAMPLES

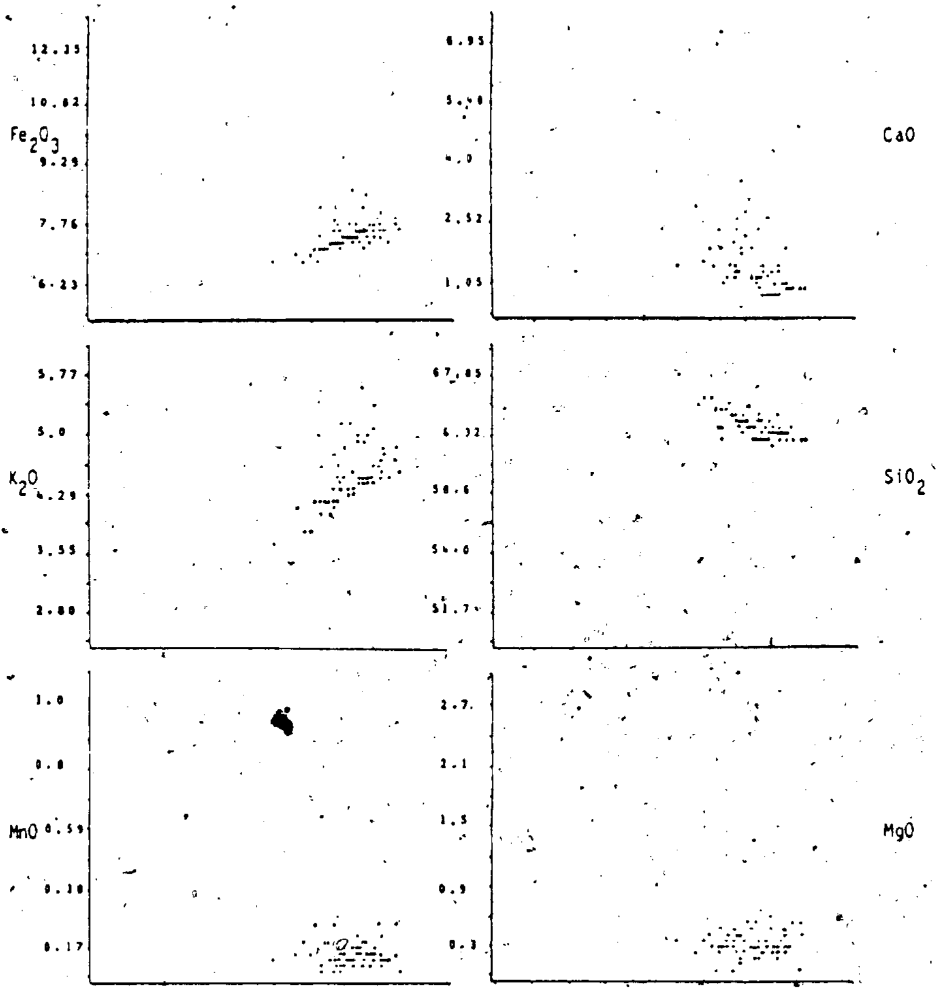

Figure III-3.

SCATTERGRAM OF Na_2O CONTENT VERSUS Al_2O_3,
ALL ANALYZED RED MUDROCKS

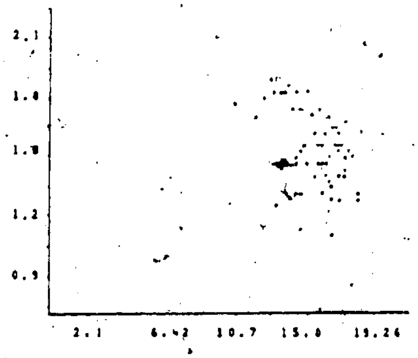

Figure III-4.

SCATTERGRAMS OF MAJOR ELEMENT CONCENTRATIONS VERSUS Al_2O_3,
ALL ANALYZED GREEN MUDROCK SAMPLES

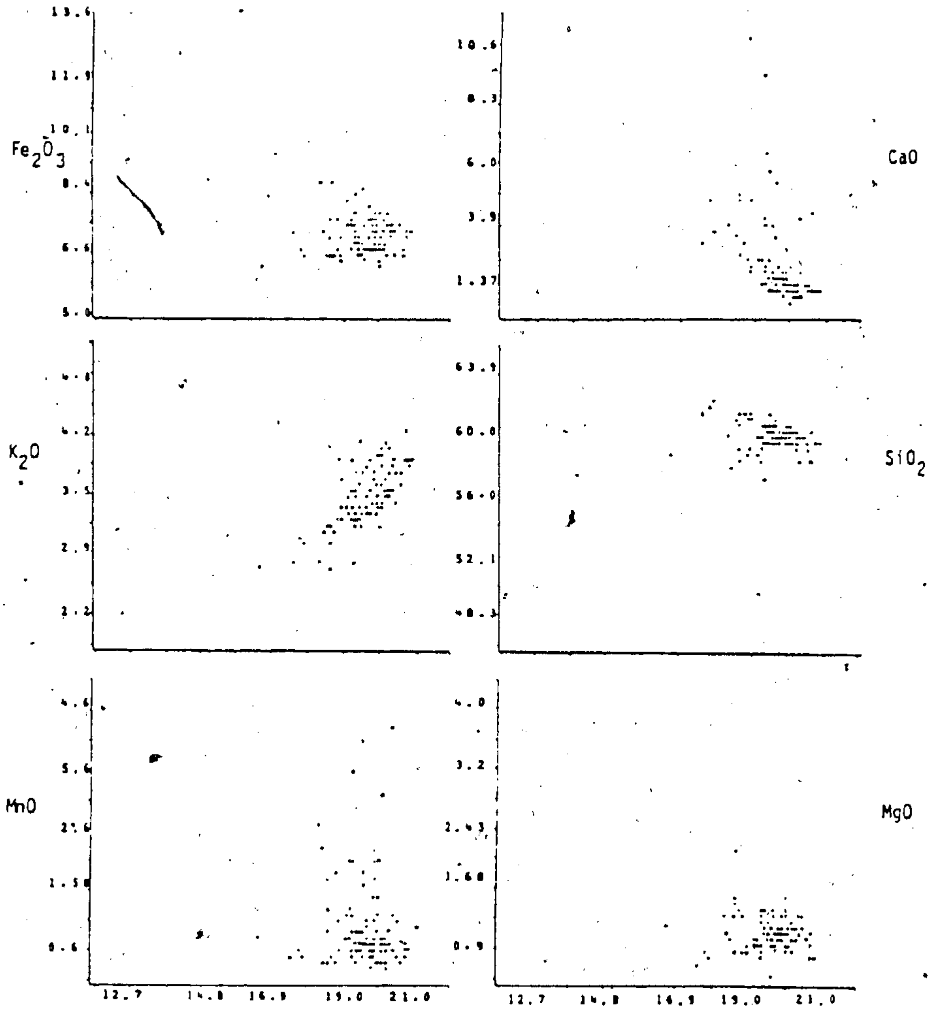

Figure III-5.

SCATTERGRAM OF Na_2O CONCENTRATIONS VERSUS Al_2O_3,
ALL ANALYZED GREEN MUDROCK SAMPLES

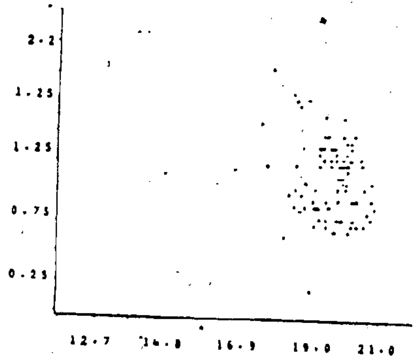

Figure III-6.